# TRAJECTORIES OF BRAIN ALTERATIONS: CHARACTERIZING THE PROGRESSION OF BRAIN AGING IN PATIENTS WITH MENTAL DISORDERS

EDITED BY: Wenjing Zhang, Wei Deng and Meiling Li

PUBLISHED IN: Frontiers in Aging Neuroscience

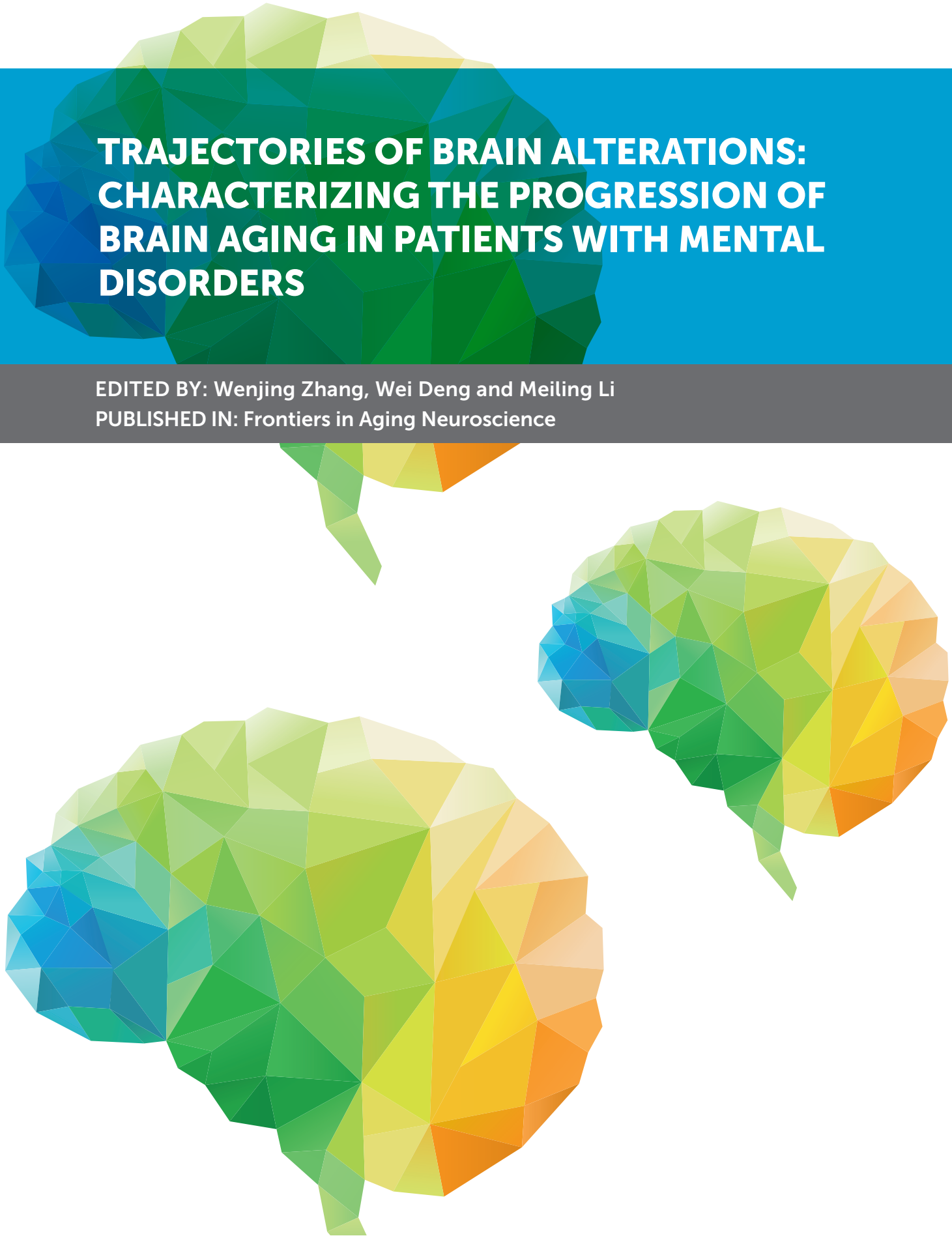

frontiers Research Topics

ISSN 1664-8714
ISBN 978-2-83250-193-1
DOI 10.3389/978-2-83250-193-1

## About Frontiers

Frontiers is more than just an open-access publisher of scholarly articles: it is a pioneering approach to the world of academia, radically improving the way scholarly research is managed. The grand vision of Frontiers is a world where all people have an equal opportunity to seek, share and generate knowledge. Frontiers provides immediate and permanent online open access to all its publications, but this alone is not enough to realize our grand goals.

## Frontiers Journal Series

The Frontiers Journal Series is a multi-tier and interdisciplinary set of open-access, online journals, promising a paradigm shift from the current review, selection and dissemination processes in academic publishing. All Frontiers journals are driven by researchers for researchers; therefore, they constitute a service to the scholarly community. At the same time, the Frontiers Journal Series operates on a revolutionary invention, the tiered publishing system, initially addressing specific communities of scholars, and gradually climbing up to broader public understanding, thus serving the interests of the lay society, too.

## Dedication to Quality

Each Frontiers article is a landmark of the highest quality, thanks to genuinely collaborative interactions between authors and review editors, who include some of the world's best academicians. Research must be certified by peers before entering a stream of knowledge that may eventually reach the public - and shape society; therefore, Frontiers only applies the most rigorous and unbiased reviews.
Frontiers revolutionizes research publishing by freely delivering the most outstanding research, evaluated with no bias from both the academic and social point of view. By applying the most advanced information technologies, Frontiers is catapulting scholarly publishing into a new generation.

## What are Frontiers Research Topics?

Frontiers Research Topics are very popular trademarks of the Frontiers Journals Series: they are collections of at least ten articles, all centered on a particular subject. With their unique mix of varied contributions from Original Research to Review Articles, Frontiers Research Topics unify the most influential researchers, the latest key findings and historical advances in a hot research area! Find out more on how to host your own Frontiers Research Topic or contribute to one as an author by contacting the Frontiers Editorial Office: frontiersin.org/about/contact

# TRAJECTORIES OF BRAIN ALTERATIONS: CHARACTERIZING THE PROGRESSION OF BRAIN AGING IN PATIENTS WITH MENTAL DISORDERS

Topic Editors:
**Wenjing Zhang,** Sichuan University, China
**Wei Deng,** Affiliated Mental Health Center & Hangzhou Seventh People's Hospital, China
**Meiling Li,** Athinoula A. Martinos Center for Biomedical Imaging, Department of Radiology, Massachusetts General Hospital, Harvard Medical School, United States

**Citation:** Zhang, W., Deng, W., Li, M., eds. (2022). Trajectories of Brain Alterations: Characterizing the Progression of Brain Aging in Patients with Mental Disorders. Lausanne: Frontiers Media SA. doi: 10.3389/978-2-83250-193-1

# Table of Contents

frontiers in Aging Neuroscience

ORIGINAL RESEARCH
published: 24 December 2021
doi: 10.3389/fnagi.2021.752575

# Longitudinal Changes in Brain Gyrification in Schizophrenia Spectrum Disorders

*Tien Viet Pham[1,2], Daiki Sasabayashi[1,2]*, Tsutomu Takahashi[1,2], Yoichiro Takayanagi[1,3], Manabu Kubota[4], Atsushi Furuichi[1,2], Mikio Kido[1,2,5], Kyo Noguchi[6] and Michio Suzuki[1,2]*

[1] Department of Neuropsychiatry, University of Toyama Graduate School of Medicine and Pharmaceutical Sciences, Toyama, Japan, [2] Research Center for Idling Brain Science, University of Toyama, Toyama, Japan, [3] Arisawabashi Hospital, Toyama, Japan, [4] Department of Psychiatry, Graduate School of Medicine, Kyoto University, Kyoto, Japan, [5] Toyama City Hospital, Toyama, Japan, [6] Department of Radiology, University of Toyama School of Medicine, Toyama, Japan

Previous magnetic resonance imaging (MRI) studies reported increased brain gyrification in schizophrenia and schizotypal disorder, a prototypic disorder within the schizophrenia spectrum. This may reflect deviations in early neurodevelopment; however, it currently remains unclear whether the gyrification pattern longitudinally changes over the course of the schizophrenia spectrum. The present MRI study using FreeSurfer compared longitudinal changes (mean inter-scan interval of 2.7 years) in the local gyrification index (LGI) in the entire cortex among 23 patients with first-episode schizophrenia, 14 with schizotypal disorder, and 39 healthy controls. Significant differences were observed in longitudinal LGI changes between these groups; the schizophrenia group exhibited a progressive decline in LGI, predominantly in the fronto-temporal regions, whereas LGI increased over time in several brain regions in the schizotypal and control groups. In the schizophrenia group, a greater reduction in LGI over time in the right precentral and post central regions correlated with smaller improvements in negative symptoms during the follow-up period. The cumulative medication dosage during follow-up negatively correlated with a longitudinal LGI increase in the right superior parietal area in the schizotypal group, but did not affect longitudinal LGI changes in the schizophrenia group. Collectively, these results suggest that gyrification patterns in the schizophrenia spectrum reflect both early neurodevelopmental abnormalities as a vulnerability factor and active brain pathology in the early stages of schizophrenia.

**Keywords: gyrification, local gyrification index, magnetic resonance imaging, schizophrenia, schizotypal disorder, longitudinal, gyrification trajectory**

OPEN ACCESS

***Edited by:***
*Wenjing Zhang,*
*Sichuan University, China*

***Reviewed by:***
*Bhoomika Kar,*
*Allahabad University, India*
*Gui Fu,*
*Sichuan University, China*

***Correspondence:**
*Daiki Sasabayashi*
*ds179@med.u-toyama.ac.jp*

***Received:*** *03 August 2021*
***Accepted:*** *25 November 2021*
***Published:*** *24 December 2021*

***Citation:***
*Pham TV, Sasabayashi D, Takahashi T, Takayanagi Y, Kubota M, Furuichi A, Kido M, Noguchi K and Suzuki M (2021) Longitudinal Changes in Brain Gyrification in Schizophrenia Spectrum Disorders. Front. Aging Neurosci. 13:752575. doi: 10.3389/fnagi.2021.752575*

## INTRODUCTION

Brain gyrification is regarded as an early neurodevelopmental marker of cortical complexity because its pattern is genetically mediated (Bartley et al., 1997) and it undergoes the greatest development during pregnancy but remains rather stable after birth (Armstrong et al., 1995; Zilles et al., 2013). Previous magnetic resonance imaging (MRI) studies demonstrated a widespread brain hypergyrification pattern in the early stages of schizophrenia (Schultz et al., 2013; Nanda et al., 2014; Sasabayashi et al., 2017a), which potentially reflects an early neurodevelopmental pathology,

including white matter maldevelopment and aberrant neural connectivity (Sasabayashi et al., 2021). Increased brain gyrification in the frontal and other cortical regions was also detected in individuals with genetic (Falkai et al., 2007; Neilson et al., 2018) and clinical risk for the development of psychosis (Tepest et al., 2013; Sasabayashi et al., 2017b) and in patients with schizotypal disorder (Sasabayashi et al., 2020), who share biological commonalities with schizophrenia patients as part of the schizophrenia spectrum in the context of the neurodevelopmental hypothesis but are mostly spared from developing overt psychosis (Siever and Davis, 2004). These findings support brain hypergyrification being an early developmental trait marker associated with vulnerability to psychosis (Sasabayashi et al., 2021).

Gyrification was previously reported to be normal (Haukvik et al., 2012) or even decreased (Nesvåg et al., 2014; Palaniyappan and Liddle, 2014) in patients with schizophrenia, particularly in chronic cases (reviewed by Harris et al., 2007; Nanda et al., 2014; Sasabayashi et al., 2021). In addition to the potential influence of different sample characteristics (e.g., clinical subtypes, Sallet et al., 2003; Takayanagi et al., 2019, and treatment responses; Palaniyappan et al., 2013b) on the gyrification pattern in schizophrenia, these discrepancies may partly be attributed to factors associated with illness stages, such as illness chronicity and antipsychotic medication (Tomelleri et al., 2009). A 2-year follow-up MRI study on first-episode schizophrenia (Palaniyappan et al., 2013a) reported a longitudinal decline in gyrification, predominantly in the fronto-temporo-limbic regions, which may be associated with treatment responses (Nelson et al., 2020). Since the cortical surface may flatten during adolescence as a late neurodevelopmental process (Alemán-Gómez et al., 2013), this longitudinal decline appears to be consistent with the notion that a progressive brain pathology in the early stages of psychosis is associated with the acceleration of normal brain maturational processes (Pantelis et al., 2007). However, these longitudinal studies only examined selected brain regions (Palaniyappan et al., 2013a) or average gyrification per hemisphere (Nelson et al., 2020). Furthermore, to the best of our knowledge, potential changes in gyrification over time have not yet been investigated in schizotypal patients using MRI.

Therefore, the present MRI study investigated potential longitudinal changes in the brain gyrification pattern in the entire cortex among patients with first-episode schizophrenia, those with schizotypal disorder, and matched healthy controls. Based on the gyrification patterns observed at different illness stages of schizophrenia and previous longitudinal findings (Palaniyappan et al., 2013a), we hypothesized that patients with first-episode schizophrenia exhibit a greater longitudinal decline in gyrification than healthy controls. We also predicted that the brain gyrification pattern is more stable in patients with schizotypal disorder who are vulnerable to psychosis, but do not exhibit active brain changes (Takahashi and Suzuki, 2018). Furthermore, we investigated whether potential longitudinal changes in brain gyrification in the patient groups are associated with medication and changes in clinical symptoms.

# MATERIALS AND METHODS

## Subjects

Subjects comprised 23 patients with first-episode schizophrenia, 14 with schizotypal disorder, and 39 healthy controls (**Table 1**), all of whom were right-handed and physically healthy and had no previous history of head trauma, neurological illness, substance abuse disorder, or serious medical disease. In the longitudinal brain assessment, all subjects were scanned twice during clinical follow-up (inter-scan interval; mean = 2.7 years, *SD* = 0.6 years) using the same MR scanner and parameters. Although this was the first follow-up study of local gyrification index (LGI) changes in our sample, we previously assessed cross-sectional LGI differences in larger cohorts (Sasabayashi et al., 2017a, 2020) that included some of the subjects in the present study (18/23 patients with first-episode schizophrenia, 8/14 with schizotypal disorder, and 17/39 healthy controls). The Committee on Medical Ethics of Toyama University approved the present study. All subjects provided their written informed consent following a detailed explanation of the study.

As previously described (Suzuki et al., 2005; Takahashi et al., 2010), patients with first-episode schizophrenia and schizotypal disorder who fulfilled the ICD-10 research criteria (World Health Organization., 1993) were recruited from the inpatient and outpatient clinics of the Department of Neuropsychiatry of Toyama University Hospital. Briefly, first-episode patients were defined as those with an illness duration of $\leq$ 1 year or those experiencing psychiatric hospitalization for the first time during baseline scanning. All schizotypal patients also met the DSM Axis II diagnosis of schizotypal personality disorder (American Psychiatric Association., 1994) and did not develop overt psychosis during the follow-up period. The Scale for the Assessment of Negative Symptoms (SANS) (Andreasen, 1983) and the Scale for the Assessment of Positive Symptoms (SAPS) (Andreasen, 1984) were used to rate clinical symptoms at the time of baseline and follow-up scanning. During the follow-up period between scans, 13 patients (7 schizophrenia and 6 schizotypal patients; typical group) were predominantly treated with typical antipsychotics or received substantial amounts of both typical and atypical ones, while 24 patients (16 schizophrenia and 8 schizotypal patients; atypical group) were treated mostly with atypical antipsychotics.

Members of the community, hospital staff, and university students were recruited as healthy controls. A questionnaire with 15 items related to personal (13 items, e.g., a previous history of traumatic head injury, seizures, neurological or psychiatric diseases, hypothyroidism, hypertension, diabetes mellitus, complications of pregnancy, and substance use) and family (2 items) histories of illness was completed, which revealed no personal or family history of psychiatric illness among first-degree relatives.

## Image Acquisition

Subjects were scanned using 1.5-T Magnetom Vision (Siemens Medical System, Inc., Erlangen, Germany) with the three-dimensional gradient-echo sequence FLASH (fast low-angle

**TABLE 1 |** Subjects characteristics in the present study.

| | HC (*N* = 39) | SzTypal (*N* = 14) | Sz (*N* = 23) | Group comparisons |
|---|---|---|---|---|
| Male/female | 22/17 | 10/4 | 15/8 | Chi-square = 1.144, $p = 0.564$ |
| Age at baseline scan (years) | 24.6 (4.7) | 23.0 (4.9) | 23.5 (4.8) | $F(2, 73) = 0.788$, $p = 0.458$ |
| Height (cm) | 165.8 (8.0) | 166.6 (9.2) | 165.0 (7.9) | $F(2, 73) = 0.169$, $p = 0.845$ |
| Education (years) | 15.6 (2.1) | 12.5 (2.4) | 13.1 (1.6) | $F(2, 73) = 17.218$, $p < 0.001$; Sz, SzTypal < C |
| Parental education (years)[a] | 13.1 (2.4) | 12.1 (1.6) | 12.7 (2.1) | $F(2, 73) = 0.947$, $p = 0.393$ |
| Inter-scan interval (years) | 2.5 (0.4) | 2.9 (0.8) | 2.6 (0.8) | $F(2, 73) = 1.867$, $p = 0.162$ |
| Onset age (years) | – | – | 22.4 (4.9) | – |
| Illness duration at baseline (months) | – | – | 9.5 (9.1) | – |
| Medication dose (haloperidol equivalent mg) | | | | |
| Dose at baseline (mg/day) | – | 6.4 (7.6) | 13.5 (11.4) | $F(1, 35) = 4.331$, $p = 0.045$; SzTypal < Sz |
| Cumulative dose during follow-up (mg) | – | 7030.7 (7243.2) | 9526.4 (8609.2) | $F(1, 35) = 0.820$, $p = 0.371$ |
| Duration of medication at baseline (months) | – | 42.3 (60.2) | 7.8 (9.7) | $F(1, 35) = 7.379$, $p = 0.010$; Sz < SzTypal |
| Total SAPS score[a] | | | | |
| Baseline | – | 17.6 (9.6) | 29.0 (24.3) | $F(1, 31) = 2.572$, $p = 0.119$ |
| Follow-up | – | 13.6 (11.3) | 17.0 (17.1) | $F(1, 34) = 0.452$, $p = 0.506$ |
| Total SANS score[a] | | | | |
| Baseline | – | 54.8 (22.1) | 52.1 (25.5) | $F(1, 31) = 0.099$, $p = 0.755$ |
| Follow-up | – | 42.3 (16.6) | 38.0 (22.5) | $F(1, 34) = 0.376$, $p = 0.544$ |

**Data are shown as means (SD).**

[a]*Data were missing for 4 patients (1 schizotypal and 3 schizophrenia patients) at baseline and for 1 schizophrenia patient in the follow-up. HC, healthy controls; SANS, scale for the assessment of negative symptoms; SAPS, scale for the assessment of positive symptoms; Sz, schizophrenia; SzTypal, schizotypal disorder.*

shots) yielding 160–180 contiguous T1-weighted slices with a thickness of 1.0 mm in the sagittal plane. Imaging parameters were as follows: repetition time = 24 ms; echo time = 5 ms; flip angle = 40; field of view = 256 mm; and matrix size = 256 × 256 pixels. The voxel size was $1.0 \times 1.0 \times 1.0$ mm$^3$.

## Imaging Processing

FreeSurfer software (version 5.3[1]) preprocessed T1-weighted images based on a standard auto-reconstruction algorithm using the normalization of non-uniform intensities, non-brain tissue removal, affine registration to the Montreal Neurological Institute (MNI) space and Talairach transformation, and the segmentation of gray/white matter tissue (Fischl, 2012). A visual inspection of reconstructed images followed by the manual editing of any inaccuracies in tissue segmentation was performed by one trained investigator (TVP) blinded to subjects' identities.

Based on the pial surface reconstruction, an algorithm for measuring 3D LGI at each vertex across each hemisphere was performed (Sasabayashi et al., 2017a,b). Details of the LGI computation may be found in the validation paper (Schaer et al., 2008) and at https://surfer.nmr.mgh.harvard.edu/fswiki/LGI. LGI changes over time were assessed using the standard and automated FreeSurfer longitudinal pipelines based on a within-subject template estimation (Reuter et al., 2012). Specifically, an unbiased within-subject template (Reuter and Fischl, 2011) was created for robust and inverse consistent registration (Reuter et al., 2010). Several processing steps, such as skull stripping, Talairach transformation, atlas registration, spherical surface mapping, and parcellation, were then initialized using common information from the within-subject template, which significantly increased reliability and statistical power (Reuter et al., 2012).

## Statistical Analysis

Demographic and clinical differences between groups were examined by the chi-squared test or a one-way analysis of variance (ANOVA).

All vertex-wise LGI values were individually mapped on a common spherical coordinate system (fsaverage) that was smoothed with a 5-mm Gaussian kernel. Regarding cross-sectional baseline group comparisons as well as longitudinal comparisons in each group (baseline vs. follow-up), LGI values at each vertex were investigated using a general linear model with age, sex, the duration of medication, and medication dosage as covariates, with the Query Design Estimate Contrast application in FreeSurfer software creating contrasts. Concerning pairwise group comparisons of longitudinal LGI changes, a longitudinal two-stage model was employed to examine LGI changes across groups with age, sex, the inter-scan interval, and cumulative medication dosage during follow-up period as covariates. In the first stage, we performed a linear fit for each subject independently to reduce the repeated measures to a single number. In the second stage, a regular cross-sectional analysis was conducted across subjects. For the medication type, we compared longitudinal LGI changes between the patients with typical and atypical subgroups using the same model. We conducted a vertex-by-vertex correlation analysis between baseline LGI and cumulative medication dosage at baseline (mean = 529.2 mg, *SD* = 535.2

[1]http://surfer.nmr.mgh.harvard.edu/

mg) in the schizophrenia group using a general linear model controlling for age and sex. The same model controlling for age, sex, and the inter-scan interval was used in the vertex-by-vertex correlation analyses between longitudinal LGI changes in patients and the cumulative medication dosage during follow-up, or symptom changes (SAPS/SANS scores in the follow-up—SAPS/SANS scores at baseline). The cumulative medication dosage during follow-up was also added as a covariate for interactions with symptom changes. To correct for multiple comparisons, a Monte Carlo simulation implemented in the AlphaSim program of Analysis of Functional NeuroImages (AFNI) was used in these analyses (Hagler et al., 2007). To define significant clusters, 10,000 iterations of the Monte Carlo simulation were conducted in each comparison using a threshold of $p < 0.05$.

# RESULTS

## Demographic Backgrounds

Although groups were matched for age, sex, height, and parental education, the control group had a higher level of education than the patient groups (**Table 1**). The schizophrenia group had a higher SAPS score than the schizotypal group, particularly at baseline. The duration of medication at baseline was significantly longer and the medication dosage at baseline was significantly higher in the schizotypal group than in the schizophrenia group (**Table 1**).

## Baseline Group Comparisons of Local Gyrification Index

Baseline group comparison revealed LGI in the bilateral frontal regions was higher in the schizotypal group, but not in the schizophrenia group, than in the control group (**Figure 1**). LGI in the bilateral fronto-temporal regions was also higher in the schizotypal group than in the schizophrenia group (**Figure 1**). There were no significant differences in baseline LGI between the combined patient group (schizophrenia and schizotypal group) and control group.

## Longitudinal Local Gyrification Index Changes in Each Group (Baseline vs. Follow-up)

No cluster exhibited significant LGI changes between baseline and follow-up scans in any diagnostic group after cluster-wise correction.

We also conducted supplementary uncorrected analyses using age, sex, and medication as nuisance variables in order to examine general tendency of LGI changes over time (i.e., increase or decrease); LGI decreased predominantly in the fronto-temporal areas in the schizophrenia group, while it increased in several brain regions in the schizotypal and control groups (**Supplementary Figure 1**). A similar progressive decline in the fronto-temporal LGI was observed in the combined patient group (**Supplementary Figure 2**).

## Pairwise Group Comparisons of Longitudinal Local Gyrification Index Changes

The progressive decline in LGI, predominantly in the fronto-temporal and parietal regions, was significantly greater in the schizophrenia group than in the control group (**Table 2** and **Figure 2**). There were no regions in which schizophrenia patients had a significant LGI increase compared with healthy control subjects. Although a progressive increase in LGI was observed in the schizotypal and control groups (**Supplementary Figure 1**), this change in gyrification was significantly greater in the left superior frontal region in the control group (**Figure 2**). The mean LGI values of these clusters with significant group differences are summarized in **Supplementary Table 1**. In addition, the combined patient group exhibited progressive LGI decline similar to that observed in schizophrenia group (**Supplementary Table 2** and **Supplementary Figure 3**).

When we included the education, parental education, or illness duration at baseline as one of the controlling factors (illness duration = 0 for the schizotypal and healthy groups), significant clusters similar to the original analyses were observed even after controlling for the parental education and illness duration (**Supplementary Figures 4**, **5**). There was no group difference in the longitudinal LGI changes when we used the education as a covariate (**Supplementary Figure 6**).

Whereas the schizophrenia subgroup treated with typical antipsychotics ($n = 7$) exhibited progressive LGI decline in the bilateral frontal regions, LGI was declined in the bilateral temporal and left parietal regions for those with atypical antipsychotics ($n = 16$) (**Supplementary Figure 7**). There was no significant difference in the longitudinal LGI changes between the schizotypal subgroup with typical ($n = 6$) and atypical ($n = 8$) antipsychotics.

## Correlation Analysis of Baseline Local Gyrification Index and Cumulative Medication Dosage at Baseline

In the schizophrenia group, baseline LGI was not related to the cumulative medication dosage at baseline.

## Correlation Analysis of Longitudinal Local Gyrification Index Changes and Clinical Variables

In the schizophrenia group, the greater progressive decline in LGI in the right pre- and post-central regions was associated with smaller improvements in negative symptoms (**Figure 3**).

The cumulative medication dosage during follow-up negatively correlated with longitudinal LGI changes in the right superior parietal region in the schizotypal group (**Figure 3**), whereas medication was not associated with longitudinal LGI changes in the schizophrenia group.

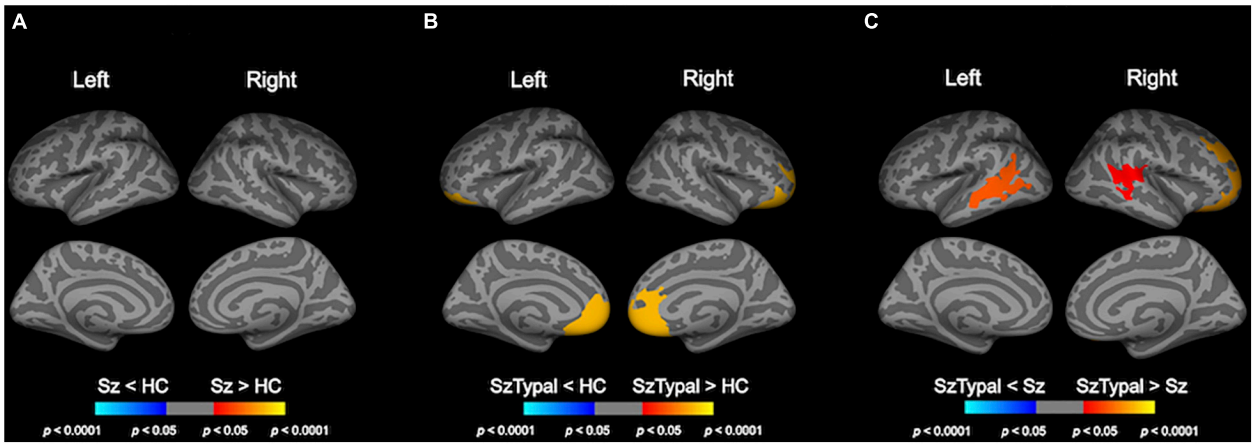


**FIGURE 1 |** Cortical statistical maps of baseline local gyrification index (LGI) comparisons. The schizophrenia (Sz) group showed no significant LGI changes from the healthy control (HC) group **(A)**. LGI in the bilateral superior frontal, medial orbitofrontal, frontal pole, and rostral anterior cingulate regions was higher in the schizotypal (SzTypal) group than in the HC group **(B)**. LGI in the bilateral superior and medial temporal, right superior, and lateral orbitofrontal regions was higher in the SzTypal group than in the Sz group **(C)**.

**TABLE 2 |** Clusters showing significant differences in pairwise group comparisons of longitudinal local gyrification index changes.

| Cluster no. | Cluster size ($mm_2$) | Cluster-wise *p* | MNI coordinates | | | Annotation |
|---|---|---|---|---|---|---|
| | | | x | y | z | |
| **Sz < HC** | | | | | | |
| 1 | 3634.8 | 0.0001 | – 21.3 | 31.3 | 28.4 | Left caudal and rostral middle frontal, pars triangularis, pars opercularis gyrus, insular cortex |
| 2 | 1998.1 | 0.0164 | – 10.8 | 19.5 | 35.8 | Left superior frontal gyrus, caudal and rostral anterior cingulate cortex |
| 3 | 3065.4 | 0.0006 | 55.3 | – 7.0 | – 7.6 | Right superior temporal, precentral, pars opercularis gyrus |
| 4 | 2304 | 0.0097 | 36.4 | – 4.5 | 45.7 | Right precentral, superior frontal, caudal middle frontal gyrus |
| **SzTypal < HC** | | | | | | |
| 5 | 2348.2 | 0.0055 | – 8.6 | 48.7 | 23.9 | Left superior frontal gyrus, rostral middle frontal, medial orbitofrontal cortex, frontal pole |
| **Sz < SzTypal** | | | | | | |
| 6 | 1707.8 | 0.0435 | 43.5 | – 18.8 | 17.9 | Right pre- and postcentral, supramarginal, transverse temporal gyrus |

*HC, healthy controls; Sz, schizophrenia; SzTypal, schizotypal disorder.*

## DISCUSSION

To the best of our knowledge, this is the first MRI study to examine and compare longitudinal changes in brain gyrification in the entire cortex among patients with first-episode schizophrenia, those with schizotypal disorder, and healthy controls. The results obtained demonstrated a greater progressive decline in LGI in the fronto-temporal and parietal regions in the schizophrenia group, but not in the schizotypal group, than in the control group, which was partly associated with smaller improvements in negative symptoms after the first episode of the illness. Among schizophrenia spectrum disorders, these changes appear to reflect active brain changes specifically observed in the early stages of schizophrenia, which are also associated with early treatment responses.

Although the formation of the brain sulcogyral pattern is mostly complete by the late second to third trimester (Armstrong et al., 1995; Zilles et al., 2013), healthy subjects may exhibit mild age-related GI changes after birth; the entire cortical GI increases by approximately 20% in the first 2 years after birth, but slowly decreases thereafter (approximately 1%/year during adolescence) (Raznahan et al., 2011; Cao et al., 2017). Although gyral formation, which is considered to be mediated by genetic factors (Bartley et al., 1997), may reflect pre- and perinatal brain development (including early axonal connections, neuronal growth and differentiation, glial proliferation, and synaptogenesis) (Toro and Burnod, 2005), the mechanisms underlying the decline in GI after birth have not yet been elucidated (Cao et al., 2017). However, age-related cortical flattening (i.e., cortical thinning in combination with a decrease

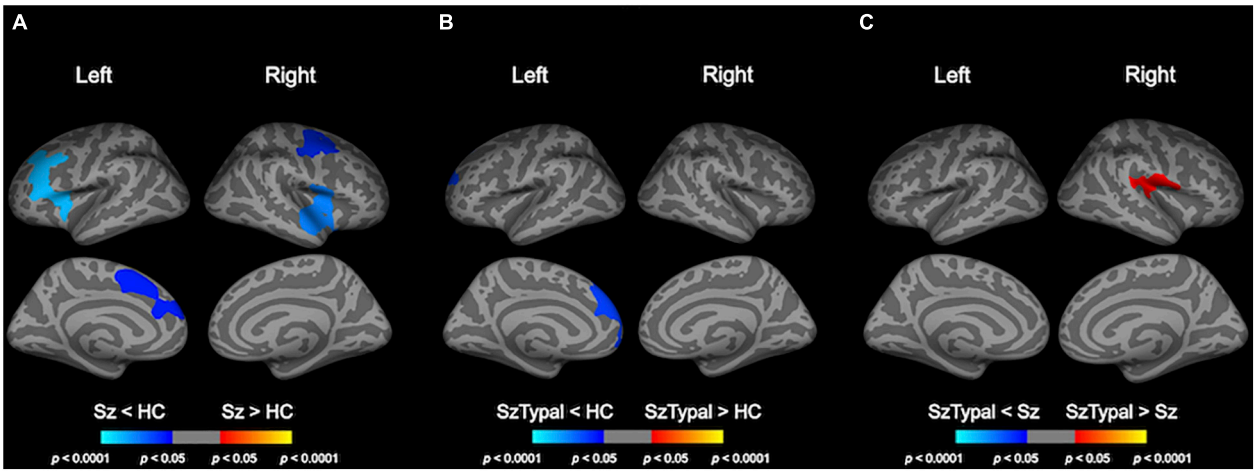


**FIGURE 2 |** Pairwise group comparisons of longitudinal local gyrification index (LGI) changes. Cortical statistical maps showed that the schizophrenia (Sz) group exhibited a significantly greater decline in LGI over time than the healthy control (HC) group in the caudal middle frontal gyrus, superior frontal gyrus, and pars opercularis gyrus bilaterally, in addition to the rostral middle frontal gyrus, pars triangularis gyrus, and caudal anterior cingulate cortex in the left hemisphere, and superior temporal gyrus, precentral gyrus in the right hemisphere **(A)**. The progressive increase in LGI in the left superior frontal area was smaller in the schizotypal (SzTypal) group than in the HC group **(B)**. The decline in LGI in the right pre- and post-central gyrus, supramarginal gyrus, and transverse temporal gyrus was greater in the Sz group than in the SzTypal group **(C)**.

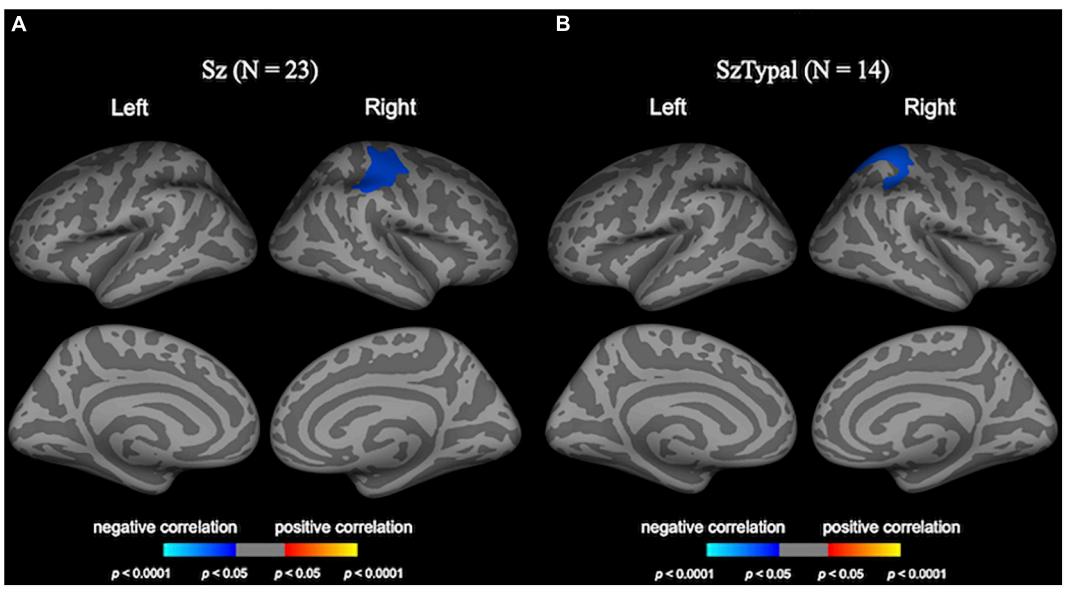


**FIGURE 3 |** Correlation analyses of longitudinal local gyrification index (LGI) changes and clinical variables. Cortical statistical maps revealed the longitudinal LGI reductions in the right pre/post-central regions negatively correlated with changes in negative symptoms in the schizophrenia (Sz) group **(A)**. The longitudinal LGI increase in the right superior parietal region in the schizotypal (SzTypal) group negatively correlated with the cumulative medication dosage during follow-up **(B)**.

in GI) during adolescence may be attributed to synaptic pruning and the effects of the maturation of white matter as a process of late neurodevelopment (Alemán-Gómez et al., 2013). The present finding of no significant longitudinal LGI changes in healthy subjects in early adulthood suggests that this maturation process predominantly occurs at earlier ages and/or gyrification changes after birth are subtle and undetectable in a small sample.

In cross-sectional comparisons, we replicated our previous findings in a larger cohort (Sasabayashi et al., 2020) of schizotypal patients exhibiting an increase in LGI predominantly in the prefrontal regions, which was also reported in the early stages of schizophrenia (Narr et al., 2004; Tepest et al., 2013) as well as in genetic (Falkai et al., 2007; Neilson et al., 2018) and clinical (Tepest et al., 2013; Sasabayashi et al., 2017b) high risk subjects for the development of psychosis. Although

hypergyrification was not detected in the schizophrenia group in the present study, which may have been due to its small sample size, we previously demonstrated a widespread brain hypergyrification pattern in an expanded cohort of first-episode schizophrenia patients ($N$ = 62) (Sasabayashi et al., 2017a). As described above, the brain gyrification pattern in humans largely depends on early neurodevelopmental processes, such as axonal connections and cortical maturation (Zilles et al., 2013). When taken together with previous findings suggesting that altered connectivity in frontal regions was common under specific clinical conditions (e.g., schizotypal, Nakamura et al., 2005; Hazlett et al., 2012, first-episode schizophrenia; Pettersson-Yeo et al., 2011; Li et al., 2017, and genetic and clinical high risk subjects, Shim et al., 2010; Yoon et al., 2015), our cross-sectional observations of frontal hypergyrification in the schizophrenia spectrum indicate that it is a vulnerability factor associated with aberrant early neurodevelopment. Direct comparison between the schizophrenia and schizotypal groups showed a significantly higher LGI in the prefrontal and temporal regions in the schizotypal group, while our previous study in a larger cohort suggested a higher frontal LGI in the schizophrenia than in the schizotypal patients (Sasabayashi et al., 2020). Thus, cross-sectional difference in LGI between these disorders and potential influencing factors (e.g., medication, clinical symptoms) should be further investigated in an independent cohort.

Consistent with previous longitudinal LGI studies including older participants (Palaniyappan et al., 2013a; Nelson et al., 2020), we observed a greater progressive decline in LGI in the first-episode schizophrenia group than in the control group, which may partly explain the discrepant gyrification findings at different stages of schizophrenia (e.g., normal or even hypogyrification in chronic schizophrenia; reviewed by Harris et al., 2007; Nanda et al., 2014). These progressive changes in LGI were specific to the schizophrenia group and were not observed in the schizotypal group, suggesting that the active brain processes associated with the decline in LGI partly explain the neural mechanisms underlying the onset of psychosis. We further demonstrated that lower educational attainment has significant influence on longitudinal LGI changes in schizophrenia, partly supporting the notion that general cognitive impairments reflect core features of schizophrenia which are evident throughout the course of the illness (Ohi et al., 2018). Likewise, a greater LGI decline of the temporo-parietal areas in the schizophrenia group than in the schizotypal group might be partly explained by progressive gray matter reduction of the corresponding regions specific to the schizophrenia patients, which may underlie positive psychotic symptoms (Takahashi et al., 2010). Based on the potential relationship between age-related changes in gyrification and late neurodevelopmental processes (e.g., synaptic pruning and myelination) in healthy subjects (Alemán-Gómez et al., 2013), the present results provide support for the hypothesis that overmaturation during adolescence and young adulthood plays a role in the development of psychosis (Pantelis et al., 2007). However, the functional significance of our longitudinal LGI results warrants further study in combination with other modalities that assess brain function/connectivity (Palaniyappan and Liddle, 2014).

One major result of the present study was the correlation between the decline in LGI in the pre-/post-central region and smaller improvements specifically in negative symptoms during the first episode of schizophrenia, which appears to support a role for functional/connectivity deficits involving this brain region in negative symptomatology in the early stages of schizophrenia (Li et al., 2015; Vanes et al., 2019). This is also consistent with findings by Palaniyappan et al. (2013a,b) showing that a decline in LGI at baseline and longitudinal reductions in LGI in first-episode schizophrenia predicted poor treatment responses and cognitive deficits; however, this relationship was detected at the fronto-insular regions. Interestingly, our previous cross-sectional study suggested LGI decline with illness chronicity in similar brain regions only for the subgroup of schizophrenia who had no persistent negative symptoms (i.e., non-deficit type) (Takayanagi et al., 2019). However, it remains unknown why longitudinal LGI changes after the onset of schizophrenia can contribute to negative but not positive symptomatology. Furthermore, a recent longitudinal study on unmedicated schizophrenia (Nelson et al., 2020) demonstrated that the decline in LGI in the fronto-parietal regions (including the precentral gyrus) was related to a "better" treatment response. As clinical symptoms of schizophrenia can persist only in some cases and can be reversibly altered, the associations of treatment responses with longitudinal LGI changes should be interpreted with caution. In addition, although the exact reasons for these discrepancies remain unclear, potential medication effects may be a contributing factor. Although a relationship was not observed between the longitudinal decline in LGI and medication in the schizophrenia group, the cumulative medication dosage during follow-up in the schizotypal group negatively correlated with changes in LGI in the parietal region. Since the schizophrenia group was previously treated for a substantial period on average at baseline, antipsychotic medication may have affected their symptom severity and LGI changes. Although the lack of longitudinal data of cognitive functioning did not enable us to test the hypothesis, our findings of a progressive LGI decline predominantly in the fronto-temporal regions, corresponding to the language-related regions around the Sylvian fissure, might be implicated in the production and perception of speech. Indeed, individuals with high-risk for psychosis and first-episode/chronic schizophrenia patients were reported to share an impaired verbal fluency with progression according to illness stages (Henry and Crawford, 2005), which may be associated with a decline in the fronto-insular gyrification (Palaniyappan et al., 2013a). Therefore, further studies are needed to clarify the potential factors affecting changes in gyrification during the course of schizophrenia.

There are a number of limitations that need to be addressed. Since a large number of patients withdrew from the clinical follow-up, the sample size of the present study was small. The unequal sample size with very few schizotypal patients would also affect the statistical power for the comparisons across the three groups. The LGI findings in the combined patient group (schizophrenia and schizotypal disorder) were

largely the same as those in schizophrenia, which could be due to small sample size of the schizotypal group. We did not replicate baseline frontal hypergyrification in patients with first-episode schizophrenia (Sasabayashi et al., 2017a) in the present study, which may have been also due to insufficient statistical power. Furthermore, although illness chronicity may affect the gyrification pattern differently depending on the subtypes of schizophrenia (Takayanagi et al., 2019), we were unable to examine this heterogeneity due to the small sample size. Therefore, future longitudinal studies with a larger and well-defined cohort in various illness stages (e.g., before and after the onset of psychosis, chronic stages) are needed to evaluate the changes in gyrification pattern and its linkage with clinical manifestation (e.g., positive or negative symptom change and cognitive decline) during the course of the schizophrenia spectrum. If the LGI findings (especially longitudinal changes at early stages) in schizophrenia spectrum are associated with later illness course (i.e., symptom severity, treatment response, and cognitive deficits), they may have a clinical utility as a predictive marker of outcome. Further, the possibility exists that longitudinal LGI changes may be a target of treatment to prevent illness chronicity, while it is unknown whether early intervention could ameliorate these LGI changes. Another limitation, as described above, is that all patients both in the schizophrenia and schizotypal group had been treated with antipsychotics even at the baseline (median = 3.0 months), which may have biased the results obtained and made it difficult to identify the pathophysiological characteristics of the two groups. Our preliminary results suggested different effects of the type of antipsychotics (typical vs. atypical) on longitudinal LGI changes in schizophrenia, but such effects as well as potential effects of other psychotropic agents (e.g., benzodiazepines, mood stabilizers) should be further tested in a larger cohort. Moreover, since an altered gyrification pattern has been reported in many neuropsychiatric disorders (e.g., mood disorders, Nenadic et al., 2015; Han et al., 2017, and autism spectrum disorder; Kohli et al., 2019), further transdiagnostic comparisons of the trajectories of gyrification are needed to clarify the disease specificity of the present results and their role in the pathophysiology of the schizophrenia spectrum. Lastly, although a multimodal neuroimaging study demonstrated the topographical overlapping between LGI and degree centrality changes (Palaniyappan and Liddle, 2014), it is still elusive whether gyrification patterns implicate connectional characteristics of corresponding regions. Confirming the potential relationship between LGI and functional connectivity measures may be useful for interpreting the present findings.

## CONCLUSION

In conclusion, combined with our previous cross-sectional findings from larger cohorts (Sasabayashi et al., 2017a, 2020), the present results suggest that the brain gyrification pattern in the schizophrenia spectrum reflects both early and late neurodevelopmental pathologies. Increases in LGI predominantly in the prefrontal regions, which were commonly observed in the schizophrenia and schizotypal groups, may represent a static vulnerability factor associated with aberrant early neurodevelopment, whereas the progressive decrease in LGI in the fronto-temporal and parietal regions specifically observed during the first episode of schizophrenia appears to reflect an exaggeration of brain maturation during adolescence.

## DATA AVAILABILITY STATEMENT

The datasets utilized for this article are not available immediately because we do not have permission to share them. Requests to access the datasets should be directed to corresponding author.

## ETHICS STATEMENT

The studies involving human participants were reviewed and approved by the Committee on Medical Ethics of Toyama University. Written informed consent to participate in this study was provided by all participants and the legal guardian/next of kin of participants under 20 years old.

## AUTHOR CONTRIBUTIONS

In this study, MS and TT conceived the idea and design of this study. DS, YT, AF, and MKi recruited subjects and were involved in clinical assessments. TVP and DS preprocessed the MRI data and conducted statistical analyses. MKu and KN provided technical support for MRI scanning and data processing. TVP, DS, TT, and MS interpreted the results. TVP wrote the manuscript. DS, TT, and MS contributed to the writing and editing of the manuscript. All authors contributed to and approved the final manuscript.

## FUNDING

This work was supported by the JSPS KAKENHI (Grant Nos. JP18K15509, JP19H03579, and JP20KK0193 to DS, JP18K07550 to TT, JP18K07549 to YT, and JP20H03598 to MS), the SENSHIN Medical Research Foundation to YT and DS, the Hokuriku Bank Grant-in-Aid for Young Scientists to DS, and by the Health and Labor Sciences Research Grants for Comprehensive Research on Persons with Disabilities from the Japan Agency for Medical Research and Development (AMED) (Grant No. 20dk0307094s0201 to MS).

## SUPPLEMENTARY MATERIAL

The Supplementary Material for this article can be found online at: https://www.frontiersin.org/articles/10.3389/fnagi.2021.752575/full#supplementary-material

## REFERENCES


Alemán-Gómez, Y., Janssen, J., Schnack, H., Balaban, E., Pina-Camacho, L., Alfaro-Almagro, F., et al. (2013). The human cerebral cortex flattens during adolescence. *J. Neurosci.* 33, 15004–15010. doi: 10.1523/JNEUROSCI.1459-13.2013

American Psychiatric Association. (1994). *Diagnostic and Statistical Manual of Mental Disorders*, 4th Edn. Washington, DC: American Psychiatric Association Press.

Andreasen, N. C. (1983). *The Scale for the Assessment of Negative Symptoms (SANS)*. Iowa City, IA: The University of Iowa.

Andreasen, N. C. (1984). *The Scale for the Assessment of Positive Symptoms (SAPS)*. Iowa City, IA: The University of Iowa.

Armstrong, E., Schleicher, A., Omran, H., Curtis, M., and Zilles, K. (1995). The ontogeny of human gyrification. *Cereb. Cortex* 5, 56–63. doi: 10.1093/cercor/5.1.56

Bartley, A. J., Jones, D. W., and Weinberger, D. R. (1997). Genetic variability of human brain size and cortical gyral patterns. *Brain* 120, 257–269. doi: 10.1093/brain/120.2.257

Cao, B., Mwangi, B., Passos, I. C., Wu, M. J., Keser, Z., Zunta-Soares, G. B., et al. (2017). Lifespan gyrification trajectories of human brain in healthy individuals and patients with major psychiatric disorders. *Sci. Rep.* 7:511. doi: 10.1038/s41598-017-00582-1

Falkai, P., Honer, W. G., Kamer, T., Dustert, S., Vogeley, K., Schneider-Axmann, T., et al. (2007). Disturbed frontal gyrification within families affected with schizophrenia. *J. Psychiatr. Res.* 41, 805–813. doi: 10.1016/j.jpsychires.2006.07.018

Fischl, B. (2012). FreeSurfer. *Neuroimage* 62, 774–781. doi: 10.1016/j.neuroimage.2012.01.021

Hagler, D. J. Jr., Saygin, A. P., and Sereno, M. I. (2007). Smoothing and cluster thresholding for cortical surface-based group analysis of fMRI data. *Neuroimage* 33, 1093–1103. doi: 10.1016/j.neuroimage.2006.07.036

Han, K. M., Won, E., Kang, J., Kim, A., Yoon, H. K., Chang, H. S., et al. (2017). Local gyrification index in patients with major depressive disorder and its association with tryptophan hydroxylase-2 (TPH2) polymorphism. *Hum. Brain Mapp.* 38, 1299–1310. doi: 10.1002/hbm.23455

Harris, J. M., Moorhead, T. W., Miller, P., McIntosh, A. M., Bonnici, H. M., Owens, D. G., et al. (2007). Increased prefrontal gyrification in a large high-risk cohort characterizes those who develop schizophrenia and reflects abnormal prefrontal development. *Biol. Psychiatry* 62, 722–729. doi: 10.1016/j.biopsych.2006.11.027

Haukvik, U. K., Schaer, M., Nesvag, R., McNeil, T., Hartberg, C. B., Jonsson, E. G., et al. (2012). Cortical folding in Broca's area relates to obstetric complications in schizophrenia patients and healthy controls. *Psychol. Med.* 42, 1329–1337. doi: 10.1017/S0033291711002315

Hazlett, E. A., Collazo, T., Zelmanova, Y., Entis, J. J., Chu, K. W., Goldstein, K. E., et al. (2012). Anterior limb of the internal capsule in schizotypal personality disorder: Fiber-tract counting, volume, and anisotropy. *Schizophr. Res.* 141, 119–127. doi: 10.1016/j.schres.2012.08.022

Henry, J. D., and Crawford, J. R. (2005). A meta-analytic review of verbal fluency deficits in schizophrenia relative to other neurocognitive deficits. *Cogn. Neuropsychiatry* 10, 1–33. doi: 10.1080/13546800344000309

Kohli, J. S., Kinnear, M. K., Fong, C. H., Fishman, I., Carper, R. A., and Müller, R. A. (2019). Local cortical gyrification is increased in children with autism spectrum disorders, but decreases rapidly in adolescents. *Cereb. Cortex* 29, 2412–2423. doi: 10.1093/cercor/bhy111

Li, H. J., Xu, Y., Zhang, K. R., Hoptman, M. J., and Zuo, X. N. (2015). Homotopic connectivity in drug-naive, first-episode, early-onset schizophrenia. *J. Child Psychol. Psychiatry* 56, 432–443. doi: 10.1111/jcpp.12307

Li, T., Wang, Q., Zhang, J., Rolls, E. T., Yang, W., Palaniyappan, L., et al. (2017). Brain-wide analysis of functional connectivity in first-episode and chronic stages of schizophrenia. *Schizophr. Bull.* 43, 436–448. doi: 10.1093/schbul/sbw099

Nakamura, M., McCarley, R. W., Kubicki, M., Dickey, C. C., Niznikiewicz, M. A., Voglmaier, M. M., et al. (2005). Fronto-temporal disconnectivity in schizotypal personality disorder: a diffusion tensor imaging study. *Biol. Psychiatry* 58, 468–478. doi: 10.1016/j.biopsych.2005.04.016

Nanda, P., Tandon, N., Mathew, I. T., Giakoumatos, C. I., Abhishekh, H. A., Clementz, B. A., et al. (2014). Local gyrification index in probands with psychotic disorders and their first-degree relatives. *Biol. Psychiatry* 76, 447–455. doi: 10.1016/j.biopsych.2013.11.018

Narr, K. L., Bilder, R. M., Kim, S., Thompson, P. M., Szeszko, P., Robinson, D., et al. (2004). Abnormal gyral complexity in first-episode schizophrenia. *Biol. Psychiatry* 55, 859–867. doi: 10.1016/j.biopsych.2003.12.027

Neilson, E., Bois, C., Clarke, T. K., Hall, L., Johnstone, E. C., Owens, D. G. C., et al. (2018). Polygenic risk for schizophrenia, transition and cortical gyrification: a high-risk study. *Psychol. Med.* 48, 1532–1539. doi: 10.1017/S0033291717003087

Nelson, E. A., Kraguljac, N. V., White, D. M., Jindal, R. D., Shin, A. L., and Lahti, A. C. (2020). A prospective longitudinal investigation of cortical thickness and gyrification in schizophrenia. *Can. J. Psychiatry* 65, 381–391. doi: 10.1177/0706743720904598

Nenadic, I., Maitra, R., Dietzek, M., Langbein, K., Smesny, S., Sauer, H., et al. (2015). Prefrontal gyrification in psychotic bipolar I disorder vs. schizophrenia. *J. Affect. Disord.* 185, 104–107. doi: 10.1016/j.jad.2015.06.014

Nesvåg, R., Schaer, M., Haukvik, U. K., Westlye, L. T., Rimol, L. M., Lange, E. H., et al. (2014). Reduced brain cortical folding in schizophrenia revealed in two independent samples. *Schizophr. Res.* 152, 333–338. doi: 10.1016/j.schres.2013.11.032

Ohi, K., Sumiyoshi, C., Fujino, H., Yasuda, Y., Yamamori, H., Fujimoto, M., et al. (2018). Genetic overlap between general cognitive function and schizophrenia: a review of cognitive GWASs. *Int. J. Mol. Sci.* 19:3822. doi: 10.3390/ijms19123822

Palaniyappan, L., Crow, T. J., Hough, M., Voets, N. L., Liddle, P. F., James, S., et al. (2013a). Gyrification of broca's region is anomalously lateralized at onset of schizophrenia in adolescence and regresses at 2 year follow-up. *Schizophr. Res.* 147, 39–45. doi: 10.1016/j.schres.2013.03.028

Palaniyappan, L., and Liddle, P. F. (2014). Diagnostic discontinuity in psychosis: a combined study of cortical gyrification and functional connectivity. *Schizophr. Bull.* 40, 675–684. doi: 10.1093/schbul/sbt050

Palaniyappan, L., Marques, T. R., Taylor, H., Handley, R., Mondelli, V., Bonaccorso, S., et al. (2013b). Cortical folding defects as markers of poor treatment response in first-episode psychosis. *JAMA Psychiatry* 70, 1031–1040. doi: 10.1001/jamapsychiatry.2013.203

Pantelis, C., Velakoulis, D., Wood, S. J., Yücel, M., Yung, A. R., Phillips, L. J., et al. (2007). Neuroimaging and emerging psychotic disorders: the Melbourne ultra-high risk studies. *Int. Rev. Psychiatry* 19, 371–381. doi: 10.1080/09540260701512079

Pettersson-Yeo, W., Allen, P., Benetti, S., McGuire, P., and Mechelli, A. (2011). Dysconnectivity in schizophrenia: where are we now? *Neurosci. Biobehav. Rev.* 35, 1110–1124. doi: 10.1016/j.neubiorev.2010.11.004

Raznahan, A., Shaw, P., Lalonde, F., Stockman, M., Wallace, G. L., Greenstein, D., et al. (2011). How does your cortex grow? *J. Neurosci.* 31, 7174–7177. doi: 10.1523/JNEUROSCI.0054-11.2011

Reuter, M., and Fischl, B. (2011). Avoiding asymmetry-induced bias in longitudinal image processing. *Neuroimage* 57, 19–21. doi: 10.1016/j.neuroimage.2011.02.076

Reuter, M., Rosas, H. D., and Fischl, B. (2010). Highly accurate inverse consistent registration: a robust approach. *Neuroimage* 53, 1181–1196. doi: 10.1016/j.neuroimage.2010.07.020

Reuter, M., Schmansky, N. J., Rosas, H. D., and Fischl, B. (2012). Within-subject template estimation for unbiased longitudinal image analysis. *Neuroimage* 61, 1402–1418. doi: 10.1016/j.neuroimage.2012.02.084

Sallet, P. C., Elkis, H., Alves, T. M., Oliveira, J. R., Sassi, E., Campi de Castro, C., et al. (2003). Reduced cortical folding in schizophrenia: an MRI morphometric study. *Am. J. Psychiatry* 160, 1606–1613. doi: 10.1176/appi.ajp.160.9.1606

Sasabayashi, D., Takahashi, T., Takayanagi, Y., and Suzuki, M. (2021). Anomalous brain gyrification patterns in major psychiatric disorders: A systematic review and trans-diagnostic integration. *Transl. Psychiatry* 11:176. doi: 10.1038/s41398-021-01297-8

Sasabayashi, D., Takayanagi, Y., Nishiyama, S., Takahashi, T., Furuichi, A., Kido, M., et al. (2017a). Increased frontal gyrification negatively correlates with executive function in patients with first-episode schizophrenia. *Cereb. Cortex* 27, 2686–2694. doi: 10.1093/cercor/bhw101

Sasabayashi, D., Takayanagi, Y., Takahashi, T., Koike, S., Yamasue, H., Katagiri, N., et al. (2017b). Increased occipital gyrification and development of psychotic disorders in individuals with an at-risk mental state: a multicenter study. *Biol. Psychiatry* 82, 737–745. doi: 10.1016/j.biopsych.2017.05.018

Sasabayashi, D., Takayanagi, Y., Takahashi, T., Nemoto, K., Furuichi, A., Kido, M., et al. (2020). Increased brain gyrification in the schizophrenia spectrum. *Psychiatry Clin. Neurosci.* 74, 70–76. doi: 10.1111/pcn.12939

Schaer, M., Cuadra, M. B., Tamarit, L., Lazeyras, F., Eliez, S., and Thiran, J. P. (2008). A surface-based approach to quantify local cortical gyrification. *IEEE Trans. Med. Imaging* 27, 161–170. doi: 10.1109/TMI.2007.903576

Schultz, C. C., Wagner, G., Koch, K., Gaser, C., Roebel, M., Schachtzabel, C., et al. (2013). The visual cortex in schizophrenia: alterations of gyrification rather than cortical thickness—a combined cortical shape analysis. *Brain Struct. Funct.* 218, 51–58. doi: 10.1007/s00429-011-0374-1

Shim, G., Oh, J. S., Jung, W. H., Jang, J. H., Choi, C. H., Kim, E., et al. (2010). Altered resting-state connectivity in subjects at ultra-high risk for psychosis: an fMRI study. *Behav. Brain Funct.* 6:58. doi: 10.1186/1744-9081-6-58

Siever, L. J., and Davis, K. L. (2004). The pathophysiology of schizophrenia disorders: perspective from the spectrum. *Am. J. Psychiatry* 161, 398–413. doi: 10.1176/appi.ajp.161.3.398

Suzuki, M., Zhou, S. Y., Takahashi, T., Hagino, H., Kawasaki, Y., Niu, L., et al. (2005). Differential contributions of prefrontal and temporolimbic pathology to mechanisms of psychosis. *Brain* 128, 2109–2122. doi: 10.1093/brain/awh554

Takahashi, T., and Suzuki, M. (2018). Brain morphologic changes in early stages of psychosis: implications for clinical application and early intervention. *Psychiatry Clin. Neurosci.* 72, 556–571. doi: 10.1111/pcn.12670

Takahashi, T., Suzuki, M., Zhou, S. Y., Tanino, R., Nakamura, K., Kawasaki, Y., et al. (2010). A follow-up MRI study of the superior temporal subregions in schizotypal disorder and first-episode schizophrenia. *Schizophr. Res.* 119, 65–74. doi: 10.1016/j.schres.2009.12.006

Takayanagi, Y., Sasabayashi, D., Takahashi, T., Komori, Y., Furuichi, A., Kido, M., et al. (2019). Altered brain gyrification in deficit and non-deficit schizophrenia. *Psychol. Med.* 49, 573–580. doi: 10.1017/S0033291718001228

Tepest, R., Schwarzbach, C. J., Krug, B., Klosterkötter, J., Ruhrmann, S., and Vogeley, K. (2013). Morphometry of structural disconnectivity indicators in subjects at risk and in age-matched patients with schizophrenia. *Eur. Arch. Psychiatry Clin. Neurosci.* 263, 15–24. doi: 10.1007/s00406-012-0343-6

Tomelleri, L., Jogia, J., Perlini, C., Bellani, M., Ferro, A., Rambaldelli, G., et al. (2009). Brain structural changes associated with chronicity and antipsychotic treatment in schizophrenia. *Eur. Neuropsychopharmacol.* 19, 835–840. doi: 10.1016/j.euroneuro.2009.07.007

Toro, R., and Burnod, Y. (2005). A morphogenetic model for the development of cortical convolutions. *Cereb. Cortex* 15, 1900–1913. doi: 10.1093/cercor/bhi068

Vanes, L. D., Mouchlianitis, E., Patel, K., Barry, E., Wong, K., Thomas, M., et al. (2019). Neural correlates of positive and negative symptoms through the illness course: an fMRI study in early psychosis and chronic schizophrenia. *Sci. Rep.* 9:14444. doi: 10.1038/s41598-019-51023-0

World Health Organization. (1993). *The ICD-10 Classification of Mental and Behavioural Disorders: Diagnostic Criteria for Research*. Geneva: World Health Organization.

Yoon, Y. B., Yun, J. Y., Jung, W. H., Cho, K. I., Kim, S. N., Lee, T. Y., et al. (2015). Altered fronto-temporal functional connectivity in individuals at ultra-high-risk of developing psychosis. *PLoS One* 10:e0135347. doi: 10.1371/journal.pone.0135347

Zilles, K., Palomero-Gallagher, N., and Amunts, K. (2013). Development of cortical folding during evolution and ontogeny. *Trends Neurosci.* 36, 275–284. doi: 10.1016/j.tins.2013.01.006

**Conflict of Interest:** The authors declare that the research was conducted in the absence of any commercial or financial relationships that could be construed as a potential conflict of interest.

**Publisher's Note:** All claims expressed in this article are solely those of the authors and do not necessarily represent those of their affiliated organizations, or those of the publisher, the editors and the reviewers. Any product that may be evaluated in this article, or claim that may be made by its manufacturer, is not guaranteed or endorsed by the publisher.

frontiers in Aging Neuroscience

ORIGINAL RESEARCH
published: 10 January 2022
doi: 10.3389/fnagi.2021.809853

# Age-Related Decrease in Default-Mode Network Functional Connectivity Is Accelerated in Patients With Major Depressive Disorder

*Shixiong Tang[1,2†], Zhipeng Wu[3†], Hengyi Cao[4,5], Xudong Chen[3], Guowei Wu[3], Wenjian Tan[3], Dayi Liu[3], Jie Yang[3], Yicheng Long[3]* and Zhening Liu[3]*

[1] Department of Radiology, The Second Xiangya Hospital, Central South University, Changsha, China, [2] Clinical Research Center for Medical Imaging in Hunan Province, Changsha, China, [3] National Clinical Research Center for Mental Disorders, and Department of Psychiatry, The Second Xiangya Hospital, Central South University, Changsha, China, [4] Center for Psychiatric Neuroscience, Feinstein Institute for Medical Research, Manhasset, NY, United States, [5] Division of Psychiatry Research, Zucker Hillside Hospital, Glen Oaks, NY, United States

Major depressive disorder (MDD) is a common psychiatric disorder which is associated with an accelerated biological aging. However, little is known whether such process would be reflected by a more rapid aging of the brain function. In this study, we tested the hypothesis that MDD would be characterized by accelerated aging of the brain's default-mode network (DMN) functions. Resting-state functional magnetic resonance imaging data of 971 MDD patients and 902 healthy controls (HCs) was analyzed, which was drawn from a publicly accessible, multicenter dataset in China. Strength of functional connectivity (FC) and temporal variability of dynamic functional connectivity (dFC) within the DMN were calculated. Age-related effects on FC/dFC were estimated by linear regression models with age, diagnosis, and diagnosis-by-age interaction as variables of interest, controlling for sex, education, site, and head motion effects. The regression models revealed (1) a significant main effect of age in the predictions of both FC strength and dFC variability; and (2) a significant main effect of diagnosis and a significant diagnosis-by-age interaction in the prediction of FC strength, which was driven by stronger negative correlation between age and FC strength in MDD patients. Our results suggest that (1) both healthy participants and MDD patients experience decrease in DMN FC strength and increase in DMN dFC variability along age; and (2) age-related decrease in DMN FC strength may occur at a faster rate in MDD patients than in HCs. However, further longitudinal studies are still needed to understand the causation between MDD and accelerated aging of brain.

**Keywords: major depressive disorder, aging, fMRI, functional connectivity, dynamic functional connectivity (dFC), dynamic brain network**

OPEN ACCESS

***Edited by:***
*Wenjing Zhang,*
*Sichuan University, China*

***Reviewed by:***
*Nicola Filippini,*
*University of Oxford, United Kingdom*
*Olga V. Martynova,*
*Institute of Higher Nervous Activity and Neurophysiology, Russian Academy of Sciences (RAS), Russia*
*Joan Guàrdia-Olmos,*
*University of Barcelona, Spain*

****Correspondence:***
*Yicheng Long*
*yichenglong@csu.edu.cn*

*† These authors have contributed equally to this work*

***Specialty section:***
*This article was submitted to Neurocognitive Aging and Behavior, a section of the journal Frontiers in Aging Neuroscience*

***Received:*** *05 November 2021*
***Accepted:*** *20 December 2021*
***Published:*** *10 January 2022*

***Citation:***
*Tang S, Wu Z, Cao H, Chen X, Wu G, Tan W, Liu D, Yang J, Long Y and Liu Z (2022) Age-Related Decrease in Default-Mode Network Functional Connectivity Is Accelerated in Patients With Major Depressive Disorder. Front. Aging Neurosci. 13:809853. doi: 10.3389/fnagi.2021.809853*

## INTRODUCTION

Major depressive disorder (MDD), one of the most common serious psychiatric disorders worldwide, is associated with increased risks of many biological and physiological pathologies such as dementia/cognitive decline (Byers and Yaffe, 2011; Holmquist et al., 2020), cardiovascular disease (Gan et al., 2014), and osteoporosis (Cizza et al., 2009) which occur in the process of normal aging. Accordingly, there are growing evidences suggesting that MDD leads to an accelerated biological aging as revealed by biochemical (Wolkowitz et al., 2011; Levada and Troyan, 2020), genetic (Simon et al., 2006; Protsenko et al., 2021), and neuroimaging (Sacchet et al., 2017; Cheng et al., 2020; Dunlop et al., 2021) characteristics. For instance, it was found that MDD patients are significantly older (with a median gap of 2 years) than their chronological age based on predictable age-related patterns of DNA methylation (Protsenko et al., 2021). Structural neuroimaging studies have also reported that age-related reductions in the brain cortical thickness (Cheng et al., 2020) and putamen volumes (Sacchet et al., 2017) are accelerated in MDD.

Apart from the above mentioned biochemical, genetic, and brain structural alterations, MDD is characterized by abnormal brain function that can be shown by functional magnetic resonance imaging (fMRI) (Mulders et al., 2015; Zhang K. et al., 2016; Zanatta et al., 2019). In previous fMRI studies, the most prominent and frequently reported findings in MDD are altered resting-state functional connectivity (FC) patterns within the default-mode network (DMN) areas (Mulders et al., 2015; Zhang K. et al., 2016; Zanatta et al., 2019; Shi et al., 2021). Such alterations include both reduced FC strengths (Chen et al., 2015; | Yan et al., 2019; Shi et al., 2020) as well as decreased temporal stability of dynamic functional connectivity (dFC) based on the recent assumption that FC patterns fluctuate over time (Wise et al., 2017; Long et al., 2020a). Interestingly, these alterations have been also associated with the process of normal aging: several previous studies have consistently reported that older age is related to decreased FC strength (Bluhm et al., 2008; Mevel et al., 2013; Vidal-Piñeiro et al., 2014; Park et al., 2017; Staffaroni et al., 2018) and increased dFC variability (Qin et al., 2015; Marusak et al., 2017; Park et al., 2017) within the DMN. Such similarities bring up the possibility that accelerated biological aging in MDD may be reflected by FC strength and dFC variability within the DMN, which has not been well examined to our knowledge. Thus, characterizing the trajectories of age-related changes in FC strength/dFC variability within the DMN may both facilitate the mechanistic understanding of MDD, as well as the development of specific treatment strategies to prevent deteriorated progression in MDD.

In the present study, we therefore investigated whether MDD would be characterized by accelerated aging of brain function in terms of FC/dFC features within the DMN. Specifically, we assessed the MDD diagnosis-by-age interactions on FC strength and dFC variability within the DMN based on the previously mentioned literatures. In order to increase the statistical power and reliability of the results, we used a large, multicenter fMRI dataset of MDD patients and healthy controls (HCs). We hypothesized that (1) age-related decreases in FC strength and increases in temporal variability of dFC within the DMN would be observed in both the MDD and healthy participants; and (2) such processes might be accelerated in MDD as reflected by significant diagnosis-by-age interactions, which are driven by stronger associations between age and FC/dFC measures in patients with MDD.

## MATERIALS AND METHODS

### Participants

The final analyzed sample in this study consisted of 971 MDD patients and 902 healthy participants from 20 study centers, which was a part of the REST-meta-MDD Consortium in China.[1] All patients were diagnosed as MDD based on the International Statistical Classification of Diseases, 10th Revision (ICD-10) or Diagnostic and Statistical Manual of Mental Disorders-IV (DSM-IV) criteria. Such a sample was drawn from the original 1300 MDD patients and 1128 HCs in the REST-meta-MDD dataset by excluding the subjects who met the following exclusion criteria: (1) $<$18 years of age; (2) demographic information such as age is incomplete; (3) fMRI scanning repetition time $\neq$2 s (to reduce biases caused by different temporal resolutions when constructing dynamic brain networks); (4) poor image quality or inaccurate spatial normalization determined by manual checking; (5) excessive head motion with framewise-displacement (FD) $>$0.2 mm; (6) bad mask coverage with signal loss in any region of interest (ROI). The data was anonymously contributed from studies which were approved by local Institutional Review Boards in each center, and written informed consent were obtained from all participants from the local institutions.

Among the analyzed 971 patients with MDD, there were 364 first-episode and 234 recurrent MDD patients, while the episodicity (first or recurrent) was unavailable for the other 373 patients. The 17-item Hamilton Depression Rating Scale (HAMD) and Hamilton Anxiety Scale (HAMA) scores were available for 813 and 561 patients, respectively. See **Tables 1**, **2** for sample details. More details of the REST-meta-MDD Consortium can be also found in previous publications (Yan et al., 2019; Liang et al., 2020; Long et al., 2020a; Ding et al., 2021; Liu et al., 2021; Yang et al., 2021).

### Imaging Data Acquisition and Preprocessing

All imaging data (including resting-state fMRI and T1-weighted structural images) was required at each center of the REST-meta-MDD Consortium (see **Table 1** for key scanning parameters). Data was preprocessed in each center locally with a standardized pipeline to obtain ROI-based fMRI time series. The raw imaging data was not shared to protect participant privacy based on the policy of REST-meta-MDD Consortium (Yan et al., 2019). The preprocessing pipeline was performed using the DPARSF software[2] (Chao-Gan and Yu-Feng, 2010; Yan et al., 2016) whose details can be found in previous published studies (Yan et al., 2019; Long et al., 2020a). Briefly, it includes removing the

[1]http://rfmri.org/REST-meta-MDD

[2]http://rfmri.org/DPARSF

**TABLE 1 |** The sample size and key data acquisition parameters of each site included in this study.

| Site serial number[a] | Samples | | Scanner | Repetition time (ms) | Echo time (ms) | Flip angle (°) | Slice number | Time points |
|---|---|---|---|---|---|---|---|---|
| | MDD | HCs | | | | | | |
| 1 | 71 | 71 | Siemens 3T | 2000 | 30 | 90 | 30 | 210 |
| 2 | 29 | 26 | Philips 3T | 2000 | 30 | 90 | 37 | 200 |
| 3 | 24 | 33 | Siemens 3T | 2000 | 40 | 90 | 26 | 150 |
| 6 | 13 | 15 | Siemens 3T | 2000 | 30 | 70 | 33 | 180 |
| 7 | 32 | 40 | GE 3T | 2000 | 30 | 90 | 37 | 184 |
| 8 | 43 | 51 | GE 3T | 2000 | 30 | 90 | 35 | 200 |
| 9 | 47 | 48 | GE 3T | 2000 | 25 | 90 | 35 | 200 |
| 10 | 28 | 11 | Siemens 3T | 2000 | 30 | 90 | 32 | 240 |
| 11 | 28 | 27 | GE 3T | 2000 | 30 | 90 | 33 | 200 |
| 12 | 31 | 4 | GE 3T | 2000 | 30 | 90 | 33 | 240 |
| 15 | 40 | 48 | Siemens 3T | 2000 | 25 | 90 | 36 | 240 |
| 16 | 28 | 29 | GE 3T | 2000 | 30 | 90 | 30 | 200 |
| 17 | 36 | 38 | GE 3T | 2000 | 40 | 90 | 33 | 240 |
| 18 | 20 | 18 | Philips 3T | 2000 | 35 | 90 | 24 | 200 |
| 20 | 265 | 241 | Siemens 3T | 2000 | 30 | 90 | 32 | 242 |
| 21 | 81 | 65 | Siemens 3T | 2000 | 30 | 90 | 33 | 240 |
| 22 | 22 | 20 | Philips 3T | 2000 | 30 | 90 | 36 | 250 |
| 23 | 27 | 29 | Philips 3T | 2000 | 30 | 90 | 38 | 240 |
| 24 | 24 | 28 | GE 1.5T | 2000 | 40 | 90 | 24 | 160 |
| 25 | 82 | 60 | Siemens 3T | 2000 | 25 | 90 | 36 | 240 |

[a]*The sample was drawn from data of the original 25 sites in the REST-meta-MDD project. More details about each site (affiliations and principal investigators) can be found at: http://rfmri.org/REST-meta-MDD.*

first 10 volumes, slice timing, motion realignment, brain tissue segmentation, spatial normalization, temporal filtering (0.01–0.10 Hz), and nuisance (including white matter, cerebrospinal fluid, and whole brain signals) regression. After preprocessing, the images were manually checked by trained researchers to ensure the quality. Data with unsatisfied quality was excluded based on the criteria above in section "Participants."

## Functional Connectivity Strength and Dynamic Functional Connectivity Variability Within Default-Mode Network

The steps of calculating DMN FC strength and dFC variability are summarized below and also shown in **Figure 1**. After preprocessing, mean time series were firstly extracted from 58 DMN ROIs defined based on the Power functional atlas (Power et al., 2011; Cole et al., 2013). The ROIs were visualized in **Figure 2** using Brainnet viewer (Xia et al., 2013) and their coordinates can be found elsewhere (Long et al., 2019).

**TABLE 2 |** Comparisons on demographic/characteristics between the MDD and HC groups.

| | MDD ($n$ = 971), mean ± SD | HCs ($n$ = 902), mean ± SD | Group comparisons |
|---|---|---|---|
| Age (years) | 37.43 ± 14.80 | 36.88 ± 16.15 | $t$ = 0.759, $p$ = 0.448 |
| Sex (male/female) | 344/627 | 368/534 | $\chi^2$ = 5.724, $p$ = 0.017 |
| Education (years) | 11.43 ± 4.09 | 12.47 ± 4.90 | $t$ = −4.996, $p$ < 0.001 |
| Mean FD (mm) | 0.07 ± 0.03 | 0.07 ± 0.04 | $t$ = −1.075, $p$ = 0.282 |
| Illness duration (months)[a] | 38.54 ± 60.64 | / | / |
| HAMD score[a] | 20.63 ± 7.83 | / | / |
| HAMA score[a] | 19.43 ± 8.90 | / | / |

[a]*Data on duration of illness, HAMD score and HAMA score was available for 747, 813, and 561 patients, respectively.*

To calculated FC strength within the DMN, the weighted adjacency FC matrices were computed for each participant. In the matrices, FC strengths between all possible ($N = 58 \times 57/2 = 1653$ here) ROI pairs were estimated by Pearson's correlation coefficients between fMRI time series. In line with previous work (Yan et al., 2019), the average FC values between all possible ROI pairs within the DMN was then defined as within-DMN FC strength.

To calculate temporal variability of dFC, a widely used sliding-windows approach (Long et al., 2020a; Huang D. et al., 2021; Huang X. et al., 2021) was applied to segment the time series of all ROIs into a number of continuous time windows; in the primary analyses, a window width of 100 s and a step length of 6 s were used according to previous recommendations (Sun et al., 2019; Long et al., 2020a). The same as static FC, weighted adjacency matrices were computed in each time window to represent dFC during different time periods. Average dFC variability within the DMN was estimated by averaging the dissimilarities of dFC profiles across different time windows. Briefly, node-wise temporal variability of dFC for a ROI $k$ ($V_k$) was firstly computed as

$$V_k = 1 - \overline{\text{corrcoef}\left(F(i,k), F(j,k)\right)}, i, j = 1, 2, 3, \ldots, T; i \neq j,$$

where $T$ is the total number of time windows depending on fMRI scanning length, $F(i, k)$ is the vector characterizing dFC between

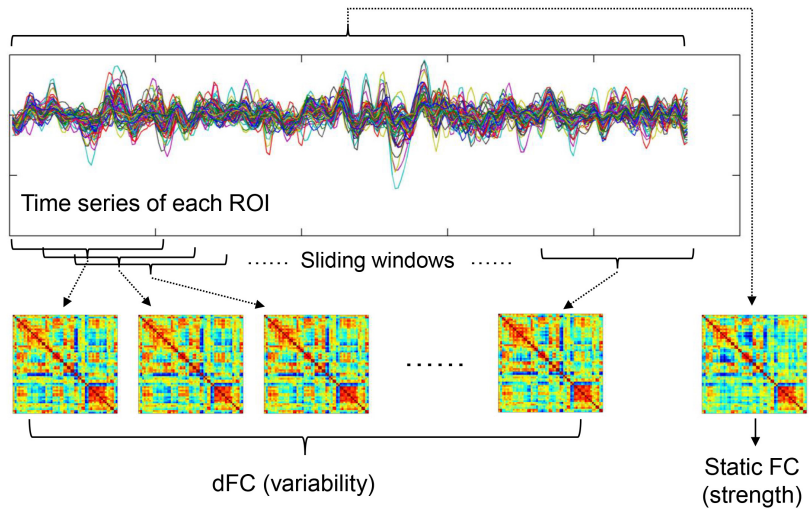


**FIGURE 1 |** A summary of how to calculate static FC strength and dFC variability (refer to section "Functional Connectivity Strength and Dynamic Functional Connectivity Variability Within Default-Mode Network" for details).

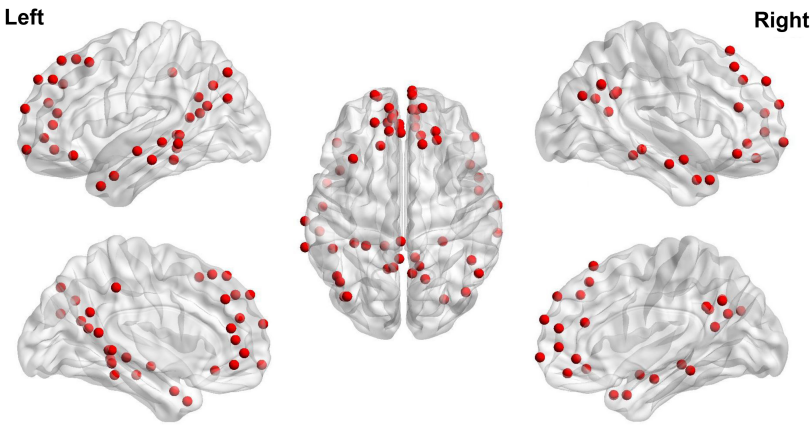


**FIGURE 2 |** Regions of interest used to define the DMN based on Power et al. (2011).

ROI *k* and all other DMN ROIs within the *i*th time window, and "corrcoef" means correlation coefficients. Temporal variability of dFC for the whole DMN ($V$) was then calculated by averaging $V_k$ of all ROIs within the DMN as

$$V = \frac{\sum_k V_k}{N},$$

where $N$ is equal to 58 here. More details about such methods can be found in prior studies (Zhang J. et al., 2016; Dong et al., 2019; Long et al., 2020a,b).

## Assessing Diagnosis by Age Effects

Referring to a number of published work (Wright et al., 2014; Sheffield et al., 2016; Sacchet et al., 2017; van Velzen et al., 2020), linear regression analyses were performed to assess the MDD diagnosis by age interactions, with diagnosis (MDD = 0 vs. HCs = 1), age, and diagnosis × age interaction as variables of interest in the prediction of FC/dFC measures, as well as sex, education level, site (as dummy variables), and head motion (mean FD) as covariates (~intercept + diagnosis + age + diagnosis × age + sex+education + site + head motion). Note that here, "site" was included as a covariate to exclude potential effects of differences in fMRI scanning parameters and in the proportions of patients/controls enrolled by each site. Associations between age and FC/dFC measures in each group were further estimated by Pearson correlation coefficients and compared between groups using an online tool, cocor[3] (Diedenhofen and Musch, 2015), utilizing the function of "comparing correlation coefficients in independent groups" in cocor which is based on procedures provided by Meng et al. (1992) and Zou (2007). All other statistical analyses (except the comparisons between correlation coefficients) were completed in SPSS v22.

[3]http://comparingcorrelations.org/

## Associations With Clinical Characteristics

Several additional analyses were performed to assess the possible associations between DMN FC/dFC and clinical characteristics. First, to investigate possible associations between the DMN FC/dFC and illness duration/HAMD scores/HAMA scores, partial Pearson correlations were calculated between them in patients whose corresponding information are available, after controlling for age, sex, education, site, and head motion. Second, to investigate if DMN FC/dFC patterns would differ by episodicity (first or recurrent), they were compared between the first-episode and recurrent patients using ANCOVA with covariates of age, sex, education, site, and head motion.

## Validation Analysis

Several supplementary analyses were performed to validate our results. Firstly, in dFC studies, there remain debates about the optimal window width and step length in constructing dynamic brain networks (Qin et al., 2015; Zhang et al., 2018; Savva et al., 2020). Therefore, we repeated the analyses on DMN dFC using a range of different window widths (80/100/120 s) and step lengths (6/8/10 s) to see if the results would be changed. Secondly, we repeated the analyses with Fisher's *r*-to-*z* transformations on Pearson's correlation coefficients in all FC/dFC matrices, which were not performed in the main analyses. Thirdly, when dealing with regression analyses, heteroscedasticity is a common problem that may reduce the precision of model (Rosopa et al., 2013). Therefore, we tested the heteroscedasticity of each regression model and when there is a significant heteroscedasticity, we mitigated possible effects of heteroscedasticity by applying a logarithmic transformation to the dependent variable (calculating the natural logarithm) as suggested (Rosopa et al., 2013).

# RESULTS

## Sample Characteristics

Demographic and clinical characteristics of the MDD and HC groups are summarized in **Table 2**. There were no significant differences in age and head motion between the MDD and HC groups (both $p > 0.05$). The MDD group had a higher proportion of females ($\chi^2 = 5.724$, $p = 0.017$) and a significantly lower education level ($t = -4.996$, $p < 0.001$) than HCs.

## Linear Regression Results

The linear regression model revealed a significant main effect of age ($\beta = -0.182$, $t = -6.115$, $p < 0.001$) in the prediction of DMN FC strength, suggesting that both MDD patients and HCs experienced a similar reduction in DMN FC with age. Moreover, the model revealed a significant main effect of diagnosis ($\beta = 0.074$, $t = 3.631$, $p < 0.001$), suggesting a lower DMN FC in MDD patients; and a significant diagnosis × age interaction ($\beta = 0.047$, $t = 2.334$, $p = 0.020$) which was driven by a significantly stronger negative correlation ($z = -2.183$, $p = 0.029$) between age and DMN FC strength in MDD patients than in HCs (**Table 3** and **Figure 3A**). Taken together, although the strength of DMN FC decreased with age in both the MDD and HC groups, such reduction may occurr at a faster rate in MDD patients. Additionally, a significant effect of sex ($\beta = 0.061$, $t = 3.030$, $p = 0.002$) was found in the model, which suggests a higher DMN FC strength in females than males.

As for DMN dFC, the linear regression model revealed a significant main effect of age ($\beta = 0.086$, $t = 3.722$, $p < 0.001$) in the prediction of dFC variability, suggesting that both MDD patients and HCs experienced a similar increase in DMN dFC variability with age. However, the model revealed no significant main effect of diagnosis ($\beta = -0.017$, $t = -1.046$, $p = 0.296$) and no significant diagnosis × age interaction ($\beta = -0.030$, $t = -1.298$, $p = 0.054$), with no between-group difference in the correlation between age and DMN dFC variability ($z = 1.043$, $p = 0.297$) (**Table 3** and **Figure 3B**). Additionally, a significant effect of sex ($\beta = -0.047$, $t = -2.894$, $p = 0.003$) was found in the model, which suggests a lower DMN dFC variability in females than males.

## Associations With Clinical Characteristics

No significant correlations were found between the DMN FC/dFC and illness duration/HAMD scores/HAMA scores (all $p > 0.05$, **Table 4**). No significant differences were found between the first-episode and recurrent patients in either the DMN FC strength ($F = 0.816$, $p = 0.367$) or dFC variability ($F = 1.699$, $p = 0.193$).

## Validation Analysis

When re-calculating the DMN dFC with using a range of different window widths and step lengths, the regression models kept showing a significant main effect of age ($p < 0.001$, see **Table 5**) in the prediction of DMN dFC variability, while the main effect of diagnosis and diagnosis-by-age interaction kept being no significant ($p > 0.05$). The results on FC and dFC were also largely unchanged when repeating the analyses with Fisher's *r*-to-*z* transformations on FC/dFC matrices (**Supplementary Table 1**). These results, therefore, suggest that the effects of age on FC strength/dFC variability were unlikely to be mainly driven by analyzing strategies.

In regression model on the DMN FC strength, there exists a significant heteroscedasticity as indicated by a significant correlation between age and absolute values of the residuals (Spearman's rho = −0.051, $p = 0.027$; shown in **Supplementary Figure 1**). Nevertheless, effects of such a heteroscedasticity can be corrected by applying

**TABLE 3 |** Comparisons on the correlation coefficients between groups.

| | In MDD ($n = 971$) | In HCs ($n = 902$) | Group comparisons on *r* |
|---|---|---|---|
| Correlation between age and FC strength | $r = -0.310$ | $r = -0.216$ | $z = -2.183$, $p = 0.029$ |
| Correlation between age and dFC variability | $r = 0.434$ | $r = 0.394$ | $z = 1.043$, $p = 0.297$ |

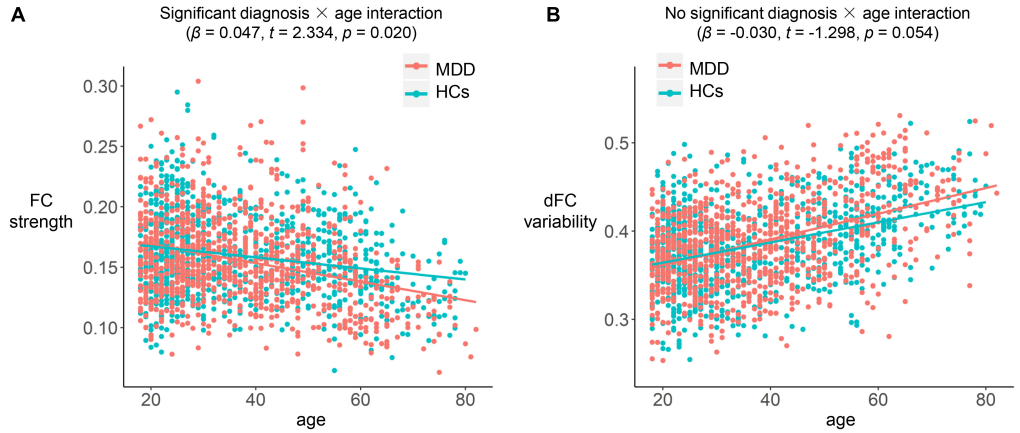


**FIGURE 3 |** Associations between age and DMN FC strength **(A)**/dFC variability **(B)** in each group.

a logarithmic transformation to the DMN FC strength (**Supplementary Figure 1**), while main results were unchanged in the corrected model (**Supplementary Table 2**). Therefore, the results were unlikely to be affected by the heteroscedasticity in regression models.

## DISCUSSION

In this study, we tested the hypothesis that MDD would be characterized by accelerated aging of brain function within the DMN as reflected by significant diagnosis-by-age interactions. Specially, age-related effects on both the strength of static FC and temporal variability of dFC within the DMN were investigated by linear regression models. Our results revealed (1) significant main effects of age in the prediction of both FC strength and dFC variability; and (2) a significant main effect of diagnosis and a significant diagnosis-by-age interaction in the prediction of FC strength within the DMN. These results may facilitate our understanding of both the process of biological aging and neural mechanisms underlying MDD.

**TABLE 4 |** Correlations between the DMN FC/dFC and clinical characteristics.

| | Illness duration | HAMD score | HAMA score |
|---|---|---|---|
| DMN FC strength | $r = -0.013$, $p = 0.729$ | $r = -0.022$, $p = 0.545$ | $r = 0.008$, $p = 0.861$ |
| DMN dFC variability | $r = 0.002$, $p = 0.963$ | $r = 0.006$, $p = 0.871$ | $r = -0.027$, $p = 0.530$ |

**TABLE 5 |** Main effect of age in the prediction of DMN dFC variability, when dFC was calculated with different window widths/step lengths.

| Window width (s) | Step length | | |
|---|---|---|---|
| | 6 s | 8 s | 10 s |
| 80 | β = 0.093, $t = 3.832$, $p < 0.001$ | β = 0.094, $t = 3.851$, $p < 0.001$ | β = 0.094, $t = 3.834$, $p < 0.001$ |
| 100 | β = 0.086, $t = 3.722$, $p < 0.001$ | β = 0.087, $t = 3.690$, $p < 0.001$ | β = 0.087, $t = 3.662$, $p < 0.001$ |
| 120 | β = 0.079, $t = 3.660$, $p < 0.001$ | β = 0.080, $t = 3.663$, $p < 0.001$ | β = 0.081, $t = 3.640$, $p < 0.001$ |

The first main finding revealed by regression model in the present study is a significant main effect of age in the prediction of both FC strength and dFC variability within the DMN. Such results indicate that both healthy participants and MDD patients experienced similar decrease in DMN FC strength and increase in DMN dFC variability along age. These results are in line with a number of previous studies, which have consistently reported that older age is associated with lower FC strength (Bluhm et al., 2008; Mevel et al., 2013; Vidal-Piñeiro et al., 2014; Park et al., 2017; Staffaroni et al., 2018) and lower dFC stability (higher variability) (Qin et al., 2015; Marusak et al., 2017; Park et al., 2017) within the DMN. It is noteworthy that compared with most of the above studies, our study has a much larger sample size which means a higher reliability (Cao et al., 2019) achieved by using a large, multicenter dataset. Therefore, our results reinforce previous studies and may further offer solid evidence that normal aging of the brain can be reflected by changed FC/dFC patterns within the DMN.

The regression model also revealed a significant main effect of diagnosis, and a significant diagnosis-by-age interaction in the prediction of FC strength within the DMN. The significant main effect of diagnosis indicates a lower DMN FC strength in MDD patients. The DMN is known to mediate brain's self-referential and internally directed processing (Whitfield-Gabrieli and Ford, 2012) and although not completely consistent (Scalabrini et al., 2020), its FC has been reported to be reduced in MDD in multiple studies (Chen et al., 2015; Jacob et al., 2020; Shi et al., 2020). Thus, our study further supports this result. The significant diagnosis-by-age interaction, which was driven by stronger negative correlation between age and DMN FC in MDD patients (**Table 3** and **Figure 3A**), suggests that age-related reduction in DMN FC may occur at a faster rate in MDD patients than in HCs. Multiple previous neuroimaging studies have reported accelerated brain aging in MDD patients in terms of brain structures (Sacchet et al., 2017; Cheng et al., 2020;

Ballester et al., 2021), but much less is known about it from a functional perspective. Here, to our knowledge, our study provides one of the first evidences of accelerated aging of FC within the DMN. Therefore, this brain subsystem may be an important target for the intervention and treatment of MDD across the lifespan.

We should note that in the regression model, no significant main effect of diagnosis and no significant diagnosis-by-age interaction (both $p > 0.05$) were found in the prediction of dFC variability. Thus, the present study failed to replicate previously reported MDD-related increase in DMN dFC variability (Wise et al., 2017; Long et al., 2020a). There are two potential reasons for such inconsistency as we proposed. First, in the analyzed sample we included participants with different fMRI scanning lengths, ranging from 300 to 500 s (**Table 1**). Although site effects have been controlled in the regression model, such diversity along the time dimension might bring bias to the results. Second, besides the reports of increased DMN dFC variability in MDD (Wise et al., 2017; Long et al., 2020a), there was also research reporting opposite results (Demirtaş et al., 2016). It is possible that subtypes with distinct DMN dFC profiles (hyper- and hypo-variability) may exist in MDD, which can be investigated in future studies.

Although we focused on age-related effects in this study, significant effects of sex were also shown in the regression models, indicating higher FC strength and lower dFC variability within the DMN in females than males. Such results are in concert with some earlier studies, which have pointed out potential sex differences in both static and dynamic brain connectome (Jiang et al., 2020; Long et al., 2021). These results might also, therefore, highlight the necessity of controlling sex-related effects in fMRI studies.

Our study has some limitations. Firstly and importantly, the current study was carried out based on cross-sectional rather than longitudinal data, and we cannot directly define the causation between MDD and accelerated aging. We are also unable to answer whether there are genetic or epigenetic deviations which cause both MDD and more rapid aging. Due to such limitations, it should be only one of possible interpretations of the presented data that MDD causes accelerated aging of brain. Secondly, the detailed clinical information for each MDD patient, such as comorbid conditions, number of prior depressive episodes and treatment details, was not fully recorded due to the variations in data management practices across different sites. This issue has limited our power to further analyze the effects of clinical variables on DMN FC/dFC patterns. Thirdly, because raw image data was not shared by the REST-meta-MDD Consortium, we are unable to further perform voxel-wise analyses (Cui et al., 2018) which may provide valuable information. Lastly, we only focused on FC strength and dFC variability within the DMN based on our literature driven hypothesis. However, other brain subsystems [e.g., salience, affective, and cognitive control networks (Zeng et al., 2012; Manoliu et al., 2014)] and other brain network measures [e.g., static and dynamic small-world metrics (Long et al., 2020a; Yang et al., 2021)] may be also relevant to the occurrence and development of MDD with age, which can be explored in further studies.

In summary, this study tested the hypothesis that MDD is characterized by accelerated aging of the brain function in terms of FC strength and dFC variability within the DMN. Diagnosis-by-age interactions on FC/dFC were estimated by linear regression models. The results suggest that both healthy participants and MDD patients experienced similar decrease in DMN FC strength and increase in DMN dFC variability along age; moreover, stronger negative correlations were found between DMN FC strength and age in MDD patients than in HCs, suggesting that age-related decrease in DMN FC may occur at a faster rate in MDD. These findings may further facilitate our understanding of mechanisms underlying the occurrence and development of MDD. However, further longitudinal studies are still needed to understand the causation between MDD and accelerated aging of brain.

## DATA AVAILABILITY STATEMENT

The datasets presented in this study can be found in online repositories. The names of the repository/repositories and accession number(s) can be found below: http://rfmri.org/REST-meta-MDD.

## ETHICS STATEMENT

The studies involving human participants were reviewed and approved by the Ethics Committee of Second Xiangya Hospital, Central South University. The patients/participants provided their written informed consent to participate in this study.

## AUTHOR CONTRIBUTIONS

ST, ZW, and YL designed the study and carried out the analysis. XC, GW, WT, YL, and ZL contributed to the data collection. ST and YL wrote the first draft of manuscript. All authors contributed to the final manuscript and have read and agreed to the published version of the manuscript.

## FUNDING

This work was supported by the Natural Science Foundation of Hunan Province, China (2021JJ40851 to YL and 2020JJ5800 to XC) and the National Natural Science Foundation of China (82071506 to ZL).

## ACKNOWLEDGMENTS

The data of this study were provided by the members of the REST-meta-MDD Consortium.

## SUPPLEMENTARY MATERIAL

The Supplementary Material for this article can be found online at: https://www.frontiersin.org/articles/10.3389/fnagi.2021.809853/full#supplementary-material

## REFERENCES


Ballester, P. L., Su, J., Nogovitsyn, N., Hassel, S., Strother, S. C., Arnott, S. R., et al. (2021). Accelerated brain aging in major depressive disorder and antidepressant treatment response: A CAN-BIND report. *Neuroimage Clin.* 32:102864. doi: 10.1016/j.nicl.2021.102864

Bluhm, R. L., Osuch, E. A., Lanius, R. A., Boksman, K., Neufeld, R. W. J., Théberge, J., et al. (2008). Default mode network connectivity: Effects of age, sex, and analytic approach. *Neuroreport* 19, 887–891. doi: 10.1097/WNR.0b013e328300ebbf

Byers, A. L., and Yaffe, K. (2011). Depression and risk of developing dementia. *Nat. Rev. Neurol.* 7, 323–331. doi: 10.1038/nrneurol.2011.60

Cao, H., McEwen, S. C., Forsyth, J. K., Gee, D. G., Bearden, C. E., Addington, J., et al. (2019). Toward leveraging human connectomic data in large consortia: Generalizability of fmri-based brain graphs across sites, sessions, and paradigms. *Cereb. Cortex* 29, 1263–1279. doi: 10.1093/cercor/bhy032

Chao-Gan, Y., and Yu-Feng, Z. (2010). DPARSF: A MATLAB toolbox for "pipeline" data analysis of resting-state fMRI. *Front. Syst. Neurosci.* 4:13. doi: 10.3389/fnsys.2010.00013

Chen, Y., Wang, C., Zhu, X., Tan, Y., and Zhong, Y. (2015). Aberrant connectivity within the default mode network in first-episode, treatment-naïve major depressive disorder. *J. Affect. Disord.* 183, 49–56. doi: 10.1016/j.jad.2015.04.052

Cheng, Y., Xu, J., Dong, C., Shen, Z., Zhou, C., Li, N., et al. (2020). Age-related atrophy of cortical thickness and genetic effect of ANK3 gene in first episode MDD patients. *Neuroimage Clin.* 28:102384. doi: 10.1016/j.nicl.2020.102384

Cizza, G., Primma, S., and Csako, G. (2009). Depression as a risk factor for osteoporosis. *Trends Endocrinol. Metab.* 20, 367–373. doi: 10.1016/j.tem.2009.05.003

Cole, M. W., Reynolds, J. R., Power, J. D., Repovs, G., Anticevic, A., and Braver, T. S. (2013). Multi-task connectivity reveals flexible hubs for adaptive task control. *Nat. Neurosci.* 16, 1348–1355. doi: 10.1038/nn.3470

Cui, X., Liu, F., Chen, J., Xie, G., Wu, R., Zhang, Z., et al. (2018). Voxel-wise brain-wide functional connectivity abnormalities in first-episode, drug-naive patients with major depressive disorder. *Am. J. Med. Genet. Part B Neuropsychiatr. Genet.* 177, 447–453. doi: 10.1002/ajmg.b.32633

Demirtaş, M., Tornador, C., Falcón, C., López-Solà, M., Hernández-Ribas, R., Pujol, J., et al. (2016). Dynamic functional connectivity reveals altered variability in functional connectivity among patients with major depressive disorder. *Hum. Brain Mapp.* 37, 2918–2930. doi: 10.1002/hbm.23215

Diedenhofen, B., and Musch, J. (2015). Cocor: A comprehensive solution for the statistical comparison of correlations. *PLoS One* 10:e0121945. doi: 10.1371/journal.pone.0121945

Ding, Y. D., Yang, R., Yan, C. G., Chen, X., Bai, T. J., Bo, Q. J., et al. (2021). Disrupted hemispheric connectivity specialization in patients with major depressive disorder: Evidence from the REST-meta-MDD Project. *J. Affect. Disord.* 284, 217–228. doi: 10.1016/j.jad.2021.02.030

Dong, D., Duan, M., Wang, Y., Zhang, X., Jia, X., Li, Y., et al. (2019). Reconfiguration of Dynamic Functional Connectivity in Sensory and Perceptual System in Schizophrenia. *Cereb. Cortex* 29, 3577–3589. doi: 10.1093/cercor/bhy232

Dunlop, K., Victoria, L. W., Downar, J., Gunning, F. M., and Liston, C. (2021). Accelerated brain aging predicts impulsivity and symptom severity in depression. *Neuropsychopharmacology* 46, 911–919. doi: 10.1038/s41386-021-00967-x

Gan, Y., Gong, Y., Tong, X., Sun, H., Cong, Y., Dong, X., et al. (2014). Depression and the risk of coronary heart disease: A meta-analysis of prospective cohort studies. *BMC Psychiatry* 14:371. doi: 10.1186/s12888-014-0371-z

Holmquist, S., Nordström, A., and Nordström, P. (2020). The association of depression with subsequent dementia diagnosis: A Swedish nationwide cohort study from 1964 to 2016. *PLoS Med* 17:e1003016. doi: 10.1371/JOURNAL.PMED.1003016

Huang, D., Liu, Z., Cao, H., Yang, J., Wu, Z., and Long, Y. (2021). Childhood trauma is linked to decreased temporal stability of functional brain networks in young adults. *J. Affect. Disord.* 290, 23–30. doi: 10.1016/j.jad.2021.04.061

Huang, X., Wu, Z., Liu, Z., Liu, D., Huang, D., and Long, Y. (2021). Acute Effect of Betel Quid Chewing on Brain Network Dynamics: A Resting-State Functional Magnetic Resonance Imaging Study. *Front. Psychiatry* 12:701420. doi: 10.3389/fpsyt.2021.701420

Jacob, Y., Morris, L. S., Huang, K. H., Schneider, M., Rutter, S., Verma, G., et al. (2020). Neural correlates of rumination in major depressive disorder: A brain network analysis. *Neuroimage Clin.* 25:102142. doi: 10.1016/j.nicl.2019.102142

Jiang, R., Calhoun, V. D., Fan, L., Zuo, N., Jung, R., Qi, S., et al. (2020). Gender Differences in Connectome-based Predictions of Individualized Intelligence Quotient and Sub-domain Scores. *Cereb. Cortex* 30, 888–900. doi: 10.1093/cercor/bhz134

Levada, O. A., and Troyan, A. S. (2020). Major depressive disorder and accelerated aging from a peripheral IGF-1 overexpression perspective. *Med. Hypotheses* 138:109610. doi: 10.1016/j.mehy.2020.109610

Liang, S., Deng, W., Li, X., Greenshaw, A. J., Wang, Q., Li, M., et al. (2020). Biotypes of major depressive disorder: Neuroimaging evidence from resting-state default mode network patterns. *Neuroimage Clin.* 28:102514. doi: 10.1016/j.nicl.2020.102514

Liu, P. H., Li, Y., Zhang, A. X., Sun, N., Li, G. Z., Chen, X., et al. (2021). Brain structural alterations in MDD patients with gastrointestinal symptoms: Evidence from the REST-meta-MDD project. *Prog. Neuro Psychopharmacol. Biol. Psychiatry* 111:110386. doi: 10.1016/j.pnpbp.2021.110386

Long, Y., Cao, H., Yan, C., Chen, X., Li, L., Castellanos, F. X., et al. (2020a). Altered resting-state dynamic functional brain networks in major depressive disorder: Findings from the REST-meta-MDD consortium. *Neuroimage Clin.* 26:102163. doi: 10.1016/j.nicl.2020.102163

Long, Y., Chen, C., Deng, M., Huang, X., Tan, W., Zhang, L., et al. (2019). Psychological resilience negatively correlates with resting-state brain network flexibility in young healthy adults: a dynamic functional magnetic resonance imaging study. *Ann. Transl. Med.* 7, 809–809. doi: 10.21037/atm.2019.12.45

Long, Y., Liu, Z., Chan, C. K. Y., Wu, G., Xue, Z., Pan, Y., et al. (2020b). Altered Temporal Variability of Local and Large-Scale Resting-State Brain Functional Connectivity Patterns in Schizophrenia and Bipolar Disorder. *Front. Psychiatry* 11:422. doi: 10.3389/fpsyt.2020.00422

Long, Y., Yan, C., Wu, Z., Huang, X., and Cao, H. (2021). Evaluating test-retest reliability and sex/age-related effects on temporal clustering coefficient of dynamic functional brain networks. *Biorxiv* doi: 10.1101/2021.10.21.465376

Manoliu, A., Meng, C., Brandl, F., Doll, A., Tahmasian, M., Scherr, M., et al. (2014). Insular dysfunction within the salience network is associated with severity of symptoms and aberrant inter-network connectivity in major depressive disorder. *Front. Hum. Neurosci.* 7:930. doi: 10.3389/fnhum.2013.00930

Marusak, H. A., Calhoun, V. D., Brown, S., Crespo, L. M., Sala-Hamrick, K., Gotlib, I. H., et al. (2017). Dynamic functional connectivity of neurocognitive networks in children. *Hum. Brain Mapp.* 38, 97–108. doi: 10.1002/hbm.23346

Meng, X. L., Rosenthal, R., and Rubin, D. B. (1992). Comparing correlated correlation coefficients. *Psychol. Bull.* 111, 172–175. doi: 10.1037/0033-2909.111.1.172

Mevel, K., Landeau, B., Fouquet, M., La Joie, R., Villain, N., Mézenge, F., et al. (2013). Age effect on the default mode network, inner thoughts, and cognitive abilities. *Neurobiol. Aging* 34, 1292–1301. doi: 10.1016/j.neurobiolaging.2012.08.018

Mulders, P. C., van Eijndhoven, P. F., Schene, A. H., Beckmann, C. F., and Tendolkar, I. (2015). Resting-state functional connectivity in major depressive disorder: A review. *Neurosci. Biobehav. Rev.* 56, 330–344. doi: 10.1016/j.neubiorev.2015.07.014

Park, J. E., Jung, S. C., Ryu, K. H., Oh, J. Y., Kim, H. S., Choi, C. G., et al. (2017). Differences in dynamic and static functional connectivity between young and elderly healthy adults. *Neuroradiology* 59, 781–789. doi: 10.1007/s00234-017-1875-2

Power, J. D., Cohen, A. L., Nelson, S. M., Wig, G. S., Barnes, K. A., Church, J. A., et al. (2011). Functional Network Organization of the Human Brain. *Neuron* 72, 665–678. doi: 10.1016/j.neuron.2011.09.006

Protsenko, E., Yang, R., Nier, B., Reus, V., Hammamieh, R., Rampersaud, R., et al. (2021). GrimAge," an epigenetic predictor of mortality, is accelerated in major depressive disorder. *Transl. Psychiatry* 11:193. doi: 10.1038/s41398-021-01302-0

Qin, J., Chen, S. G., Hu, D., Zeng, L. L., Fan, Y. M., Chen, X. P., et al. (2015). Predicting individual brain maturity using dynamic functional connectivity. *Front. Hum. Neurosci.* 9:418. doi: 10.3389/fnhum.2015.00418

Rosopa, P. J., Schaffer, M. M., and Schroeder, A. N. (2013). Managing heteroscedasticity in general linear models. *Psychol. Methods* 18, 335–351. doi: 10.1037/a0032553

Sacchet, M. D., Camacho, M. C., Livermore, E. E., Thomas, E. A. C., and Gotlib, I. H. (2017). Accelerated aging of the putamen in patients with major depressive disorder. *J. Psychiatry Neurosci.* 42, 164–171. doi: 10.1503/jpn.160010

Savva, A. D., Kassinopoulos, M., Smyrnis, N., Matsopoulos, G. K., and Mitsis, G. D. (2020). Effects of motion related outliers in dynamic functional connectivity using the sliding window method. *J. Neurosci. Methods* 330:108519. doi: 10.1016/j.jneumeth.2019.108519

Scalabrini, A., Vai, B., Poletti, S., Damiani, S., Mucci, C., Colombo, C., et al. (2020). All roads lead to the default-mode network—global source of DMN abnormalities in major depressive disorder. *Neuropsychopharmacology* 45, 2058–2069. doi: 10.1038/s41386-020-0785-x

Sheffield, J. M., Repovs, G., Harms, M. P., Carter, C. S., Gold, J. M., Macdonald, A. W., et al. (2016). Evidence for accelerated decline of functional brain network efficiency in schizophrenia. *Schizophr. Bull.* 42, 753–761. doi: 10.1093/schbul/sbv148

Shi, Y., Li, J., Feng, Z., Xie, H., Duan, J., Chen, F., et al. (2020). Abnormal functional connectivity strength in first-episode, drug-naïve adult patients with major depressive disorder. *Prog. Neuro Psychopharmacol. Biol. Psychiatry* 97:109759. doi: 10.1016/j.pnpbp.2019.109759

Shi, Y., Zhang, L., Wang, Z., Lu, X., Wang, T., Zhou, D., et al. (2021). Multivariate Machine Learning Analyses in Identification of Major Depressive Disorder Using Resting-State Functional Connectivity: A Multicentral Study. *ACS Chem. Neurosci.* 12, 2878–2886. doi: 10.1021/acschemneuro.1c00256

Simon, N. M., Smoller, J. W., McNamara, K. L., Maser, R. S., Zalta, A. K., Pollack, M. H., et al. (2006). Telomere Shortening and Mood Disorders: Preliminary Support for a Chronic Stress Model of Accelerated Aging. *Biol. Psychiatry* 60, 432–435. doi: 10.1016/j.biopsych.2006.02.004

Staffaroni, A. M., Brown, J. A., Casaletto, K. B., Elahi, F. M., Deng, J., Neuhaus, J., et al. (2018). The longitudinal trajectory of default mode network connectivity in healthy older adults varies as a function of age and is associated with changes in episodic memory and processing speed. *J. Neurosci.* 38, 2809–2817. doi: 10.1523/JNEUROSCI.3067-17.2018

Sun, Y., Collinson, S. L., Suckling, J., and Sim, K. (2019). Dynamic reorganization of functional connectivity reveals abnormal temporal efficiency in schizophrenia. *Schizophr. Bull.* 45, 659–669. doi: 10.1093/schbul/sby077

van Velzen, L. S., Kelly, S., Isaev, D., Aleman, A., Aftanas, L. I., Bauer, J., et al. (2020). White matter disturbances in major depressive disorder: a coordinated analysis across 20 international cohorts in the ENIGMA MDD working group. *Mol. Psychiatry* 25, 1511–1525. doi: 10.1038/s41380-019-0477-2

Vidal-Piñeiro, D., Valls-Pedret, C., FernÃ¡ndez-Cabello, S., Arenaza-Urquijo, E. M., Sala-Llonch, R., and Solana, E. (2014). Decreased Default Mode Network connectivity correlates with age-associated structural and cognitive changes. *Front. Aging Neurosci.* 6:256. doi: 10.3389/fnagi.2014.00256

Whitfield-Gabrieli, S., and Ford, J. M. (2012). Default mode network activity and connectivity in psychopathology. *Annu. Rev. Clin. Psychol.* 8, 49–76. doi: 10.1146/annurev-clinpsy-032511-143049

Wise, T., Marwood, L., Perkins, A. M., Herane-Vives, A., Joules, R., Lythgoe, D. J., et al. (2017). Instability of default mode network connectivity in major depression: A two-sample confirmation study. *Transl. Psychiatry* 7:e1105. doi: 10.1038/tp.2017.40

Wolkowitz, O. M., Reus, V. I., and Mellon, S. H. (2011). Of sound mind and body: Depression, disease, and accelerated aging. *Dialogues Clin. Neurosci.* 13, 25–40. doi: 10.31887/dcns.2011.13.1/owolkowitz

Wright, S. N., Kochunov, P., Chiappelli, J., McMahon, R. P., Muellerklein, F., Wijtenburg, S. A., et al. (2014). Accelerated white matter aging in schizophrenia: Role of white matter blood perfusion. *Neurobiol. Aging* 35, 2411–2418. doi: 10.1016/j.neurobiolaging.2014.02.016

Xia, M., Wang, J., and He, Y. (2013). BrainNet Viewer: A Network Visualization Tool for Human Brain Connectomics. *PLoS One* 8:e68910. doi: 10.1371/journal.pone.0068910

Yan, C. G., Chen, X., Li, L., Castellanos, F. X., Bai, T. J., Bo, Q. J., et al. (2019). Reduced default mode network functional connectivity in patients with recurrent major depressive disorder. *Proc. Natl. Acad. Sci. U. S. A.* 116, 9078–9083. doi: 10.1073/pnas.1900390116

Yan, C. G., Di Wang, X, Zuo, X. N., and Zang, Y. F. (2016). DPABI: Data Processing & Analysis for (Resting-State) Brain Imaging. *Neuroinformatics* 14, 339–351. doi: 10.1007/s12021-016-9299-4

Yang, H., Chen, X., Chen, Z.-B., Li, L., Li, X.-Y., Castellanos, F. X., et al. (2021). Disrupted intrinsic functional brain topology in patients with major depressive disorder. *Mol. Psychiatry* 3058:15. doi: 10.1038/s41380-021-01247-2

Zanatta, D. P., Rondinoni, C., Salmon, C. E. G., and Del Ben, C. M. (2019). Brain alterations in first episode depressive disorder and resting state fMRI: A systematic review. *Psychol. Neurosci.* 12, 407–429. doi: 10.1037/pne0000165

Zeng, L. L., Shen, H., Liu, L., Wang, L., Li, B., Fang, P., et al. (2012). Identifying major depression using whole-brain functional connectivity: A multivariate pattern analysis. *Brain* 135, 1498–1507. doi: 10.1093/brain/aws059

Zhang, C., Baum, S. A., Adduru, V. R., Biswal, B. B., and Michael, A. M. (2018). Test-retest reliability of dynamic functional connectivity in resting state fMRI. *Neuroimage* 183, 907–918. doi: 10.1016/j.neuroimage.2018.08.021

Zhang, J., Cheng, W., Liu, Z., Zhang, K., Lei, X., Yao, Y., et al. (2016). Neural, electrophysiological and anatomical basis of brain-network variability and its characteristic changes in mental disorders. *Brain* 139, 2307–2321. doi: 10.1093/brain/aww143

Zhang, K., Zhu, Y., Zhu, Y., Wu, S., Liu, H., Zhang, W., et al. (2016). Molecular, Functional, and Structural Imaging of Major Depressive Disorder. *Neurosci. Bull.* 32, 273–285. doi: 10.1007/s12264-016-0030-0

Zou, G. Y. (2007). Toward Using Confidence Intervals to Compare Correlations. *Psychol. Methods* 12, 399–413. doi: 10.1037/1082-989X.12.4.399

**Conflict of Interest:** The authors declare that the research was conducted in the absence of any commercial or financial relationships that could be construed as a potential conflict of interest.

**Publisher's Note:** All claims expressed in this article are solely those of the authors and do not necessarily represent those of their affiliated organizations, or those of the publisher, the editors and the reviewers. Any product that may be evaluated in this article, or claim that may be made by its manufacturer, is not guaranteed or endorsed by the publisher.

frontiers in Aging Neuroscience

ORIGINAL RESEARCH
published: 10 February 2022
doi: 10.3389/fnagi.2022.817607

# The Relationship Between Vitamin D, Clinical Manifestations, and Functional Network Connectivity in Female Patients With Major Depressive Disorder

*Dao-min Zhu[1,2,3,4†], Wenming Zhao[1,5,6†], Shunshun Cui[1,5,6], Ping Jiang[1,5,6], Yu Zhang[2,3,4], Cun Zhang[1,5,6], Jiajia Zhu[1,5,6*] and Yongqiang Yu[1,5,6*]*

[1] Department of Radiology, The First Affiliated Hospital of Anhui Medical University, Hefei, China, [2] Department of Sleep Disorders, Affiliated Psychological Hospital of Anhui Medical University, Hefei, China, [3] Hefei Fourth People's Hospital, Hefei, China, [4] Anhui Mental Health Center, Hefei, China, [5] Research Center of Clinical Medical Imaging, Anhui Province, Hefei, China, [6] Anhui Provincial Institute of Translational Medicine, Hefei, China

OPEN ACCESS

**Edited by:**
*Wenjing Zhang,*
*Sichuan University, China*

**Reviewed by:**
*Wenbin Guo,*
*Central South University, China*
*Jiaojian Wang,*
*University of Electronic Science and Technology of China, China*

***Correspondence:**
*Jiajia Zhu*
*zhujiajiagraduate@163.com*
*Yongqiang Yu*
*cjr.yuyongqiang@vip.163.com*

*† These authors have contributed equally to this work*

**Specialty section:**
*This article was submitted to Neurocognitive Aging and Behavior, a section of the journal Frontiers in Aging Neuroscience*

**Received:** *18 November 2021*
**Accepted:** *05 January 2022*
**Published:** *10 February 2022*

**Citation:**
*Zhu D-m, Zhao W, Cui S, Jiang P, Zhang Y, Zhang C, Zhu J and Yu Y (2022) The Relationship Between Vitamin D, Clinical Manifestations, and Functional Network Connectivity in Female Patients With Major Depressive Disorder. Front. Aging Neurosci. 14:817607. doi: 10.3389/fnagi.2022.817607*

Evidence suggests the pivotal role of vitamin D in the pathophysiology of major depressive disorder (MDD) via its effects on the brain. Gender differences exist in both depression and vitamin D level. Our objective was to investigate the association between gender, vitamin D, clinical manifestations, and functional network connectivity in a large sample of MDD patients and healthy controls. Resting-state functional MRI data were collected from 122 patients and 119 controls, with independent component analysis adopted to examine large-scale inter- and intranetwork functional connectivity. Serum concentration of vitamin D (SCVD) and clinical manifestations were also assessed. MDD patients exhibited lower SCVD than controls in females but not males. Moreover, we identified a female-specific association between lower SCVD and poorer cognitive performance. Concurrently, MDD-related functional network connectivity changes were correlated with SCVD in females as well as depression and anxiety symptoms in female patients. Remarkably, MDD- and SCVD-related functional network connectivity alterations mediated the associations between SCVD and cognition in females. Aside from providing evidence for a female-specific neurobiological mechanism whereby low vitamin D might contribute to MDD and its associated clinical characteristics, our findings inform a novel conceptualization that adjuvant vitamin D supplementation therapy may yield clinical benefits in improving treatment outcomes in female patients with MDD.

**Keywords: major depressive disorder, vitamin D, gender, functional network connectivity, functional MRI**

## INTRODUCTION

Major depressive disorder (MDD) is a prevalent major psychiatric disorder that typically begins in adolescence (Jones, 2013). Despite decades of clinical and preclinical research, the pathogenesis of MDD is still not well understood (Holtzheimer and Nemeroff, 2006). It is now generally accepted that depressive mood tends to follow a seasonal pattern, peaking in summer and winter

(Wehr and Rosenthal, 1989). It is likely that vitamin D, through its action on the brain, might account for the link between seasonal photoperiod changes and seasonal mood swings (Berk et al., 2007). Fundamentally, there is abundant evidence for an intimate association between vitamin D deficiency and MDD (Bertone-Johnson et al., 2011; Kjaergaard et al., 2011; Anglin et al., 2013; Ju et al., 2013; Milaneschi et al., 2014; Aghajafari et al., 2018; Wong et al., 2018; Briggs et al., 2019; Zhu et al., 2019). Moreover, longitudinal studies have documented that vitamin D supplementation is beneficial for the treatment of depression (de Koning et al., 2015; Gowda et al., 2015; Casseb et al., 2019; Alghamdi et al., 2020). These findings converge to support the pivotal role of vitamin D in the pathophysiology of MDD.

There is intense research on the potential pathways through which vitamin D exerts its effects on brain development and functioning. One plausible mechanism lies in the fact that vitamin D status affects the synthesis and release of key neurotransmitters in the brain, such as dopamine and serotonin (Eyles et al., 2013; Patrick and Ames, 2014). Acting as a neurosteroid hormone, vitamin D may also play a regulatory role in neurotransmission, neuroprotection, and neuroimmunomodulation (Fernandes de Abreu et al., 2009). In addition, metabolites of vitamin D can cross the blood-brain barrier and bind to vitamin D receptors, which are widely distributed in the brain (Eyles et al., 2005). Given the prior reports that vitamin D is related to both depression and the brain, it is appealing to investigate the neural substrates underlying the association between vitamin D and MDD. Although our earlier preliminary work showed that the relationship between serum concentration of vitamin D (SCVD) and depressive symptoms was mediated by total intracranial volume in MDD patients (Zhu et al., 2019), it offers insufficient material to attempt a more thorough characterization of such neural underpinnings.

Epidemiological studies demonstrate that females are more likely to develop depression than males (Nolen-Hoeksema and Girgus, 1994; Ferrari et al., 2013). While marked gender difference in depression has long been a topic of active investigation, the exact mechanisms responsible for this gender dimorphism remain elusive. Possible explanations include but not limited to gender divergence in the monoamine systems, stress responses, hypothalamus-pituitary-adrenal (HPA) axis function, and the levels of gonadal steroid hormones (e.g., estrogens) (Amin et al., 2005; Solomon and Herman, 2009; Bourke et al., 2012; Fernandez-Guasti et al., 2012; Bangasser and Valentino, 2014; Zagni et al., 2016). In parallel, a large number of studies have reported gender difference in vitamin D status characterized by the fact that SCVD is lower in females than males (Milaneschi et al., 2010; Toffanello et al., 2014b; Song et al., 2016; Yan et al., 2019; Choi et al., 2020; Rhee et al., 2020). Moreover, researchers have demonstrated a gender-dependent relationship between SCVD and depression, with most studies showing a strong and specific SCVD-depression association in females (Milaneschi et al., 2010; Toffanello et al., 2014b; Serati et al., 2016; Amini et al., 2019; Boulkrane et al., 2020). It is well established that vitamin D is related to the production/release of gonadal hormones (Kinuta et al., 2000; Lorenzen et al., 2017), which may offer a mechanistic account for the gender-dependent association between SCVD and MDD.

Previous data have provided solid evidence for a link between vitamin D and cognition, such that vitamin D deficiency is associated with worse cognitive performance in healthy adults (Balion et al., 2012; Annweiler et al., 2013; Mayne and Burne, 2019) and low vitamin D status is causally related to cognitive decline in older adults (Llewellyn et al., 2011; Slinin et al., 2012; Toffanello et al., 2014a; Miller et al., 2015; Pavlovic et al., 2018). Furthermore, a randomized trial revealed that high dose vitamin D supplementation enhanced cognitive ability in healthy adults, especially among those with insufficient vitamin D at baseline (Pettersen, 2017). It is largely known that cognitive deficits are commonly present in MDD patients (Bortolato et al., 2016; Pan et al., 2019). Past research suggests that cognitive dysfunction persists following symptomatic remission (Bortolato et al., 2016) and retention of cognitive impairment may interact with existing emotional and social vulnerability, increasing the risk of recurrent depressive episodes (Knight and Baune, 2018). As such, cognitive symptoms are considered suitable targets and primary outcomes of psychological and pharmacological treatments in MDD (Knight and Baune, 2018). Collectively, it is natural to assume a potential association between vitamin D, cognitive impairment, and depression. Despite recent attempts to clarify this issue (Lerner et al., 2018; Roy, 2021), such association is rather complex and warrants further investigation.

As a non-invasive imaging technique, resting-state functional magnetic resonance imaging (rs-fMRI) has been frequently used to measure spontaneous brain activity based on the blood-oxygen-level-dependent (BOLD) signal (Biswal et al., 1995). The human brain comprises multiple functional networks subserving different functions (Damoiseaux et al., 2006; Power et al., 2011), each network consisting of several brain regions demonstrating similar patterns of BOLD signal change over time whereas different networks showing distinct patterns. Independent component analysis (ICA) is a useful data-driven approach that can be applied to brain rs-fMRI data to extract different functional networks and further examine large-scale inter- and intranetwork functional connectivity (Calhoun et al., 2001a,b; van de Ven et al., 2004; Wang et al., 2020; Cai et al., 2021). By leveraging this approach, investigators have shown functional dysconnectivity of multiple brain networks in MDD (Sacchet et al., 2016; Wu et al., 2017; Albert et al., 2019; Chen et al., 2019; Liu et al., 2019, 2020, 2021; Yu et al., 2019; Jiao et al., 2020).

The objective of the current study was to investigate the relationship between gender, SCVD, clinical manifestations, and functional network connectivity in a large sample of MDD patients and healthy subjects. On the basis of previous literature, we aimed to test three hypotheses: (1) a diagnosis by gender interaction for SCVD, (2) a gender-specific association of SCVD with clinical manifestations and MDD-related functional network connectivity changes, and (3) a mediative role of MDD- and SCVD-related functional network connectivity alterations in accounting for the association between SCVD and clinical manifestations in a gender-specific manner.

# MATERIALS AND METHODS

## Participants

Major depressive disorder patients were enrolled from Affiliated Psychological Hospital of Anhui Medical University. Healthy controls (HC) were recruited from the local community via poster advertisements. A total of 244 participants with right-handedness were included, consisting of 122 MDD patients and 122 gender- and age-matched HC. Two well-trained clinical psychiatrists confirmed the diagnoses of depression using the MINI-International Neuropsychiatric Interview (M.I.N.I.) in accordance with the International Classification of Diseases (ICD-10) criteria. HC were carefully screened to confirm an absence of any psychiatric illness using the M.I.N.I. The exclusion criteria for all participants were (1) the presence of other psychiatric disorders, e.g., schizophrenia, bipolar disorder, substance-induced mood disorder, anxiety disorders, substance abuse or dependence; (2) a history of severe physical or neurological diseases; (3) a history of head injury leading to a loss of consciousness; (4) contraindications for magnetic resonance imaging (MRI). Additional exclusion criterion for HC was a family history of serious neurological or psychiatric illnesses among their first-degree relatives. It is noteworthy that participants with SCVD values greater than mean + 3 × standard deviation (SD) or smaller than mean − 3 × SD (i.e., outliers, $n = 3$) were excluded. This brought the final sample into 241 participants, comprising 122 MDD patients and 119 HC. The 24-item Hamilton Rating Scale for Depression (HAMD) (Williams, 1988) and the 14-item Hamilton Rating Scale for Anxiety (HAMA) (Thompson, 2015) were utilized to evaluate the severity of depression and anxiety symptoms. All MDD patients were receiving regular antidepressant medications, including selective serotonin reuptake inhibitors (SSRIs), serotonin-norepinephrine reuptake inhibitors (SNRIs), and noradrenergic and specific serotonergic antidepressants (NaSSA). The ethics committee of The First Affiliated Hospital of Anhui Medical University approved this study. After being given a complete description of the study, written informed consent was obtained from all participants.

## Cognitive Assessment

There is convergent evidence that cognitive impairments in prospective memory (PM) and sustained attention appear to be typical characteristics in depression (Han et al., 2012; Rock et al., 2014; Zhou et al., 2017; McFarland and Vasterling, 2018), such that we examined these two cognitive functions here. The cognitive assessment was conducted by a psychiatrist trained in neuropsychological testing. PM is defined as the ability to remember to carry out an intended action after a delay without any explicit instruction (Einstein and McDaniel, 1990; McDaniel and Einstein, 2011). PM is commonly classified into event-based prospective memory (EBPM; i.e., the ability to remember to carry out an intended action at the occurrence of a certain event) and time-based prospective memory (TBPM; i.e., the ability to remember to carry out an intended action at a certain time). Details of the EBPM and TBPM tests can be found in prior literature (Cheng et al., 2013; Yang et al., 2015). For the EBPM test, the experimental stimuli were 30 cards with each containing 12 Chinese words, of which 10 belonged to one major category and the other two to one minor category. Participants were instructed to read out the two words belonging to the minor category on each card. If the selected words belonged to the category of animals (target events), participants were required to tap the table. After the test, participants should write down their telephone number without any hints at the end of the test. There were six target cards (card numbers 5, 10, 15, 20, 24, and 29) in this test. Participants received one point for each correct response to a target card, and they received two points for remembering to write down their phone number. The maximum score was 8 points. For the TBPM test, the experimental stimuli were 100 cards with each containing 12 two-digit numbers. Participants were asked to pick out the smallest and the largest numbers on each card and to tap the table at the target time points (5, 10, and 15 min after the start of the test). The test stopped at the 17-min time point. Participants received two points if they responded within 10 s around the target time, and one point if within 30 s. The maximum score was 6 points.

Sustained attention was measured with a computerized version of the Continuous Performance Task-Identical Pairs (CPT-IP) (Cornblatt et al., 1988). The stimuli were 2−, 3−, or 4-digit numbers in separate conditions, generating separate scores reflecting increasing memory load on digit span. Participants were asked to monitor numbers on a computer screen and respond to any consecutive presentation of identical stimuli by key pressing as quickly as possible. Responses to target trials (pairs that were identical and required a response) and catch trials (pairs that were similar but not identical) were scored as true and false positive responses. The main outcome variable of interest was $d'$ -a well-established discrimination sensitivity index incorporating both true and false positive responses. $d'$ was calculated as $z$(hit rate) − $z$(false alarm rate) [in Matlab, norminv(hit rate) − norminv(false alarm rate)]. CPT-IP-2, −3, and −4 represented $d'$ values corresponding to the number of digits, with higher scores reflecting better sustained attention performance.

## Serum Concentration of Vitamin D Measurement

After an overnight fasting period, we collected peripheral venous blood samples (2 ml) from all participants in the morning of MRI scanning. Samples were sent to the Department of Clinical Laboratory, Affiliated Psychological Hospital of Anhui Medical University immediately for centrifugation to separate serum. Serum vitamin D [25(OH)D] was measured using a chemiluminescence immunoassay (CLIA) technique in a fully automated Maglumi 1000 analyzer (SNIBE Co., Ltd., Shenzhen, China). Internal quality control provided by the manufacturer was employed to assure quality. SCVD was stratified as sufficiency: 30–100 ng/ml (75–250 nmol/L), insufficiency: 20–30 ng/ml (50–75 nmol/L), and deficiency: <20 ng/ml (50 nmol/L) (Ringe and Kipshoven, 2012).

## Image Acquisition

Magnetic resonance imaging data were acquired using a 3.0-Tesla MR system (Discovery MR750w, General Electric, Milwaukee, WI, United States) with a 24-channel head coil. During scanning, tight but comfortable foam and earplugs were used to minimize head movement and scanner noise. All participants were instructed to relax, keep their eyes closed but not fall asleep, think of nothing in particular, and move as little as possible. All participants underwent a high-resolution three-dimensional T1-weighted brain volume (BRAVO) sequence with the following parameters: repetition time (TR) = 8.5 ms; echo time (TE) = 3.2 ms; inversion time (TI) = 450 ms; flip angle (FA) = 12°; field of view (FOV) = 256 mm × 256 mm; matrix size = 256 × 256; slice thickness = 1 mm, no gap; voxel size = 1mm × 1mm × 1mm; 188 sagittal slices; and acquisition time = 296 s. Resting-state BOLD fMRI data were acquired using a gradient-echo single-shot echo planar imaging (GRE-SS-EPI) sequence with the following parameters: TR = 2,000 ms; TE = 30 ms; FA = 90°; FOV = 220 mm × 220 mm; matrix size = 64 × 64; slice thickness = 3 mm, slice gap = 1 mm; 35 interleaved axial slices; 185 volumes; and acquisition time = 370 s. Routine T2-weighted images were also collected to exclude any organic brain abnormality. All images were visually inspected to ensure that only images without visible artifacts (e.g., ghosting artifacts arising from subject movement and pulsating large arteries, metal artifacts, susceptibility artifacts, and blooming artifacts) were included in subsequent analyses. None of the participants were excluded for visually inspected imaging artifacts.

## fMRI Data Preprocessing

Resting-state fMRI data were preprocessed using Statistical Parametric Mapping software (SPM12[1]) and Data Processing and Analysis for Brain Imaging (DPABI[2]) (Yan et al., 2016). The first 10 volumes for each participant were discarded, and the remaining volumes were corrected for the acquisition time delay between slices. Realignment was then performed to correct the motion between time points. Head motion parameters were computed by estimating the translation in each direction and the angular rotation on each axis for each volume. All participants' BOLD data were within the defined motion thresholds (i.e., maximum translational or rotational motion parameters less than 2 mm or 2°). We also calculated FD, which indexes the volume-to-volume changes in head position. In the normalization step, individual structural images were firstly co-registered with the mean functional image; the transformed structural images were then segmented and normalized to the Montreal Neurological Institute (MNI) space using a high-level non-linear warping algorithm, i.e., the diffeomorphic anatomical registration through exponentiated Lie algebra (DARTEL) technique (Ashburner, 2007). Finally, each functional volume was spatially normalized to the MNI space using the deformation parameters estimated during the above step and resampled into a 3-mm isotropic voxel. After spatial normalization, all data sets were smoothed with a 6 mm full-width at half-maximum (FWHM) Gaussian kernel.

## Independent Component Analysis

Independent component analysis was performed for the preprocessed fMRI data with the GIFT toolbox[3] and the number of independent components ($N$ = 21) was estimated automatically by the software using the minimum description length criteria. Spatial ICA decomposes the participant data into linear mixtures of spatially independent components that exhibit a unique time course profile. This was realized by using two data reduction steps. First, principal component analysis was adopted to reduce the subject-specific data into 32 principle components. Next, reduced data of all participants were concatenated across time and decomposed into 21 independent components using the infomax algorithm. To ensure estimation stability, the infomax algorithm was repeated 20 times in ICASSO[4], and the most central run was selected and analyzed further. Finally, participant specific spatial maps and time courses were obtained using the GICA back reconstruction approach.

We identified several independent components as functional networks. These independent components had peak activations in gray matter, showed low spatial overlap with known vascular, ventricular, motion, and susceptibility artifacts, and exhibited primarily low frequency power. This selection procedure yielded 11 functional networks out of the 21 independent components obtained (**Figure 1**): anterior and posterior default mode networks (aDMN and pDMN), dorsal and ventral attention networks (DAN and VAN), posterior and medial visual networks (pVN and mVN), left and right frontoparietal networks (lFPN and rFPN), sensorimotor network (SMN), salience network (SN), and auditory network (AN).

Before internetwork functional connectivity calculation, the following additional postprocessing steps were carried out on the time courses of selected functional networks: (1) detrending linear, quadratic, and cubic trends; (2) despiking detected outliers; and (3) low-pass filtering with a cut-off frequency of 0.15 Hz. Then, internetwork functional connectivity was estimated as the Pearson correlation coefficients between pairs of time courses of the functional networks, resulting in a symmetric 11 × 11 correlation matrix per participant. Finally, correlations were transformed to $z$-scores using Fisher's transformation to improve the normality. Intranetwork connectivity was examined via the spatial maps, indexing the contribution of the time course to each voxel comprising a given independent component.

## Statistical Analysis

Demographic and clinical data were analyzed using the SPSS 23.0 software package (SPSS, Chicago, IL, United States). Two-sample $t$-tests were utilized to compare MDD patients and HC in age, educational level, body mass index (BMI), FD, HAMD, HAMA, EBPM, TBPM, and CPT-IP. Pearson Chi-square test was adopted to examine group difference in gender. A threshold of $P < 0.05$ was considered statistically significant (two-sided).

[1] http://www.fil.ion.ucl.ac.uk/spm

[2] http://rfmri.org/dpabi

[3] mialab.mrn.org/software/gift/

[4] http://research.ics.tkk.fi/ica/icasso/

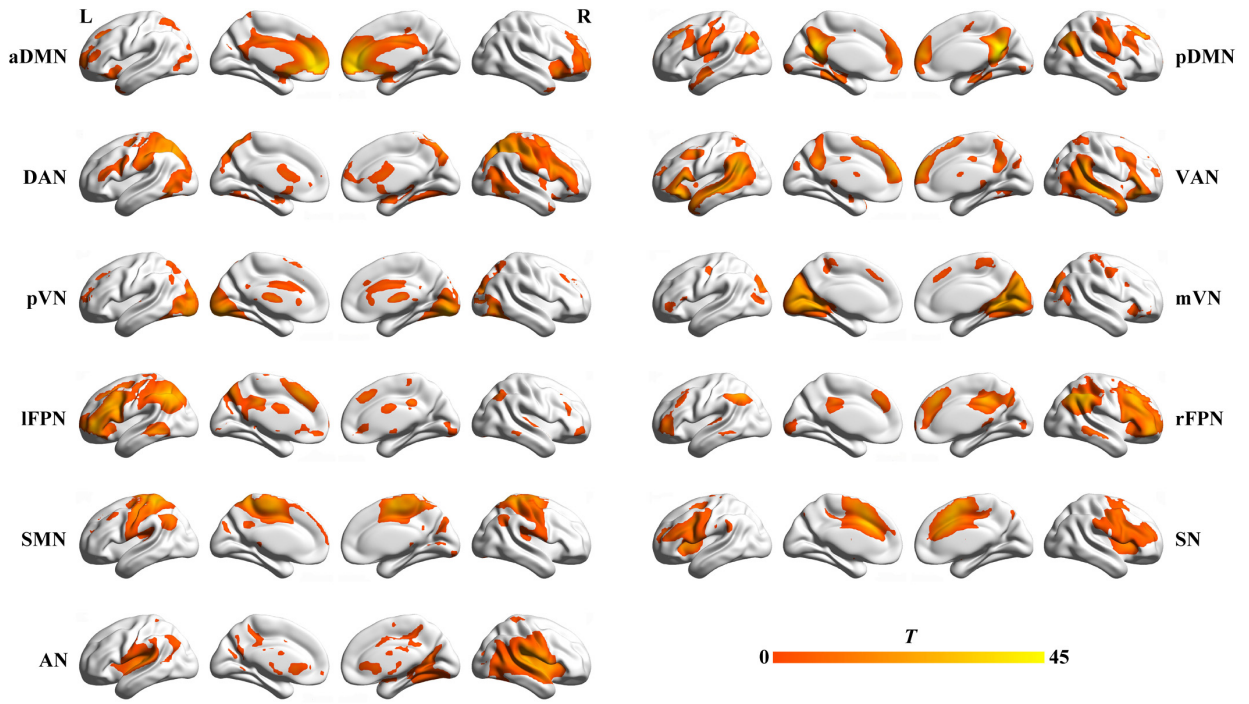


**FIGURE 1 |** Spatial maps of 11 selected functional networks. aDMN, anterior default mode network; pDMN, posterior default mode network; DAN, dorsal attention network; VAN, ventral attention network; pVN, posterior visual network; mVN, medial visual network; lFPN, left frontoparietal network; rFPN, right frontoparietal network; SMN, sensorimotor network; SN, salience network; AN, auditory network; L, left; R, right.

Since our principal focus was set on the group × gender interaction effect on SCVD, a general linear model was utilized to examine this effect with age and education as nuisance variables. In case of significant interaction, we performed *post hoc* pairwise comparisons in SCVD between patients and HC in females and males, respectively. For a gender exhibiting significant group differences, subsequent analyses examining the relationships of SCVD with clinical and neuroimaging data were conducted in this gender. With respect to clinical data, we examined their associations with SCVD using partial correlation analyses controlling for age and education. Multiple comparisons were corrected using the false discovery rate (FDR) method with a corrected significance threshold of $P < 0.05$. In terms of neuroimaging data, inter- and intranetwork functional connectivity were analyzed, respectively. Briefly, differences in internetwork functional connectivity between patients and HC were tested using a general linear model with age, education and FD as nuisance variables. For intranetwork functional connectivity, all participants' spatial maps for each functional network were initially entered into a random-effect one-sample *t*-test. Brain regions were considered to be within each network if they met a height threshold of $P < 0.05$ corrected for multiple comparisons using a family-wise error (FWE) method and an extent threshold of 100 voxels. Within each network, a voxel-wise two-sample *t*-test was then used to examine intranetwork connectivity differences between patients and HC controlling for age, education and FD. Multiple comparisons were corrected using the cluster-level FWE method, resulting in a cluster defining threshold of $P = 0.001$ and a corrected cluster significance of $P < 0.05$. After group comparisons, inter- and intranetwork functional connectivity with significant group differences were extracted for subsequent correlation analyses with SCVD. Finally, we further tested the associations of the SCVD-sensitive functional network connectivity with clinical variables.

To examine the potential relationship among SCVD, functional network connectivity and clinical variables, we tested the SCVD-functional connectivity-clinical variables mediation model where functional connectivity mediated the relation between SCVD and clinical variables. The PROCESS macro[5] available for SPSS (Hayes, 2009, 2014) was used to conduct the mediation analyses. Only variables that showed a significant correlation with others were considered independent, dependent or mediating variables in the mediation analyses. Age, education and FD were included as nuisance variables. Based on 5,000 bootstrap realizations, the significance of mediation effects was determined by the bootstrap 95% confidence interval (CI) in the way a significant indirect effect is indicated when the bootstrap 95% CI does not include zero.

## Sensitivity and Specificity Analyses

Considering a significant effect of BMI on SCVD (Wortsman et al., 2000), we repeated the above-mentioned analyses after additionally adjustment for BMI. To test the specificity of our

[5]http://www.processmacro.org/

results, we also conducted the same analyses in the gender demonstrating no group effect on SCVD.

# RESULTS

## Demographic and Clinical Characteristics

In agreement with our hypothesis, a significant interaction effect ($F = 6.050$, $P = 0.015$) of group × gender on SCVD was observed (**Supplementary Figure 1**). *Post hoc* analyses demonstrated that MDD patients presented with a significant SCVD reduction compared with HC in females ($P < 0.001$) but not males ($P > 0.05$), indicative of a gender-specific effect. As such, we focused our subsequent analyses on females. Demographic and clinical characteristics of the females are shown in **Table 1**. Briefly, there were no significant differences in age (two-sample $t$-test, $t = 0.061$, $P = 0.952$), BMI ($t = -1.076$, $P = 0.284$), and FD ($t = -0.003$, $P = 0.998$) between female patients and controls. Nevertheless, female MDD patients showed lower SCVD ($t = -5.940$, $P < 0.001$), educational level ($t = -4.100$, $P < 0.001$), EBPM ($t = -7.638$, $P < 0.001$), TBPM ($t = -11.482$, $P < 0.001$), CPT-IP-2 ($t = -6.559$, $P < 0.001$), CPT-IP-3 ($t = -4.954$, $P < 0.001$), and CPT-IP-4 ($t = -3.273$, $P = 0.001$), and higher HAMD ($t = 22.244$, $P < 0.001$) and HAMA ($t = 21.287$, $P < 0.001$) than female HC. Among 82 female patients, 11 (13.41%) were classified as vitamin D insufficiency and 70 (85.37%) as deficiency. Additionally, demographic and clinical characteristics of all participants are listed in **Supplementary Table 1**

**TABLE 1 |** Demographic and clinical characteristics of the females.

| Characteristics | MDD ($n$ = 82) | HC ($n$ = 82) | Statistics | $P$-value |
|---|---|---|---|---|
| Age (years) | 44.35 ± 10.28 (21–62) | 44.24 ± 12.75 (21–62) | $t$ = 0.061 | 0.952 |
| Education (years) | 8.45 ± 3.76 (0–16) | 11.15 ± 4.63 (3–20) | $t$ = −4.100 | <0.001 |
| BMI (kg/m$^2$) | 22.39 ± 3.66 (13.93–32.44) | 22.93 ± 2.67 (15.98–31.22) | $t$ = −1.076 | 0.284 |
| HAMD | 30.06 ± 11.25 (1–52) | 1.49 ± 2.97 (0–19) | $t$ = 22.244 | <0.001 |
| HAMA | 20.68 ± 7.40 (2–35) | 1.63 ± 3.31 (0–21) | $t$ = 21.287 | <0.001 |
| EBPM | 2.28 ± 2.55 (0–8) | 5.49 ± 2.82 (0–8) | $t$ = −7.638 | <0.001 |
| TBPM | 1.89 ± 2.27 (0–6) | 5.30 ± 1.45 (0–6) | $t$ = −11.482 | <0.001 |
| CPT-IP-2 | 2.07 ± 1.09 (−0.12–4.24) | 3.11 ± 0.93 (1.11–4.24) | $t$ = −6.559 | <0.001 |
| CPT-IP-3 | 1.50 ± 0.97 (−0.26–4.24) | 2.29 ± 1.08 (0.28–4.24) | $t$ = −4.954 | <0.001 |
| CPT-IP-4 | 0.85 ± 0.69 (−0.41–3.12) | 1.24 ± 0.83 (−0.44–3.34) | $t$ = −3.273 | 0.001 |
| SCVD (nmol/L) | 38.87 ± 12.05 (15.95–78.36) | 50.91 ± 15.83 (21.50–86.25) | $t$ = −5.940 | <0.001 |
| FD (mm) | 0.13 ± 0.09 (0.05–0.60) | 0.13 ± 0.07 (0.06–0.40) | $t$ = −0.003 | 0.998 |
| Illness duration (months) | 62.74 ± 71.44 (0.30–306) | – | – | – |
| Onset age (years) | 38.95 ± 10.46 (19–55) | – | – | – |
| Episode number | 2.52 ± 2.40 (1–21) | – | – | – |
| Antidepressant medications | | | | |
| SSRIs | 58 | – | – | – |
| SNRIs | 19 | – | – | – |
| NaSSA | 5 | – | – | – |

*Data are expressed as means ± standard deviations. Numbers in parentheses are the range. MDD, major depressive disorder; HC, healthy controls; BMI, body mass index; HAMD, Hamilton Rating Scale for Depression; HAMA, Hamilton Rating Scale for Anxiety; EBPM, event-based prospective memory; TBPM, time-based prospective memory; CPT-IP, Continuous Performance Task-Identical Pairs; SCVD, serum concentration of vitamin D; FD, frame-wise displacement; SSRIs, selective serotonin reuptake inhibitors; SNRIs, serotonin norepinephrine reuptake inhibitors; NaSSA, noradrenergic and specific serotonergic antidepressant.*

## Associations Between Serum Concentration of Vitamin D and Clinical Variables in Females

There were significant positive correlations of SCVD with EBPM (partial correlation coefficient [$pr$] = 0.267, $P < 0.001$), TBPM ($pr = 0.355$, $P < 0.001$), and CPT-IP-2 ($pr = 0.215$, $P = 0.006$) in females ($P < 0.05$, FDR corrected). Correlations between SCVD and clinical symptoms (HAMD and HAMA) were not observed in female MDD patients (**Supplementary Table 2**).

## Group Differences of Functional Network Connectivity in Females

In comparison with female HC, female MDD patients manifested reduced functional connectivity between AN and DAN ($F = 3.987$, $P = 0.048$) and between pVN and lFPN ($F = 7.007$, $P = 0.009$) as well as increased connectivity between AN and aDMN ($F = 4.068$, $P = 0.045$), between VAN and SMN ($F = 6.230$, $P = 0.014$) and between SMN and SN ($F = 7.709$, $P = 0.006$).

Voxel-wise intranetwork functional connectivity analyses revealed that female MDD patients exhibited increased connectivity in the bilateral lateral parietal cortex (LPC) of DAN, the right anterior angular gyrus (aANG) and posterior angular gyrus (pANG) of pDMN, the right inferior parietal gyrus (IPG) of rFPN, the left middle cingulate cortex (MCC) of SMN, and the right calcarine sulcus (CAL) of mVN relative to female HC ($P < 0.05$, cluster-level FWE corrected) (**Table 2** and **Supplementary Figure 2**).

## Associations Between Serum Concentration of Vitamin D and Functional Network Connectivity in Females

For internetwork functional connectivity, SCVD was negatively correlated with VAN-SMN connectivity ($pr = -0.272$, $P < 0.001$, **Figures 2A,B**) in females. For intranetwork functional connectivity, SCVD was negatively correlated with connectivity in the right aANG ($pr = -0.253$, $P = 0.001$,

**TABLE 2 |** Brain regions showing increased intranetwork functional connectivity in female MDD patients relative to female HC.

| Regions | Cluster size (voxels) | Peak *t*-values | Coordinates in MNI (*x*-, *y*-, *z*-) |
|---|---|---|---|
| DAN | | | |
| Left lateral parietal cortex | 108 | 4.688 | −27, −69, 39 |
| Right lateral parietal cortex | 437 | 6.650 | 33, −66, 42 |
| pDMN | | | |
| Right anterior angular gyrus | 60 | 5.176 | 54, −60, 30 |
| Right posterior angular gyrus | 29 | 4.615 | 36, −63, 45 |
| rFPN | | | |
| Right inferior parietal gyrus | 53 | 4.699 | 39, −45, 51 |
| SMN | | | |
| Left middle cingulate cortex | 29 | 4.567 | −12, −21, 42 |
| mVN | | | |
| Right calcarine sulcus | 28 | 3.757 | 15, −81, 12 |

*DAN, dorsal attention network; pDMN, posterior default mode network; rFPN, right frontoparietal network; SMN, sensorimotor network; mVN, medial visual network; MDD, major depressive disorder; HC, healthy controls; MNI, Montreal Neurological Institute.*

**Figure 3A**) and pANG ($pr = -0.183$, $P = 0.020$, **Figure 3A**) of pDMN, the right LPC ($pr = -0.276$, $P < 0.001$, **Figure 3B**) of DAN, the right CAL ($pr = -0.167$, $P = 0.034$, **Figure 3C**) of mVN, the right IPG ($pr = -0.180$, $P = 0.023$, **Figure 3D**) of rFPN, and the left MCC ($pr = -0.181$, $P = 0.022$, **Figure 3E**) of SMN in females ($P < 0.05$, FDR corrected).

## Associations Between Serum Concentration of Vitamin D, Functional Network Connectivity and Clinical Variables in Females

For internetwork functional connectivity, VAN-SMN connectivity was negatively correlated with CPT-IP-2 ($pr = -0.221$, $P = 0.005$, **Figure 2C**) in females. In the mediation analysis model, all paths were reported as unstandardized ordinary least squares regression coefficients, namely, total effect of $X$ on $Y$ ($c$) = indirect effect of $X$ on $Y$ through $M$ ($a \times b$) + direct effect of $X$ on $Y$ ($c'$). We found that the relationship between SCVD and CPT-IP-2 was significantly mediated by VAN-SMN connectivity (indirect effect = 0.0031, $SE$ = 0.0018, 95% CI: 0.0005, 0.0076, **Figure 2D**) in females. Moreover, we observed significant negative correlations of VAN-SMN connectivity with HAMD ($pr = -0.231$, $P = 0.040$, **Figure 2E**) and HAMA ($pr = -0.232$, $P = 0.040$, **Figure 2F**) in female MDD patients.

Regarding intranetwork functional connectivity, EBPM was negatively correlated with connectivity in the right aANG ($pr = -0.194$, $P = 0.014$, **Figure 4A**), right LPC ($pr = -0.288$, $P < 0.001$, **Figure 4B**), right CAL ($pr = -0.234$, $P = 0.003$, **Figure 4C**), and right IPG ($pr = -0.188$, $P = 0.017$, **Figure 4D**) in females ($P < 0.05$, FDR corrected). To summarize individual differences in intranetwork functional connectivity, a principal component analysis (PCA) was performed to identify latent components underlying the EBPM-related intranetwork functional connectivity. Based on the Kaiser-Guttman criterion, components with an eigenvalue (EV) < 1.5 were removed. Consequently, only the first intranetwork connectivity component that accounted for 50.73% of the variance was retained and extracted for subsequent mediation analysis. The relationship between SCVD and EBPM was significantly mediated by the first intranetwork connectivity component (indirect effect = 0.0143, $SE$ = 0.0053, 95% CI: 0.0059, 0.0272, **Figure 4E**) in females. In addition, TBPM was negatively correlated with connectivity in the right aANG ($pr = -0.234$, $P = 0.003$, **Figure 5A**), right pANG ($pr = -0.195$, $P = 0.013$, **Figure 5B**), right LPC ($pr = -0.334$, $P < 0.001$, **Figure 5C**), and right IPG ($pr = -0.244$, $P = 0.002$, **Figure 5D**) in females ($P < 0.05$, FDR corrected). PCA revealed that the first intranetwork connectivity component accounted for 51.78% of the variance. The relationship between SCVD and TBPM was significantly mediated by the first intranetwork connectivity component (indirect effect = 0.0127, $SE$ = 0.0048, 95% CI: 0.0048, 0.0240, **Figure 5E**) in females. Finally, CPT-IP-2 was negatively correlated with connectivity in the right LPC ($pr = -0.281$, $P < 0.001$, **Figure 6A**) in females ($P < 0.05$, FDR corrected). Moreover, connectivity in the right LPC significantly mediated the relationship between SCVD and CPT-IP-2 (indirect effect = 0.0043, $SE$ = 0.0018, 95% CI: 0.0015, 0.0086, **Figure 6B**) in females.

No significant correlations were found between functional network connectivity and other clinical variables (**Supplementary Table 3**).

## Sensitivity and Specificity Analyses

After additionally controlling for BMI, the interaction effect of group × gender on SCVD remained significant ($F = 6.066$, $P = 0.015$) and the correlations of SCVD with clinical variables and functional network connectivity were unchanged (**Supplementary Tables 4, 5**), suggesting no influence of BMI on our results. In males, no significant correlations were found between SCVD and clinical variables (**Supplementary Table 6**). The correlations between SCVD and functional network connectivity were non-significant or showed opposite directions in males (**Supplementary Table 7**). In addition, most of the significant correlations between functional network connectivity and clinical variables in females were absent in males (**Supplementary Table 8**).

# DISCUSSION

Our data represent the first report to date exploring the relationship between gender, SCVD, clinical manifestations, and functional network connectivity in a large sample of MDD patients and HC. There were four main findings observed in the present study. First, there was a significant group-by-gender interaction effect on SCVD in the way MDD patients exhibited lower SCVD relative to HC in females rather than males. Second, we identified a female-specific association between lower SCVD and poorer cognitive performance (i.e., prospective memory and

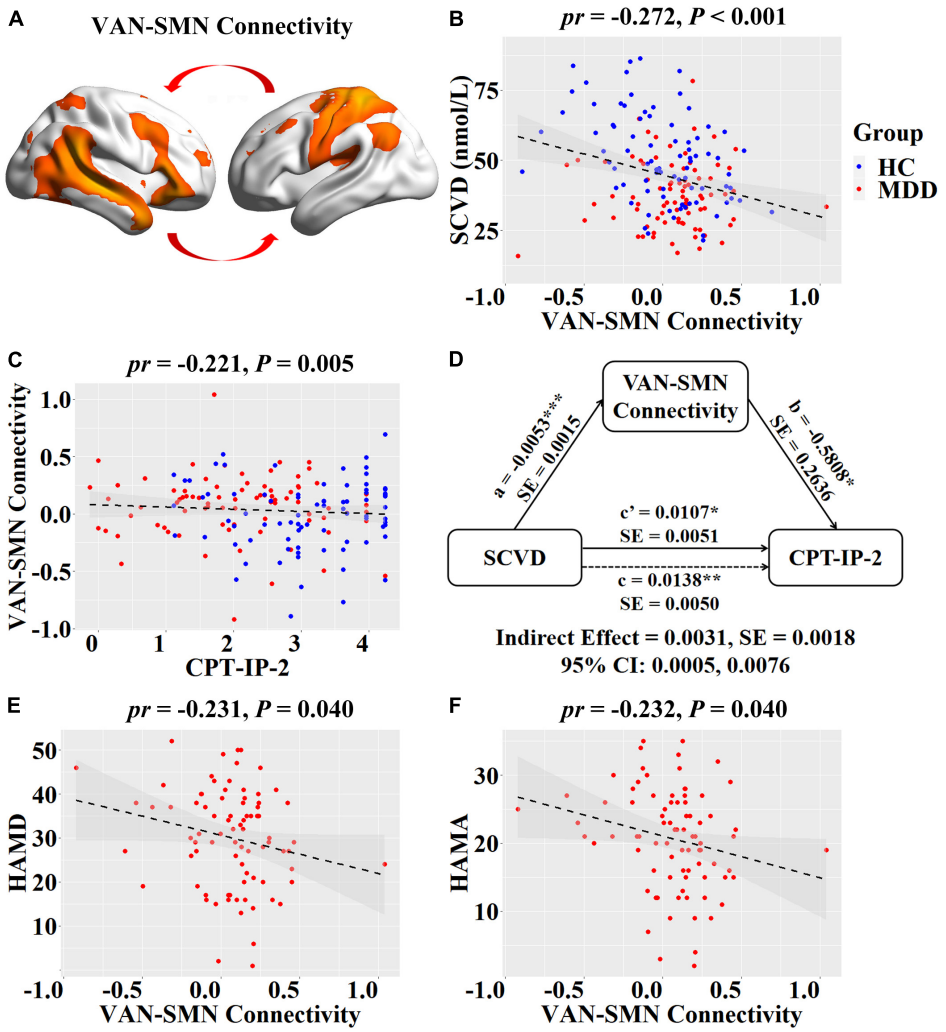


**FIGURE 2 |** Associations between SCVD, internetwork functional connectivity, and clinical variables in females. **(A)** Female patients and controls differed in functional connectivity between VAN and SMN. **(B)** A scatter plot shows correlation between SCVD and VAN-SMN connectivity in females. **(C)** A scatter plot shows correlation between VAN-SMN connectivity and CPT-IP-2 in females. **(D)** Graphical representation of the mediation analysis between SCVD and CPT-IP-2 in females with VAN-SMN connectivity as mediator: estimates of the mediated ($a \times b$), direct ($c'$), and total (c) effects. **(E,F)** Scatter plots show correlations of VAN-SMN connectivity with HAMD and HAMA scores. $^{*}P < 0.05$, $^{**}P < 0.01$, $^{***}P < 0.001$. SCVD, serum concentration of vitamin D; VAN, ventral attention network; SMN, sensorimotor network; CPT-IP, Continuous Performance Task-Identical Pairs; HAMD, Hamilton Rating Scale for Depression; HAMA, Hamilton Rating Scale for Anxiety; HC, healthy controls; MDD, major depressive disorder; *pr*, partial correlation coefficient; SE, standard error; CI, confidence interval.

sustained attention). Third, MDD-related functional network connectivity changes were correlated with SCVD in females as well as depression and anxiety symptoms in female patients with MDD. Finally, MDD- and SCVD-related functional network connectivity alterations mediated the associations between SCVD and cognition in females.

A large number of cross-sectional and longitudinal studies have established an intimate link between low vitamin D and depression (Milaneschi et al., 2010, 2014; Anglin et al., 2013; Ju et al., 2013; Aghajafari et al., 2018; Wong et al., 2018; Briggs et al., 2019), indicating the critical role of low vitamin D in the pathophysiology of MDD. Furthermore, vitamin D supplementation has been shown to hold promise as an effective antidepressant intervention approach (de Koning et al., 2015; Gowda et al., 2015; Casseb et al., 2019; Alghamdi et al., 2020). Overall, these previous findings are coincident with our current observation that MDD patients had significantly lower SCVD (vitamin D insufficiency or deficiency) relative to HC in females.

This study revealed that vitamin D insufficiency and deficiency was more common in females than males, which is in line with many previous studies (Milaneschi et al., 2010; Toffanello et al., 2014b; Song et al., 2016; Yan et al., 2019; Choi et al., 2020; Rhee et al., 2020). Several factors might explain this gender difference, such as insufficient sunlight exposure, higher BMI, more fat tissue, and more sedentary life in females relative to males. Interestingly, females are more likely to suffer from depression than males (Nolen-Hoeksema and Girgus, 1994; Ferrari et al., 2013), with the high-risk periods for developing

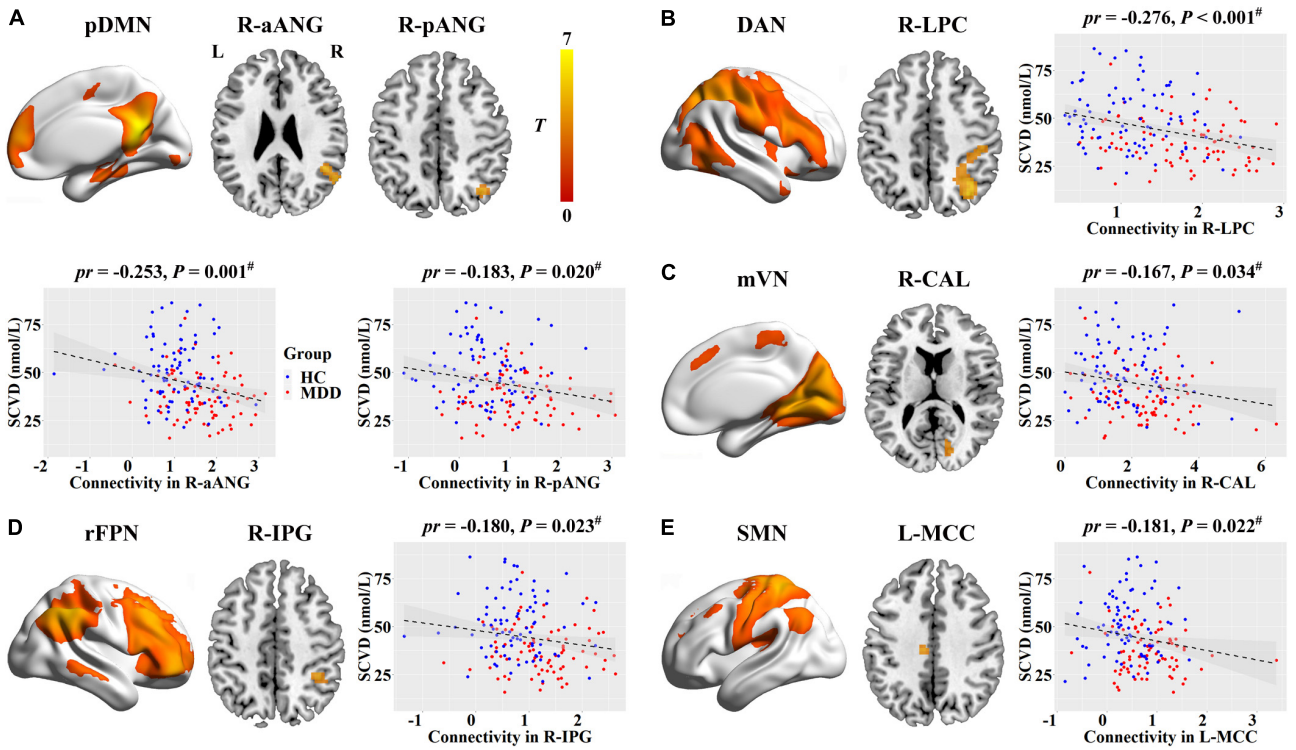


**FIGURE 3 |** Associations between SCVD and intranetwork functional connectivity in females. **(A–E)** SCVD was correlated with intranetwork connectivity in brain regions showing group differences; scatter plots show the correlations between SCVD and intranetwork connectivity. The warm color denotes increased intranetwork connectivity in MDD patients. $^{\#}P < 0.05$, false discovery rate correction for multiple comparisons. SCVD, serum concentration of vitamin D; pDMN, posterior default mode network; aANG, anterior angular gyrus; pANG, posterior angular gyrus; DAN, dorsal attention network; LPC, lateral parietal cortex; mVN, medial visual network; CAL, calcarine sulcus; rFPN, right frontoparietal network; IPG, inferior parietal gyrus; SMN, sensorimotor network; MCC, middle cingulate cortex; HC, healthy controls; MDD, major depressive disorder; L, left; R, right.

depression including adolescence, pregnancy, parturition, and perimenopause (Kessler, 2003; Woods et al., 2008; Amini et al., 2019). Crucially, these periods are typically characterized by a profound hormonal shift, which indicates the importance of gonadal hormones in the heightened predominance of depression among females. Here, we found that MDD patients presented a lower SCVD than HC in females but not males, suggesting a female-specific involvement of vitamin D in the pathogenesis of depression. Combined, these findings might have led to some speculation that abnormal changes of gonadal hormones in females, arising from low vitamin D status, may lead to the development of depression given that vitamin D is related to the production/release of gonadal hormones (Kinuta et al., 2000; Lorenzen et al., 2017). In support of this view, previous research has provided evidence that the gender difference in prevalence of depression is less apparent in later middle age, particularly during menopause when gonadal hormonal flux stabilizes (Bebbington et al., 1998). Besides, it is evident that hormone replacement therapy during the perimenopausal period can be effective in preventing postmenopausal depression (Gordon and Girdler, 2014).

Cognitive dysfunction represents a characteristic feature of MDD (Bortolato et al., 2016; Pan et al., 2019), which is closely linked to depression severity (McDermott and Ebmeier, 2009) and persists following treatment of affective symptoms as well as increases the risk of recurrent depressive episodes (Knight and Baune, 2018), highlighting the need to treat cognitive impairment separately from mood symptoms. In agreement with previous findings, we found that sustained attention and prospective memory were worse in female MDD patients than female HC. Moreover, the worse cognitive performance was related to lower SCVD, extending prior reports of a potentially causal relationship between low vitamin D and cognitive dysfunction in healthy populations (Llewellyn et al., 2011; Balion et al., 2012; Slinin et al., 2012; Annweiler et al., 2013; Toffanello et al., 2014a; Miller et al., 2015; Pettersen, 2017; Pavlovic et al., 2018; Mayne and Burne, 2019) by unraveling such vitamin D-cognition association in a psychiatric population. The present observation also has clinical implications for the development of a precision medicine approach in antidepressant treatment, i.e., assignment of female patients with comorbid MDD and cognitive deficits to adjuvant vitamin D supplementation therapy.

Major depressive disorder patients have been extensively shown to exhibit resting-state functional connectivity abnormalities involving a wide range of functional networks (Sacchet et al., 2016; Wu et al., 2017; Albert et al., 2019; Chen et al., 2019; Liu et al., 2019, 2020, 2021; Yu et al., 2019; Jiao et al., 2020). In the current study, we identified

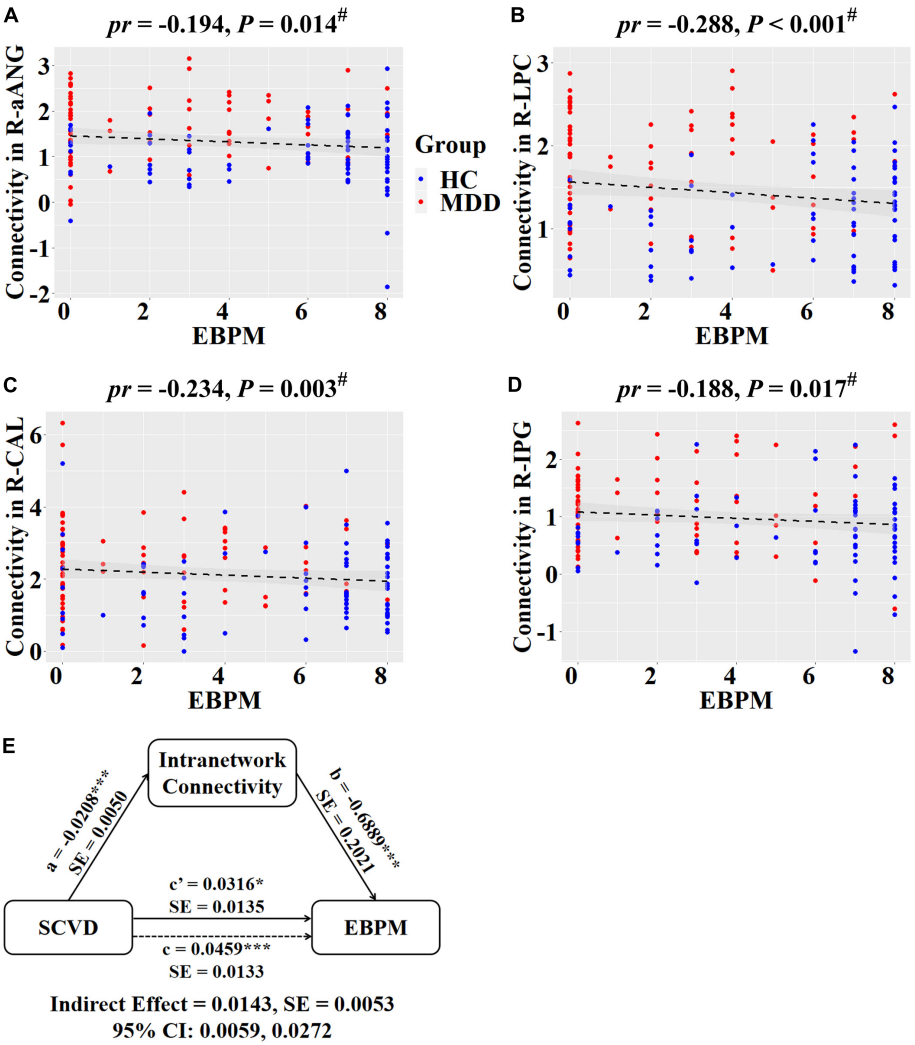


**FIGURE 4 |** Associations between SCVD, intranetwork functional connectivity, and EBPM in females. **(A–D)** Scatter plots show correlations between SCVD-related intranetwork connectivity and EBPM. **(E)** Graphical representation of the mediation analysis between SCVD and EBPM with first intranetwork functional connectivity component as the mediator: estimates of the mediated ($a \times b$), direct ($c'$), and total (c) effects. $^{\#}P < 0.05$, false discovery rate correction for multiple comparisons. $^{*}P < 0.05$, $^{***}P < 0.001$. SCVD, serum concentration of vitamin D; EBPM, event-based prospective memory; aANG, anterior angular gyrus; LPC, lateral parietal cortex; CAL, calcarine sulcus; IPG, inferior parietal gyrus; HC, healthy controls; MDD, major depressive disorder; R, right; *pr*, partial correlation coefficient; SE, standard error; CI, confidence interval.

a complex pattern of decreased (AN-DAN and pVN-lFPN connectivity) and increased (AN-aDMN, VAN-SMN, and SMN-SN connectivity) internetwork functional connectivity as well as increased intranetwork connectivity (DAN, pDMN, rFPN, SMN, and mVN) in female MDD patients. Although some of these functional network connectivity alterations are coherent with prior reports, some are at odds with previous findings of decreased intranetwork functional connectivity in particular. The commonalities and differences with earlier research may be due to the fact that we focused our analysis on females and thus identified functional network connectivity alterations specific to female patients with MDD, whereas earlier research has examined functional network connectivity changes in mixed patients.

Vitamin D plays an important role in neuronal development and brain function as well as the synthesis, release, and regulation of neurotransmitters (Fernandes de Abreu et al., 2009; Eyles et al., 2013; Patrick and Ames, 2014, 2015; Kesby et al., 2017). Vitamin D exerts its effects on the brain via binding to vitamin D receptors (Ryan et al., 2015), which are broadly distributed in the prefrontal cortex, cingulate cortex, and limbic system (Eyles et al., 2005). In recent years, the relationship between vitamin D and the brain has attracted much interest from neuroimaging investigators. For instance, Annweiler et al. (2014) found that vitamin D depletion was associated with smaller brain volume and larger lateral cerebral ventricles. Another structural MRI study reported a negative correlation between vitamin D and intracranial volume as well as total cortical gray and cerebral white matter volumes in

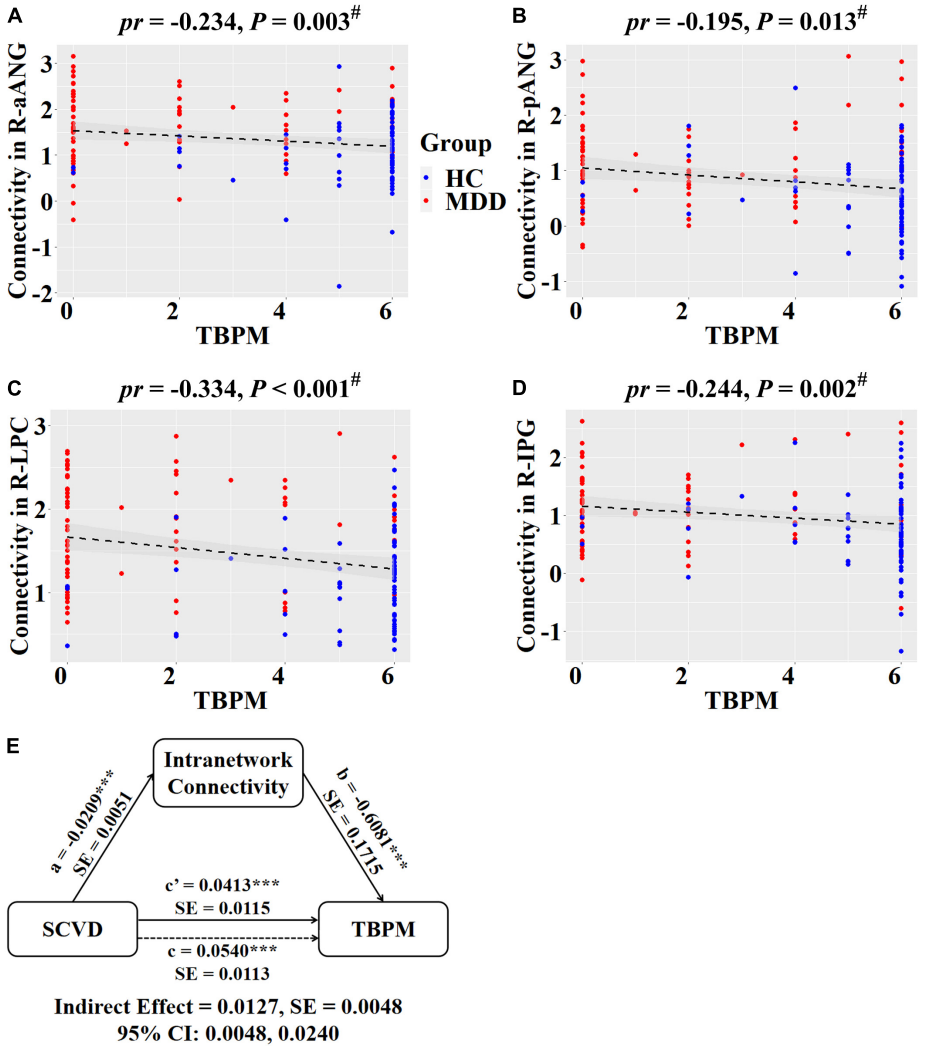


**FIGURE 5 |** Associations between SCVD, intranetwork functional connectivity, and TBPM in females. **(A–D)** Scatter plots show correlations between SCVD-related intranetwork connectivity and TBPM. **(E)** Graphical representation of the mediation analysis between SCVD and TBPM with first intranetwork functional connectivity component as the mediator: estimates of the mediated ($a \times b$), direct ($c'$), and total ($c$) effects. $^{\#}P < 0.05$, false discovery rate correction for multiple comparisons. $^{***}P < 0.001$. SCVD, serum concentration of vitamin D; TBPM, time-based prospective memory; aANG, anterior angular gyrus; pANG, posterior angular gyrus; LPC, lateral parietal cortex; IPG, inferior parietal gyrus; HC, healthy controls; MDD, major depressive disorder; R, right; *pr*, partial correlation coefficient; SE, standard error; CI, confidence interval.

healthy young women (Plozer et al., 2015). In older adults, lower vitamin D has been found to relate to lower gray matter volume of the hippocampus (Karakis et al., 2016) and calcarine sulcus (Ali et al., 2020) as well as thinner cingulate cortex (Foucault et al., 2019). Of note, our earlier work identified an association between lower SCVD and more severe depressive symptoms in MDD patients, which was mediated by total intracranial volume (Zhu et al., 2019). Nevertheless, these prior studies place less emphasis on brain functional measures that may represent a more sensitive and specific index of state-related changes and instead focus on structural measures that are more stable and thus may reflect more enduring signatures. By means of functional network connectivity analysis, we observed that lower SCVD was associated with higher VAN-SMN functional connectivity and higher intranetwork connectivity of pDMN, DAN, mVN, rFPN, and SMN that characterized MDD in females. Moreover, higher VAN-SMN functional connectivity was associated with depression and anxiety symptoms in female patients, which is consistent with previous research (Yu et al., 2019). Our data support the concept that brain functional measures are able to more sensitively detect small effects and more closely track symptom expression.

Critically, we found that the MDD- and SCVD-related functional network connectivity changes were related to sustained attention and prospective memory in females. Furthermore, the functional network connectivity alterations mediated the relationship between SCVD and cognitive performance. These findings endorse the notion that complex

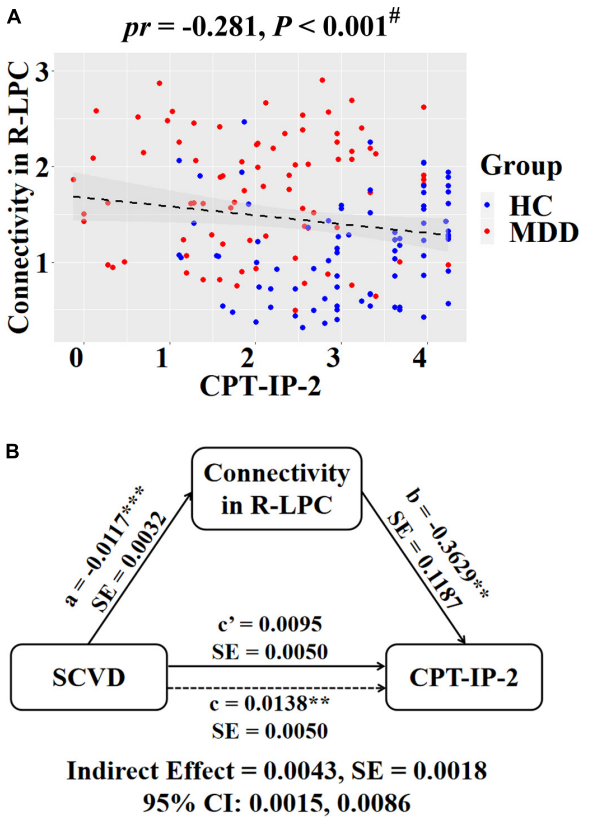


**FIGURE 6 |** Associations between SCVD, intranetwork functional connectivity, and CPT-IP-2 in females. **(A)** A scatter plot shows correlation between intranetwork connectivity in the right LPC and CPT-IP-2. **(B)** Graphical representation of the mediation analysis between SCVD and CPT-IP-2 with intranetwork connectivity in the right LPC as the mediator: estimates of the mediated ($a \times b$), direct ($c'$), and total ($c$) effects. $^{\#}P < 0.05$, false discovery rate correction for multiple comparisons. $^{**}P < 0.01$, $^{***}P < 0.001$. SCVD, serum concentration of vitamin D; CPT-IP, Continuous Performance Task-Identical Pairs; LPC, lateral parietal cortex; HC, healthy controls; MDD, major depressive disorder; R, right; *pr*, partial correlation coefficient; SE, standard error; CI, confidence interval.

cognitive functions are supposed to rely on a variety of neural processes arising from integration and segregation of different functional networks. Specifically, sustained attention was related to VAN-SMN functional connectivity and intranetwork connectivity of DAN. DAN is involved in goal-directed (top-down) control of attention and VAN, coupled with sensory systems, is implicated in stimulus-driven control of attention (Corbetta and Shulman, 2002; Vossel et al., 2014). Our results corroborate the importance of both attention networks in attention-demanding cognitive tasks. In addition, EBPM was related to intranetwork connectivity of pDMN, DAN, rFPN and mVN, and TBPM was linked to intranetwork connectivity of pDMN, DAN and rFPN. DMN can be typically divided into anterior and posterior sub-networks (Andrews-Hanna et al., 2010), with pDMN predominantly engaged in memory processing (Andrews-Hanna et al., 2014; Raichle, 2015). FPN appears to be most active during cognitive tasks involving working memory (Mulders et al., 2015). Notably, the prominent involvement of mVN in EBPM but not TBPM may be attributable to the fact that detecting and processing of visual stimuli are a prerequisite for EBPM tasks. Altogether, our data might help elucidate the potential neural mechanisms by which lower SCVD contributes to cognitive dysfunction in female MDD patients.

There are several limitations that should be mentioned. First, our results might be influenced by the confounds of antidepressant treatment and illness chronicity. Future studies in a sample of first-episode, medication-naive patients with MDD are required to validate our preliminary findings. Second, despite several independent components identified as meaningful functional networks according to a strict selection procedure, there are possible biases, e.g., some non-typical but physiologically important functional networks might have been ignored. Third, MDD patients and HC differed significantly in educational level. While education was included as a covariate of no interest in our analyses, its potential residual effects cannot be ruled out completely. Fourth, it should be noted that patients with anxiety disorders were excluded. Since anxiety is frequently comorbid with MDD, this reduces the generalizability of the findings to the general population with MDD. Fifth, this study is cross-sectional and therefore cannot discern between cause and effect. Longitudinal studies are necessary for determining causality between determinant and outcome. Finally, we did not collect more information concerning the participants' lifestyle characteristics. Analyzing these relevant data may aid in further understanding our findings.

In summary, the current work demonstrated a plausible relationship between low vitamin D, functional network dysconnectivity, and clinical presentations in female patients with MDD. Our data provide evidence for a female-specific neurobiological mechanism whereby low vitamin D might give rise to MDD and its associated clinical characteristics. More broadly, these findings may inform a novel conceptualization that adjuvant vitamin D supplementation therapy may yield clinical benefits in improving treatment outcomes in female patients with MDD.

## DATA AVAILABILITY STATEMENT

The raw data supporting the conclusions of this article will be made available by the authors, without undue reservation.

## ETHICS STATEMENT

The studies involving human participants were reviewed and approved by The First Affiliated Hospital of Anhui Medical University. The patients/participants provided their written informed consent to participate in this study.

## AUTHOR CONTRIBUTIONS

WZ and YY designed the research, analyzed the data, and wrote the manuscript. D-MZ conducted the clinical evaluation and

acquired the clinical data. SC, PJ, CZ, and YZ acquired the MRI data. JZ reviewed the manuscript for intellectual content. All authors contributed to and have approved the final manuscript.

## FUNDING

This study was supported by the National Natural Science Foundation of China (grant numbers: 81801679, 82071905, and 81771817).

## ACKNOWLEDGMENTS

The authors are grateful to study participants for volunteering their time.

## SUPPLEMENTARY MATERIAL

The Supplementary Material for this article can be found online at: https://www.frontiersin.org/articles/10.3389/fnagi.2022.817607/full#supplementary-material

## REFERENCES

Aghajafari, F., Letourneau, N., Mahinpey, N., Cosic, N., and Giesbrecht, G. (2018). Vitamin D deficiency and antenatal and postpartum depression: a systematic review. *Nutrients* 10:478. doi: 10.3390/nu10040478

Albert, K. M., Potter, G. G., Boyd, B. D., Kang, H., and Taylor, W. D. (2019). Brain network functional connectivity and cognitive performance in major depressive disorder. *J. Psychiatr. Res.* 110, 51–56. doi: 10.1016/j.jpsychires.2018.11.020

Alghamdi, S., Alsulami, N., Khoja, S., Alsufiani, H., Tayeb, H. O., and Tarazi, F. I. (2020). Vitamin D supplementation ameliorates severity of major depressive disorder. *J. Mol. Neurosci.* 70, 230–235. doi: 10.1007/s12031-019-01461-2

Ali, P., Labriffe, M., Navasiolava, N., Custaud, M. A., Dinomais, M., and Annweiler, C. (2020). Vitamin D concentration and focal brain atrophy in older adults: a voxel-based morphometric study. *Ann. Clin. Transl. Neurol.* 7, 554–558. doi: 10.1002/acn3.50997

Amin, Z., Canli, T., and Epperson, C. N. (2005). Effect of estrogen-serotonin interactions on mood and cognition. *Behav. Cogn. Neurosci. Rev.* 4, 43–58. doi: 10.1177/1534582305277152

Amini, S., Jafarirad, S., and Amani, R. (2019). Postpartum depression and vitamin D: a systematic review. *Crit. Rev. Food Sci. Nutr.* 59, 1514–1520. doi: 10.1080/10408398.2017.1423276

Andrews-Hanna, J. R., Reidler, J. S., Sepulcre, J., Poulin, R., and Buckner, R. L. (2010). Functional-anatomic fractionation of the brain's default network. *Neuron* 65, 550–562. doi: 10.1016/j.neuron.2010.02.005

Andrews-Hanna, J. R., Smallwood, J., and Spreng, R. N. (2014). The default network and self-generated thought: component processes, dynamic control, and clinical relevance. *Ann. N. Y. Acad. Sci.* 1316, 29–52. doi: 10.1111/nyas.12360

Anglin, R. E., Samaan, Z., Walter, S. D., and McDonald, S. D. (2013). Vitamin D deficiency and depression in adults: systematic review and meta-analysis. *Br. J. Psychiatry* 202, 100–107. doi: 10.1192/bjp.bp.111.106666

Annweiler, C., Annweiler, T., Montero-Odasso, M., Bartha, R., and Beauchet, O. (2014). Vitamin D and brain volumetric changes: systematic review and meta-analysis. *Maturitas* 78, 30–39. doi: 10.1016/j.maturitas.2014.02.013

Annweiler, C., Montero-Odasso, M., Llewellyn, D. J., Richard-Devantoy, S., Duque, G., and Beauchet, O. (2013). Meta-analysis of memory and executive dysfunctions in relation to vitamin D. *J. Alzheimers Dis.* 37, 147–171. doi: 10.3233/JAD-130452

Ashburner, J. (2007). A fast diffeomorphic image registration algorithm. *Neuroimage* 38, 95–113. doi: 10.1016/j.neuroimage.2007.07.007

Balion, C., Griffith, L. E., Strifler, L., Henderson, M., Patterson, C., Heckman, G., et al. (2012). Vitamin D, cognition, and dementia: a systematic review and meta-analysis. *Neurology* 79, 1397–1405. doi: 10.1212/WNL.0b013e31826c197f

Bangasser, D. A., and Valentino, R. J. (2014). Sex differences in stress-related psychiatric disorders: neurobiological perspectives. *Front. Neuroendocrinol.* 35:303–319. doi: 10.1016/j.yfrne.2014.03.008

Bebbington, P. E., Dunn, G., Jenkins, R., Lewis, G., Brugha, T., Farrell, M., et al. (1998). The influence of age and sex on the prevalence of depressive conditions: report from the National Survey of Psychiatric Morbidity. *Psychol. Med.* 28, 9–19. doi: 10.1017/s0033291797006077

Berk, M., Sanders, K. M., Pasco, J. A., Jacka, F. N., Williams, L. J., Hayles, A. L., et al. (2007). Vitamin D deficiency may play a role in depression. *Med. Hypotheses* 69, 1316–1319. doi: 10.1016/j.mehy.2007.04.001

Bertone-Johnson, E. R., Powers, S. I., Spangler, L., Brunner, R. L., Michael, Y. L., Larson, J. C., et al. (2011). Vitamin D intake from foods and supplements and depressive symptoms in a diverse population of older women. *Am. J. Clin. Nutr.* 94, 1104–1112. doi: 10.3945/ajcn.111.017384

Biswal, B., Yetkin, F. Z., Haughton, V. M., and Hyde, J. S. (1995). Functional connectivity in the motor cortex of resting human brain using echo-planar MRI. *Magn. Reson. Med.* 34, 537–541. doi: 10.1002/mrm.1910340409

Bortolato, B., Miskowiak, K. W., Kohler, C. A., Maes, M., Fernandes, B. S., Berk, M., et al. (2016). Cognitive remission: a novel objective for the treatment of major depression? *BMC Med.* 14:9. doi: 10.1186/s12916-016-0560-3

Boulkrane, M. S., Fedotova, J., Kolodyaznaya, V., Micale, V., Drago, F., van den Tol, A. J. M., et al. (2020). Vitamin D and depression in women: a mini-review. *Curr. Neuropharmacol.* 18, 288–300. doi: 10.2174/1570159X17666191108111120

Bourke, C. H., Harrell, C. S., and Neigh, G. N. (2012). Stress-induced sex differences: adaptations mediated by the glucocorticoid receptor. *Horm. Behav.* 62, 210–218. doi: 10.1016/j.yhbeh.2012.02.024

Briggs, R., McCarroll, K., O'Halloran, A., Healy, M., Kenny, R. A., and Laird, E. (2019). Vitamin D deficiency is associated with an increased likelihood of incident depression in community-dwelling older adults. *J. Am. Med. Dir. Assoc.* 20, 517–523. doi: 10.1016/j.jamda.2018.10.006

Cai, H., Wang, C., Qian, Y., Zhang, S., Zhang, C., Zhao, W., et al. (2021). Large-scale functional network connectivity mediate the associations of gut microbiota with sleep quality and executive functions. *Hum. Brain Mapp.* 42, 3088–3101. doi: 10.1002/hbm.25419

Calhoun, V. D., Adali, T., Pearlson, G. D., and Pekar, J. J. (2001a). A method for making group inferences from functional MRI data using independent component analysis. *Hum. Brain Mapp.* 14, 140–151. doi: 10.1002/hbm.1048

Calhoun, V. D., Adali, T., Pearlson, G. D., and Pekar, J. J. (2001b). Spatial and temporal independent component analysis of functional MRI data containing a pair of task-related waveforms. *Hum. Brain Mapp.* 13, 43–53. doi: 10.1002/hbm.1024

Casseb, G. A. S., Kaster, M. P., and Rodrigues, A. L. S. (2019). Potential role of Vitamin D for the management of depression and anxiety. *CNS Drugs* 33, 619–637. doi: 10.1007/s40263-019-00640-4

Chen, H., Liu, K., Zhang, B., Zhang, J., Xue, X., Lin, Y., et al. (2019). More optimal but less regulated dorsal and ventral visual networks in patients with major depressive disorder. *J. Psychiatr. Res.* 110, 172–178. doi: 10.1016/j.jpsychires.2019.01.005

Cheng, H., Yang, Z., Dong, B., Chen, C., Zhang, M., Huang, Z., et al. (2013). Chemotherapy-induced prospective memory impairment in patients with breast cancer. *Psychooncology* 22, 2391–2395. doi: 10.1002/pon.3291

Choi, J. H., Lee, B., Lee, J. Y., Kim, C. H., Park, B., Kim, D. Y., et al. (2020). Relationship between sleep duration, sun exposure, and serum 25-hydroxyvitamin d status: a cross-sectional study. *Sci. Rep.* 10:4168. doi: 10.1038/s41598-020-61061-8

Corbetta, M., and Shulman, G. L. (2002). Control of goal-directed and stimulus-driven attention in the brain. *Nat. Rev. Neurosci.* 3, 201–215. doi: 10.1038/nrn755

Cornblatt, B. A., Risch, N. J., Faris, G., Friedman, D., and Erlenmeyer-Kimling, L. (1988). The Continuous Performance Test, identical pairs version (CPT-IP): I. New findings about sustained attention in normal families. *Psychiatry Res.* 26, 223–238. doi: 10.1016/0165-1781(88)90076-5

Damoiseaux, J. S., Rombouts, S. A., Barkhof, F., Scheltens, P., Stam, C. J., Smith, S. M., et al. (2006). Consistent resting-state networks across healthy subjects. *Proc. Natl. Acad. Sci. U.S.A.* 103, 13848–13853. doi: 10.1073/pnas.0601417103

de Koning, E. J., van Schoor, N. M., Penninx, B. W., Elders, P. J., Heijboer, A. C., Smit, J. H., et al. (2015). Vitamin D supplementation to prevent depression and poor physical function in older adults: study protocol of the D-Vitaal study, a randomized placebo-controlled clinical trial. *BMC Geriatr.* 15:151. doi: 10.1186/s12877-015-0148-3

Einstein, G. O., and McDaniel, M. A. (1990). Normal aging and prospective memory. *J. Exp. Psychol. Learn. Mem. Cogn.* 16, 717–726. doi: 10.1037//0278-7393.16.4.717

Eyles, D. W., Burne, T. H., and McGrath, J. J. (2013). Vitamin D, effects on brain development, adult brain function and the links between low levels of vitamin D and neuropsychiatric disease. *Front. Neuroendocrinol.* 34:47–64. doi: 10.1016/j.yfrne.2012.07.001

Eyles, D. W., Smith, S., Kinobe, R., Hewison, M., and McGrath, J. J. (2005). Distribution of the vitamin D receptor and 1 alpha-hydroxylase in human brain. *J. Chem. Neuroanat.* 29, 21–30. doi: 10.1016/j.jchemneu.2004.08.006

Fernandes de Abreu, D. A., Eyles, D., and Feron, F. (2009). Vitamin D, a neuro-immunomodulator: implications for neurodegenerative and autoimmune diseases. *Psychoneuroendocrinology* 34(Suppl. 1), S265–S277. doi: 10.1016/j.psyneuen.2009.05.023

Fernandez-Guasti, A., Fiedler, J. L., Herrera, L., and Handa, R. J. (2012). Sex, stress, and mood disorders: at the intersection of adrenal and gonadal hormones. *Horm. Metab. Res.* 44, 607–618. doi: 10.1055/s-0032-1312592

Ferrari, A. J., Charlson, F. J., Norman, R. E., Patten, S. B., Freedman, G., Murray, C. J., et al. (2013). Burden of depressive disorders by country, sex, age, and year: findings from the global burden of disease study 2010. *PLoS Med.* 10:e1001547. doi: 10.1371/journal.pmed.1001547

Foucault, G., Duval, G. T., Simon, R., Beauchet, O., Dinomais, M., and Annweiler, C. (2019). Serum Vitamin D and cingulate cortex thickness in older adults: quantitative MRI of the brain. *Curr. Alzheimer Res.* 16, 1063–1071. doi: 10.2174/1567205016666191113124356

Gordon, J. L., and Girdler, S. S. (2014). Hormone replacement therapy in the treatment of perimenopausal depression. *Curr. Psychiatry Rep.* 16:517. doi: 10.1007/s11920-014-0517-1

Gowda, U., Mutowo, M. P., Smith, B. J., Wluka, A. E., and Renzaho, A. M. (2015). Vitamin D supplementation to reduce depression in adults: meta-analysis of randomized controlled trials. *Nutrition* 31, 421–429. doi: 10.1016/j.nut.2014.06.017

Han, G., Klimes-Dougan, B., Jepsen, S., Ballard, K., Nelson, M., Houri, A., et al. (2012). Selective neurocognitive impairments in adolescents with major depressive disorder. *J. Adolesc.* 35, 11–20. doi: 10.1016/j.adolescence.2011.06.009

Hayes, A. F. (2009). Beyond baron and kenny: statistical mediation analysis in the new millennium. *Commun. Monogr.* 76, 408–420. doi: 10.1080/03637750903310360

Hayes, A. F. (2014). Introduction to mediation, moderation, and conditional process analysis: a regression-based approach. *J. Educ. Meas.* 51, 335–337. doi: 10.1111/jedm.12050

Holtzheimer, P. E. III, and Nemeroff, C. B. (2006). Future prospects in depression research. *Dialogues Clin. Neurosci.* 8, 175–189.

Jiao, K., Xu, H., Teng, C., Song, X., Xiao, C., Fox, P. T., et al. (2020). Connectivity patterns of cognitive control network in first episode medication-naive depression and remitted depression. *Behav. Brain Res.* 379:112381. doi: 10.1016/j.bbr.2019.112381

Jones, P. B. (2013). Adult mental health disorders and their age at onset. *Br. J. Psychiatry Suppl.* 54, s5–s10. doi: 10.1192/bjp.bp.112.119164

Ju, S. Y., Lee, Y. J., and Jeong, S. N. (2013). Serum 25-hydroxyvitamin D levels and the risk of depression: a systematic review and meta-analysis. *J. Nutr. Health Aging* 17, 447–455. doi: 10.1007/s12603-012-0418-0

Karakis, I., Pase, M. P., Beiser, A., Booth, S. L., Jacques, P. F., Rogers, G., et al. (2016). Association of serum Vitamin D with the risk of incident dementia and subclinical indices of brain aging: the framingham heart study. *J. Alzheimers Dis.* 51, 451–461. doi: 10.3233/JAD-150991

Kesby, J. P., Turner, K. M., Alexander, S., Eyles, D. W., McGrath, J. J., and Burne, T. H. J. (2017). Developmental vitamin D deficiency alters multiple neurotransmitter systems in the neonatal rat brain. *Int. J. Dev. Neurosci.* 62, 1–7. doi: 10.1016/j.ijdevneu.2017.07.002

Kessler, R. (2003). Epidemiology of women and depression. *J. Affect. Disord.* 74, 5–13. doi: 10.1016/s0165-0327(02)00426-3

Kinuta, K., Tanaka, H., Moriwake, T., Aya, K., Kato, S., and Seino, Y. (2000). Vitamin D is an important factor in estrogen biosynthesis of both female and male gonads. *Endocrinology* 141, 1317–1324. doi: 10.1210/endo.141.4.7403

Kjaergaard, M., Joakimsen, R., and Jorde, R. (2011). Low serum 25-hydroxyvitamin D levels are associated with depression in an adult Norwegian population. *Psychiatry Res.* 190, 221–225. doi: 10.1016/j.psychres.2011.06.024

Knight, M. J., and Baune, B. T. (2018). Cognitive dysfunction in major depressive disorder. *Curr. Opin. Psychiatry* 31, 26–31. doi: 10.1097/YCO.0000000000000378

Lerner, P. P., Sharony, L., and Miodownik, C. (2018). Association between mental disorders, cognitive disturbances and vitamin D serum level: current state. *Clin. Nutr. ESPEN* 23, 89–102. doi: 10.1016/j.clnesp.2017.11.011

Liu, G., Jiao, K., Zhong, Y., Hao, Z., Wang, C., Xu, H., et al. (2021). The alteration of cognitive function networks in remitted patients with major depressive disorder: an independent component analysis. *Behav. Brain Res* .400:113018. doi: 10.1016/j.bbr.2020.113018

Liu, J., Xu, P., Zhang, J., Jiang, N., Li, X., and Luo, Y. (2019). Ventral attention-network effective connectivity predicts individual differences in adolescent depression. *J. Affect. Disord.* 252, 55–59. doi: 10.1016/j.jad.2019.04.033

Liu, Y., Chen, Y., Liang, X., Li, D., Zheng, Y., Zhang, H., et al. (2020). Altered resting-state functional connectivity of multiple networks and disrupted correlation with executive function in major depressive disorder. *Front. Neurol.* 11:272. doi: 10.3389/fneur.2020.00272

Llewellyn, D. J., Lang, I. A., Langa, K. M., and Melzer, D. (2011). Vitamin D and cognitive impairment in the elderly U.S. population. *J. Gerontol. A Biol. Sci. Med. Sci.* 66, 59–65. doi: 10.1093/gerona/glq185

Lorenzen, M., Boisen, I. M., Mortensen, L. J., Lanske, B., Juul, A., and Blomberg Jensen, M. (2017). Reproductive endocrinology of vitamin D. *Mol. Cell Endocrinol.* 453, 103–112. doi: 10.1016/j.mce.2017.03.023

Mayne, P. E., and Burne, T. H. J. (2019). Vitamin D in synaptic plasticity, cognitive function, and neuropsychiatric illness. *Trends Neurosci.* 42, 293–306. doi: 10.1016/j.tins.2019.01.003

McDaniel, M. A., and Einstein, G. O. (2011). The neuropsychology of prospective memory in normal aging: a componential approach. *Neuropsychologia* 49, 2147–2155. doi: 10.1016/j.neuropsychologia.2010.12.029

McDermott, L. M., and Ebmeier, K. P. (2009). A meta-analysis of depression severity and cognitive function. *J. Affect. Disord.* 119, 1–8. doi: 10.1016/j.jad.2009.04.022

McFarland, C. P., and Vasterling, J. J. (2018). Prospective memory in depression: review of an emerging field. *Arch. Clin. Neuropsychol.* 33, 912–930. doi: 10.1093/arclin/acx118

Milaneschi, Y., Hoogendijk, W., Lips, P., Heijboer, A. C., Schoevers, R., van Hemert, A. M., et al. (2014). The association between low vitamin D and depressive disorders. *Mol. Psychiatry* 19, 444–451. doi: 10.1038/mp.2013.36

Milaneschi, Y., Shardell, M., Corsi, A. M., Vazzana, R., Bandinelli, S., Guralnik, J. M., et al. (2010). Serum 25-hydroxyvitamin D and depressive symptoms in older women and men. *J. Clin. Endocrinol. Metab.* 95, 3225–3233. doi: 10.1210/jc.2010-0347

Miller, J. W., Harvey, D. J., Beckett, L. A., Green, R., Farias, S. T., Reed, B. R., et al. (2015). Vitamin D status and rates of cognitive decline in a multiethnic cohort of older adults. *JAMA Neurol.* 72, 1295–1303. doi: 10.1001/jamaneurol.2015.2115

Mulders, P. C., van Eijndhoven, P. F., Schene, A. H., Beckmann, C. F., and Tendolkar, I. (2015). Resting-state functional connectivity in major depressive disorder: a review. *Neurosci. Biobehav. Rev.* 56, 330–344. doi: 10.1016/j.neubiorev.2015.07.014

Nolen-Hoeksema, S., and Girgus, J. S. (1994). The emergence of gender differences in depression during adolescence. *Psychol. Bull.* 115, 424–443. doi: 10.1037/0033-2909.115.3.424

Pan, Z., Park, C., Brietzke, E., Zuckerman, H., Rong, C., Mansur, R. B., et al. (2019). Cognitive impairment in major depressive disorder. *CNS Spectr.* 24, 22–29. doi: 10.1017/S1092852918001207

Patrick, R. P., and Ames, B. N. (2014). Vitamin D hormone regulates serotonin synthesis. Part 1: relevance for autism. *FASEB J.* 28, 2398–2413. doi: 10.1096/fj.13-246546

Patrick, R. P., and Ames, B. N. (2015). Vitamin D and the omega-3 fatty acids control serotonin synthesis and action, part 2: relevance for ADHD, bipolar disorder, schizophrenia, and impulsive behavior. *FASEB J.* 29, 2207–2222. doi: 10.1096/fj.14-268342

Pavlovic, A., Abel, K., Barlow, C. E., Farrell, S. W., Weiner, M., and DeFina, L. F. (2018). The association between serum vitamin d level and cognitive function in older adults: cooper center longitudinal study. *Prev. Med.* 113, 57–61. doi: 10.1016/j.ypmed.2018.05.010

Pettersen, J. A. (2017). Does high dose vitamin D supplementation enhance cognition?: A randomized trial in healthy adults. *Exp. Gerontol.* 90, 90–97. doi: 10.1016/j.exger.2017.01.019

Plozer, E., Altbacker, A., Darnai, G., Perlaki, G., Orsi, G., Nagy, S. A., et al. (2015). Intracranial volume inversely correlates with serum 25(OH)D level in healthy young women. *Nutr. Neurosci.* 18, 37–40. doi: 10.1179/1476830514Y.0000000109

Power, J. D., Cohen, A. L., Nelson, S. M., Wig, G. S., Barnes, K. A., Church, J. A., et al. (2011). Functional network organization of the human brain. *Neuron* 72, 665–678. doi: 10.1016/j.neuron.2011.09.006

Raichle, M. E. (2015). The brain's default mode network. *Annu. Rev. Neurosci.* 38, 433–447. doi: 10.1146/annurev-neuro-071013-014030

Rhee, S. J., Lee, H., and Ahn, Y. M. (2020). Serum Vitamin D concentrations are associated with depressive symptoms in men: the sixth korea national health and nutrition examination survey 2014. *Front. Psychiatry* 11:756. doi: 10.3389/fpsyt.2020.00756

Ringe, J. D., and Kipshoven, C. (2012). Vitamin D-insufficiency: an estimate of the situation in Germany. *Dermatoendocrinology* 4, 72–80. doi: 10.4161/derm.19829

Rock, P. L., Roiser, J. P., Riedel, W. J., and Blackwell, A. D. (2014). Cognitive impairment in depression: a systematic review and meta-analysis. *Psychol. Med.* 44, 2029–2040. doi: 10.1017/S0033291713002535

Roy, N. M. (2021). Impact of vitamin D on neurocognitive function in dementia, depression, schizophrenia and ADHD. *Front. Biosci.* 26:566–611. doi: 10.2741/4908

Ryan, J. W., Anderson, P. H., and Morris, H. A. (2015). Pleiotropic activities of vitamin d receptors – adequate activation for multiple health outcomes. *Clin. Biochem. Rev* 36, 53–61.

Sacchet, M. D., Ho, T. C., Connolly, C. G., Tymofiyeva, O., Lewinn, K. Z., Han, L. K., et al. (2016). Large-scale hypoconnectivity between resting-state functional networks in unmedicated adolescent major depressive disorder. *Neuropsychopharmacology* 41, 2951–2960. doi: 10.1038/npp.2016.76

Serati, M., Redaelli, M., Buoli, M., and Altamura, A. C. (2016). Perinatal major depression biomarkers: a systematic review. *J. Affect. Disord.* 193, 391–404. doi: 10.1016/j.jad.2016.01.027

Slinin, Y., Paudel, M., Taylor, B. C., Ishani, A., Rossom, R., Yaffe, K., et al. (2012). Association between serum 25(OH) vitamin D and the risk of cognitive decline in older women. *J. Gerontol. A Biol. Sci. Med. Sci.* 67, 1092–1098. doi: 10.1093/gerona/gls075

Solomon, M. B., and Herman, J. P. (2009). Sex differences in psychopathology: of gonads, adrenals and mental illness. *Physiol. Behav.* 97, 250–258. doi: 10.1016/j.physbeh.2009.02.033

Song, B. M., Kim, H. C., Rhee, Y., Youm, Y., and Kim, C. O. (2016). Association between serum 25-hydroxyvitamin D concentrations and depressive symptoms in an older korean population: a cross-sectional study. *J. Affect. Disord.* 189, 357–364. doi: 10.1016/j.jad.2015.09.043

Thompson, E. (2015). Hamilton rating scale for anxiety (HAM-A). *Occup. Med. (Lond.)* 65:601. doi: 10.1093/occmed/kqv054

Toffanello, E. D., Sergi, G., Veronese, N., Perissinotto, E., Zambon, S., Coin, A., et al. (2014b). Serum 25-hydroxyvitamin d and the onset of late-life depressive mood in older men and women: the Pro.V.A. study. *J. Gerontol. A Biol. Sci. Med. Sci.* 69, 1554–1561. doi: 10.1093/gerona/glu081

Toffanello, E. D., Coin, A., Perissinotto, E., Zambon, S., Sarti, S., Veronese, N., et al. (2014a). Vitamin D deficiency predicts cognitive decline in older men and women: the Pro.V.A. Study. *Neurology* 83, 2292–2298. doi: 10.1212/WNL.0000000000001080

van de Ven, V. G., Formisano, E., Prvulovic, D., Roeder, C. H., and Linden, D. E. (2004). Functional connectivity as revealed by spatial independent component analysis of fMRI measurements during rest. *Hum. Brain Mapp.* 22, 165–178. doi: 10.1002/hbm.20022

Vossel, S., Geng, J. J., and Fink, G. R. (2014). Dorsal and ventral attention systems: distinct neural circuits but collaborative roles. *Neuroscientist* 20, 150–159. doi: 10.1177/1073858413494269

Wang, C., Cai, H., Sun, X., Si, L., Zhang, M., Xu, Y., et al. (2020). Large-scale internetwork functional connectivity mediates the relationship between serum triglyceride and working memory in young adulthood. *Neural Plast* 2020:8894868. doi: 10.1155/2020/8894868

Wehr, T. A., and Rosenthal, N. E. (1989). Seasonality and affective illness. *Am. J. Psychiatry* 146, 829–839. doi: 10.1176/ajp.146.7.829

Williams, J. B. (1988). A structured interview guide for the hamilton depression rating scale. *Arch. Gen. Psychiatry* 45, 742–747. doi: 10.1001/archpsyc.1988.01800320058007

Wong, S. K., Chin, K. Y., and Ima-Nirwana, S. (2018). Vitamin D and depression: the evidence from an indirect clue to treatment strategy. *Curr. Drug Targets* 19, 888–897. doi: 10.2174/1389450118666170913161030

Woods, N. F., Smith-DiJulio, K., Percival, D. B., Tao, E. Y., Mariella, A., and Mitchell, S. (2008). Depressed mood during the menopausal transition and early postmenopause: observations from the Seattle Midlife Women's Health Study. *Menopause* 15, 223–232. doi: 10.1097/gme.0b013e3181450fc2

Wortsman, J., Matsuoka, L. Y., Chen, T. C., Lu, Z., and Holick, M. F. (2000). Decreased bioavailability of vitamin D in obesity. *Am. J. Clin. Nutr.* 72, 690–693. doi: 10.1093/ajcn/72.3.690

Wu, X. J., Zeng, L. L., Shen, H., Yuan, L., Qin, J., Zhang, P., et al. (2017). Functional network connectivity alterations in schizophrenia and depression. *Psychiatry Res. Neuroimaging* 263, 113–120. doi: 10.1016/j.pscychresns.2017.03.012

Yan, C. G., Wang, X. D., Zuo, X. N., and Zang, Y. F. (2016). DPABI: data processing & analysis for (resting-state) brain imaging. *Neuroinformatics* 14, 339–351. doi: 10.1007/s12021-016-9299-4

Yan, X., Zhang, N., Cheng, S., Wang, Z., and Qin, Y. (2019). Gender differences in Vitamin D status in china. *Med. Sci. Monit.* 25, 7094–7099. doi: 10.12659/MSM.916326

Yang, J., Zhong, F., Qiu, J., Cheng, H., and Wang, K. (2015). Dissociation of event-based prospective memory and time-based prospective memory in patients with prostate cancer receiving androgen-deprivation therapy: a neuropsychological study. *Eur. J. Cancer Care (Engl.)* 24, 198–204. doi: 10.1111/ecc.12299

Yu, M., Linn, K. A., Shinohara, R. T., Oathes, D. J., Cook, P. A., Duprat, R., et al. (2019). Childhood trauma history is linked to abnormal brain connectivity in major depression. *Proc. Natl. Acad. Sci. U.S.A.* 116, 8582–8590. doi: 10.1073/pnas.1900801116

Zagni, E., Simoni, L., and Colombo, D. (2016). Sex and gender differences in central nervous system-related disorders. *Neurosci. J.* 2016:2827090. doi: 10.1155/2016/2827090

Zhou, F. C., Wang, Y. Y., Zheng, W., Zhang, Q., Ungvari, G. S., Ng, C. H., et al. (2017). Prospective memory deficits in patients with depression: a meta-analysis. *J. Affect. Disord.* 220, 79–85. doi: 10.1016/j.jad.2017.05.042

Zhu, D.-M., Zhao, W., Zhang, B., Zhang, Y., Yang, Y., Zhang, C., et al. (2019). The relationship between serum concentration of Vitamin D, total intracranial volume, and severity of depressive symptoms in patients with major depressive disorder. *Front. Psychiatry* 10:322. doi: 10.3389/fpsyt.2019.00322

**Conflict of Interest:** The authors declare that the research was conducted in the absence of any commercial or financial relationships that could be construed as a potential conflict of interest.

**Publisher's Note:** All claims expressed in this article are solely those of the authors and do not necessarily represent those of their affiliated organizations, or those of the publisher, the editors and the reviewers. Any product that may be evaluated in this article, or claim that may be made by its manufacturer, is not guaranteed or endorsed by the publisher.

frontiers in Aging Neuroscience

SYSTEMATIC REVIEW
published: 16 February 2022
doi: 10.3389/fnagi.2022.847218

# Cerebral Blood Flow Alterations in Type 2 Diabetes Mellitus: A Systematic Review and Meta-Analysis of Arterial Spin Labeling Studies

*Jieke Liu†, Xi Yang†, Yong Li, Hao Xu, Jing Ren and Peng Zhou**

*Department of Radiology, Sichuan Cancer Center, School of Medicine, Sichuan Cancer Hospital and Institute, University of Electronic Science and Technology of China, Chengdu, China*

OPEN ACCESS

**Edited by:**
*Wenjing Zhang, Sichuan University, China*

**Reviewed by:**
*David Ellis Crane, Sunnybrook Research Institute, Canada*
*Matthias Günther, University of Bremen, Germany*
*Xun Yang, Chongqing University, China*

***Correspondence:**
*Peng Zhou*
*penghyzhou@126.com*

*†These authors have contributed equally to this work*

**Specialty section:**
*This article was submitted to Neurocognitive Aging and Behavior, a section of the journal Frontiers in Aging Neuroscience*

**Received:** *01 January 2022*
**Accepted:** *26 January 2022*
**Published:** *16 February 2022*

**Citation:**
*Liu J, Yang X, Li Y, Xu H, Ren J and Zhou P (2022) Cerebral Blood Flow Alterations in Type 2 Diabetes Mellitus: A Systematic Review and Meta-Analysis of Arterial Spin Labeling Studies. Front. Aging Neurosci. 14:847218. doi: 10.3389/fnagi.2022.847218*

**Objective:** Arterial spin labeling (ASL) studies have revealed inconsistent regional cerebral blood flow (CBF) alterations in patients with type 2 diabetes mellitus (T2DM). The aim of this systematic review and meta-analysis was to identify concordant regional CBF alterations in T2DM.

**Methods:** A systematic review was conducted to the published literatures comparing cerebral perfusion between patients with T2DM and healthy controls using ASL. The seed-based *d* mapping (SDM) was further used to perform quantitative meta-analysis on voxel-based literatures and to estimate the regional CBF alterations in patients with T2DM. Metaregression was performed to explore the associations between clinical characteristics and cerebral perfusion alterations.

**Results:** A total of 13 studies with 14 reports were included in the systematic review and 7 studies with 7 reports were included in the quantitative meta-analysis. The qualitative review found widespread CBF reduction in cerebral lobes in T2DM. The meta-analysis found increased regional CBF in right supplementary motor area and decreased regional CBF in bilateral middle occipital gyrus, left caudate nucleus, right superior parietal gyrus, and left calcarine fissure/surrounding cortex in T2DM.

**Conclusion:** The patterns of cerebral perfusion alterations, characterized by the decreased CBF in occipital and parietal lobes, might be the neuropathology of visual impairment and cognitive aging in T2DM.

**Keywords: type 2 diabetes mellitus, arterial spin labeling, cerebral blood flow, meta-analysis, seed-based *d* mapping**

## INTRODUCTION

Type 2 diabetes mellitus (T2DM) is a common metabolic disease in middle-aged and older adults characterized by chronic hyperglycemia, which leads to long-term macrovascular and microvascular complications of various organ systems. The epidemic of T2DM and its complications raise a global health threat (Zheng et al., 2018). The present literatures have proved

that T2DM is a significant risk factor of developing certain mental disorders, including cognitive dysfunction, dementia, and depression (Biessels and Despa, 2018; van Sloten and Schram, 2018; Xue et al., 2019), and older individuals with T2DM progress to dementia at faster rates (Xu et al., 2010; Morris et al., 2014). Although the underlying mechanisms of these disorders are still unaddressed, growing evidences indicate that cerebral microvascular dysfunction is one of the key mechanisms, which may be driven by hyperglycemia, obesity, insulin resistance, and hypertension (van Sloten et al., 2020). Therefore, characterizing the phenotype of cerebral perfusion alterations may advance our understanding of the underlying mechanisms of cognitive aging and mental impairments in T2DM.

As the brain is a highly metabolic organ with limited energy reserves, the metabolically active regions need abundant supply of glucose and oxygen *via* cerebral perfusion (Coucha et al., 2018). Cerebral blood flow (CBF), commonly defined as the volume of blood delivered to a unit of brain tissue per minute, is responsible for the delivery of nutrients to the brain (Fantini et al., 2016). CBF is also correlated to brain activity, and there is a coupling between metabolically active regions and CBF under normal circumstances (Hoge et al., 1999). Recent studies have observed neurovascular decoupling in T2DM (Hu et al., 2019; Yu et al., 2019; Zhang et al., 2021). Therefore, the cerebral perfusion impairment may cause oxidative metabolism dysfunction of brain and neuronal damage, leading to mental disorders in T2DM.

CBF can be quantitatively measured using single-photon emission computerized tomography (SPECT), positron emission tomography (PET), perfusion computed tomography (PCT), dynamic susceptibility contrast magnetic resonance imaging (DSC-MRI), and arterial spin labeling (ASL). However, SPECT and PET require injection of radiotracers while PCT and DSC-MRI require injection of intravenous contrast agent (Wintermark et al., 2005). Besides, SPECT, PET, and PCT are associated with radiation exposure. Compared with the aforementioned methods, ASL is a non-invasive method to measure CBF by magnetically labeling the inflowing arterial blood water *in vivo* as an endogenous tracer (Williams et al., 1992). Due to its non-radiation, non-invasiveness, and reliability, ASL is proposed as a promising method to reveal cerebral perfusion biomarkers in various mental disorders (Alsop et al., 2015; Haller et al., 2016; Zhang, 2016).

In the last three decades, growing literatures have attempted to characterize cerebral perfusion patterns in T2DM, but the findings are varied across studies. A recent study systematically reviewed literatures on cerebral perfusion in T2DM and found the reduction of regional cerebral perfusion in multiple locations, including occipital lobe, domains involved in the default mode network and the cerebellum (Wang et al., 2021). However, this study involved various modalities including SPECT, DSC-MRI, and ASL. More importantly, no quantitative synthesizing method was used to conduct meta-analysis of voxel-based studies. As the region of interest (ROI) method has inherent bias and is more liberal in statistical threshold than voxel-based analysis (VBA) method (Radua and Mataix-Cols, 2009; Yao et al., 2021), the quantitative meta-analysis of voxel-based studies can objectively identify regional CBF differences at whole-brain level without any *priori* hypothesis.

Therefore, we first systematically reviewed literatures on cerebral perfusion in T2DM using ASL and then conducted a quantitative meta-analysis on these voxel-based literatures using Seed-based *d* Mapping (SDM, formerly Signed Differential Mapping) as primary tool. The SDM is a well-recognized synthesizing method for voxel-based studies and has been used in meta-analysis of cerebral structural and functional alterations in T2DM (Liu J. et al., 2017; Liu et al., 2021; Yao et al., 2021). This study aimed to identify consistent regional CBF alterations in T2DM and explore the potential effects of the clinical characteristics on these perfusion alterations.

# METHODS

## Search Strategy and Study Selection

A systematic search was conducted for relevant studies in the PubMed, Web of Knowledge, and Embase databases before November 30, 2021 according to the Preferred Reporting Items for Systematic reviews and Meta-Analyses (PRISMA) guidelines (Page et al., 2021a,b). The keywords were ("diabetes" or "diabetic") and ("arterial spin labeling" or "ASL"). Besides, the references of the retrieved studies and suitable reviews were manually checked for additional eligible studies.

Studies were included in systematic review according to the following criteria: (1) Original article published in peer-reviewed journal and in English; (2) conducted group comparison between patients with T2DM and healthy controls; (3) measured whole-brain or regional CBF using ASL. Studies were further included in meta-analysis according to the additional criteria: (1) Used VBA to estimate CBF changes; (2) reported coordinates of significant clusters in Montreal Neurological Institute (MNI) or Talairach space. The exclusion criteria were as follows: (1) studies that re-analyzed previously published data; (2) studies without available full-text record; (3) studies that only reported ROI findings or without available coordinates were further excluded in meta-analysis.

For each included study in systematic review, the extracted information included sample size, gender, age, comorbidity, brain regions and their CBF alterations. For each included study in meta-analysis, additional information was recorded as follows: (1) Clinical characteristics including years of education, diabetic duration, onset age, body mass index (BMI), hemoglobin $A_{1c}$ ($HbA_{1c}$), and Mini Mental State Examination (MMSE) score; (2) acquisition parameters including scanner, sequence, labeling duration, post labeling delay (PLD), and spatial resolution; (3) analytic methods including software package, full width at half maximum (FWHM), partial volume effect (PVE) correction, and statistical threshold. The corresponding author were contacted *via* email for additional data that were required in the meta-analysis. Two radiologist (JL and XY) independently conducted the literature search and extracted data. The discrepancies between the two radiologists were resolved by consensus.

## Voxel-Based Meta-Analysis

Voxel-based meta-analysis was conducted with SDM software package (version 5.15)[1]. The procedures including the data preparation, preprocessing, mean analysis, and statistic test were summarized here in brief (Radua and Mataix-Cols, 2009; Radua et al., 2012, 2014).

First, the peak coordinates and *t*-values were written in a text file for each study. Only the peak coordinates at the whole-brain level were extracted to avoid biases toward liberally thresholded brain regions in ROI studies (Friston et al., 2006; Radua and Mataix-Cols, 2009). The studies with non-statistically significant unreported effects (NSUEs) were also included, and their text files were recorded with no content and named with the extension of ".no_peaks.txt." Second, an anisotropic non-normalized Gaussian kernel was used to recreate an effect-size map and its variance map for each study. Both positive and negative coordinates were reconstructed in the same map to avoid any voxel erroneously appearing positive and negative simultaneously. The FWHM was set at 20 mm as it was found to optimally balance the sensitivity and specificity in SDM, according to previous simulations (Radua et al., 2012). Third, the mean map was obtained by performing a voxel-wise calculation of the mean of the study maps, weighted by the sample size, the inverse of the variance of each study, and the inter-study heterogeneity. Finally, the statistic test was conducted with the default SDM threshold, which were proposed to optimally balance sensitivity and specificity and to be an approximate equivalent to a corrected *P*-value of 0.05 for effect-size in SDM ($p < 0.005$, peak height $z = 1$, cluster extent $> 50$ voxels) (Radua and Mataix-Cols, 2009; Radua et al., 2012).

## Reliability, Heterogeneity and Publication Bias Analyses

The jackknife sensitivity analysis was performed to test the replicability of the results by iteratively repeating the analyses, discarding one dataset each time. We presumed that the findings might be highly conclusive and replicable if previous significant results could be replicated in all or most study combinations.

The inter-study heterogeneity of each significant cluster was tested using a random-effects model. Magnitude of heterogeneity was estimated using $I^2$ index, computed as $100\% \times (Q—df)/Q$, where *df* is the degree of freedom, which estimated the proportion of variability due to non-random differences between studies. The value of $I^2$ less than 25% indicated low heterogeneity (Higgins et al., 2003).

The funnel plot of each significant cluster was created by Egger's test to estimate the publication bias. The result with $p < 0.05$ was considered significant for publication bias (Egger et al., 1997).

## Subgroup Meta-Analysis

To explore the potential biases that were introduced by the different acquisition parameters and analytic methods between the studies, we conducted subgroup analyses. We repeated the analysis for those studies acquiring images with pulsed ASL (PASL), with pseudo-continuous ASL (PCASL), and with a slice thickness 4 mm. We also repeated the analysis for those studies using PVE correction.

## Metaregression Meta-Analysis

The potential effects of relevant clinical variables on regional brain CBF alterations in patients with T2DM were examined by a random-effects general linear metaregression. The independent variables explored by the metaregression included percentage of males, mean age, years of education, diabetic duration, onset age, body mass index (BMI), hemoglobin $A_{1c}$ ($HbA_{1c}$), Mini Mental State Examination (MMSE) score. The dependent variable was the SDM-Z value. As reported in a previous study, we decreased the probability threshold to 0.0005 to reduce false positives (Radua and Mataix-Cols, 2009). In the findings of metaregression analysis, the regions that did not overlap with those in the main between-group analysis were discarded. Finally, regression plots were visually inspected to discard fittings driven by few studies (Radua and Mataix-Cols, 2009; Radua et al., 2012).

# RESULTS

## Included Studies and Sample Characteristics

A total of 369 records were identified through database searching and citation searching, and **Figure 1** shows the flowchart of literature search and study selection. We finally included 13 studies with 14 reports in the systematic review (Last et al., 2007; Jor'dan et al., 2014; Novak et al., 2014; Rusinek et al., 2015; Xia et al., 2015; Jansen et al., 2016; Cui et al., 2017; Dai et al., 2017; Shen et al., 2017; Bangen et al., 2018; Zhang et al., 2019; Chau et al., 2020; Huang et al., 2021). One study performed analysis using both ROI and VBA methods (Jansen et al., 2016). As 1 of 8 VBA reports had no available coordinate (Novak et al., 2014), 7 studies with 7 reports were finally included in the meta-analysis (Xia et al., 2015; Jansen et al., 2016; Cui et al., 2017; Dai et al., 2017; Shen et al., 2017; Zhang et al., 2019; Huang et al., 2021).

The search revealed 407 patients with T2DM and 443 healthy controls in the systematic review and 253 patients with T2DM and 247 healthy controls in the meta-analysis. The basic characteristics of the studies in the systematic review including sample size, gender, age, comorbidity, and the main findings of brain regions and their CBF alterations are summarized in **Table 1**. The relevant clinical characteristics, acquisition parameters, and analytic methods of the included studies in the meta-analysis are presented in **Tables 2**, **3**.

## Findings of Qualitative Review

In 3 of 6 ROI studies, researchers reported no significant regional CBF alterations in T2DM patients compared with healthy controls (Jor'dan et al., 2014; Rusinek et al., 2015; Jansen et al., 2016). The other 3 ROI studies reported significant reduction of regional CBF in T2DM patients, mainly involving frontal, temporal, and parietal lobe (Last et al., 2007; Bangen et al., 2018;

[1]http://www.sdmproject.com

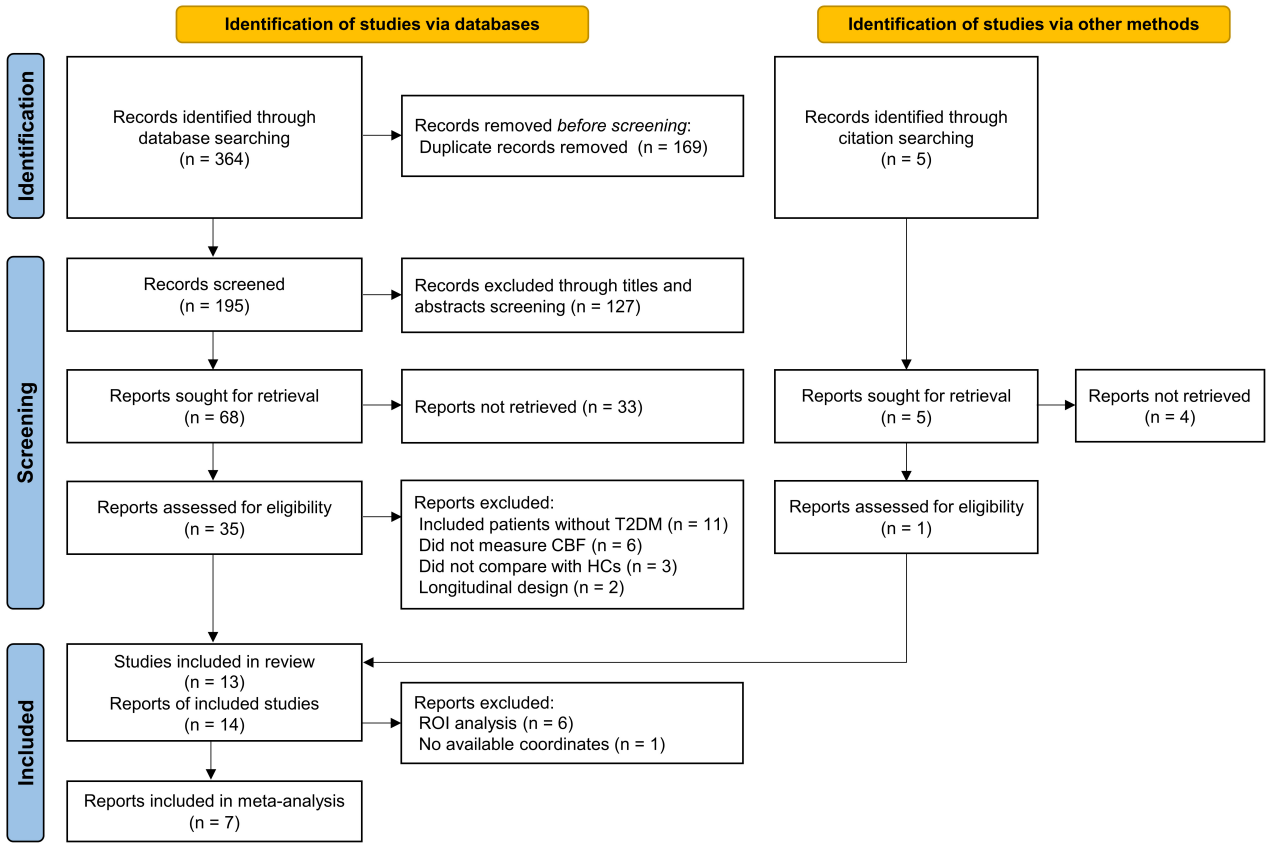


**FIGURE 1 |** PRISMA flow diagram for literature search and study selection. PRISMA, Preferred Reporting Items for Systematic reviews and Meta-Analyses; T2DM, type 2 diabetes mellitus; HCs, healthy controls; CBF, cerebral blood flow; ROI, region of interest.

Chau et al., 2020), as well as occipital lobe (Last et al., 2007; Chau et al., 2020). Another VBA study without available coordinate reported reduced CBF in insular cortex (Novak et al., 2014; **Table 1**).

## Findings of Meta-Analysis

In the voxel-based meta-analysis, 2 of 7 reports had NSUE (Jansen et al., 2016; Shen et al., 2017). Patients with T2DM showed increased regional CBF in right supplementary motor area compared with healthy controls, and decreased regional CBF in bilateral middle occipital gyrus, left caudate nucleus, right superior parietal gyrus, and left calcarine fissure/surrounding cortex (**Table 4** and **Figure 2**).

## Reliability, Heterogeneity, and Publication Bias Analyses

The jackknife analysis showed that decreased CBF in right middle occipital gyrus and right superior parietal gyrus were highly replicable and remained significant in all the combinations. The increased CBF in right supplementary motor area and the decreased CBF in left middle occipital gyrus and left calcarine fissure/surrounding cortex remained significant in 6/7 combinations. The decreased CBF in left caudate nucleus remained significant in 5/7 combinations (**Supplementary Table 1**).

All brain regions with CBF alterations showed low between-study heterogeneity ($I^2$ ranged from 3.35 to 22.65%) (**Supplementary Table 2**). The Egger test was significant only in the right supplementary motor area ($p = 0.001$). All the brain regions with decreased CBF did not show publication bias (all $p > 0.05$) (**Supplementary Table 3**).

## Subgroup Meta-Analysis

The meta-analysis of PASL studies showed decreased regional CBF in right middle occipital gyrus and superior parietal gyrus. The meta-analysis of PCASL studies showed increased regional CBF in right supplementary motor area and decreased regional CBF in left middle occipital gyrus, caudate nucleus, and calcarine fissure/surrounding cortex. The meta-analysis of studies with a slice thickness 4 mm showed increased regional CBF in right supplementary motor area and decreased regional CBF in right middle occipital gyrus and superior parietal gyrus. The meta-analysis of studies using PVE correction showed increased regional CBF in right supplementary motor area and decreased regional CBF in bilateral middle occipital gyrus, right superior parietal gyrus, and left calcarine fissure/surrounding cortex (**Supplementary Table 4**).

**TABLE 1 |** Arterial spin labeling studies investigating cerebral blood flow alterations in patients with T2DM relative to healthy controls.

| References | T2DM | | | Healthy controls | | Method | Brain regions | CBF alteration |
|---|---|---|---|---|---|---|---|---|
| | No. (male/female) | Age (years) | Comorbidity (No.) | No. (male/female) | Age (years) | | | |
| Last et al. (2007) | 26 (13/13) | 61.6 ± 6.6 | Hyperlipidemia (10), hypertension (10), retinopathy (10) | 25 (13/12) | 60.4 ± 8.6 | ROI | Frontal, temporal, and parieto-occipital lobe | ↓ |
| Jor'dan et al. (2014) | 61 (31/30) | 65 ± 8 | Hyperlipidemia (34), hypertension (38), peripheral neuropathy (31) | 67 (28/39) | 67 ± 9 | ROI | Cerebellum, frontal, temporal, parietal, and occipital lobe | n.s. |
| Novak et al. (2014) | 15 (8/7) | 62.0 ± 7.9 | Hyperlipidemia (10) | 14 (4/10) | 60.1 ± 9.9 | VBA | Insular cortex | ↓ |
| Rusinek et al. (2015) | 23 (9/14) | 54.2 ± 5.2 | NA | 37 (15/22) | 51.8 ± 3.8 | ROI | Frontal and parietal lobe | n.s. |
| Xia et al. (2015) | 38 (17/21) | 56.0 ± 6.1 | Hypertension (29) | 40 (21/19) | 57.1 ± 7.6 | VBA | R middle occipital gyrus, R and L inferior parietal lobe, R precuneus | ↓ |
| Jansen et al. (2016) | 41 (NA) | NA | Hypertension (39), cardiovascular disease (8) | 39 (NA) | NA | ROI | Whole cerebral cortex, frontal, temporal, parietal, and occipital cortex, and subcortical gray matter | n.s. |
| | | | | | | VBA | | n.s. |
| Cui et al. (2017) | 40 (21/19) | 60.5 ± 6.9 | Lacunar infarcts (9) | 41 (13/28) | 57.9 ± 6.5 | VBA | Dorsal anterior cingulate cortex | ↑ |
| | | | | | | | R and L middle occipital gyrus, R precuneus, cuneus | ↓ |
| Dai et al. (2017) | 41 (19/22) | 65.5 ± 8.3 | Hypertension (32) | 32 (16/16) | 67.3 ± 10.1 | VBA | Cerebellum, frontal lobe | ↓ |
| Shen et al. (2017) | 36 (17/19) | 57.6 ± 6.2 | Hyperlipidemia (9), hypertension (20), white matter hyperintensities (29) | 36 (14/22) | 56.2 ± 6.8 | VBA | | n.s. |
| Bangen et al. (2018) | 11 (8/3) | 72.3 ± 2.8 | Hypertension (11), cardiovascular disease (1), atrial fibrillation (1) | 38 (13/25) | 73.6 ± 5.9 | ROI | R and L hippocampus, R inferior parietal cortex, R inferior temporal cortex, R rostral middle frontal gyrus | ↓ |
| | | | | | | | L inferior parietal cortex, L inferior temporal cortex, R and L medial orbitofrontal cortex, L rostral middle frontal gyrus | n.s. |
| Zhang et al. (2019) | 26 (10/16) | 51.9 ± 10.7 | Hyperlipidemia (9), hypertension (7), cardiovascular disease (1) | 26 (11/15) | 48.2 ± 6.7 | VBA | R temporopolar, R superior and middle frontal gyrus | ↑ |
| Chau et al. (2020) | 18 (15/3) | 62.5 ± 3.7 | Hyperlipidemia (16), hypertension (9) | 15 (3/12) | 71.8 ± 6.1 | ROI | Global cortex, R and L cerebral, prefrontal, rostral anterior cingulate, precuneus/posterior cingulate, parietal, lateral temporal, mesial temporal, occipital, and sensorimotor cortex | ↓ |
| Huang et al. (2021) | 31 (15/16) | 53.4 ± 9.1 | Retinopathy (31) | 33 (12/21) | 51.6 ± 9.8 | VBA | L middle temporal gyrus, R and L supplementary motor area | ↑ |
| | | | | | | | R and L calcarine, and caudate | ↓ |

*T2DM, type 2 diabetes mellitus; CBF, cerebral blood flow; ROI, region of interest; VBA, voxel-based analysis; NA, not available; R, right; L, left; n.s., no significant difference between T2DM and healthy controls; downward arrow (↓), decreased CBF in T2DM; upward arrow (↑), increased CBF in T2DM.*

**TABLE 2 |** Clinical characteristics of the included studies in the meta-analysis.

| References | Education (years) | Duration (year) | Onset (year) | BMI ($kg/m^2$) | HbAlc (%) | MMSE |
|---|---|---|---|---|---|---|
| Xia et al. (2015) | 9.6 ± 3.0 | 7.1 ± 3.5 | 48.9 | 24.4 ± 2.6 | 7.2 ± 1.1 | 29.0 ± 0.9 |
| Jansen et al. (2016) | NA | 9.8 ± 6.7 | NA | 29.2 ± 3.5 | 6.7 ± 0.4 | 28.6 ± 1.4 |
| Cui et al. (2017) | 10.0 ± 3.4 | 8.9 ± 5.0 | 51.6 | 24.4 ± 2.7 | 7.7 ± 1.6 | 28.3 ± 1.0 |
| Dai et al. (2017) | 15.4 ± 3.8 | 9.9 ± 7.9 | 55.6 | 29.1 ± 6.8 | 7.3 ± 1.25 | 28.6 ± 1.5 |
| Shen et al. (2017) | 9.1 ± 1.5 | 5.4 ± 4.9 | 52.2 | 26.0 ± 2.9 | NA | NA |
| Zhang et al. (2019) | 10.3 ± 3.7 | 9.2 ± 7.1 | 42.7 | 24.0 ± 3.6 | NA | 26.9 ± 3.9 |
| Huang et al. (2021) | NA | NA | NA | NA | 7.3 ± 1.4 | NA |

*T2DM, type 2 diabetes mellitus; BMI, body mass index; $HbA_{1c}$, hemoglobin $A_{1c}$; MMSE, Mini Mental State Examination; NA, not available.*

**TABLE 3 |** Acquisition parameters and analytic methods of the included studies in the meta-analysis.

| References | Acquisition parameters | | | | | Analytic methods | | | |
|---|---|---|---|---|---|---|---|---|---|
| | Scanner | Sequence | Labeling duration (ms)* | PLD (ms)** | Resolution (mm) | Software | FWHM (mm) | PVE correction | Threshold |
| Xia et al. (2015) | 3T Siemens Trio | PASL | 600 | 1000 | 3.4 × 3.4 × 4 | SPM8 | 6 | NA | Cluster-level FWE $p < 0.01$ corrected |
| Jansen et al. (2016) | 3T Philips Achieva | PCASL | 1,650 | 1,525 | 3 × 3 × 7 | SPM8 | NA | NA | FDR $p < 0.05$ corrected |
| Cui et al. (2017) | 3T Siemens Trio | PASL | 600 | 1,000 | 3.4 × 3.4 × 4 | AFNI | 6 | GM + 0.4 × WM | AlphaSim $p < 0.05$ corrected |
| Dai et al. (2017) | 3T GE Signa Hdxt | PCASL | 1,500 | 1,500 | 1.9 × 1.9 × 4 | SPM8 | 8 | Volume of GM | Cluster-level FWE $p < 0.05$ corrected |
| Shen et al. (2017) | 3T Siemens Skyra | PASL | Multiple TI*** | | 3.4 × 3.4 × 4 | SPM8 | NA | GM + 0.4 × WM | FDR $p < 0.05$ corrected |
| Zhang et al. (2019) | 3T GE Discovery 750 | PCASL | 1,525 | 1,525 | Thickness 4 | SPM8 | 8 | Volume of brain | AlphaSim $p < 0.01$ corrected |
| Huang et al. (2021) | 3T GE Discovery 750 | PCASL | 1,525 | 1,525 | Thickness 3.5 | SPM8 | 6 | NA | Gaussian random field $p < 0.05$ corrected |

*PASL, pulsed arterial spin labeling; PCASL, pseudo-continuous arterial spin labeling; PLD, post labeling delay PLD; TI, inversion time; SPM, Statistical Parametric Mapping; AFNI, Analysis of Functional NeuroImages; FWHM, full width at half maximum; PVE, partial volume effect; GM, gray matter; WM, white matter; FWE, familywise error rate; FDR, false discovery rate; NA, not available.*

**The labeling duration in PCASL is analogous to the bolus duration (TI1) in PASL.*

***The PLD in PCASL is analogous to the difference between TI and TI1 in PASL.*

****The Multiple TI includes 16 TIs from 480 to 4,080 ms with a step of 225 ms.*

## Metaregression Meta-Analysis

The metaregression analysis showed that the percentage of males, mean age, years of education, diabetic duration, onset age, BMI, $HbA_{1c}$%, and MMSE scores were not linearly associated with regional CBF alterations in patients with T2DM.

# DISCUSSION

To our knowledge, this is the first quantitative meta-analysis to pool the ASL studies to identify the consistent pattern of CBF alterations in T2DM. This systematic review and meta-analysis revealed that the regional CBF was significantly reduced in the patients with T2DM, mainly involving occipital and parietal lobes. These findings indicated the potential neuropathology of visual impairment and cognitive aging in T2DM (Meusel et al., 2014).

The most consistent and significant finding was that the perfusion of occipital lobe was impaired in T2DM. The middle occipital gyrus and calcarine fissure/surrounding cortex in the occipital lobe were important components of visual cortex, which were responsible for vision processing and visual memory (Tootell et al., 1998; Wandell et al., 2007). Previous studies demonstrated that the decreased perfusion in middle occipital gyrus was associated with impaired visuospatial function and visual memory (Xia et al., 2015; Cui et al., 2017). A recent meta-analysis study of functional magnetic resonance imaging (fMRI) also revealed consistent hypoactivity in the middle occipital gyrus and calcarine fissure/surrounding cortex in T2DM (Yao et al., 2021). Beside, recent studies focusing on patients with diabetic retinopathy observed decreased CBF in the bilateral calcarine fissure/surrounding cortex (Huang et al., 2021) and hypoactivity in the middle occipital gyrus (Wang et al., 2017; Qi et al., 2020). These findings indicated that the perfusion and function alterations in occipital lobe, which involving vasculopathy and neuropathy along the visual pathway (Heravian et al., 2012), might be attribute to the potential visual impairment, a common comorbidity of diabetes.

**TABLE 4 |** Differences in regional cerebral blood flow alterations between patients with T2DM and healthy controls.

| | MNI coordinates | SDM-*Z* value | *p*-value | No. of voxels | Cluster breakdown (no. of voxels) |
|---|---|---|---|---|---|
| **T2DM > Control** | | | | | |
| R supplementary motor area | 6, –12, 68 | 1.320 | 0.0002 | 438 | R supplementary motor area (273)<br>R superior frontal gyrus, dorsolateral (83)<br>L supplementary motor area (40)<br>L paracentral lobule (37)<br>R precentral gyrus (5) |
| **T2DM < Control** | | | | | |
| L middle occipital gyrus | –18, –94, –2 | –1.543 | 0.0004 | 822 | L middle occipital gyrus (337)<br>L calcarine fissure/surrounding cortex (233)<br>L inferior occipital gyrus (128)<br>L lingual gyrus (73)<br>L superior occipital gyrus (46)<br>L fusiform gyrus (3)<br>L cuneus cortex (2) |
| R middle occipital gyrus | 30, –90, 10 | –1.380 | 0.0010 | 309 | R middle occipital gyrus (194)<br>R superior occipital gyrus (56)<br>R inferior occipital gyrus (26)<br>R cuneus cortex (30)<br>L cuneus cortex (2)<br>R calcarine fissure/surrounding cortex (1) |
| L caudate nucleus | –12, –2, 18 | –1.365 | 0.0011 | 53 | L caudate nucleus (48)<br>L thalamus (5) |
| R superior parietal gyrus | 16, –64, 56 | –1.201 | 0.0023 | 54 | R superior parietal gyrus (44)<br>R precuneus (9)<br>R inferior parietal gyrus (1) |
| L calcarine fissure/surrounding cortex | 2, –86, 8 | –1.227 | 0.0021 | 52 | L calcarine fissure/surrounding cortex (45)<br>L cuneus cortex (4)<br>R calcarine fissure/surrounding cortex (3) |

*T2DM, type 2 diabetes mellitus; MNI, Montreal Neurological Institute; SDM, seed-based d mapping; R, right; L, left.*

Another consistent finding was the reduced perfusion in parietal lobe in T2DM. Our quantitative meta-analysis identified decreased CBF in superior parietal gyrus. Previous neuroimaging studies also demonstrated gray matter volume loss (Roy et al., 2020) and functional dysconnectivity (Cui et al., 2016; Liu L. et al., 2017) in superior parietal gyrus in patients with T2DM. The superior parietal gyrus was involved in aspects of attention and visuospatial orientation, including the manipulation of information in working memory (Koenigs et al., 2009), which was impaired in patients with T2DM (Chen et al., 2014; Huang et al., 2016). Working memory is a fundamental cognitive process in the brain and it is crucially important for most higher-order cognitive functions (Baddeley, 2003). T2DM has been consistently associated with an increased risk of dementia and mild cognitive impairment (Reijmer et al., 2010; Beeri and Bendlin, 2020), and the structural and functional abnormalities in the brain are thought to underlie these cognitive deficits (Yao et al., 2021). Previous studies indicated that increased activation strength in parietal lobe was positively associated with memory improvement in patients with mild cognitive impairment (Belleville et al., 2011; Corriveau-Lecavalier et al., 2019). Therefore, it suggests that the decreased perfusion in superior parietal area may underlie the neuropathology of cognitive deficits in T2DM.

Our meta-analysis results also showed decreased CBF in the left caudate nucleus and increased CBF in the right supplementary motor area in T2DM, which were not commonly reported in ROI studies. Besides, it should be noted that the right supplementary motor area showed significant publication bias (Egger test $p = 0.001$). The caudate nucleus, a component of the dorsal striatum, has an important role in cognitive function and spatial working memory (Postle and D'Esposito, 2003; Grahn et al., 2008). The functional abnormalities of the caudate nucleus may also lead to motor dysfunctions (McColgan et al., 2015; Ji et al., 2018), which have been observed in patients with T2DM (Gorniak et al., 2014; Ochoa et al., 2016). Meanwhile, the supplementary motor area play a role in the direct control of movement, especially in finger movement (Shibasaki et al., 1993; Tanji and Shima, 1994), and the diabetic peripheral neuropathy may lead to sensory impairments in the motor system (Allen et al., 2016). Thus the deficits of corticostriatal circuit between the head of caudate nucleus and supplementary motor area may be the neuropathology for motor dysfunction in T2DM. The increased perfusion in supplementary motor area might suggest a compensation for the functional deficits of corticostriatal circuit in T2DM.

Although ASL has been the widely used neuroimaging approach in brain perfusion, the acquisition parameters and analytic methods varies among ASL studies, bringing potential bias. For example, quantitative assessment of perfusion with ASL is hampered by the transport time from the labeling position to the tissue, known as arterial transit time (ATT)

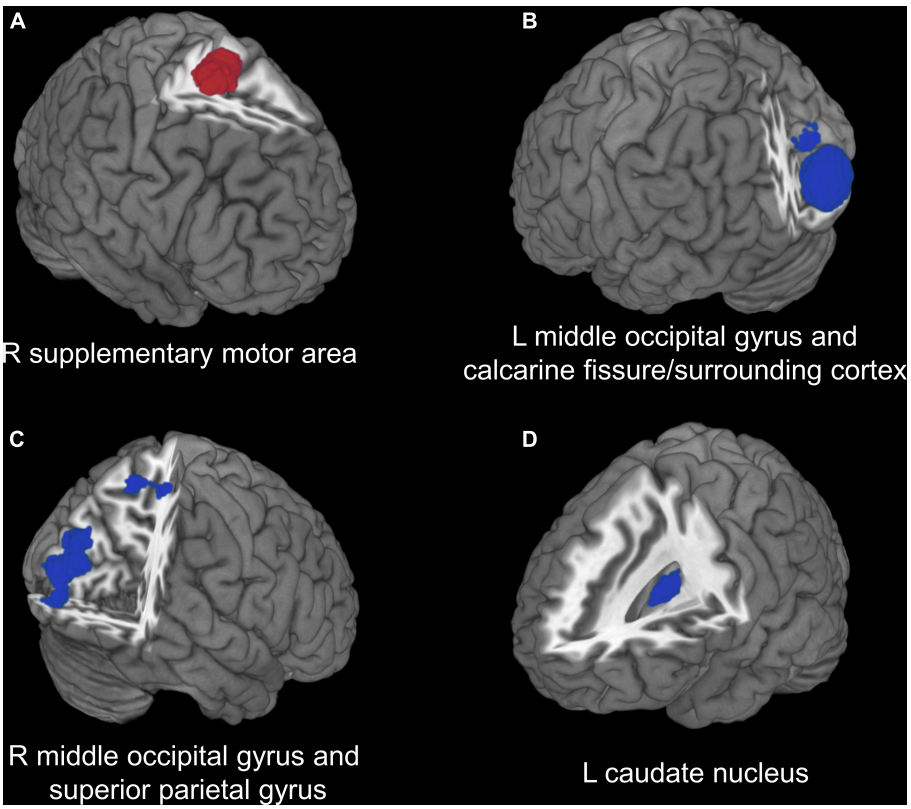


**FIGURE 2 |** Voxel-based meta-analysis results of regions with cerebral perfusion alterations in T2DM. **(A)** Red region indicates increased CBF in patients with T2DM compared with healthy controls. **(B–D)** Blue regions indicate decreased CBF in patients with T2DM compared with healthy controls. T2DM, type 2 diabetes mellitus; CBF, cerebral blood flow; R, right; L, left.

(Alsop et al., 2015). PASL and PCASL are both labeling approaches using single PLD/inversion time (TI) but differ fundamentally in spatial extent and time of labeling and labeling delay (As shown in **Table 3**). Besides, one of the PASL study used multiple TI approach (Shen et al., 2017), which estimated both CBF and ATT *via* fitting data. Our subgroup meta-analysis found no overlap of regional CBF alteration between PASL and PCASL, suggesting the labeling approach might have a great impact on cerebral perfusion. As for the spatial resolution and PVE, our subgroup meta-analysis showed that the cerebral perfusion alteration in left caudate nucleus were not reproducible. One possible reason might be that the caudate nucleus was close to lateral ventricle and more likely to contain a mixture of gray matter and cerebrospinal fluid (Jezzard et al., 2018). Besides, as gray matter atrophy was observed in T2DM (Yao et al., 2021), there might be potential overestimation of decreased perfusion in regions where both perfusion and gray matter volume were reduced (Chappell et al., 2021). Future studies should attempt to conduct analysis with and without PVE correction to investigate its influence. In summary, even though some regional perfusion alterations could be affected by the heterogeneity of acquisition parameters and analytic methods, the increased CBF in right supplementary motor area and decreased regional CBF in right middle occipital gyrus and superior parietal gyrus were robust in 3 of 4 subgroup analyses.

There are several limitations in this study. First, the sample size of patients with T2DM included in some studies was relatively small. Second, near half of ASL studies in T2DM were not included in quantitative meta-analysis because of the use of ROI approach without available coordinates and corresponding effect sizes. Third, there were heterogeneity between the included studies. The confounding factors such as age, illness duration, blood glucose control, and comorbidities might affect CBF. Although we sought to identify the potential effects of some confounding factors, the results were negative, which also should be taken caution as only few data were available in the metaregression analysis. It is also difficult to avoid false-negative results even though voxel-based meta-analytical methods have good control for false-positive results (Radua et al., 2012). Fourth, although this review reveals the association between neuropathology and visual impairment and cognitive aging in T2DM, whether the vascular mechanism underlying these disorders remains inconclusive. Further research would be required to determine causation.

In conclusion, this systematic review and meta-analysis revealed consistent cerebral perfusion alterations in T2DM, characterized by decreased CBF in occipital and parietal

lobes. These findings suggested the neuropathology of visual impairment and cognitive aging in T2DM.

## DATA AVAILABILITY STATEMENT

The original contributions presented in the study are included in the article/**Supplementary Material**, further inquiries can be directed to the corresponding author/s.

## AUTHOR CONTRIBUTIONS

JL and PZ conceived and designed the study. JL, XY, YL, and HX collected the data. JL and XY analyzed the data and drafted the manuscript. PZ revised the final manuscript. JL, JR, and PZ provided funding for the study. All authors reviewed the manuscript, contributed to the article and approved the submitted version.

## FUNDING

This study was supported by the Sichuan Science and Technology Program (grant nos. 2021YFS0075, 2021YFG0125, and 2021YFS0225).

## SUPPLEMENTARY MATERIAL

The Supplementary Material for this article can be found online at: https://www.frontiersin.org/articles/10.3389/fnagi.2022.847218/full#supplementary-material

## REFERENCES

Allen, M. D., Doherty, T. J., Rice, C. L., and Kimpinski, K. (2016). Physiology in Medicine: neuromuscular consequences of diabetic neuropathy. *J. Appl. Physiol.* 121, 1–6. doi: 10.1152/japplphysiol.00733.2015

Alsop, D. C., Detre, J. A., Golay, X., Gunther, M., Hendrikse, J., Hernandez-Garcia, L., et al. (2015). Recommended implementation of arterial spin-labeled perfusion MRI for clinical applications:a consensus of the ISMRM perfusion study group and the European consortium for ASL in dementia. *Magn. Reson. Med.* 73, 102–116. doi: 10.1002/mrm.25197

Baddeley, A. (2003). Working memory: looking back and looking forward. *Nat. Rev. Neurosci.* 4, 829–839. doi: 10.1038/nrn1201

Bangen, K. J., Werhane, M. L., Weigand, A. J., Edmonds, E. C., Delano-Wood, L., Thomas, K. R., et al. (2018). Reduced Regional Cerebral Blood Flow Relates to Poorer Cognition in Older Adults With Type 2 Diabetes. *Front. Aging Neurosci.* 10:270. doi: 10.3389/fnagi.2018.00270

Beeri, M. S., and Bendlin, B. B. (2020). The link between type 2 diabetes and dementia: from biomarkers to treatment. *Lancet Diabetes Endocrinol.* 8, 736–738. doi: 10.1016/S2213-8587(20)30267-9

Belleville, S., Clement, F., Mellah, S., Gilbert, B., Fontaine, F., and Gauthier, S. (2011). Training-related brain plasticity in subjects at risk of developing Alzheimer's disease. *Brain* 134, 1623–1634. doi: 10.1093/brain/awr037

Biessels, G. J., and Despa, F. (2018). Cognitive decline and dementia in diabetes mellitus:mechanisms and clinical implications. *Nat. Rev. Endocrinol.* 14, 591–604. doi: 10.1038/s41574-018-0048-7

Chappell, M. A., McConnell, F. A. K., Golay, X., Gunther, M., Hernandez-Tamames, J. A., van Osch, M. J., et al. (2021). Partial volume correction in arterial spin labeling perfusion MRI:a method to disentangle anatomy from physiology or an analysis step too far? *Neuroimage* 238:118236. doi: 10.1016/j.neuroimage.2021.118236

Chau, A. C. M., Cheung, E. Y. W., Chan, K. H., Chow, W. S., Shea, Y. F., Chiu, P. K. C., et al. (2020). Impaired cerebral blood flow in type 2 diabetes mellitus - A comparative study with subjective cognitive decline, vascular dementia and Alzheimer's disease subjects. *Neuroimage Clin.* 27:102302. doi: 10.1002/trc2.12008

Chen, Y., Liu, Z., Zhang, J., Xu, K., Zhang, S., Wei, D., et al. (2014). Altered brain activation patterns under different working memory loads in patients with type 2 diabetes. *Diabetes Care* 37, 3157–3163. doi: 10.2337/dc14-1683

Corriveau-Lecavalier, N., Mellah, S., Clement, F., and Belleville, S. (2019). Evidence of parietal hyperactivation in individuals with mild cognitive impairment who progressed to dementia:a longitudinal fMRI study. *Neuroimage Clin.* 24:101958. doi: 10.1016/j.nicl.2019.101958

Coucha, M., Abdelsaid, M., Ward, R., Abdul, Y., and Ergul, A. (2018). Impact of Metabolic Diseases on Cerebral Circulation:structural and Functional Consequences. *Compr. Physiol.* 8, 773–799. doi: 10.1002/cphy.c170019

Cui, Y., Li, S. F., Gu, H., Hu, Y. Z., Liang, X., Lu, C. Q., et al. (2016). Disrupted Brain Connectivity Patterns in Patients with Type 2 Diabetes. *AJNR Am. J. Neuroradiol.* 37, 2115–2122. doi: 10.3174/ajnr.A4858

Cui, Y., Liang, X., Gu, H., Hu, Y., Zhao, Z., Yang, X. Y., et al. (2017). Cerebral perfusion alterations in type 2 diabetes and its relation to insulin resistance and cognitive dysfunction. *Brain Imaging Behav.* 11, 1248–1257. doi: 10.1007/s11682-016-9583-9

Dai, W., Duan, W., Alfaro, F. J., Gavrieli, A., Kourtelidis, F., and Novak, V. (2017). The resting perfusion pattern associates with functional decline in type 2 diabetes. *Neurobiol. Aging* 60, 192–202. doi: 10.1016/j.neurobiolaging.2017.09.004

Egger, M., Davey Smith, G., Schneider, M., and Minder, C. (1997). Bias in meta-analysis detected by a simple, graphical test. *BMJ* 315, 629–634. doi: 10.1136/bmj.315.7109.629

Fantini, S., Sassaroli, A., Tgavalekos, K. T., and Kornbluth, J. (2016). Cerebral blood flow and autoregulation:current measurement techniques and prospects for noninvasive optical methods. *Neurophotonics* 3:031411. doi: 10.1117/1.NPh.3.3.031411

Friston, K. J., Rotshtein, P., Geng, J. J., Sterzer, P., and Henson, R. N. (2006). A critique of functional localisers. *Neuroimage* 30, 1077–1087. doi: 10.1016/j.neuroimage.2005.08.012

Gorniak, S. L., Khan, A., Ochoa, N., Sharma, M. D., and Phan, C. L. (2014). Detecting subtle fingertip sensory and motor dysfunction in adults with type II diabetes. *Exp. Brain Res.* 232, 1283–1291. doi: 10.1007/s00221-014-3844-x

Grahn, J. A., Parkinson, J. A., and Owen, A. M. (2008). The cognitive functions of the caudate nucleus. *Prog. Neurobiol.* 86, 141–155. doi: 10.1016/j.pneurobio.2008.09.004

Haller, S., Zaharchuk, G., Thomas, D. L., Lovblad, K. O., Barkhof, F., and Golay, X. (2016). Arterial Spin Labeling Perfusion of the Brain:emerging Clinical Applications. *Radiology* 281, 337–356. doi: 10.1148/radiol.2016150789

Heravian, J., Ehyaei, A., Shoeibi, N., Azimi, A., Ostadi-Moghaddam, H., Yekta, A. A., et al. (2012). Pattern Visual Evoked Potentials in Patients with Type II Diabetes Mellitus. *J. Ophthalmic. Vis. Res.* 7, 225–230.

Higgins, J. P., Thompson, S. G., Deeks, J. J., and Altman, D. G. (2003). Measuring inconsistency in meta-analyses. *BMJ* 327, 557–560. doi: 10.1136/bmj.327.7414.557

Hoge, R. D., Atkinson, J., Gill, B., Crelier, G. R., Marrett, S., and Pike, G. B. (1999). Linear coupling between cerebral blood flow and oxygen consumption in activated human cortex. *Proc. Natl. Acad. Sci. U.S.A.* 96, 9403–9408. doi: 10.1073/pnas.96.16.9403

Hu, B., Yan, L. F., Sun, Q., Yu, Y., Zhang, J., Dai, Y. J., et al. (2019). Disturbed neurovascular coupling in type 2 diabetes mellitus patients:evidence from a comprehensive fMRI analysis. *Neuroimage Clin.* 22:101802. doi: 10.1007/s00330-019-06096-w

Huang, R. R., Jia, B. H., Xie, L., Ma, S. H., Yin, J. J., Sun, Z. B., et al. (2016). Spatial working memory impairment in primary onset middle-age type 2 diabetes

mellitus:an ethology and BOLD-fMRI study. *J. Magn. Reson Imaging* 43, 75–87. doi: 10.1002/jmri.24967

Huang, X., Wen, Z., Tong, Y., Qi, C. X., and Shen, Y. (2021). Altered resting cerebral blood flow specific to patients with diabetic retinopathy revealed by arterial spin labeling perfusion magnetic resonance imaging. *Acta Radiol.* 62, 524–532. doi: 10.1016/j.nicl.2020.102302

Jansen, J. F., van Bussel, F. C., van de Haar, H. J., van Osch, M. J., Hofman, P. A., van Boxtel, M. P., et al. (2016). Cerebral blood flow, blood supply, and cognition in Type 2 Diabetes Mellitus. *Sci. Rep.* 6:10.

Jezzard, P., Chappell, M. A., and Okell, T. W. (2018). Arterial spin labeling for the measurement of cerebral perfusion and angiography. *J. Cereb. Blood Flow Metab.* 38, 603–626. doi: 10.1177/0271678X17743240

Ji, G. J., Hu, P., Liu, T. T., Li, Y., Chen, X., Zhu, C., et al. (2018). Functional Connectivity of the Corticobasal Ganglia-Thalamocortical Network in Parkinson Disease:a Systematic Review and Meta-Analysis with Cross-Validation. *Radiology* 287, 973–982. doi: 10.1148/radiol.2018172183

Jor'dan, A. J., Manor, B., and Novak, V. (2014). Slow gait speed - an indicator of lower cerebral vasoreactivity in type 2 diabetes mellitus. *Front. Aging Neurosci.* 6:135. doi: 10.3389/fnagi.2014.00135

Koenigs, M., Barbey, A. K., Postle, B. R., and Grafman, J. (2009). Superior parietal cortex is critical for the manipulation of information in working memory. *J. Neurosci.* 29, 14980–14986. doi: 10.1523/JNEUROSCI.3706-09.2009

Last, D., Alsop, D. C., Abduljalil, A. M., Marquis, R. P., de Bazelaire, C., Hu, K., et al. (2007). Global and regional effects of type 2 diabetes on brain tissue volumes and cerebral vasoreactivity. *Diabetes Care* 30, 1193–1199. doi: 10.2337/dc06-2052

Liu, J., Li, Y., Yang, X., Xu, H., Ren, J., and Zhou, P. (2021). Regional Spontaneous Neural Activity Alterations in Type 2 Diabetes Mellitus:a Meta-Analysis of Resting-State Functional MRI Studies. *Front. Aging Neurosci.* 13:678359. doi: 10.3389/fnagi.2021.678359

Liu, J., Liu, T., Wang, W., Ma, L., Ma, X., Shi, S., et al. (2017). Reduced Gray Matter Volume in Patients with Type 2 Diabetes Mellitus. *Front. Aging Neurosci.* 9:161. doi: 10.3389/fnagi.2017.00161

Liu, L., Li, W., Zhang, Y., Qin, W., Lu, S., and Zhang, Q. (2017). Weaker Functional Connectivity Strength in Patients with Type 2 Diabetes Mellitus. *Front. Neurosci.* 11:390. doi: 10.3389/fnins.2017.00390

McColgan, P., Seunarine, K. K., Razi, A., Cole, J. H., Gregory, S., Durr, A., et al. (2015). Selective vulnerability of Rich Club brain regions is an organizational principle of structural connectivity loss in Huntington's disease. *Brain* 138, 3327–3344. doi: 10.1093/brain/awv259

Meusel, L. A., Kansal, N., Tchistiakova, E., Yuen, W., MacIntosh, B. J., Greenwood, C. E., et al. (2014). A systematic review of type 2 diabetes mellitus and hypertension in imaging studies of cognitive aging:time to establish new norms. *Front. Aging Neurosci.* 6:148. doi: 10.3389/fnagi.2014.00148

Morris, J. K., Vidoni, E. D., Honea, R. A., Burns, J. M., and Alzheimer's Disease Neuroimaging initiative (2014). Impaired glycemia increases disease progression in mild cognitive impairment. *Neurobiol. Aging* 35, 585–589. doi: 10.1016/j.neurobiolaging.2013.09.033

Novak, V., Milberg, W., Hao, Y., Munshi, M., Novak, P., Galica, A., et al. (2014). Enhancement of vasoreactivity and cognition by intranasal insulin in type 2 diabetes. *Diabetes Care* 37, 751–759. doi: 10.2337/dc13-1672

Ochoa, N., Gogola, G. R., and Gorniak, S. L. (2016). Contribution of tactile dysfunction to manual motor dysfunction in type II diabetes. *Muscle Nerve* 54, 895–902. doi: 10.1002/mus.25137

Page, M. J., McKenzie, J. E., Bossuyt, P. M., Boutron, I., Hoffmann, T. C., Mulrow, C. D., et al. (2021a). The PRISMA 2020 statement:an updated guideline for reporting systematic reviews. *BMJ* 372:n71. doi: 10.1136/bmj.n71

Page, M. J., Moher, D., Bossuyt, P. M., Boutron, I., Hoffmann, T. C., Mulrow, C. D., et al. (2021b). PRISMA 2020 explanation and elaboration:updated guidance and exemplars for reporting systematic reviews. *BMJ* 372:n160. doi: 10.1136/bmj.n160

Postle, B. R., and D'Esposito, M. (2003). Spatial working memory activity of the caudate nucleus is sensitive to frame of reference. *Cogn. Affect. Behav. Neurosci.* 3, 133–144. doi: 10.3758/cabn.3.2.133

Qi, C. X., Huang, X., and Shen, Y. (2020). Altered Intrinsic Brain Activities in Patients with Diabetic Retinopathy Using Amplitude of Low-frequency Fluctuation:a Resting-state fMRI Study. *Diabetes Metab. Syndr. Obes.* 13, 2833–2842. doi: 10.2147/DMSO.S259476

Radua, J., and Mataix-Cols, D. (2009). Voxel-wise meta-analysis of grey matter changes in obsessive-compulsive disorder. *Br. J. Psychiatry* 195, 393–402. doi: 10.1192/bjp.bp.108.055046

Radua, J., Mataix-Cols, D., Phillips, M. L., El-Hage, W., Kronhaus, D. M., Cardoner, N., et al. (2012). A new meta-analytic method for neuroimaging studies that combines reported peak coordinates and statistical parametric maps. *Eur. Psychiatry* 27, 605–611. doi: 10.1016/j.eurpsy.2011.04.001

Radua, J., Rubia, K., Canales-Rodriguez, E. J., Pomarol-Clotet, E., Fusar-Poli, P., and Mataix-Cols, D. (2014). Anisotropic kernels for coordinate-based meta-analyses of neuroimaging studies. *Front. Psychiatry* 5:13. doi: 10.3389/fpsyt.2014.00013

Reijmer, Y. D., van den Berg, E., Ruis, C., Kappelle, L. J., and Biessels, G. J. (2010). Cognitive dysfunction in patients with type 2 diabetes. *Diabetes Metab. Res. Rev.* 26, 507–519. doi: 10.1002/dmrr.1112

Roy, B., Ehlert, L., Mullur, R., Freeby, M. J., Woo, M. A., Kumar, R., et al. (2020). Regional Brain Gray Matter Changes in Patients with Type 2 Diabetes Mellitus. *Sci. Rep.* 10:9925. doi: 10.1038/s41598-020-67022-5

Rusinek, H., Ha, J., Yau, P. L., Storey, P., Tirsi, A., Tsui, W. H., et al. (2015). Cerebral perfusion in insulin resistance and type 2 diabetes. *J. Cereb. Blood Flow Metab.* 35, 95–102. doi: 10.1038/jcbfm.2014.173

Shen, Y., Zhao, B., Yan, L., Jann, K., Wang, G., Wang, J., et al. (2017). Cerebral Hemodynamic and White Matter Changes of Type 2 Diabetes Revealed by Multi-TI Arterial Spin Labeling and Double Inversion Recovery Sequence. *Front. Neurol.* 8:717. doi: 10.3389/fneur.2017.00717

Shibasaki, H., Sadato, N., Lyshkow, H., Yonekura, Y., Honda, M., Nagamine, T., et al. (1993). Both primary motor cortex and supplementary motor area play an important role in complex finger movement. *Brain* 116, 1387–1398. doi: 10.1093/brain/116.6.1387

Tanji, J., and Shima, K. (1994). Role for supplementary motor area cells in planning several movements ahead. *Nature* 371, 413–416. doi: 10.1038/371413a0

Tootell, R. B., Hadjikhani, N. K., Vanduffel, W., Liu, A. K., Mendola, J. D., Sereno, M. I., et al. (1998). Functional analysis of primary visual cortex (V1) in humans. *Proc. Natl. Acad. Sci. U.S.A.* 95, 811–817. doi: 10.1073/pnas.95.3.811

van Sloten, T., and Schram, M. (2018). Understanding depression in type 2 diabetes:a biological approach in observational studies. *F1000Res* 7:1283. doi: 10.12688/f1000research.13898.1

van Sloten, T. T., Sedaghat, S., Carnethon, M. R., Launer, L. J., and Stehouwer, C. D. A. (2020). Cerebral microvascular complications of type 2 diabetes:stroke, cognitive dysfunction, and depression. *Lancet Diabetes Endocrinol.* 8, 325–336. doi: 10.1016/S2213-8587(19)30405-X

Wandell, B. A., Dumoulin, S. O., and Brewer, A. A. (2007). Visual field maps in human cortex. *Neuron* 56, 366–383. doi: 10.1016/j.neuron.2007.10.012

Wang, Y., Sun, L., He, G., Gang, X., Zhao, X., Wang, G., et al. (2021). Cerebral perfusion alterations in type 2 diabetes mellitus - a systematic review. *Front. Neuroendocrinol.* 62:100916. doi: 10.1016/j.yfrne.2021.100916

Wang, Z. L., Zou, L., Lu, Z. W., Xie, X. Q., Jia, Z. Z., Pan, C. J., et al. (2017). Abnormal spontaneous brain activity in type 2 diabetic retinopathy revealed by amplitude of low-frequency fluctuations:a resting-state fMRI study. *Clin. Radiol.* 72, 340.e1–340.e7. doi: 10.1016/j.crad.2016.11.012

Williams, D. S., Detre, J. A., Leigh, J. S., and Koretsky, A. P. (1992). Magnetic resonance imaging of perfusion using spin inversion of arterial water. *Proc. Natl. Acad. Sci. U.S.A.* 89, 212–216. doi: 10.1073/pnas.89.1.212

Wintermark, M., Sesay, M., Barbier, E., Borbely, K., Dillon, W. P., Eastwood, J. D., et al. (2005). Comparative overview of brain perfusion imaging techniques. *J. Neuroradiol.* 32, 294–314. doi: 10.1016/s0150-9861(05)83159-1

Xia, W., Rao, H., Spaeth, A. M., Huang, R., Tian, S., Cai, R., et al. (2015). Blood Pressure is Associated With Cerebral Blood Flow Alterations in Patients With T2DM as Revealed by Perfusion Functional MRI. *Medicine* 94:e2231. doi: 10.1097/md.0000000000002231

Xu, W., Caracciolo, B., Wang, H. X., Winblad, B., Backman, L., Qiu, C., et al. (2010). Accelerated progression from mild cognitive impairment to dementia in people with diabetes. *Diabetes* 59, 2928–2935. doi: 10.2337/db10-0539

Xue, M., Xu, W., Ou, Y. N., Cao, X. P., Tan, M. S., Tan, L., et al. (2019). Diabetes mellitus and risks of cognitive impairment and dementia:a systematic review and meta-analysis of 144 prospective studies. *Ageing Res. Rev.* 55:100944. doi: 10.1016/j.arr.2019.100944

Yao, L., Yang, C., Zhang, W., Li, S., Li, Q., Chen, L., et al. (2021). A multimodal meta-analysis of regional structural and functional brain alterations in type 2 diabetes. *Front. Neuroendocrinol.* 62:100915. doi: 10.1016/j.yfrne.2021.100915

Yu, Y., Yan, L. F., Sun, Q., Hu, B., Zhang, J., Yang, Y., et al. (2019). Neurovascular decoupling in type 2 diabetes mellitus without mild cognitive impairment:potential biomarker for early cognitive impairment. *Neuroimage* 200, 644–658. doi: 10.1016/j.neuroimage.2019.06.058

Zhang, D., Shi, L., Song, X., Shi, C., Sun, P., Lou, W., et al. (2019). Neuroimaging endophenotypes of type 2 diabetes mellitus:a discordant sibling pair study. *Quant. Imaging Med. Surg.* 9, 1000–1013. doi: 10.21037/qims.2019.05.18

Zhang, J. (2016). How far is arterial spin labeling MRI from a clinical reality? *J. Magn. Reson. Imaging* 43, 1020–1045. doi: 10.1002/jmri.25022

Zhang, Y., Zhang, X., Ma, G., Qin, W., Yang, J., Lin, J., et al. (2021). Neurovascular coupling alterations in type 2 diabetes:a 5-year longitudinal MRI study. *BMJ Open Diabetes Res. Care* 9:e001433. doi: 10.1136/bmjdrc-2020-001433

Zheng, Y., Ley, S. H., and Hu, F. B. (2018). Global aetiology and epidemiology of type 2 diabetes mellitus and its complications. *Nat. Rev. Endocrinol.* 14, 88–98. doi: 10.1038/nrendo.2017.151

**Conflict of Interest:** The authors declare that the research was conducted in the absence of any commercial or financial relationships that could be construed as a potential conflict of interest.

**Publisher's Note:** All claims expressed in this article are solely those of the authors and do not necessarily represent those of their affiliated organizations, or those of the publisher, the editors and the reviewers. Any product that may be evaluated in this article, or claim that may be made by its manufacturer, is not guaranteed or endorsed by the publisher.

frontiers in Aging Neuroscience

ORIGINAL RESEARCH
published: 17 February 2022
doi: 10.3389/fnagi.2021.803080

# Global Functional Connectivity Analysis Indicating Dysconnectivity of the Hate Circuit in Major Depressive Disorder

*Pan Pan[1], Lu Wang[1], Chujun Wu[1], Kun Jin[1], Song Cao[1], Yan Qiu[1], Ziwei Teng[1], Sujuan Li[1], Tiannan Shao[1], Jing Huang[1], Haishan Wu[1], Hui Xiang[1], Jindong Chen[1], Feng Liu[2], Hui Tang[1]* and Wenbin Guo[1,3]**

[1] National Clinical Research Center on Mental Disorders and Department of Psychiatry, The Second Xiangya Hospital of Central South University, Changsha, China, [2] Department of Radiology, Tianjin Medical University General Hospital, Tianjin, China, [3] Department of Psychiatry, The Third People's Hospital of Foshan, Foshan, China

OPEN ACCESS

**Edited by:**
*Wenjing Zhang,*
*Sichuan University, China*

**Reviewed by:**
*Jiajia Zhu,*
*The First Affiliated Hospital of Anhui Medical University, China*
*Dongrong Xu,*
*Columbia University, United States*

***Correspondence:**
*Hui Tang*
*tanghui2017@csu.edu.cn*
*Wenbin Guo*
*guowenbin76@csu.edu.cn*

**Specialty section:**
*This article was submitted to Neurocognitive Aging and Behavior, a section of the journal Frontiers in Aging Neuroscience*

**Received:** *27 October 2021*
**Accepted:** *30 December 2021*
**Published:** *17 February 2022*

**Citation:**
*Pan P, Wang L, Wu C, Jin K, Cao S, Qiu Y, Teng Z, Li S, Shao T, Huang J, Wu H, Xiang H, Chen J, Liu F, Tang H and Guo W (2022) Global Functional Connectivity Analysis Indicating Dysconnectivity of the Hate Circuit in Major Depressive Disorder. Front. Aging Neurosci. 13:803080. doi: 10.3389/fnagi.2021.803080*

**Background:** Abnormalities of functional connectivity (FC) in certain brain regions are closely related to the pathophysiology of major depressive disorder (MDD). Findings are inconsistent with different presuppositions in regions of interest. Our research focused on voxel-wise brain-wide FC changes in patients with MDD in an unbiased manner.

**Method:** We examined resting-state functional MRI in 23 patients with MDD and 26 healthy controls. Imaging data were analyzed by using global-brain FC (GFC) and used to explore the correlation of abnormal GFC values with clinical variables.

**Results:** Increased GFC values in the left medial superior frontal gyrus (SFGmed) and decreased GFC values in the right supplementary motor area (SMA) were observed in the patients with MDD compared with the controls. The decreased GFC values in the right SMA had a positive correlation with vitamin D and Hamilton Anxiety Scale (HAM-A) scores.

**Conclusion:** Abnormal GFC in the hate circuit, particularly increased GFC in the left SFGmed and decreased GFC in the right SMA, appears to be a new sight for comprehending the pathological alterations in MDD.

**Keywords: major depressive disorder, fMRI, global-brain functional connectivity, network, hate circuit**

## INTRODUCTION

Typical signs of major depressive disorder (MDD) include persistent negative emotions, reduced volitional activity, and cognitive dysfunction. MDD brings a heavy burden to the patients and their families due to its significant characteristics of high morbidity and mortality. However, the pathophysiology of MDD remains unclear. Several abnormal biochemical serum indices exhibit potential diagnostic significance for MDD. For example, the levels of some monoamine metabolites are significantly associated with the incidence of MDD (Richelson, 2001; Moret and Briley, 2011).

Vitamin D is involved in the synthesis of monoamine neurotransmitters as a common fat-soluble vitamin. Previous studies found a significantly negative correlation between vitamin D levels in serum and MDD occurrence in participants (Hoang et al., 2011; Jääskeläinen et al., 2015). In other words, vitamin D deficiency might be involved in the incidence of MDD. Patients with MDD have a higher rate of vitamin D deficiency than the general population (Anglin et al., 2013; Gelaye et al., 2015). Lower levels of vitamin D in serum reduced neurotransmitters such as cholinergic, dopamine, and norepinephrine, thereby increasing the risk of MDD. Lower levels of vitamin D in older adults may be considered a biomarker for the depressive state (Adibfar et al., 2016).

Several previous studies on the pathogenesis for MDD have focused on genetic factors, social environment, and other aspects. Nonetheless, no single hypothesis could perfectly explain all the characteristics and prognosis of this disease. The development of brain imaging has provided a new sight and method for exploring the pathogenesis of MDD in recent years. Researchers have achieved important progress in probing the neurobiological mechanisms of MDD from the aspects of brain structure and function. Neuroimaging studies indicated that MDD may be caused by disruptions within discrete brain networks rather than abnormalities in isolated brain regions (Wang et al., 2012). Neural networks that have been studied extensively in patients with MDD include the default mode network (DMN) and fronto-limbic network, where functional defects have been observed (Lee et al., 2008; Guo et al., 2015b; Scalabrini et al., 2020). Notably, the location of abnormally activated brain regions in previous studies focusing on brain dysfunction in MDD was involved in the main component of the hate circuit (Tao et al., 2013; Guo et al., 2015a). Hate, an intense basic human emotional response, plays an important role in psychological behavior and human evolution (Halperin, 2012). The hate circuit shows an altered activation when people watch stimuli they hate (Zeki and Romaya, 2008). Disgust at its core feeling of hate has been implicated in a wide range of psychological and mental conditions (Turnell et al., 2019). A number of studies have shown that hate is closely associated with depressive symptoms. For example, high levels of self-hate are directly related to the depressive state. Self-lathing in patients with MDD is associated with increased activity of the hate circuit (Surguladze et al., 2010; Turnell et al., 2019).

Resting-state functional connectivity (FC) between brain regions reflects its correlation with brain activity, which is an important tool to understand changes in FC between brain regions in patients with mood disorders. A number of studies have reported abnormal FC with inconsistent results in patients with MDD. For instance, patients with MDD in one study showed decreased FC between the medial orbitofrontal gyrus (Yu et al., 2021) and cerebellum (Zhu et al., 2020), whereas patients in another work exhibited increased homotopic FC (Liu et al., 2020) in the same brain regions.

One important factor contributing to these inconsistent results may be sample differences in age, population, locations, living style, etc. For example, patients with treatment-sensitive depression exhibited dysfunction in the frontoparietal top-down control network at specific frequency bands. However, patients with treatment-resistant depression showed abnormal FCs in the affective network, auditory network, visual network, and language processing cortex at the same frequency bands (He et al., 2016). Therefore, it is important to select first-episode, drug-naive patients with MDD to provide naive FC information to the pathophysiology of MDD.

Another important factor may be that previous studies focused on FC in specific brain regions. The region of interest (ROI) method was applied to these studies without a whole-brain examination. Critical areas associated with the core pathological alteration in MDD may be omitted by using this approach. Different ROI selections may result in different consequences. In this study, we adopted a data-driven approach, global-brain functional connectivity (GFC), to explore the pathophysiology of MDD and remedy the disadvantages of the ROI-based analysis (Preller et al., 2020). This method could be independent of the ROI selection. Therefore, GFC is helpful to obtain whole-brain FCs (Anticevic et al., 2014; Abdallah et al., 2017; Preller et al., 2018).

This study aims to utilize the GFC method, which belongs to the analysis method of the functional connectome, to probe the FC alterations in the whole brain of patients with MDD based on the aforementioned studies in MDD. We hypothesized that patients with MDD would exhibit GFC abnormalities in certain brain networks. Abnormal GFC in these brain regions may be related to the vitamin D levels in patients with MDD.

# MATERIALS AND METHODS

## Participants

A total of 28 first-episode, drug-naive patients with MDD were involved from the Inpatient Department of the Second Xiangya Hospital of Central South University. The age of patients was between 16 and 45 years. Each patient was diagnosed and screened by two psychiatric experts according to the *Diagnostic and Statistical Manual of Mental Disorders*, Fifth Edition (DSM-5) (First, 2013). The participants were right-handed. The enrolled patients were first-episode patients and with the course of the disease not exceeding 1 year. All patients were required to complete the Hamilton Depression Rating Scale-17 (HAMD-17) (Hamilton, 1967), the Hamilton Anxiety Scale (Hamilton, 1959), and the Beck Depression Inventory-II (BDI-II) (Steer, 1993) to evaluate the clinical sign of MDD. Meanwhile, the cognitive functions of all patients were evaluated by the Repeatable Battery for the Assessment of Neuropsychological Status (RBANS) (Randolph et al., 1998). The exclusion criteria for the participants included serious physical disease and any other mental disorders consistent with DSM-5, any history of alcohol or drug abuse, any drug treatment to MDD, lipid-lowering therapy or vitamin D supplementation, pregnancy, and any contraindications to MRI scanning.

Thirty healthy controls who matched the patients with age, sex ratio, and education were involved by advertising in the local community. The DSM-5, Non-patients Version, was adopted to screen the healthy controls. The exclusion conditions

included the history of serious neurological disorders, psychiatric disorders, and drugs or alcohol abuse in either the controls or their first-degree relatives.

All participants signed an informed consent form after obtaining an adequate explanation. Consent of the guardian was required for participants who aged under 18 years. This study is approved by the Ethics Committee of the Second Xiangya Hospital of Central South University and carried out in accordance with the Helsinki Declaration.

## Sample Collection

To avoid circadian rhythms interfering with the data, fasting blood samples for biochemical analyses were collected between 7 a.m. and 9 a.m. for all participants. Liver and kidney function, blood glucose, lipid series, and vitamin D levels were analyzed by serum tests.

## Neuroimaging Data Acquisition and Preprocessing

We used a Siemens 3.0 T scanner to obtain the resting-state images. The participants were required to lay on their back in a relaxed state and stay still during scanning. The neuroimaging data were automatically preprocessed using DPARBI and SPM8 in MATLAB (Yan et al., 2016). Detailed neuroimaging acquisition and preprocessing procedures are described in the **Supplementary Material**.

## Global-Brain FC Analysis

Global-brain functional connectivity is a measurement tool that computes the mean time series correlation between a given voxel with every other voxel for an unbiased method to determine the location of abnormal FCs (Anticevic et al., 2013, 2014; Murrough et al., 2016; Pan et al., 2019, 2021). The gray matter mask is produced by using the gray matter probability map (probability > 0.2) in the SPM8 software (Donishi et al., 2018). Such a threshold was chosen to eliminate the voxel with weak correlations that possibly originated from signal noises. A voxel-based GFC map was generated by composing GFC values of all voxels within the gray matter mask, where each voxel value represents the mean connectivity between the voxel and the rest of the brain. We computed the average Pearson's coefficient ($r$) between the time series of each seed voxel and that of all other seed voxels throughout the whole brain after selecting each voxel within the gray matter mask as the seed voxel (Cole et al., 2010). GFC was calculated as average voxel-to-voxel connectivity throughout the gray matter mask as follows:

$$GFCa = \sum_{b=1}^{n} \frac{r(T_a, T_b)}{n-1}$$

where the Pearson correlation coefficient ($r$) of time series Ts for a pair of given voxels a and b was calculated. Finally, the mean correlation coefficient within the gray matter mask of the entire brain was calculated using the MATLAB software (Scheinost et al., 2016; Pan et al., 2021), and the data were normalized and converted into $z$-values using Fisher $r$-to-$z$ transformation (Cole et al., 2010; Kaneoke et al., 2012; Thompson and Fransson, 2016).

The GFC maps between patients with MDD and controls were evaluated using two-sample $t$-tests. The framewise displacement (FD) values for each participant were calculated based on a previous study (Tozzi and Peters, 2017). The mean FD, education level, and age were substituted into the calculation as non-interest covariates. The threshold-free cluster enhancement (TFCE) was adopted to set the significance level as $p < 0.05$, a strict multiple comparison correction strategy that could achieve the optimal balance between the family-wise error rate and test-retest reliability/repeatability (Chen et al., 2018).

## Functional Connectivity Within the Hate Circuit Analysis

We performed a pairwise correlation analysis of six brain regions of the hate circuit in each subject by using the region-wise

**TABLE 1** | Characteristics of the participants.

| | Patients ($n$ = 23) | Controls ($n$ = 26) | $P$-value |
|---|---|---|---|
| Sex (male/female) | 7/16 | 11/15 | 0.390[a] |
| Age (years) | 23.17 ± 4.30 | 20.85 ± 3.13 | 0.118[b] |
| Education level (years) | 14.13 ± 2.30 | 14.62 ± 2.06 | 0.213[b] |
| HAMD-17 | 29.13 ± 8.59 | | |
| HAMA-14 | 21.04 ± 6.02 | | |
| BDI-II | 27.46 ± 10.35 | | |
| VITD-T | 24.50 ± 8.89 | | |
| Blood glucose | 3.69 ± 0.86 | | |
| TG | 0.72 ± 0.31 | | |
| CHOL | 3.75 ± 0.92 | | |
| HDL-C | 1.61 ± 1.79 | | |
| LDL-C | 2.08 ± 0.83 | | |
| Vocabulary learning | 25.30 ± 5.49 | | |
| Story retelling | 12.17 ± 5.25 | | |
| Immediate memory total score | 37.48 ± 9.51 | | |
| Graphic copy | 19.09 ± 1.35 | | |
| Line positioning | 16.35 ± 1.85 | | |
| Visual span total score | 35.43 ± 2.04 | | |
| Picture named | 9.96 ± 0.21 | | |
| Verbal fluency test | 18.35 ± 4.98 | | |
| Verbal function total score | 28.30 ± 4.97 | | |
| Digit span | 15.26 ± 1.21 | | |
| Coding test | 51.04 ± 11.42 | | |
| Attention total score | 66.30 ± 11.55 | | |
| Vocabulary memory | 6.65 ± 1.97 | | |
| Vocabulary recognition | 19.78 ± 0.52 | | |
| Story recall | 6.70 ± 2.89 | | |
| Figure memory | 15.61 ± 2.64 | | |
| Delayed memory score | 48.74 ± 6.36 | | |
| Stroop word | 98.30 ± 10.36 | | |
| Stroop Color | 65.17 ± 13.33 | | |
| Stroop Color-word | 39.04 ± 7.38 | | |

[a] *A p-value was obtained using a chi-square test.*
[b] *The p-values were obtained using two-sample t-tests.*
*HAMD-17, Hamilton Depression Scale-17; HAMA, Hamilton Anxiety Scale; BDI-II, Baker Depression Inventory-II; VITD-T, vitamin D.*

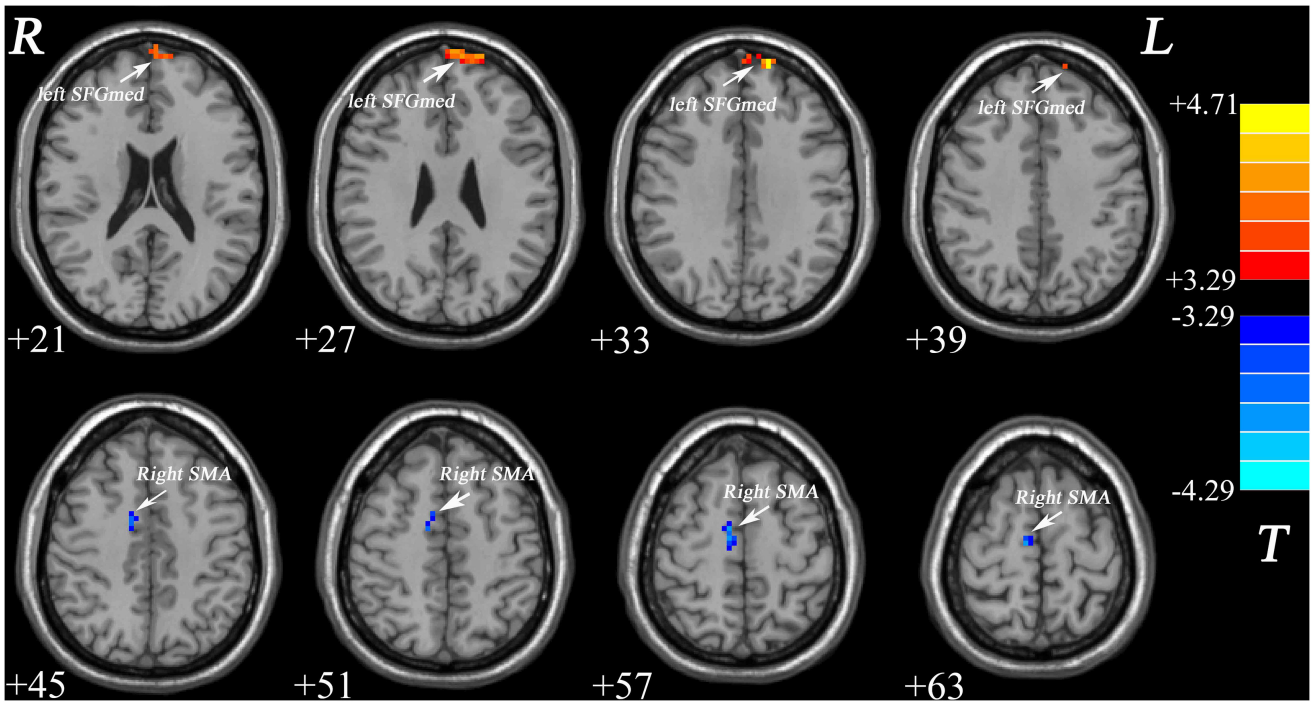


**FIGURE 1 |** Increased GFC values in the left SFGmed and decreased GFC values in the right SMA were observed in patients with MDD relative to healthy controls. GFC, global-brain functional connectivity; SFGmed, medial superior frontal gyrus; SMA, supplementary motor area; MDD, major depressive disorder.

FC method in the RESTplus software package and obtained correlation coefficient $r$. Fisher $r$-to-$z$ coefficients were adopted to transform into $z$-values to obtain a 6 × 6 FC matrix. The FC matrix between the patients with MDD and the controls was evaluated by two-sample $t$-tests.

## Statistical Analysis

Two-sample $t$-tests were conducted on continuous variables. A chi-square test was performed for gender distribution. Pearson correlation analyses were performed between GFC values in patients with MDD and clinical characteristics including vitamin D, blood lipid series, and HAMD-17, HAMA, BDI-II, or RBANS scores. The significance level was Bonferroni corrected at $p < 0.05$.

**TABLE 2 |** Significant differences in GFC values between groups.

| Cluster location | Peak (MNI) | | | Number of voxels | *T*-value |
|---|---|---|---|---|---|
| | x | y | z | | |
| Patients > Controls | | | | | |
| Left SFGmed | −15 | 63 | 33 | 64 | 4.6536 |
| Patients < Controls | | | | | |
| Right SMA | 9 | −15 | 63 | 42 | −4.2841 |

*MDD, major depressive disorder; GFC, global functional connectivity; SFGmed: medial superior frontal gyrus; SMA: supplementary motor area; MNI, Montreal Neurological Institute.*

# RESULTS

## Demographic and Clinical Characteristics

Five patients and four controls were excluded because they had excessive head movement during functional MRI (fMRI) scans after preprocessing the neuroimaging data. The final sample included 23 patients with MDD and 26 healthy controls. No significant differences in sex ratio, age, and years of education were observed between patients with MDD and healthy controls. The demographic and clinical characteristics of the participants are summarized in **Table 1**.

## Group Differences in Global-Brain FC

As shown in **Figure 1** and **Table 2**, patients with MDD exhibited decreased GFC values in the right supplementary motor area (SMA) ($t = -4.2841$, $p < 0.001$) and increased GFC values in the left medial superior frontal gyrus (SFGmed) ($t = 4.6535$, $p < 0.001$) compared with the control group. No other differences were observed in the patients.

## Correlations Between Global-Brain FC and Clinical Characteristics

Decreased GFC values in the right SMA were positively correlated with HAMA scores ($r = 0.500$, $p = 0.015$) and vitamin D ($r = 0.473$, $p = 0.033$) (**Figure 2**). No significant correlations were found between the GFC values in the left SFGmed and the

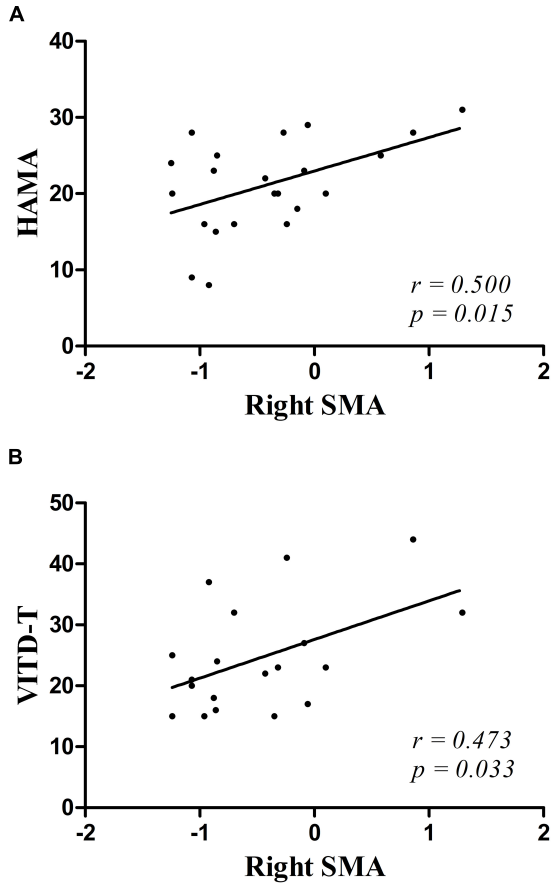


**FIGURE 2 | (A,B)** Positive correlations were observed between the GFC values in the right SMA and the scores of HAMA and the vitamin D in patients with MDD. HAMA, Hamilton Anxiety Scale; VITD-T, vitamin D.

clinical variables. No relationships between GFC and age, years of education, blood lipid series, and HAMD-17, BDI-II, or RBANS scores were observed.

## Functional Connectivity Difference Within the Hate Circuit

Compared with controls, patients with MDD showed increased FC between the left insula and the left putamen, between the left putamen and the right putamen, and between the left SFG and the right SFG. FC between the right insula and the left SFG decreased (**Figure 3**).

# DISCUSSION

Patients with MDD exhibit abnormal GFC in the brain regions of hate circuit in this study. Compared with the controls, significantly decreased GFC in the right SMA and increased GFC in the left SFGmed were observed in patients with MDD. The GFC in right SMA was positively correlated with vitamin D and the scores of HAMA.

Global-brain FC applies the basic image theory to study the overall connection between each voxel and every other voxel in the whole brain (Cole et al., 2010). This holistic approach was adopted to identify altered FC in the brain of patients with MDD and has proved to be very informative. This approach emphasizes qualitative data. Brain regions with abnormal FC may play a crucial role in coordinating massive brain activity patterns. Decreased GFC values may indicate low involvement of specific brain regions in diseases. Conversely, increased GFC values may indicate higher pathologies in specific brain regions (Buckner et al., 2009).

Superior frontal gyrus located in the upper prefrontal cortex (Shi et al., 2015) is considered to be composed of several subregions with different cellular structures (Petrides and Pandya, 1999, 2002), including Brodmann areas 6, 8, and 32 (Li et al., 2013). Previous studies on both task and resting-state fMRI have shown that different parts of SFG were involved in two anticorrelation networks, namely, task-positive network and DMN. These findings indicate that subregions exist in the SFG of humans (Li et al., 2013). Each subregion participates in different functional networks with its specific connectivity patterns of anatomical and functional levels. SFGmed plays as a pivotal node for DMN to participate in self-referential processing. The self-referential processing refers to the process of encoding, storing, and extracting information closely related to self-experience, which is often accompanied by special affective meaning and motivation (Northoff et al., 2006). Increased GFC in the left SFGmed indicates that it is abnormally activated in this brain region of patients with MDD at rest compared with controls in this study. Abnormal activation in SFGmed was closely related to excessive self-focus under the influence of MDD. The excessive self-focus often takes the form of rumination, which is a common clinical symptom in patients with MDD. Previous neuroimaging studies have revealed that patients with MDD of abnormal FC in SFGmed were more likely to cause excessive self-focus when they encounter negative emotional events (Lemogne et al., 2012). The suppression was enhanced abnormally in irrelevant information outside the self in patients with MDD when they were excessively self-focused. This reactive mode aggravated negative emotion and eventually formed into negative automatic thoughts (Morawetz et al., 2016). Previous studies have exhibited that a deceptive reaction requires more complex cognitive processing or stronger mind control, which may involve cognitive controls, including cognitive inhibition, conflict monitoring, resolution, and generativity (Spence et al., 2001; Nuñez et al., 2005). SFGmed is the physiological basis for performing cognitive control (Sohn et al., 2007; Ursu et al., 2009; Pourtois et al., 2010; Xu et al., 2021). SFGmed plays a role in working memory processing, and abnormal FC in this region is the basis of the deterioration of working memory for patients with MDD (Vasic et al., 2008). Significant activation in the SFGmed was associated with feigned long-term memory impairment, suggesting that SFGmed may underlie the physiological basis for the execution of feigned memory (Chen et al., 2015). The most active brain region frequently observed during lying is SFG, indicating that the region is the basic neural circuit for lying (Kozel et al., 2004; Spence et al., 2004). Increased GFC in SFGmed suggests

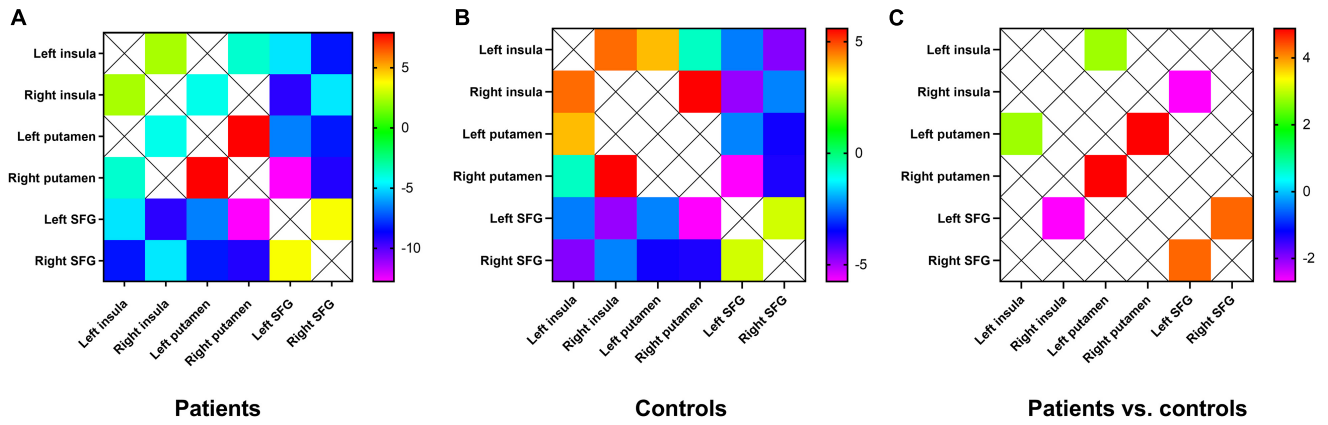


**FIGURE 3 | (A)** Mean FC between the brain regions of the hate circuit in the patient group. One-sample t-tests on the FCs were conducted. The warm color denotes higher FC values, and the cold color denotes lower FC in the patients. **(B)** Mean FC between the brain regions of the hate circuit in the control group. The range from red to green denotes higher FC values. Blue and purple denote lower FC. One-sample t-tests on the FCs were conducted. **(C)** Increased FC between the left insula and the right insula, between the left putamen and the right putamen, between the left SFG and the right SFG and decreased FC values in the right insula and the left SFG were observed in patients with MDD relative to healthy controls. FC, functional connectivity; SFG, superior frontal gyrus; MDD, major depressive disorder.

that compensatory activation occurs in this brain region affected by MDD in this study. Patients with MDD showed increased cognitive control during feigned memory disorders.

Supplementary motor area belongs to the posterior SFG, located in the medial side of hemispheres, which is mainly activated by motor tasks (Li et al., 2013). Generally, SMA takes part in controlled movement as the secondary motor cortex. A previous study has found significantly increased FC in SMA in patients with MDD, suggesting that impaired function to this brain region may be involved in the pathophysiology of MDD (Frodl et al., 2010). This study reveals decreased GFC in the right SMA, which speculated spontaneous neural activity, and functional inhibition in severe depressive symptoms would cause thinking retardation, delayed speech, decreased initiative, and a series of involuntary motor behaviors such as akathisia and unconscious standing in several patients.

Tao et al. (2013) first reported FC alteration in the hate circuit of patients with MDD. They provided a perspective that the hate circuit may reflect reduced cognitive control over oneself and others in resentment generation. This study also focuses on FC within the hate circuit. The circuit includes the SFG, insula, and putamen. The SFG exhibited increased activities as well as enhanced activation in response to positive emotional stimuli. The putamen contains neurons in the preparation phase for motor behavior and participates in the perception of contempt and disgust. This brain region may have been involved in preparing offensive activity. The insula may be the physiological basis of activity in response to painful sensory stimuli. Damage to putamen and insula could affect the ability to recognize disgust signals in patients. The analysis of FC within the hate circuit exhibited abnormal FC between the SFG, putamen, and insula. Abnormal FC between these regions may be the physiological basis for the aggressive tendency and somatic discomfort in patients with MDD. Several studies have demonstrated that hate is closely associated with depressive symptoms (Overton et al., 2008; Surguladze et al., 2010). Reduced cognitive control in emotion is one of the important factors that cause MDD (Ebmeier et al., 2006). Patients with MDD have trouble in controlling negative thoughts. The hate circuit has been considered to be responsible for emotional and cognitive control regulation (Phillips et al., 2008; Fan et al., 2020). Impaired hate circuit might result in impaired cognitive control over pervasive internal self-loathing or hate of the external environment.

Decreased GFC values in the right SMA were positively correlated with vitamin D and HAMA scores. This finding indicates that decreased GFC in the right SMA may influence the anxiety level and provides theoretical foundation for the pathophysiology of anxiety signs in patients with MDD. Vitamin D deficiency has been shown to be causally associated with MDD (Milaneschi et al., 2014). Low vitamin D is closely related to the onset of MDD (Hoang et al., 2011), which probably explains that the treatment effect of MDD could be improved by adding vitamin D in addition to conventional antidepressant therapy. The cognitive function and spontaneous neural activity in patients with MDD may be affected by abnormal GFC in SMA due to alteration in vitamin D.

Several constraints should be taken into account in this research. First, the difference in age may have a bias effect on the present results although age has been treated as a covariate. Second, the vitamin D level may vary between genders, but no significant difference was found in this research. Finally, the alterations in gray/white matter were not explored. Therefore, the mechanism of change in gray/white matter underlying GFC remains unclear.

## CONCLUSION

Despite the limitation, this study presents that GFC abnormalities in the brain areas are associated with the hate circuit in patients with MDD. Abnormal GFC values in the right SMA might be one of the brain functional bases that cause alterations in the anxiety

level. This study provides preliminary evidence that the vitamin D level in patients with MDD might be associated with abnormal FC in the hate circuit.

## DATA AVAILABILITY STATEMENT

The original contributions presented in the study are included in the article/**Supplementary Material**, further inquiries can be directed to the corresponding authors.

## ETHICS STATEMENT

The studies involving human participants were reviewed and approved by the Ethics Committee of the Second Xiangya Hospital of Central South University. The patients/participants provided their written informed consent to participate in this study.

## AUTHOR CONTRIBUTIONS

WG, JC, HT, and HW provided the conception of the work. LW, CW, SL, YQ, ZT, KJ, and SC collected the data. FL, PP, TS, HX, and JH were responsible for the data analysis and interpretation. PP drafted the manuscript. WG critically revised the manuscript. All authors contributed to the article and approved the final version of the manuscript.

## FUNDING

This study was supported by grants from the National Natural Science Foundation of China (Grant Nos. 82171508, 81771447, and 81630033), the Natural Science Foundation of Hunan (Grant No. 2020JJ4784), the Science and Technology Program of Hunan Province (Grant No. 2020SK53413), the Commission Scientific Research Project of Hunan (Grant No. C2019164), and the Natural Science Foundation of Tianjin (Grant No. 18JCQNJC10900).

## ACKNOWLEDGMENTS

We thank all individuals who served as the research participants.

## SUPPLEMENTARY MATERIAL

The Supplementary Material for this article can be found online at: https://www.frontiersin.org/articles/10.3389/fnagi.2021.803080/full#supplementary-material

## REFERENCES

Abdallah, C. G., Averill, L. A., Collins, K. A., Geha, P., Schwartz, J., Averill, C., et al. (2017). Ketamine Treatment and Global Brain Connectivity in Major Depression. *Neuropsychopharmacology* 42, 1210–1219. doi: 10.1038/npp.2016.186

Adibfar, A., Saleem, M., Lanctot, K. L., and Herrmann, N. (2016). Potential Biomarkers for Depression Associated with Coronary Artery Disease: a Critical Review. *Curr. Mol. Med.* 16, 137–164. doi: 10.2174/1566524016666160126144143

Anglin, R. E., Samaan, Z., Walter, S. D., and McDonald, S. D. (2013). Vitamin D deficiency and depression in adults: systematic review and meta-analysis. *Br. J. Psychiatr.* 202, 100–107. doi: 10.1192/bjp.bp.111.106666

Anticevic, A., Brumbaugh, M. S., Winkler, A. M., Lombardo, L. E., Barrett, J., Corlett, P. R., et al. (2013). Global prefrontal and fronto-amygdala dysconnectivity in bipolar I disorder with psychosis history. *Biol. Psychiatr.* 73, 565–573. doi: 10.1016/j.biopsych.2012.07.031

Anticevic, A., Hu, S., Zhang, S., Savic, A., Billingslea, E., Wasylink, S., et al. (2014). Global resting-state functional magnetic resonance imaging analysis identifies frontal cortex, striatal, and cerebellar dysconnectivity in obsessive-compulsive disorder. *Biol. Psychiatr.* 75, 595–605. doi: 10.1016/j.biopsych.2013.10.021

Buckner, R. L., Sepulcre, J., Talukdar, T., Krienen, F. M., Liu, H., Hedden, T., et al. (2009). Cortical hubs revealed by intrinsic functional connectivity: mapping, assessment of stability, and relation to Alzheimer's disease. *J. Neurosci.* 29, 1860–1873. doi: 10.1523/JNEUROSCI.5062-08.2009

Chen, X., Lu, B., and Yan, C. G. (2018). Reproducibility of R-fMRI metrics on the impact of different strategies for multiple comparison correction and sample sizes. *Hum. Brain Mapp.* 39, 300–318. doi: 10.1002/hbm.23843

Chen, Z. X., Xue, L., Liang, C. Y., Wang, L. L., Mei, W., Zhang, Q., et al. (2015). Specific marker of feigned memory impairment: the activation of left superior frontal gyrus. *J. Forensic Leg. Med.* 36, 164–171. doi: 10.1016/j.jflm.2015.09.008

Cole, M. W., Pathak, S., and Schneider, W. (2010). Identifying the brain's most globally connected regions. *NeuroImage* 49, 3132–3148. doi: 10.1016/j.neuroimage.2009.11.001

Donishi, T., Terada, M., and Kaneoke, Y. (2018). Effects of gender, digit ratio, and menstrual cycle on intrinsic brain functional connectivity: a whole-brain, voxel-wise exploratory study using simultaneous local and global functional connectivity mapping. *Brain Behav.* 8:e00890. doi: 10.1002/brb3.890

Ebmeier, K., Rose, E., and Steele, D. (2006). Cognitive impairment and fMRI in major depression. *Neurotox. Res.* 10, 87–92. doi: 10.1007/BF03033237

Fan, Z., Yang, J., Zeng, C., Xi, C., Wu, G., Guo, S., et al. (2020). Bipolar Mood State Reflected in Functional Connectivity of the Hate Circuit: a Resting-State Functional Magnetic Resonance Imaging Study. *Front. Psychiatr.* 11:556126. doi: 10.3389/fpsyt.2020.556126

First, M. (2013). Diagnostic and Statistical Manual of Mental Disorders, 5th Edition, and Clinical Utility. *J. Nerv. Ment. Dis.* 201, 727–729. doi: 10.1097/nmd.0b013e3182a2168a

Frodl, T., Bokde, A. L., Scheuerecker, J., Lisiecka, D., Schoepf, V., Hampel, H., et al. (2010). Functional connectivity bias of the orbitofrontal cortex in drug-free patients with major depression. *Biol. Psychiatr.* 67, 161–167. doi: 10.1016/j.biopsych.2009.08.022

Gelaye, B., Williams, M. A., Lemma, S., Berhane, Y., Fann, J. R., Vander Stoep, A., et al. (2015). Major depressive disorder and cardiometabolic disease risk among sub-Saharan African adults. *Diabetes Metab. Syndr.* 9, 183–191. doi: 10.1016/j.dsx.2014.05.003

Guo, W., Liu, F., Xiao, C., Zhang, Z., Liu, J., Yu, M., et al. (2015a). Decreased insular connectivity in drug-naïve major depressive disorder at rest. *J. Affect. Dis.* 179, 31–37. doi: 10.1016/j.jad.2015.03.028

Guo, W., Liu, F., Yu, M., Zhang, J., Zhang, Z., Liu, J., et al. (2015b). Decreased regional activity and network homogeneity of the fronto-limbic network at rest in naïvenaive major depressive disorder. *Aus. N. Z. J. Psychiatr.* 49, 550–556. doi: 10.1177/0004867415577978

Halperin, E. (2012). The Nature of Hate. *Peace confl.* 18, 101–103.

Hamilton, M. (1959). The assessment of anxiety states by rating. *Br. J. Med. Psychol.* 32, 50–55. doi: 10.1111/j.2044-8341.1959.tb00467.x

Hamilton, M. (1967). Development of a rating scale for primary depressive illness. *Br. J. Soc. Clin. Psychol.* 6, 278–296. doi: 10.1111/j.2044-8260.1967.tb00530.x

He, Z., Cui, Q., Zheng, J., Duan, X., Pang, Y., Gao, Q., et al. (2016). Frequency-specific alterations in functional connectivity in treatment-resistant and -sensitive major depressive disorder. *J. Psychiatr. Res.* 82, 30–39. doi: 10.1016/j.jpsychires.2016.07.011

Hoang, M. T., Defina, L. F., Willis, B. L., Leonard, D. S., Weiner, M. F., and Brown, E. S. (2011). Association between low serum 25-hydroxyvitamin D and depression in a large sample of healthy adults: the Cooper Center longitudinal study. *Mayo Clin. Proc.* 86, 1050–1055. doi: 10.4065/mcp.2011.0208

Jääskeläinen, T., Knekt, P., Suvisaari, J., Männistö, S., Partonen, T., Sääksjärvi, K., et al. (2015). Higher serum 25-hydroxyvitamin D concentrations are related to a reduced risk of depression. *Br. J. Nutr.* 113, 1418–1426. doi: 10.1017/S0007114515000689

Kaneoke, Y., Donishi, T., Iwatani, J., Ukai, S., Shinosaki, K., and Terada, M. (2012). Variance and autocorrelation of the spontaneous slow brain activity. *PLoS One* 7:e38131. doi: 10.1371/journal.pone.0038131

Kozel, F. A., Revell, L. J., Lorberbaum, J. P., Shastri, A., Elhai, J. D., Horner, M. D., et al. (2004). A pilot study of functional magnetic resonance imaging brain correlates of deception in healthy young men. *J. NeuroPsychiatr. Clin. Neurosci.* 16, 295–305. doi: 10.1176/jnp.16.3.295

Lee, B. T., Seok, J. H., Lee, B. C., Cho, S. W., Yoon, B. J., Lee, K. U., et al. (2008). Neural correlates of affective processing in response to sad and angry facial stimuli in patients with major depressive disorder. *Prog. Neuropsychopharmacol. Biol. Psychiatr.* 32, 778–785. doi: 10.1016/j.pnpbp.2007.12.009

Lemogne, C., Delaveau, P., Freton, M., Guionnet, S., and Fossati, P. (2012). Medial prefrontal cortex and the self in major depression. *J. Affect. Dis.* 136, e1–e11. doi: 10.1016/j.jad.2010.11.034

Li, W., Qin, W., Liu, H., Fan, L., Wang, J., Jiang, T., et al. (2013). Subregions of the human superior frontal gyrus and their connections. *NeuroImage* 78, 46–58. doi: 10.1016/j.neuroimage.2013.04.011

Liu, Y., Chen, Y., Liang, X., Li, D., Zheng, Y., Zhang, H., et al. (2020). Altered Resting-State Functional Connectivity of Multiple Networks and Disrupted Correlation With Executive Function in Major Depressive Disorder. *Front. Neurol.* 11:272. doi: 10.3389/fneur.2020.00272

Milaneschi, Y., Hoogendijk, W., Lips, P., Heijboer, A. C., Schoevers, R., van Hemert, A. M., et al. (2014). The association between low vitamin D and depressive disorders. *Mol. Psychiatr.* 19, 444–451. doi: 10.1038/mp.2013.36

Morawetz, C., Bode, S., Baudewig, J., Kirilina, E., and Heekeren, H. R. (2016). Changes in Effective Connectivity Between Dorsal and Ventral Prefrontal Regions Moderate Emotion Regulation. *Cereb. Cortex* 26, 1923–1937. doi: 10.1093/cercor/bhv005

Moret, C., and Briley, M. (2011). The importance of norepinephrine in depression. *NeuroPsychiatr. Dis. Treat.* 7, 9–13. doi: 10.2147/NDT.S19619

Murrough, J. W., Abdallah, C. G., Anticevic, A., Collins, K. A., Geha, P., Averill, L. A., et al. (2016). Reduced global functional connectivity of the medial prefrontal cortex in major depressive disorder. *Hum. Brain Mapp.* 37, 3214–3223. doi: 10.1002/hbm.23235

Northoff, G., Heinzel, A., de Greck, M., Bermpohl, F., Dobrowolny, H., and Panksepp, J. (2006). Self-referential processing in our brain–a meta-analysis of imaging studies on the self. *NeuroImage* 31, 440–457. doi: 10.1016/j.neuroimage.2005.12.002

Nuñez, J. M., Casey, B. J., Egner, T., Hare, T., and Hirsch, J. (2005). Intentional false responding shares neural substrates with response conflict and cognitive control. *NeuroImage* 25, 267–277. doi: 10.1016/j.neuroimage.2004.10.041

Overton, P. G., Markland, F. E., Taggart, H. S., Bagshaw, G. L., and Simpson, J. (2008). Self-disgust mediates the relationship between dysfunctional cognitions and depressive symptomatology. *Emotion* 8, 379–385. doi: 10.1037/1528-3542.8.3.379

Pan, P., Ou, Y., Su, Q., Liu, F., Chen, J., Zhao, J., et al. (2019). Voxel-based global-brain functional connectivity alterations in first-epinaïvedrug-naive patients with somatization disorder. *J. Affect. Dis.* 254, 82–89. doi: 10.1016/j.jad.2019.04.099

Pan, P., Qiu, Y., Teng, Z., Li, S., Huang, J., Xiang, H., et al. (2021). Increased Global-Brain Functional Connectivity Is Associated with Dyslipidemia and Cognitive Impairment in Firstnaïveode, Drug-Naive Patients with Bipolar Disorder. *Neural Plast.* 2021:5560453. doi: 10.1155/2021/5560453

Petrides, M., and Pandya, D. N. (1999). Dorsolateral prefrontal cortex: comparative cytoarchitectonic analysis in the human and the macaque brain and corticocortical connection patterns. *Eur. J. Neurosci.* 11, 1011–1036. doi: 10.1046/j.1460-9568.1999.00518.x

Petrides, M., and Pandya, D. N. (2002). Comparative cytoarchitectonic analysis of the human and the macaque ventrolateral prefrontal cortex and corticocortical connection patterns in the monkey. *Eur. J. Neurosci.* 16, 291–310. doi: 10.1046/j.1460-9568.2001.02090.x

Phillips, M. L., Ladouceur, C. D., and Drevets, W. C. (2008). A neural model of voluntary and automatic emotion regulation: implications for understanding the pathophysiology and neurodevelopment of bipolar disorder. *Mol. Psychiatr.* 13, 833–857. doi: 10.1038/mp.2008.65

Pourtois, G., Vocat, R., N'Diaye, K., Spinelli, L., Seeck, M., and Vuilleumier, P. (2010). Errors recruit both cognitive and emotional monitoring systems: simultaneous intracranial recordings in the dorsal anterior cingulate gyrus and amygdala combined with fMRI. *Neuropsychologia* 48, 1144–1159. doi: 10.1016/j.neuropsychologia.2009.12.020

Preller, K. H., Burt, J. B., Ji, J. L., Schleifer, C. H., Adkinson, B. D., Stämpfli, P., et al. (2018). Changes in global and thalamic brain connectivity in LSD-induced altered states of consciousness are attributable to the 5-HT2A receptor. *eLife* 7:e35082. doi: 10.7554/eLife.35082

Preller, K. H., Duerler, P., Burt, J. B., Ji, J. L., Adkinson, B., Stämpfli, P., et al. (2020). Psilocybin Induces Time-Dependent Changes in Global Functional Connectivity. *Biol. Psychiatr.* 88, 197–207. doi: 10.1016/j.biopsych.2019.12.027

Randolph, C., Tierney, M. C., Mohr, E., and Chase, T. N. (1998). The Repeatable Battery for the Assessment of Neuropsychological Status (RBANS): preliminary clinical validity. *J. Clin. Exp. Neuropsychol.* 20, 310–319. doi: 10.1076/jcen.20.3.310.823

Richelson, E. (2001). Pharmacology of antidepressants. *Mayo Clin. Proc.* 76, 511–527.

Scalabrini, A., Vai, B., Poletti, S., Damiani, S., Mucci, C., Colombo, C., et al. (2020). All roads lead to the default-mode network-global source of DMN abnormalities in major depressive disorder. *Neuropsychopharmacology* 45, 2058–2069. doi: 10.1038/s41386-020-0785-x

Scheinost, D., Tokoglu, F., Shen, X., Finn, E. S., Noble, S., Papademetris, X., et al. (2016). Fluctuations in Global Brain Activity Are Associated With Changes in Whole-Brain Connectivity of Functional Networks. *IEEE Trans. Biomed. Eng.* 63, 2540–2549. doi: 10.1109/TBME.2016.2600248

Shi, Y., Zeng, W., Wang, N., Wang, S., and Huang, Z. (2015). Early warning for human mental sub-health based on fMRI data analysis: an example from a seafarers' resting-data study. *Front. Psychol.* 6:1030. doi: 10.3389/fpsyg.2015.01030

Sohn, M. H., Albert, M. V., Jung, K., Carter, C. S., and Anderson, J. R. (2007). Anticipation of conflict monitoring in the anterior cingulate cortex and the prefrontal cortex. *Proc. Natl. Acad. Sci. U S A* 104, 10330–10334. doi: 10.1073/pnas.0703225104

Spence, S. A., Farrow, T. F., Herford, A. E., Wilkinson, I. D., Zheng, Y., and Woodruff, P. W. (2001). Behavioural and functional anatomical correlates of deception in humans. *Neuroreport* 12, 2849–2853. doi: 10.1097/00001756-200109170-00019

Spence, S. A., Hunter, M. D., Farrow, T. F., Green, R. D., Leung, D. H., Hughes, C. J., et al. (2004). A cognitive neurobiological account of deception: evidence from functional neuroimaging. *Philos. Trans. Phys. Sci. Eng.* 359, 1755–1762. doi: 10.1098/rstb.2004.1555

Steer, R. (1993). *Manual for the Beck Depression Inventory-II*. Agra: Psychological Corporation.

Surguladze, S. A., El-Hage, W., Dalgleish, T., Radua, J., Gohier, B., and Phillips, M. L. (2010). Depression is associated with increased sensitivity to signals of disgust: a functional magnetic resonance imaging study. *J. Psychiatr. Res.* 44, 894–902. doi: 10.1016/j.jpsychires.2010.02.010

Tao, H., Guo, S., Ge, T., Kendrick, K. M., Xue, Z., Liu, Z., et al. (2013). Depression uncouples brain hate circuit. *Mol. Psychiatr.* 18, 101–111. doi: 10.1038/mp.2011.127

Thompson, W. H., and Fransson, P. (2016). On Stabilizing the Variance of Dynamic Functional Brain Connectivity Time Series. *Brain Connectivity* 6, 735–746. doi: 10.1089/brain.2016.0454

Tozzi, A., and Peters, J. F. (2017). From abstract topology to real thermodynamic brain activity. *Cogn. Neurodyn.* 11, 283–292. doi: 10.1007/s11571-017-9431-7

Turnell, A. I., Fassnacht, D. B., Batterham, P. J., Calear, A. L., and Kyrios, M. (2019). The Self-Hate Scale: development and validation of a brief measure and its relationship to suicidal ideation. *J. Affect. Dis.* 245, 779–787. doi: 10.1016/j.jad.2018.11.047

Ursu, S., Clark, K. A., Aizenstein, H. J., Stenger, V. A., and Carter, C. S. (2009). Conflict-related activity in the caudal anterior cingulate cortex in the absence of awareness. *Biol. Psychol.* 80, 279–286. doi: 10.1016/j.biopsycho.2008.10.008

Vasic, N., Walter, H., Sambataro, F., and Wolf, R. C. (2008). Aberrant functional connectivity of dorsolateral prefrontal and cingulate networks in patients with major depression during working memory processing. *Psychol. Med.* 39, 977–987. doi: 10.1017/S0033291708004443

Wang, L., Hermens, D. F., Hickie, I. B., and Lagopoulos, J. (2012). A systematic review of resting-state functional-MRI studies in major depression. *J. Affect. Dis.* 142, 6–12. doi: 10.1016/j.jad.2012.04.013

Xu, Y., Zhang, X., Xiang, Z., Wang, Q., Huang, X., Liu, T., et al. (2021). Abnormal Functional Connectivity Between the Left Medial Superior Frontal Gyrus and Amygdala Underlying Abnormal Emotion and Premature Ejaculation: a Resting State fMRI Study. *Front. Neurosci.* 15:704920. doi: 10.3389/fnins.2021.704920

Yan, C. G., Wang, X. D., Zuo, X. N., and Zang, Y. F. (2016). DPABI: data Processing & Analysis for (Resting-State) Brain Imaging. *Neuroinformatics* 14, 339–351. doi: 10.1007/s12021-016-9299-4

Yu, R., Tan, H., Peng, G., Du, L., Wang, P., Zhang, Z., et al. (2021). Anomalous functional connectivity within the default-mode nnaïvek in treatment-naive patients possessing first-episode major depressive disorder. *Medicine* 100:e26281. doi: 10.1097/MD.0000000000026281

Zeki, S., and Romaya, J. P. (2008). Neural correlates of hate. *PLoS One* 3:e3556. doi: 10.1371/journal.pone.0003556

Zhu, D. M., Yang, Y., Zhang, Y., Wang, C., Wang, Y., Zhang, C., et al. (2020). Cerebellar-cerebral dynamic functional connectivity alterations in major depressive disorder. *J. Affect. Dis.* 275, 319–328. doi: 10.1016/j.jad.2020.06.062

**Conflict of Interest:** The authors declare that the research was conducted in the absence of any commercial or financial relationships that could be construed as a potential conflict of interest.

**Publisher's Note:** All claims expressed in this article are solely those of the authors and do not necessarily represent those of their affiliated organizations, or those of the publisher, the editors and the reviewers. Any product that may be evaluated in this article, or claim that may be made by its manufacturer, is not guaranteed or endorsed by the publisher.

frontiers in Aging Neuroscience

ORIGINAL RESEARCH
published: 03 March 2022
doi: 10.3389/fnagi.2022.823502

# Multimodal Magnetic Resonance Imaging Reveals Aberrant Brain Age Trajectory During Youth in Schizophrenia Patients

*Jiayuan Huang[1,2], Pengfei Ke[1], Xiaoyi Chen[1,2], Shijia Li[1], Jing Zhou[1], Dongsheng Xiong[1], Yuanyuan Huang[3,4], Hehua Li[3,4], Yuping Ning[3,4], Xujun Duan[5], Xiaobo Li[6], Wensheng Zhang[7], Fengchun Wu[3]* and Kai Wu[2,8,9,10,11,12]**

[1] Department of Biomedical Engineering, School of Material Science and Engineering, South China University of Technology, Guangzhou, China, [2] School of Biomedical Sciences and Engineering, South China University of Technology, Guangzhou International Campus, Guangzhou, China, [3] The Affiliated Brain Hospital of Guangzhou Medical University, Guangzhou Huiai Hospital, Guangzhou, China, [4] Guangdong Engineering Technology Research Center for Translational Medicine of Mental Disorders, Guangzhou, China, [5] MOE Key Lab for Neuroinformation, High-Field Magnetic Resonance Brain Imaging Key Laboratory of Sichuan Province, University of Electronic Science and Technology of China, Chengdu, China, [6] Department of Biomedical Engineering, New Jersey Institute of Technology, Newark, NJ, United States, [7] Institute of Automation, Chinese Academy of Sciences, Beijing, China, [8] National Engineering Research Center for Tissue Restoration and Reconstruction, South China University of Technology, Guangzhou, China, [9] Guangdong Province Key Laboratory of Biomedical Engineering, South China University of Technology, Guangzhou, China, [10] Guangdong Engineering Technology Research Center for Diagnosis and Rehabilitation of Dementia, Guangzhou, China, [11] Institute for Healthcare Artificial Intelligence Application, Guangdong Second Provincial General Hospital, Guangzhou, China, [12] Department of Nuclear Medicine and Radiology, Institute of Development, Aging and Cancer, Tohoku University, Sendai, Japan

OPEN ACCESS

**Edited by:**
*Wenjing Zhang,*
*Sichuan University, China*

**Reviewed by:**
*Asier Erramuzpe,*
*University of Mondragón, Spain*
*Jaroslav Rokicki,*
*Oslo University Hospital, Norway*

***Correspondence:**
*Fengchun Wu*
*13580380071@163.com*
*Kai Wu*
*kaiwu@scut.edu.cn*

**Specialty section:**
*This article was submitted to Neurocognitive Aging and Behavior, a section of the journal Frontiers in Aging Neuroscience*

**Received:** *27 November 2021*
**Accepted:** *18 January 2022*
**Published:** *03 March 2022*

**Citation:**
*Huang J, Ke P, Chen X, Li S, Zhou J, Xiong D, Huang Y, Li H, Ning Y, Duan X, Li X, Zhang W, Wu F and Wu K (2022) Multimodal Magnetic Resonance Imaging Reveals Aberrant Brain Age Trajectory During Youth in Schizophrenia Patients. Front. Aging Neurosci. 14:823502. doi: 10.3389/fnagi.2022.823502*

Accelerated brain aging had been widely reported in patients with schizophrenia (SZ). However, brain aging trajectories in SZ patients have not been well-documented using three-modal magnetic resonance imaging (MRI) data. In this study, 138 schizophrenia patients and 205 normal controls aged 20–60 were included and multimodal MRI data were acquired for each individual, including structural MRI, resting state-functional MRI and diffusion tensor imaging. The brain age of each participant was estimated by features extracted from multimodal MRI data using linear multiple regression. The correlation between the brain age gap and chronological age in SZ patients was best fitted by a positive quadratic curve with a peak chronological age of 47.33 years. We used the peak to divide the subjects into a youth group and a middle age group. In the normal controls, brain age matched chronological age well for both the youth and middle age groups, but this was not the case for schizophrenia patients. More importantly, schizophrenia patients exhibited increased brain age in the youth group but not in the middle age group. In this study, we aimed to investigate brain aging trajectories in SZ patients using multimodal MRI data and revealed an aberrant brain age trajectory in young schizophrenia patients, providing new insights into the pathophysiological mechanisms of schizophrenia.

**Keywords: schizophrenia, accelerated brain aging, brain age gap, multimodal magnetic resonance imaging, machine learning**

## INTRODUCTION

Schizophrenia (SZ) is one of the costliest mental disorders in terms of human suffering and societal expenditure, with a 1% lifetime risk, chronicity, severity, and an impaired quality of life (van Os and Kapur, 2009; Cocchi et al., 2011; Charlson et al., 2018). Regretfully, etiology of the disease is unknown. Recent studies have found structural abnormalities in SZ patients, including decreased fractional anisotropy, gray matter volume (GMV) and hippocampal volume (Ellison-Wright and Bullmore, 2009; Bois et al., 2016; Wu et al., 2018; Duan et al., 2021), but brain volume changes are not constant throughout the course of the illness (van Haren et al., 2008). Functional magnetic resonance imaging (MRI) studies have shown similar abnormalities in the brains of SZ patients, such as a decrease in the amplitude of low-frequency fluctuations (Huang et al., 2010), an increase in functional connectivity within the default mode network (He et al., 2013), and changes in network homogeneity (Guo et al., 2014). Importantly, structural and functional abnormalities result in different brain aging trajectories (Mitelman et al., 2009; Mandl et al., 2010). Several recent studies have revealed that some of the changes observed in SZ patients are similar to those seen in physiological aging (Douaud et al., 2009; Nenadic et al., 2012).

During the normal aging process, brain changes include highly coordinated and sequenced events characterized by both progressive (myelination) and regressive (synaptic pruning) processes (Silk and Wood, 2011). Healthy brain aging demonstrates a specific pattern, in which cortical GMV decreases curvilinearly, cortical white matter volume (WMV) remains constant, and cortical cerebrospinal fluid increases (Pfefferbaum et al., 1994). Therefore, brain age (BA) could be estimated by analyzing brain structure, function, and connectivity features over time (Dosenbach et al., 2010). Recently, machine learning methods for BA estimation modeling were introduced, in which individual neuroimage features were used for model training (Huang et al., 2017; Lewis et al., 2018; Bashyam et al., 2020), and the model can provide potential brain aging biomarkers (Kondo et al., 2015; Qin et al., 2015; Valizadeh et al., 2017).

Individuals with the same chronological age (CA) might experience different trajectories of brain aging. Such differences might result in a mismatch between the CA and the BA. Previous studies have shown that this mismatch occurs simultaneously with brain changes (Cole et al., 2015, 2018a). Importantly, this kind of mismatch has been observed in neuropsychiatric disorders (Koutsouleris et al., 2014; Nenadic et al., 2017; Kaufmann et al., 2019; He et al., 2020), and the degree of deviation from the CA might help in the detection of clinical outcomes (Franke et al., 2010; Wang et al., 2019). Cole et al. found that the brain age gap (BAG) between the BA and the CA of elderly individuals was associated with a higher risk of mental or physical problems, as well as premature death (Cole et al., 2018b, 2019). Boyle et al. revealed that the BAG was related to specific cognitive functions (Boyle et al., 2021). However, the BA trajectory in SZ patients based on three-modal MRI data has not been well-documented.

In this study, we used the Brainnetome Atlas (BNA)[1] (Fan et al., 2016) and the white matter parcellation map (WMPM) (Mori et al., 2008) to build feature vectors from multimodal MRI data, including structural MRI (sMRI), resting state-functional MRI (rs-fMRI) and diffusion tensor imaging (DTI) data. The value of the BAG was computed and provided an indication of deviation from normal aging trajectories. We estimated the BA and assessed specific patterns of brain aging trajectories in both the SZ and normal control (NC) groups. Based on previous evidence (van Haren et al., 2008; Mitelman et al., 2009; Mandl et al., 2010; Nenadic et al., 2012), we hypothesized that brain age in SZ patients might be increased and that the degree of brain aging might differ between age groups.

## MATERIALS AND METHODS

### Participants

In this study, we recruited 363 subjects, including 154 SZ patients and 209 NCs, and collected their sMRI, rs-fMRI, and DTI data. SZ patients met the diagnostic criteria for the fourth edition of the Diagnostic and Statistical Manual of Mental Disorders (DSM-IV). SZ patients were recruited from the Affiliated Brain Hospital of Guangzhou Medical University, Guangzhou. All subjects were fully informed of the details of the experiment. They signed an informed consent before undergoing the clinical trial and MRI. This study was carried out in compliance with the Declaration of Helsinki and approved by the Ethics Committee of the Affiliated Brain Hospital of Guangzhou Medical University.

### Magnetic Resonance Imaging Acquisition

MRI data were acquired using a Philips 3T MR system (Philips, Achieva, Netherlands) located at the Affiliated Brain Hospital of Guangzhou Medical University. To ensure data quality, all MRI data were scanned using scanning protocols designed by experienced experts, and the instrument was operated by an imaging technologist. The participants were instructed to keep their eyes closed, relax but not sleep, and move as little as possible. For each subject, rs-fMRI data were collected using an echo-planar imaging (EPI) sequence (64*64 scan matrix with 3.4*3.4*4 $mm^3$ spatial resolution, repetition time = 2,000 ms, echo time = 30 ms, field of view = 220*220 $mm^2$, flip angle = 90°, number of layers = 36, and layer thickness = 4 mm, total time = 486 s). The sMRI data were obtained using a sagittal three-dimensional gradient-echo T1-weighted sequence (256*256*188 matrix with 1*1*1 $mm^3$ spatial resolution, repetition time = 8.2 ms, echo time = 3.7 ms, flip angle = 7°, and layer thickness = 1 mm). The DTI data were acquired by applying a single-shot EPI-based sequence (spatial resolution = 2*2*3 $mm^3$, field of view = 256*256 $mm^2$, repetition time = 6,000 ms, echo time = 70 ms, flip angle = 90°, number of layers = 50, and layer thickness = 3 mm, 33 nonlinear diffusion weighting directions with b = 1,000 s/$mm^2$, and one direction without diffusion weighting).

[1] http://atlas.brainnetome.org/

## Image Preprocessing

The preprocessing steps of multimodal MRI data were same to those in our previous studies (Wu et al., 2018; Kong et al., 2021; Zang et al., 2021). More details were described in the **Supplementary Material**. After the correction of head motion, 20 subjects (16 SZ patients and 4 NCs) with excessive head motion (2 mm or 2°) were excluded. Therefore, 138 SZ patients and 205 NCs were included in the analysis (**Table 1**).

### Structural Magnetic Resonance Imaging

The SPM12[2] packages were used to preprocess the sMRI data. The whole brain was parcellated by the BNA containing 210 cortical and 36 subcortical regions. The GMV and WMV values of 246 brain regions were calculated.

### Resting-State Functional Magnetic Resonance Imaging

The SPM12 and DPARSF[3] packages (Yan and Zang, 2010) were used to preprocess the rs-fMRI data. The amplitude of low frequency fluctuation (ALFF), regional homogeneity (ReHo), and degree centrality (DC) values of 246 brain regions were computed.

### Diffusion Tensor Imaging

Diffusion tensor imaging data were preprocessed using the PANDA toolbox (Cui et al., 2013). The values of fractional anisotropy (FA), mean diffusivity (MD), axial diffusivity (AD), and radial diffusivity (RD) of 50 white matter regions defined by the WMPM were calculated.

## Age Estimation Analysis

### Feature Selection

In the current study, 2 sMRI indices (i.e., GMV and WMV), 3 rs-fMRI indices (i.e., ALFF, ReHo, and DC) of 246 brain regions, as well as 4 DTI indices (i.e., FA, MD, AD and RD) of 50 brain regions were extracted for each subject. As a result, a feature vector with 1,430 dimensions was obtained for each subject. The vectors were normalized by the following formula:

$$Z = (x-u)/s$$

where $u$ and $s$ are the mean and standard deviation of the training subjects' features, respectively.

The model is likely to overfit when the number of features is much larger than the number of samples (Erickson et al., 2017). Thus, the feature selection procedure might be useful and critical for improving prediction accuracy. To obtain the age-related features, least absolute shrinkage and selection operator with cross-validation (LASSOCV) (Tibshirani, 1996) was performed. The LASSOCV sets most features to zeros and retains correlated ones by using L1-norm, which results in a very sparse features matrix and reduce dimensions of features.

### Brain Age Estimation

Multiple linear regression (MLR) is a standard statistical technique for predicting the criterion or the independent variable by linearly combining several variables. MLR does not have algorithm-specific parameters. The measure of MLR is the mean absolute error (MAE), Pearson correlation, coefficient of determination and root mean squared error (rMSE). Notably, MLR has been successfully used in neuroimaging studies to assess age (Valizadeh et al., 2017) and other scores (Rosenberg et al., 2016; Shen et al., 2017). BA was estimated in NCs using leave-one-out cross-validation (LOOCV) (**Figure 1**). Furthermore, to investigate MLR prediction accuracy with different modal features, we repeated the above processes using different modal features. Data from SZ patients were used for testing based on the model of MLR trained by all NC subjects. The BA numeric value may indicate the degree of brain aging. The mean BAG of the NC group should consequently be or close to zero.

### Statistical Analysis

Two-sample $t$-tests were used for the statistical analysis of between-group differences in age and education years. A chi-square test was used for the statistical analysis of gender differences. We employed linear regression to remove the effects of gender on features (Kondo et al., 2015). A permutation test was applied to estimate the statistical significance of the MAE results like classification (Golland and Fischl, 2003). In our analysis, we randomly permuted the age labels of the training data 1,000 times and performed all regression processes with each set of permuted labels. Quadratic and linear models were used to fit the BAG and the CA in the SZ group, with the positive quadratic model performing better (**Supplementary Figure 1**), similar result was acquired by BA estimation based on sMRI and DTI (**Supplementary Figure 3**). Thus, the CA of the peak of the positive quadratic curve was used to divide the subjects into a youth group and a middle age group. The Pearson correlation analysis between BA and CA in NC group was used to estimate model prediction accuracy, while correlation analyses between BAG and CA in SZ group were used to identify the relation between BAG and CA. We defined subjects with age less than the peak of the quadratic curve as the youth group, others as the middle age group. Because the brain structure

[2]http://www.fil.ion.ucl.ac.uk/spm/
[3]http://rfmri.org/DPARSF

**TABLE 1** | Participant demographics.

| | NC group | SZ group | *p* value |
|---|---|---|---|
| Gender | 110/95 | 95/43 | $< 0.05^a$ |
| Education years | 12.84 ± 2.83 | 10.74 ± 3.29 | $< 0.05^b$ |
| Age (years) | 32.51 ± 8.37 | 33.75 ± 7.23 | $0.15^b$ |
| PANSS positive symptom scale score | – | 23.26 ± 5.16 | – |
| PANSS negative symptom scale score | – | 22.60 ± 7.47 | – |
| PANSS general psychopathology scale score | – | 40.03 ± 9.55 | – |

*PANSS, positive and negative syndrome scale.*
*[a]p value was obtained by a chi-square test.*
*[b]p value was obtained by a two-sample t-test.*

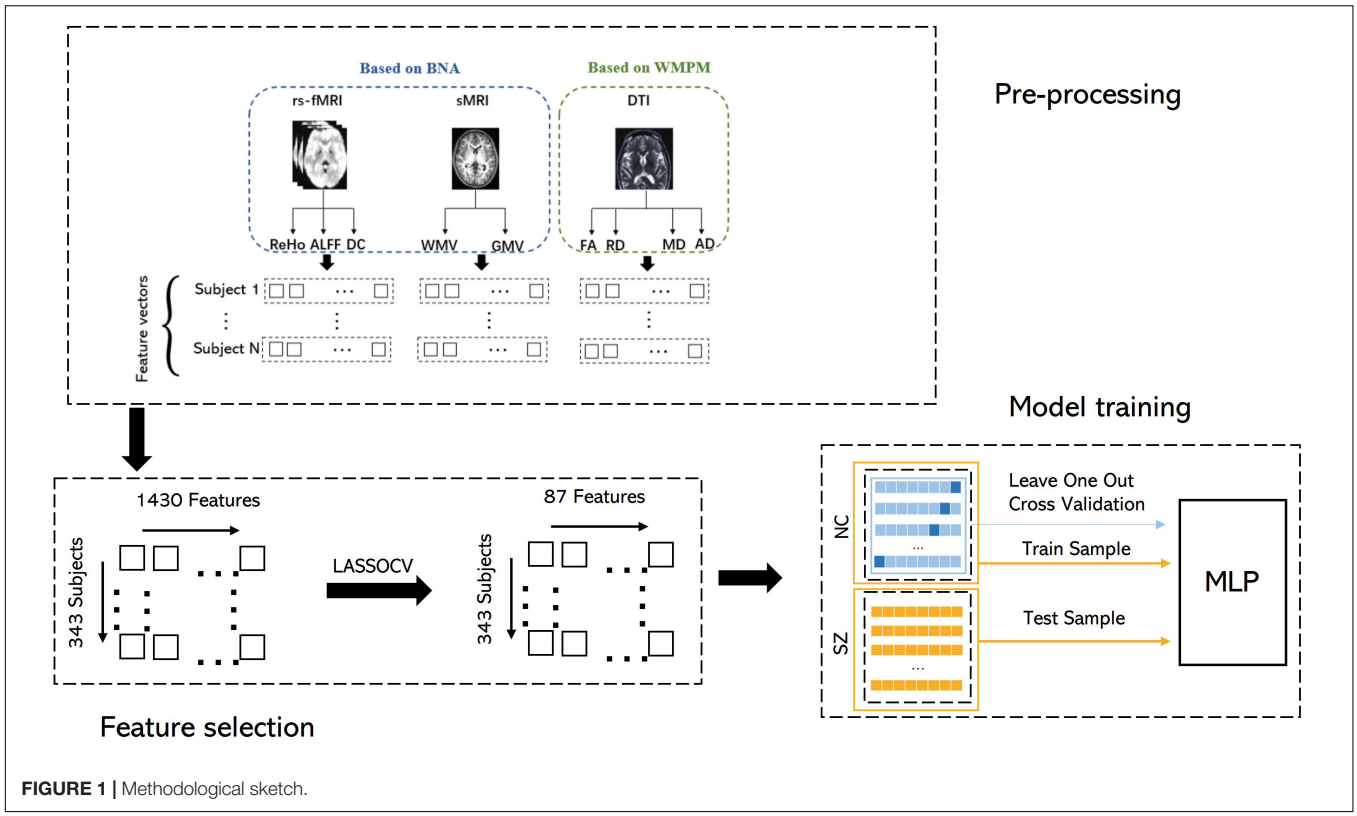


**FIGURE 1 |** Methodological sketch.

and function of SZ patients differed from those of NCs (Mori et al., 2007; Bose et al., 2009), differences in the BA and the CA were investigated by two-sample *t*-tests in the SZ and NC groups, the BAG between the SZ and NC groups was compared in the youth and middle age groups. Prior to statistical analyses, the BA was corrected with the following formula (de Lange and Cole, 2020):

$$offset = \alpha \times CA + \beta$$

$$corrected\ BA = BA - offset$$

Where the offset = BA-CA, the coefficient α and β represent the slope and intercept.

# RESULTS

## Characterization of Age-Related Features

Eighty-seven of the 1,430 features were more relevant to age and were used for the BA estimation in the NC group after LASSOCV (alpha = 0.3). The sMRI, rs-fMRI, and DTI data accounted respectively for 50, 24, and 13 features in the final feature set, respectively. After ranking the weights of all features in the MLR, the 20 best descriptors were as follows: the values of 11 brain regions in the BNA (the orbital gyrus, fusiform gyrus, striatum, precentral gyrus, superior frontal gyrus, postcentral gyrus, parahippocampal gyrus, middle temporal gyrus, insular gyrus, inferior parietal lobule and inferior frontal gyrus); and the values of 6 brain regions in the WMPM (fornix, posterior limb of internal capsule, superior corona radiata, superior longitudinal fasciculus, splenium of corpus callosum and external capsule) (see **Table 2** and **Figure 2**).

## Correlation Between Brain Age and Chronological Age in the Youth and Middle Age Groups in Normal Controls and Schizophrenia Patients

The MLR in the NC group had the best accuracy based on different model MRI combinations (**Supplementary Table 1**), in which the Pearson correlation, MAE, coefficient of determination and rMSE of the MLR were 0.88, 3.24 years, 0.77 and 4.14 years respectively (uncorrected) and significant in the permutation test. In the SZ group, the best model used to fit the BAG and CA was the positive quadratic regression, in which the peak CA was 47.33 years (**Figure 3** and **Supplementary Figure 1**). The peak was then used to divide the subjects into the youth (age range: 22–46 years, NC: 183, SZ: 128) and middle age (age range: 47–60 years, NC: 22, SZ: 10) groups. Before two-sample *t*-tests performed, BA was corrected (see in **Supplementary Figure 2** and **Supplementary Table 3**). In the youth SZ group, the BA values were significantly higher than the CA values. In the middle age SZ group, the BA and CA values were not significantly different. When the same analysis was performed on the NC group, no significant differences were found in the youth group or in the middle age group. Accordingly, the BAG of the youth

**TABLE 2 |** Brain regions with high weights in BA estimation.

| Feature | Weight | Atlas | Region |
|---|---|---|---|
| MD | −6.517 | WMPM | Fornix (column and body of fornix) |
| FA | −4.094 | WMPM | Fornix (column and body of fornix) |
| GMV | −1.522 | BNA | Subcortical nuclei/Striatum (L) |
| MD | −1.448 | WMPM | Posterior limb of internal capsule (R) |
| GMV | −1.398 | BNA | Parietal lobe/Postcentral gyrus (R) |
| ReHo | −1.193 | BNA | Temporal lobe/Parahippocampal gyrus (R) |
| FA | −1.115 | WMPM | Splenium of corpus callosum |
| FA | −1.091 | WMPM | Superior longitudinal fasciculus (L) |
| ReHo | −1.055 | BNA | Temporal lobe/Middle temporal gyrus (R) |
| FA | −0.889 | WMPM | Superior corona radiata (L) |
| AD | 3.857 | WMPM | Fornix (column and body of fornix) |
| WMV | 1.133 | BNA | Frontal lobe/Orbital gyrus (L) |
| ALFF | 0.922 | BNA | Insular lobe/Insular gyrus (L) |
| WMV | 0.849 | BNA | Temporal lobe/Fusiform gyrus (L) |
| DC | 0.845 | BNA | Parietal lobe/Inferior parietal lobule (L) |
| WMV | 0.838 | BNA | Frontal lobe/Inferior frontal gyrus (L) |
| MD | 0.821 | WMPM | External capsule (L) |
| WMV | 0.705 | BNA | Frontal lobe/Orbital gyrus (L) |
| WMV | 0.705 | BNA | Frontal lobe/Precentral gyrus (L) |
| WMV | 0.635 | BNA | Frontal lobe/Superior frontal gyrus (R) |

*L is left and R is right.*

SZ group was significantly higher than that of the youth NC group. However, the BAG of the middle age SZ group was also higher than that of the middle age NC group, despite the fact that the difference was not statistically significant (**Figure 4**). The results were similar in BA estimation based on sMRI and DTI (**Supplementary Figure 4**). This finding might be associated with the atypical brain structure and function observed in SZ patients.

# DISCUSSION

To the best of our knowledge, this was the first study to use three-modal MRI data to analyze brain aging trajectories in SZ patients. A positive quadratic trajectory of the BAG with the CA was found in the SZ group. SZ patients showed significantly higher BA than CA in the youth group, implying that youth SZ patients have increased brain age.

## Methodology Consideration

Recent studies have predicted the BA based on unimodal neuroimaging and biological information, but few have combined three-modal MRI features (Dosenbach et al., 2010; Brown et al., 2012; Lewis et al., 2018). In the current study, we combined sMRI, rs-fMRI and DTI to estimate the BA. Combined multimodal MRI features are of crucial importance because they can identify different patterns of alterations in the microstructure and macrostructure of the brain (Cherubini et al., 2016). de Lange et al. showed that combining features from multimodal MRI data (T1-weighted MRI, DTI, and rs-fMRI) yielded better age prediction performance than using unimodal features (de Lange et al., 2020). The combination of T1-weighted and T2-weighted image features also yielded better prediction performance than unimodal features (Rokicki et al., 2021). Similarly, our results showed that combining multimodal MRI data can achieve sensitive detection of aberrant patterns in brain aging (**Supplementary Table 1**).

In addition, the LASSOCV was applied to selected features which were more relevant to age (Zhang and Huang, 2008). The MLR model allowed for fast computation and straightforward interpretation of feature weights. Due to number of subjects limitation, LOOCV was used to estimate model prediction accuracy.

## Brain Age Trajectories in Youth Schizophrenia Patients

In the SZ group, we found that the correlation between the BAG and the CA was best fitted by a positive quadratic curve. On the left side of the positive quadratic curve, the BAG decreased with CA. We speculated that the BA and CA trajectories became more convergent in young SZ patients. This result was consistent with previous findings of age-related abnormalities in the brain, showing that the brains of SZ patients undergo a recovery process to realign the brain to that of a NC (Bose et al., 2009; Voineskos et al., 2010). Moreover, Schnack et al. found that the acceleration of brain aging in SZ patients decreased from 2.5 years/year to a normal rate approximately 5 years after illness onset, which could be attributed to the medication effect (Schnack et al., 2016). Recent studies have shown that the medication effect has a nonlinear relationship with antipsychotic treatment dosage (Rhindress et al., 2017) and is related to the mean dynamic network interaction index of SZ patients (Wang et al., 2021). White matter trajectories are also changed in SZ patients. Disturbances during maturation would be reflected by different ascending slopes and a shift in peak white matter maturation (Cetin-Karayumak et al., 2020), implying that the white matter trajectories of SZ patients and NCs intersect (Bose et al., 2009; Wright et al., 2014; de Moura et al., 2018). Our results were consistent with previous findings that showed changing difference between the CA and the BA in SZ patients and further suggested that such abnormalities might differ at different ages. Therefore, we divided the participants into youth and middle age groups using the peak CA and found a trajectory of increased brain age in youth SZ patients. Specifically, the BA was significantly higher than the CA in youth SZ patients, whereas the BA and CA showed no significant difference in the middle age SZ patients. Similarly, Voineskos et al. found that young SZ patients had a significantly lower FA than young NCs, but no differences were found when the older groups were compared (Voineskos et al., 2010). van Haren et al. showed that excessive volume loss in SZ patients did not occur to the same degree throughout the course of the illness, and it was most prominent during the first two decades (van Haren et al., 2008).

## Important Features for Brain Age Estimation Based on the Brainnetome Atlas

Our results suggested that subcortical nuclei, the frontal lobe and the temporal lobe all play important roles in BA estimation.

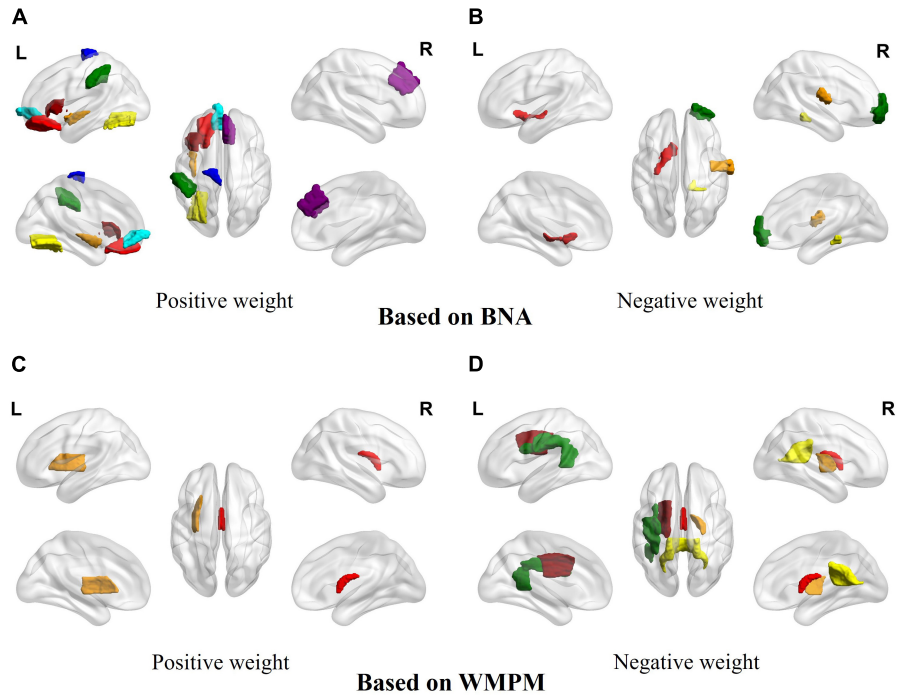


**FIGURE 2 |** The signed importance of brain regions for BA predictions in the MLP model. **(A)** Brain areas with positive weights based on the BNA. Red: orbital gyrus/frontal lobe; brown: insular gyrus/insula lobe; yellow: fusiform gyrus/temporal lobe; green: parietal lobule/inferior parietal lobe; dark red: inferior frontal gyrus/frontal lobe; cyan: orbital gyrus/frontal lobe; blue: precentral gyrus/frontal lobe; purple: superior frontal gyrus/frontal lobe. **(B)** Brain areas with negative weights based on the BNA. Red: striatum/subcortical nuclei; brown: postcentral gyrus/parietal lobe; yellow: parahippocampal gyrus/temporal lobe; green: middle temporal gyrus/temporal lobe. **(C)** Brain areas with positive weights based on the WMPM. Red: fornix; brown: external capsule. **(D)** Brain areas with negative weights based on the WMPM. Red: fornix; brown: posterior limb of internal capsule; yellow: splenium of corpus callosum; green: superior longitudinal fasciculus; dark red: superior corona radiata.

Subcortical structures are responsible for exerting cognitive, affective, and social functions in humans (Koshiyama et al., 2018). Our results showed that key subcortical structure was the striatum, which play important roles in decision-making (Goulet-Kennedy et al., 2016). Previous studies have indicated that aging causes significant changes in intrinsic functional connectivity in the striatum (Porter et al., 2015). Abnormalities in the striatum may be related to various neuropsychiatric disorders, including SZ, bipolar disorder, and attention deficit hyperactivity disorder (Emond et al., 2009; Karcher et al., 2019).

The frontal lobe is thought to manage incoming information and select appropriate actions based on one's goals in a particular context (Rosch and Mostofsky, 2019). The orbital and precentral gyri in the frontal lobe were also important for BA estimation and which are associated with emotional expression and motor behaviors (Dixon et al., 2017; Zhou et al., 2020). Accumulating evidence suggests that the orbital and precentral gyri may be abnormal in neuropsychiatric diseases such as somatic depression, bipolar disorder, autism spectrum disorder and SZ (Stanfield et al., 2009; Nebel et al., 2014; Zarei, 2018; Yan et al., 2019).

The main functions of the temporal lobe are to process auditory information and encode of memory (Hamberger et al., 2003; Dickerson et al., 2004). The fusiform and parahippocampal gyri in the temporal lobe with high weight are responsible for processing visual information and memory (Luck et al., 2010; Weiner and Zilles, 2016). Fusiform abnormality has been linked to SZ (McKenna et al., 2019). Atrophy of the parahippocampal gyrus has also been implicated as an early indicator of Alzheimer's disease (Echavarri et al., 2011).

## Important Features for Brain Age Estimation Based on the White Matter Parcellation Map

Different brain regions are linked by white matter fibers, and different white matter fibers are associated with various behaviors. The splenium of corpus callosum and external capsule, which are linking different brain regions, played major roles in BA estimation model. The functions of splenium of corpus callosum and external capsule are linking primary and secondary visual areas and serving as a route for cholinergic fibers from basal forebrain to the cerebral cortex (Knyazeva, 2013; Nolze-Charron et al., 2020), respectively. These fibers would change during the course of normal aging (Nolze-Charron et al., 2020; Delvenne et al., 2021). Abnormalities of the fibers were found in SZ (Francis et al., 2011; Joo et al., 2021).

The superior longitudinal fasciculus, posterior limb of the internal capsule, superior corona radiata and fornix, which are associated with the language, motor and memory (Jang, 2009;

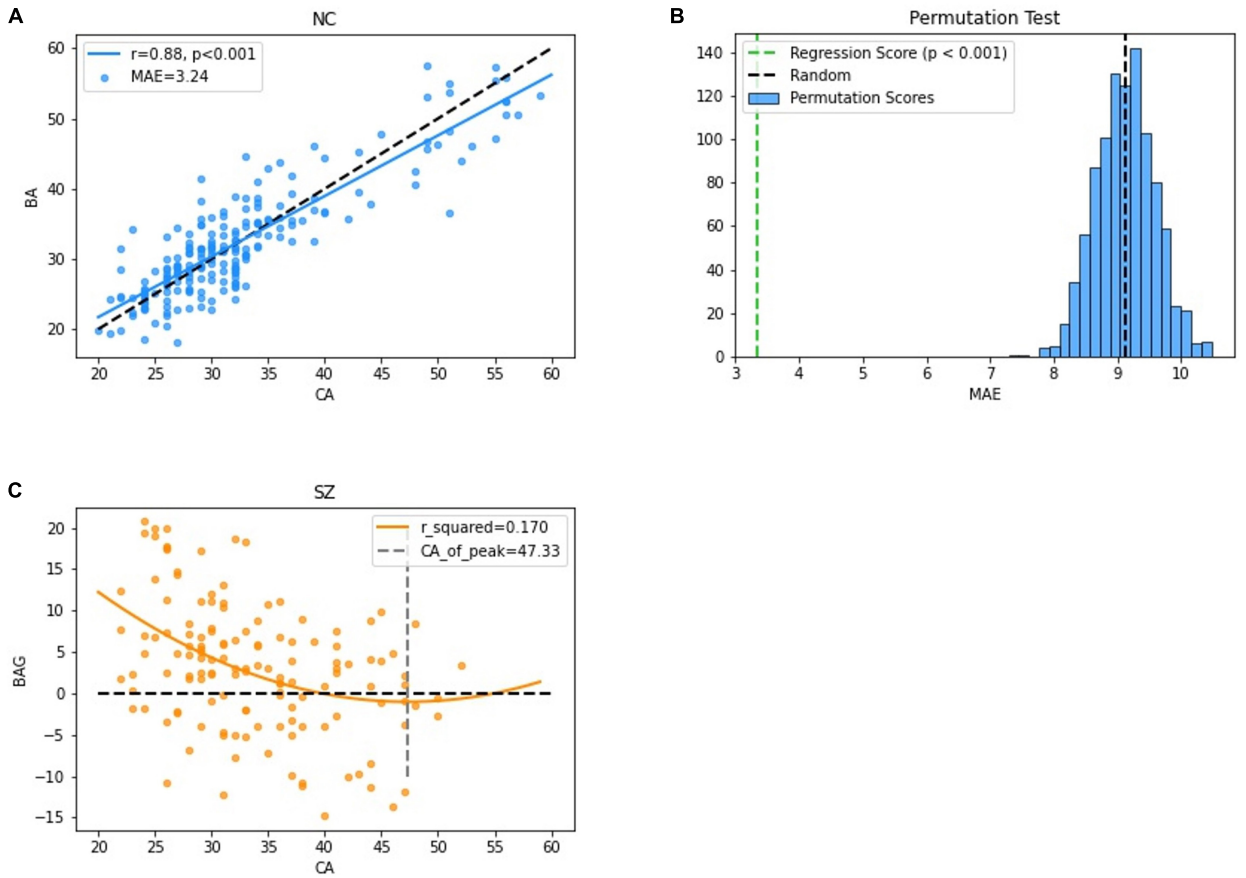


**FIGURE 3 |** Performance of the BA estimation model. **(A)** The correlation between the CA and the BA in the NC group. **(B)** The results of permutation tests of the BA estimation model. **(C)** The correlation between the BAG and the CA in the SZ group.

Bernal and Altman, 2010; Adnan et al., 2013), were all given high weight in the BA estimation model. A recent study found that some of these brain regions are age-related and showed lower FA values in SZ patients than in NCs (Yoshimura and Kurashige, 2000; Peters et al., 2010; Kochunov et al., 2016; Tesli et al., 2021). Accumulating evidence suggests that the brain regions are affected in psychiatric disorders, such as SZ, bipolar disorder and Alzheimer's disease (Koshiyama et al., 2020; Linke et al., 2020).

## Contribution of Simultaneous Multimodal Magnetic Resonance Imaging Data

Our findings demonstrated that both some brain regions have critical contributions to BA estimation. The use of multimodal neuroimages results in a more sensitive model that captures alterations in brain structure and function (Cherubini et al., 2016). The results for the BAG in SZ youth group could explain altered brain functions such as decision-making as well as changes in visual, language, motor, memory, and emotional expression. Thus, future studies using multimodal neuroimaging are necessary for broadening our understanding of brain aging.

## Limitations

The findings of this study should be considered in light of some limitations. First, the sample size was relatively small, especially in the middle age group. The lack of significant results between NC and SZ in the middle age group could be explained by a small group sample size. We utilized the data of the NC group to train the model and discover age-related brain regions that provided useful information on normal aging patterns rather than an independent NC dataset. Future work should train predictive models using data from a large number of NCs and test the models using an independent dataset. Second, we did not consider factors such as the years of illness and medication. Third, a longitudinal study can be used to validate the aberrant trajectories in SZ patients.

# CONCLUSION

We found a positive quadratic trajectory between the BAG and the CA in SZ patients. BA was significantly higher than CA only in the youth SZ group but not significantly in the middle age group. These results suggested that discrepancies between BA and CA might be attributed to abnormal brain aging

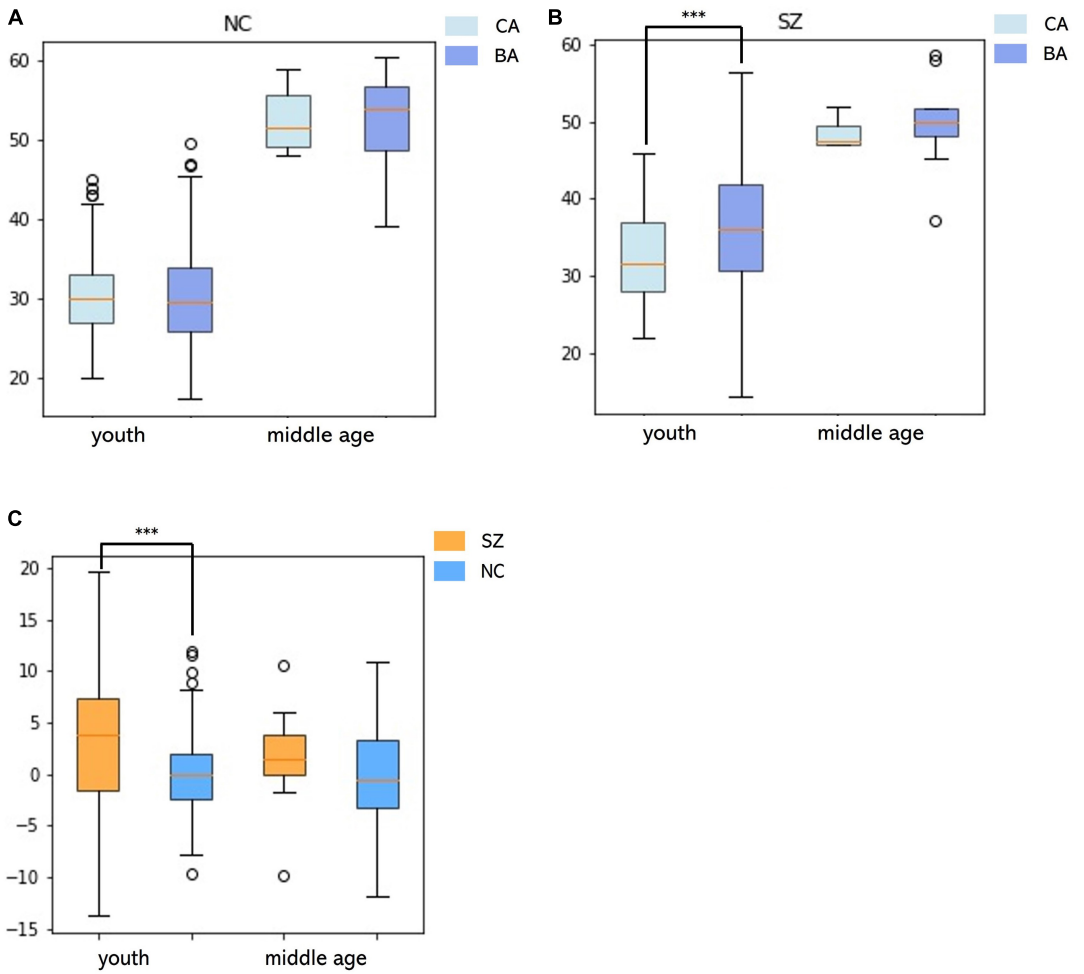


**FIGURE 4 |** Relationships between the BA and the CA and differences in the BAG in youth and middle age for the SZ and NC groups. **(A)** In the NC group, differences between BA and CA in the youth and middle age groups. **(B)** In the SZ group, differences between BA and CA in the youth and middle age groups. **(C)** Differences in BAG between SZ and NC groups in youth and middle age.

trajectories in SZ patients and demonstrated that SZ patients exhibit varying degrees of increased brain age at different age ranges. Furthermore, we suggest that the BA predicted by three-modal MRI data support more comprehensive biomarker for understanding abnormal brain aging patterns in SZ patients.

## DATA AVAILABILITY STATEMENT

The datasets presented in this article are not readily available because this is a private dataset. Requests to access the datasets should be directed to KW, kaiwu@scut.edu.cn.

## ETHICS STATEMENT

The studies involving human participants were reviewed and approved by Affiliated Brain Hospital of Guangzhou Medical University. The patients/participants provided their written informed consent to participate in this study. Written informed consent was obtained from the individual(s) for the publication of any potentially identifiable images or data included in this article.

## AUTHOR CONTRIBUTIONS

All authors contributed to data analysis, drafting and critically revising the manuscript, gave final approval of the version to be published, and agreed to be accountable for all aspects of the work.

## FUNDING

This work was supported by the National Key Research and Development Program of China (2020YFC2004300, 2020YFC2004301, 2019YFC0118800, 2019YFC0118802, 2019YFC0118804, 2019YFC0118805, 2021YFC2009400, and

2021YFC2009404), the National Natural Science Foundation of China (31771074, 81802230, and 72174082), Guangdong Basic and Applied Basic Research Foundation Outstanding Youth Project (2021B1515020064), the Key Research and Development Program of Guangdong (2018B030335001, 2020B0101130020, and 2020B0404010002), the Science and Technology Program of Guangzhou (201807010064, 201803010100, 201903010032, and 202103000032), Key Laboratory Program of Guangdong Provincial Education Department (2020KSYS001), and the Open Fund of the Guangdong Provincial Key Laboratory of Physical Activity and Health Promotion (2021B1212040014).

## SUPPLEMENTARY MATERIAL

The Supplementary Material for this article can be found online at: https://www.frontiersin.org/articles/10.3389/fnagi.2022.823502/full#supplementary-material

## REFERENCES

Adnan, A., Crawley, A., Mikulis, D., Moscovitch, M., Colella, B., and Green, R. (2013). Moderate-severe traumatic brain injury causes delayed loss of white matter integrity: evidence of fornix deterioration in the chronic stage of injury. *Brain* Inj. 27, 1415–1422. doi: 10.3109/02699052.2013.823659

Bashyam, V. M., Erus, G., Doshi, J., Habes, M., Nasralah, I., Truelove-Hill, M., et al. (2020). MRI signatures of brain age and disease over the lifespan based on a deep brain network and 14 468 individuals worldwide. *Brain* 143, 2312–2324. doi: 10.1093/brain/awaa160

Bernal, B., and Altman, N. (2010). The connectivity of the superior longitudinal fasciculus: a tractography DTI study. *Magn. Reson. Imaging* 28, 217–225. doi: 10.1016/j.mri.2009.07.008

Bois, C., Levita, L., Ripp, I., Owens, D. C. G., Johnstone, E. C., Whalley, H. C., et al. (2016). Longitudinal changes in hippocampal volume in the Edinburgh high risk study of schizophrenia. *Schizophr. Res.* 173, 146–151. doi: 10.1016/j.schres.2014.12.003

Bose, S. K., Mackinnon, T., Mehta, M. A., Turkheimer, F. E., Howes, O. D., Selvaraj, S., et al. (2009). The effect of ageing on grey and white matter reductions in schizophrenia. *Schizophr. Res.* 112, 7–13. doi: 10.1016/j.schres.2009.04.023

Boyle, R., Jollans, L., Rueda-Delgado, L. M., Rizzo, R., Yener, G. G., McMorrow, J. P., et al. (2021). Brain-predicted age difference score is related to specific cognitive functions: a multi-site replication analysis. *Brain Imaging Behav.* 15, 327–345. doi: 10.1007/s11682-020-00260-3

Brown, T. T., Kuperman, J. M., Chung, Y., Erhart, M., McCabe, C., Hagler, D. J. Jr., et al. (2012). Neuroanatomical assessment of biological maturity. *Curr. Biol.* 22, 1693–1698. doi: 10.1016/j.cub.2012.07.002

Cetin-Karayumak, S., Di Biase, M. A., Chunga, N., Reid, B., Somes, N., Lyall, A. E., et al. (2020). White matter abnormalities across the lifespan of schizophrenia: a harmonized multi-site diffusion MRI study. *Mol. Psychiatry* 25, 3208–3219. doi: 10.1038/s41380-019-0509-y

Charlson, F. J., Ferrari, A. J., Santomauro, D. F., Diminic, S., Stockings, E., Scott, J. G., et al. (2018). Global epidemiology and burden of schizophrenia: findings from the global burden of disease study 2016. *Schizophr. Bull.* 44, 1195–1203. doi: 10.1093/schbul/sby058

Cherubini, A., Caligiuri, M. E., Peran, P., Sabatini, U., Cosentino, C., and Amato, F. (2016). Importance of multimodal MRI in characterizing brain tissue and its potential application for individual age prediction. *IEEE J. Biomed. Health Inform.* 20, 1232–1239. doi: 10.1109/JBHI.2016.2559938

Cocchi, A., Mapelli, V., Meneghelli, A., and Preti, A. (2011). Cost-effectiveness of treating first-episode psychosis: five-year follow-up results from an Italian early intervention programme. *Early Interv. Psychiatry* 5, 203–211. doi: 10.1111/j.1751-7893.2011.00261.x

Cole, J. H., Jolly, A., de Simoni, S., Bourke, N., Patel, M. C., Scott, G., et al. (2018a). Spatial patterns of progressive brain volume loss after moderate-severe traumatic brain injury. *Brain* 141, 822–836. doi: 10.1093/brain/awx354

Cole, J. H., Leech, R., and Sharp, D. J. (2015). Prediction of brain age suggests accelerated atrophy after traumatic brain injury. *Ann. Neurol.* 77, 571–581. doi: 10.1002/ana.24367

Cole, J. H., Marioni, R. E., Harris, S. E., and Deary, I. J. (2019). Brain age and other bodily 'ages': implications for neuropsychiatry. *Mol. Psychiatry* 24, 266–281. doi: 10.1038/s41380-018-0098-1

Cole, J. H., Ritchie, S. J., Bastin, M. E., Valdes Hernandez, M. C., Munoz Maniega, S., Royle, N., et al. (2018b). Brain age predicts mortality. *Mol. Psychiatry* 23, 1385–1392. doi: 10.1038/mp.2017.62

Cui, Z., Zhong, S., Xu, P., He, Y., and Gong, G. (2013). PANDA: a pipeline toolbox for analyzing brain diffusion images. *Front. Hum. Neurosci.* 7:42. doi: 10.3389/fnhum.2013.00042

de Lange, A. G., Anatürk, M., Suri, S., Kaufmann, T., Cole, J. H., Griffanti, L., et al. (2020). Multimodal brain-age prediction and cardiovascular risk: the whitehall II MRI sub-study. *Neuroimage* 222:117292. doi: 10.1016/j.neuroimage.2020.117292

de Lange, A. G., and Cole, J. H. (2020). Commentary: correction procedures in brain-age prediction. *Neuroimage Clin.* 26:102229. doi: 10.1016/j.nicl.2020.102229

de Moura, M. T. M., Zanetti, M. V., Duran, F. L. S., Schaufelberger, M. S., Menezes, P. R., Scazufca, M., et al. (2018). Corpus callosum volumes in the 5years following the first-episode of schizophrenia: effects of antipsychotics, chronicity and maturation. *Neuroimage Clin.* 18, 932–942. doi: 10.1016/j.nicl.2018.03.015

Delvenne, J. F., Scally, B., Bunce, D., and Burke, M. R. (2021). Splenium tracts of the corpus callosum degrade in old age. *Neurosci. Lett.* 742:135549. doi: 10.1016/j.neulet.2020.135549

Dickerson, B. C., Salat, D. H., Bates, J. F., Atiya, M., Killiany, R. J., Greve, D. N., et al. (2004). Medial temporal lobe function and structure in mild cognitive impairment. *Ann. Neurol.* 56, 27–35. doi: 10.1002/ana.20163

Dixon, M. L., Thiruchselvam, R., Todd, R., and Christoff, K. (2017). Emotion and the prefrontal cortex: an integrative review. *Psychol. Bull.* 143, 1033–1081. doi: 10.1037/bul0000096

Dosenbach, N. U., Nardos, B., Cohen, A. L., Fair, D. A., Power, J. D., Church, J. A., et al. (2010). Prediction of individual brain maturity using fMRI. *Science* 329, 1358–1361. doi: 10.1126/science.1194144

Douaud, G., Mackay, C., Andersson, J., James, S., Quested, D., Ray, M. K., et al. (2009). Schizophrenia delays and alters maturation of the brain in adolescence. *Brain* 132(Pt 9), 2437–2448. doi: 10.1093/brain/awp126

Duan, X., He, C., Ou, J., Wang, R., Xiao, J., Li, L., et al. (2021). Reduced hippocampal volume and its relationship with verbal memory and negative symptoms in treatment-naive first-episode adolescent-onset schizophrenia. *Schizophr. Bull.* 47, 64–74. doi: 10.1093/schbul/sbaa092

Echavarri, C., Aalten, P., Uylings, H. B., Jacobs, H. I., Visser, P. J., Gronenschild, E. H., et al. (2011). Atrophy in the parahippocampal gyrus as an early biomarker of Alzheimer's disease. *Brain Struct. Funct.* 215, 265–271. doi: 10.1007/s00429-010-0283-8

Ellison-Wright, I., and Bullmore, E. (2009). Meta-analysis of diffusion tensor imaging studies in schizophrenia. *Schizophr. Res.* 108, 3–10. doi: 10.1016/j.schres.2008.11.021

Emond, V., Joyal, C., and Poissant, H. (2009). [Structural and functional neuroanatomy of attention-deficit hyperactivity disorder (ADHD)]. *Encephale* 35, 107–114. doi: 10.1016/j.encep.2008.01.005

Erickson, B. J., Korfiatis, P., Akkus, Z., and Kline, T. L. (2017). Machine learning for medical imaging. *Radiographics* 37, 505–515.

Fan, L., Li, H., Zhuo, J., Zhang, Y., Wang, J., Chen, L., et al. (2016). The human brainnetome atlas: a new brain atlas based on connectional architecture. *Cereb. Cortex* 26, 3508–3526. doi: 10.1093/cercor/bhw157

Francis, A. N., Bhojraj, T. S., Prasad, K. M., Kulkarni, S., Montrose, D. M., Eack, S. M., et al. (2011). Abnormalities of the corpus callosum in non-psychotic high-risk offspring of schizophrenia patients. *Psychiatry Res.* 191, 9–15. doi: 10.1016/j.pscychresns.2010.09.007

Franke, K., Ziegler, G., Kloppel, S., Gaser, C., and Alzheimer's Disease Neuroimaging Initiative. (2010). Estimating the age of healthy subjects from T1-weighted MRI scans using kernel methods: exploring the influence of

various parameters. *Neuroimage* 50, 883–892. doi: 10.1016/j.neuroimage.2010.01.005

Golland, P., and Fischl, B. (2003). "Permutation tests for classification: towards statistical significance in image-based studies," in *Information Processing in Medical Imaging*, eds C. Taylor and J. A. Noble (Berlin: Springer), 330–341.

Goulet-Kennedy, J., Labbe, S., and Fecteau, S. (2016). The involvement of the striatum in decision making. *Dialogues Clin. Neurosci.* 18, 55–63. doi: 10.31887/DCNS.2016.18.1/sfecteau

Guo, W. B., Yao, D. P., Jiang, J. J., Su, Q., Zhang, Z., Zhang, J., et al. (2014). Abnormal default-mode network homogeneity in first-episode, drug-naive schizophrenia at rest. *Prog. Neuropsychopharmacol. Biol. Psychiatry* 49, 16–20. doi: 10.1016/j.pnpbp.2013.10.021

Hamberger, M. J., Seidel, W. T., Goodman, R. R., Perrine, K., and McKhann, G. M. (2003). Temporal lobe stimulation reveals anatomic distinction between auditory naming processes. *Neurology* 60, 1478–1483. doi: 10.1212/01.wnl.0000061489.25675.3e

He, C., Chen, H., Uddin, L. Q., Erramuzpe, A., Bonifazi, P., Guo, X., et al. (2020). Structure-function connectomics reveals aberrant developmental trajectory occurring at preadolescence in the autistic brain. *Cereb. Cortex* 30, 5028–5037. doi: 10.1093/cercor/bhaa098

He, Z., Deng, W., Li, M., Chen, Z., Jiang, L., Wang, Q., et al. (2013). Aberrant intrinsic brain activity and cognitive deficit in first-episode treatment-naive patients with schizophrenia. *Psychol. Med.* 43, 769–780. doi: 10.1017/S0033291712001638

Huang, T.-W., Chen, H.-T., Fujimoto, R., Ito, K., Wu, K., Sato, K., et al. (2017). "Age estimation from brain MRI images using deep learning," in *Proceedings of the 2017 IEEE 14th International Symposium on Biomedical Imaging (ISBI 2017)*, (Melbourne, VIC: IEEE), 849–852.

Huang, X. Q., Lui, S., Deng, W., Chan, R. C., Wu, Q. Z., Jiang, L. J., et al. (2010). Localization of cerebral functional deficits in treatment-naive, first-episode schizophrenia using resting-state fMRI. *Neuroimage* 49, 2901–2906. doi: 10.1016/j.neuroimage.2009.11.072

Jang, S. H. (2009). A review of corticospinal tract location at corona radiata and posterior limb of the internal capsule in human brain. *NeuroRehabilitation* 24, 279–283. doi: 10.3233/NRE-2009-0479

Joo, S. W., Kim, H., Jo, Y. T., Yoon, W., Kim, Y., and Lee, J. (2021). Shared and distinct white matter abnormalities in schizophrenia and bipolar disorder. *Prog. Neuropsychopharmacol. Biol. Psychiatry* 108:110175. doi: 10.1016/j.pnpbp.2020.110175

Karcher, N. R., Rogers, B. P., and Woodward, N. D. (2019). Functional connectivity of the striatum in schizophrenia and psychotic bipolar disorder. *Biol. Psychiatry Cogn. Neurosci. Neuroimaging* 4, 956–965. doi: 10.1016/j.bpsc.2019.05.017

Kaufmann, T., van der Meer, D., Doan, N. T., Schwarz, E., Lund, M. J., Agartz, I., et al. (2019). Common brain disorders are associated with heritable patterns of apparent aging of the brain. *Nat. Neurosci.* 22, 1617–1623. doi: 10.1038/s41593-019-0471-7

Knyazeva, M. G. (2013). Splenium of corpus callosum: patterns of interhemispheric interaction in children and adults. *Neural Plast.* 2013:639430. doi: 10.1155/2013/639430

Kochunov, P., Ganjgahi, H., Winkler, A., Kelly, S., Shukla, D. K., Du, X., et al. (2016). Heterochronicity of white matter development and aging explains regional patient control differences in schizophrenia. *Hum. Brain Mapp.* 37, 4673–4688. doi: 10.1002/hbm.23336

Kondo, C., Ito, K., Kai Wu, Sato, K., Taki, Y., Fukuda, H., et al. (2015). "An age estimation method using brain local features for T1-weighted images," in *Proceedings of the 2015 37th Annual International Conference of the IEEE Engineering in Medicine and Biology Society (EMBC)*, (Milan: IEEE), 666–669.

Kong, L. Y., Huang, Y. Y., Lei, B. Y., Ke, P. F., Li, H. H., Zhou, J., et al. (2021). Divergent alterations of structural-functional connectivity couplings in first-episode and chronic schizophrenia patients. *Neuroscience* 460, 1–12. doi: 10.1016/j.neuroscience.2021.02.008

Koshiyama, D., Fukunaga, M., Okada, N., Morita, K., Nemoto, K., Usui, K., et al. (2020). White matter microstructural alterations across four major psychiatric disorders: mega-analysis study in 2937 individuals. *Mol. Psychiatry* 25, 883–895. doi: 10.1038/s41380-019-0553-7

Koshiyama, D., Fukunaga, M., Okada, N., Yamashita, F., Yamamori, H., Yasuda, Y., et al. (2018). Role of subcortical structures on cognitive and social function in schizophrenia. *Sci. Rep.* 8:1183. doi: 10.1038/s41598-017-18950-2

Koutsouleris, N., Davatzikos, C., Borgwardt, S., Gaser, C., Bottlender, R., Frodl, T., et al. (2014). Accelerated brain aging in schizophrenia and beyond: a neuroanatomical marker of psychiatric disorders. *Schizophr. Bull.* 40, 1140–1153. doi: 10.1093/schbul/sbt142

Lewis, J. D., Evans, A. C., Tohka, J., Brain Development Cooperative Group, and Pediatric Imaging, Neurocognition, and Genetics Study (2018). T1 white/gray contrast as a predictor of chronological age, and an index of cognitive performance. *Neuroimage* 173, 341–350. doi: 10.1016/j.neuroimage.2018.02.050

Linke, J. O., Stavish, C., Adleman, N. E., Sarlls, J., Towbin, K. E., Leibenluft, E., et al. (2020). White matter microstructure in youth with and at risk for bipolar disorder. *Bipolar Disord.* 22, 163–173. doi: 10.1111/bdi.12885

Luck, D., Danion, J. M., Marrer, C., Pham, B. T., Gounot, D., and Foucher, J. (2010). The right parahippocampal gyrus contributes to the formation and maintenance of bound information in working memory. *Brain Cogn.* 72, 255–263. doi: 10.1016/j.bandc.2009.09.009

Mandl, R. C., Schnack, H. G., Luigjes, J., van den Heuvel, M. P., Cahn, W., Kahn, R. S., et al. (2010). Tract-based analysis of magnetization transfer ratio and diffusion tensor imaging of the frontal and frontotemporal connections in schizophrenia. *Schizophr. Bull.* 36, 778–787. doi: 10.1093/schbul/sbn161

McKenna, F. F., Miles, L., Babb, J. S., Goff, D. C., and Lazar, M. (2019). Diffusion kurtosis imaging of gray matter in schizophrenia. *Cortex* 121, 201–224. doi: 10.1016/j.cortex.2019.08.013

Mitelman, S. A., Canfield, E. L., Newmark, R. E., Brickman, A. M., Torosjan, Y., Chu, K. W., et al. (2009). Longitudinal assessment of gray and white matter in chronic schizophrenia: a combined diffusion-tensor and structural magnetic resonance imaging study. *Open Neuroimage J.* 3, 31–47. doi: 10.2174/1874440000903010031

Mori, S., Oishi, K., Jiang, H., Jiang, L., Li, X., Akhter, K., et al. (2008). Stereotaxic white matter atlas based on diffusion tensor imaging in an ICBM template. *Neuroimage* 40, 570–582. doi: 10.1016/j.neuroimage.2007.12.035

Mori, T., Ohnishi, T., Hashimoto, R., Nemoto, K., Moriguchi, Y., Noguchi, H., et al. (2007). Progressive changes of white matter integrity in schizophrenia revealed by diffusion tensor imaging. *Psychiatry Res.* 154, 133–145. doi: 10.1016/j.pscychresns.2006.09.004

Nebel, M. B., Eloyan, A., Barber, A. D., and Mostofsky, S. H. (2014). Precentral gyrus functional connectivity signatures of autism. *Front. Syst. Neurosci.* 8:80. doi: 10.3389/fnsys.2014.00080

Nenadic, I., Dietzek, M., Langbein, K., Sauer, H., and Gaser, C. (2017). BrainAGE score indicates accelerated brain aging in schizophrenia, but not bipolar disorder. *Psychiatry Res. Neuroimaging* 266, 86–89. doi: 10.1016/j.pscychresns.2017.05.006

Nenadic, I., Sauer, H., Smesny, S., and Gaser, C. (2012). Aging effects on regional brain structural changes in schizophrenia. *Schizophr. Bull.* 38, 838–844. doi: 10.1093/schbul/sbq140

Nolze-Charron, G., Dufort-Rouleau, R., Houde, J. C., Dumont, M., Castellano, C. A., Cunnane, S., et al. (2020). Tractography of the external capsule and cognition: a diffusion MRI study of cholinergic fibers. *Exp. Gerontol.* 130:110792. doi: 10.1016/j.exger.2019.110792

Peters, A., Sethares, C., and Moss, M. B. (2010). How the primate fornix is affected by age. *J. Comp. Neurol.* 518, 3962–3980. doi: 10.1002/cne.22434

Pfefferbaum, A., Mathalon, D. H., Sullivan, E. V., Rawles, J. M., Zipursky, R. B., and Lim, K. O. (1994). A quantitative magnetic resonance imaging study of changes in brain morphology from infancy to late adulthood. *Arch. Neurol.* 51, 874–887. doi: 10.1001/archneur.1994.00540210046012

Porter, J. N., Roy, A. K., Benson, B., Carlisi, C., Collins, P. F., Leibenluft, E., et al. (2015). Age-related changes in the intrinsic functional connectivity of the human ventral vs. dorsal striatum from childhood to middle age. *Dev. Cogn. Neurosci.* 11, 83–95. doi: 10.1016/j.dcn.2014.08.011

Qin, J., Chen, S. G., Hu, D. W., Zeng, L. L., Fan, Y. M., Chen, X. P., et al. (2015). Predicting individual brain maturity using dynamic functional connectivity. *Front. Hum. Neurosci.* 9:418. doi: 10.3389/fnhum.2015.00418

Rhindress, K., Robinson, D. G., Gallego, J. A., Wellington, R., Malhotra, A. K., and Szeszko, P. R. (2017). Hippocampal subregion volume changes associated with antipsychotic treatment in first-episode psychosis. *Psychol. Med.* 47, 1706–1718. doi: 10.1017/S0033291717000137

Rokicki, J., Wolfers, T., Nordhoy, W., Tesli, N., Quintana, D. S., Alnaes, D., et al. (2021). Multimodal imaging improves brain age prediction and reveals distinct

abnormalities in patients with psychiatric and neurological disorders. *Hum. Brain Mapp.* 42, 1714–1726. doi: 10.1002/hbm.25323

Rosch, K. S., and Mostofsky, S. (2019). Development of the frontal lobe. *Handb. Clin. Neurol.* 163, 351–367. doi: 10.1016/B978-0-12-804281-6.00019-7

Rosenberg, M. D., Finn, E. S., Scheinost, D., Papademetris, X., Shen, X., Constable, R. T., et al. (2016). A neuromarker of sustained attention from whole-brain functional connectivity. *Nat. Neurosci.* 19, 165–171. doi: 10.1038/nn.4179

Schnack, H. G., van Haren, N. E., Nieuwenhuis, M., Hulshoff Pol, H. E., Cahn, W., and Kahn, R. S. (2016). Accelerated brain aging in schizophrenia: a longitudinal pattern recognition study. *Am. J. Psychiatry* 173, 607–616. doi: 10.1176/appi.ajp.2015.15070922

Shen, X., Finn, E. S., Scheinost, D., Rosenberg, M. D., Chun, M. M., Papademetris, X., et al. (2017). Using connectome-based predictive modeling to predict individual behavior from brain connectivity. *Nat. Protoc.* 12, 506–518. doi: 10.1038/nprot.2016.178

Silk, T. J., and Wood, A. G. (2011). Lessons about neurodevelopment from anatomical magnetic resonance imaging. *J. Dev. Behav. Pediatr.* 32, 158–168. doi: 10.1097/DBP.0b013e318206d58f

Stanfield, A. C., Moorhead, T. W., Job, D. E., McKirdy, J., Sussmann, J. E., Hall, J., et al. (2009). Structural abnormalities of ventrolateral and orbitofrontal cortex in patients with familial bipolar disorder. *Bipolar Disord.* 11, 135–144. doi: 10.1111/j.1399-5618.2009.00666.x

Tesli, N., Rokicki, J., Maximov, I. I., Bell, C., Hjell, G., Gurholt, T., et al. (2021). White matter matters: unraveling violence in psychosis and psychopathy. *Schizophr. Bull. Open* 2:sgab026. doi: 10.1093/schizbullopen/sgab026

Tibshirani, R. (1996). Regression shrinkage and selection via the lasso. *J. R. Stat. Soc. Ser. B* 58, 267–288.

Valizadeh, S. A., Hanggi, J., Merillat, S., and Jancke, L. (2017). Age prediction on the basis of brain anatomical measures. *Hum. Brain Mapp.* 38, 997–1008. doi: 10.1002/hbm.23434

van Haren, N. E., Hulshoff Pol, H. E., Schnack, H. G., Cahn, W., Brans, R., Carati, I., et al. (2008). Progressive brain volume loss in schizophrenia over the course of the illness: evidence of maturational abnormalities in early adulthood. *Biol. Psychiatry* 63, 106–113. doi: 10.1016/j.biopsych.2007.01.004

van Os, J., and Kapur, S. (2009). Schizophrenia. *Lancet* 374, 635–645. doi: 10.1016/s0140-6736(09)60995-8

Voineskos, A. N., Lobaugh, N. J., Bouix, S., Rajji, T. K., Miranda, D., Kennedy, J. L., et al. (2010). Diffusion tensor tractography findings in schizophrenia across the adult lifespan. *Brain* 133(Pt 5), 1494–1504. doi: 10.1093/brain/awq040

Wang, J., Knol, M. J., Tiulpin, A., Dubost, F., de Bruijne, M., Vernooij, M. W., et al. (2019). Gray matter age prediction as a biomarker for risk of dementia. *Proc. Natl. Acad. Sci. U.S.A.* 116, 21213–21218. doi: 10.1073/pnas.1902376116

Wang, Y., Jiang, Y., Collin, G., Liu, D., Su, W., Xu, L., et al. (2021). The effects of antipsychotics on interactions of dynamic functional connectivity in the triple-network in first episode schizophrenia. *Schizophr. Res.* 236, 29–37. doi: 10.1016/j.schres.2021.07.038

Weiner, K. S., and Zilles, K. (2016). The anatomical and functional specialization of the fusiform gyrus. *Neuropsychologia* 83, 48–62. doi: 10.1016/j.neuropsychologia.2015.06.033

Wright, S., Kochunov, P., Chiappelli, J., McMahon, R., Muellerklein, F., Wijtenburg, S. A., et al. (2014). Accelerated white matter aging in schizophrenia: role of white matter blood perfusion. *Neurobiol. Aging* 35, 2411–2418. doi: 10.1016/j.neurobiolaging.2014.02.016

Wu, F. C., Zhang, Y., Yang, Y. Z., Lu, X., Fang, Z., Huang, J., et al. (2018). Structural and functional brain abnormalities in drug-naive, first-episode, and chronic patients with schizophrenia: a multimodal MRI study. *Neuropsychiatr. Dis. Treat.* 14, 2889–2904. doi: 10.2147/NDT.S174356

Yan, C., and Zang, Y. (2010). DPARSF: a MATLAB toolbox for "pipeline" data analysis of resting-state fMRI. *Front. Syst. Neurosci.* 4:13. doi: 10.3389/fnsys.2010.00013

Yan, R., Tao, S., Liu, H., Chen, Y., Shi, J., Yang, Y., et al. (2019). Abnormal alterations of regional spontaneous neuronal activity in inferior frontal orbital gyrus and corresponding brain circuit alterations: a resting-state fMRI study in somatic depression. *Front. Psychiatry* 10:267. doi: 10.3389/fpsyt.2019.00267

Yoshimura, K., and Kurashige, T. (2000). Age-related changes in the posterior limb of the internal capsule revealed by magnetic resonance imaging. *Brain Dev.* 22, 118–122. doi: 10.1016/s0387-7604(00)00088-7

Zang, J., Huang, Y., Kong, L., Lei, B., Ke, P., Li, H., et al. (2021). Effects of brain atlases and machine learning methods on the discrimination of schizophrenia patients: a multimodal MRI study. *Front. Neurosci.* 15:697168. doi: 10.3389/fnins.2021.697168

Zarei, M. (2018). Precentral gyrus abnormal connectivity in male and female patients with schizophrenia. *Neuroimmunol. Neuroinflammation* 5:13. doi: 10.20517/2347-8659.2018.02

Zhang, C.-H., and Huang, J. (2008). The sparsity and bias of the lasso selection in high-dimensional linear regression. *Ann. Statist.* 36, 1567–1594.

Zhou, L., Tian, N., Geng, Z. J., Wu, B. K., Dong, L. Y., and Wang, M. R. (2020). Diffusion tensor imaging study of brain precentral gyrus and postcentral gyrus during normal brain aging process. *Brain Behav.* 10:e01758. doi: 10.1002/brb3.1758

**Conflict of Interest:** The authors declare that the research was conducted in the absence of any commercial or financial relationships that could be construed as a potential conflict of interest.

frontiers in Aging Neuroscience

ORIGINAL RESEARCH
published: 30 March 2022
doi: 10.3389/fnagi.2022.804621

# Abnormal Default Mode Network Homogeneity in Major Depressive Disorder With Gastrointestinal Symptoms at Rest

*Meiqi Yan[1], Jindong Chen[1], Feng Liu[2], Huabing Li[3], Jingping Zhao[1] and Wenbin Guo[1,4]**

*[1] Department of Psychiatry, National Clinical Research Center for Mental Disorders, The Second Xiangya Hospital of Central South University, Changsha, China, [2] Department of Radiology, Tianjin Medical University General Hospital, Tianjin, China, [3] Department of Radiology, The Second Xiangya Hospital of Central South University, Changsha, China, [4] Department of Psychiatry, The Third People's Hospital of Foshan, Foshan, China*

**Background:** Gastrointestinal (GI) symptoms are prominent in many patients with major depressive disorder (MDD). However, it remains unclear whether MDD patients with GI symptoms have brain imaging alterations in the default mode network (DMN) regions.

**Methods:** A total of 35 MDD patients with GI symptoms, 17 MDD patients without GI symptoms, and 28 healthy controls (HCs) were recruited. All participants underwent resting-state functional magnetic resonance imaging scans. Network homogeneity (NH) and support vector machine (SVM) methods were used to analyze the imaging data.

**Results:** Gastrointestinal group showed higher 17-item Hamilton Rating Scale for Depression total scores and factor scores than the non-GI group. Compared with the non-GI group and HCs, the GI group showed decreased NH in the right middle temporal gyrus (MTG) and increased NH in the right precuneus (PCu). The SVM results showed that a combination of NH values of the right PCu and the right MTG exhibited the highest accuracy of 88.46% (46/52) to discriminate MDD patients with GI symptoms from those without GI symptoms.

**Conclusion:** Major depressive disorder patients with GI symptoms have more severe depressive symptoms than those without GI symptoms. Distinctive NH patterns in the DMN exist in MDD patients with GI symptoms, which can be applied as a potential brain imaging marker to discriminate MDD patients with GI symptoms from those without GI symptoms.

**Keywords: major depressive disorder, default mode network, network homogeneity, gastrointestinal symptoms, magnetic resonance imaging**

OPEN ACCESS

***Edited by:***
*Wei Deng,*
*Affiliated Mental Health Center and Hangzhou Seventh People's Hospital, China*

***Reviewed by:***
*Zhiliang Long,*
*Southwest University, China*
*Jiajia Zhu,*
*The First Affiliated Hospital of Anhui Medical University, China*

***Correspondence:**
*Wenbin Guo*
*guowenbin76@csu.edu.cn*

***Specialty section:***
*This article was submitted to Alzheimer's Disease and Related Dementias, a section of the journal Frontiers in Aging Neuroscience*

***Received:*** *29 October 2021*
***Accepted:*** *01 March 2022*
***Published:*** *30 March 2022*

***Citation:***
*Yan M, Chen J, Liu F, Li H, Zhao J and Guo W (2022) Abnormal Default Mode Network Homogeneity in Major Depressive Disorder With Gastrointestinal Symptoms at Rest. Front. Aging Neurosci. 14:804621. doi: 10.3389/fnagi.2022.804621*

## INTRODUCTION

Major depressive disorder (MDD) is a globally common, severe, and recurrent mental disorder (Smith, 2014). The World Health Organization (WHO) predicted that MDD will be the leading cause of the global burden of disease by 2030 (Malhi and Mann, 2018). However, the resources of professional psychiatric medical staff are scarce. Almost half of the whole world's population lives

in countries with only two professional psychiatrists per 100,000 people (Smith, 2014). A previous study has indicated that more healthcare resources were required during the episodes of MDD, resulting in a higher economic burden (Painchault et al., 2014). Comorbidity was reported as an important cause of the increasing economic burden of MDD (Greenberg et al., 2015). Many patients with MDD often have some non-specific somatic symptoms as their chief complaints [such as medically unexplained pain, insomnia, blurred vision, chest tightness, tachycardia, and gastrointestinal (GI) symptoms], with the prominent GI symptoms (such as loss of appetite, gastralgia, gastric distention, heartburn, acid reflux, nausea, vomiting, constipation, and diarrhea). In a large study of the general population, 54% of people with depressive symptoms suffered from frequent abdominal pain, constipation, diarrhea, dyspepsia, or irritable bowel syndrome (IBS), whereas only 29% of people with non-depressive symptoms (Hillilä et al., 2008). It has been indicated that somatic symptoms in MDD patients are associated with more severe clinical symptoms, lower remission rates (Novick et al., 2013), and worse prognosis (Bekhuis et al., 2016). Somatic symptoms also led to more utilization of health resources in patients with MDD (García-Campayo et al., 2008). In addition, patients with depressive-anxiety disorder comorbidities were reported to exhibit more several chronic physical conditions than patients without depression and anxiety comorbidities, and having depression and anxiety at the same time further increased the risk of a number of physical conditions co-occurring (Scott et al., 2007). Unfortunately, due to the scarcity of mental health resources, coupled with the social stigma of mental illness/disorders, MDD patients with somatic symptoms as chief complaints tend to seek treatment at general hospitals for the first time, even over and over again, leading to a lack of correct diagnosis and effective treatment (Kirmayer et al., 1993; García-Campayo et al., 2008), which is often called as "masked depression" (Verster and Gagiano, 1995). Thus, correct identifications and diagnoses of MDD patients with GI symptoms as chief complaints and effective treatments for them are urgent. It is not a one-way story that only patients with MDD can have GI symptoms. In clinical practice, patients with the digestive disease can also have psychological problems, such as anxiety, self-reported depressive mood, and even depression. A previous study has reported that most patients with GI motility disorders, IBS, and functional dyspepsia had a number of mental and psychological problems. When patients with IBS were exposed to stressors, their GI symptoms seem to be greatly increased (Whitehead, 1996). In another study, 44.4% of patients with inflammatory bowel disease (IBD) suffered from anxiety or depression or both, resulting in more therapies and healthcare resources (Navabi et al., 2018). IBD patients with baseline depression were reported to show more aggressive symptoms and poorer long-term progress than IBD patients without baseline depression (Kochar et al., 2018). Therefore, it is very important to find out the etiology of GI symptoms in patients with MDD.

But to date, the definite cause of MDD remains unknown. In recent years, the gut-brain axis has become a hot research topic, which is believed as one possible critical mechanism of affective disorders (Mayer et al., 2015). It has previously been reported that the GI microbiota can activate neural pathways and the central nervous system signaling systems, thereby affecting MDD-related symptoms (Foster and McVey Neufeld, 2013). However, it still remains unclear whether MDD patients with GI symptoms have brain imaging alterations. Structural (Bell-McGinty et al., 2002; Depping et al., 2016; Hyett et al., 2018) and functional (Bluhm et al., 2009; Guo et al., 2013b, Chen et al., 2015; Guo et al., 2018a) brain changes have already been reported in many previous studies of MDD. Meanwhile, some previous studies have reported structural and functional brain image changes in digestive system diseases (Kwan et al., 2005; Song et al., 2006; Blankstein et al., 2010; Skrobisz et al., 2020). Thus, some researchers tried to study whether MDD patients with GI symptoms exhibited abnormal brain imaging data and observed altered gray matter volume (GMV) and regional homogeneity (ReHo) (Yan et al., 2019; Liu et al., 2020). However, there are still few functional imaging studies conducted on MDD patients with GI symptoms, and the researchers did not further examine whether these abnormal GMV or ReHo could be used as good neuroimaging markers to discriminate the GI group from the non-GI group in both abovementioned studies.

The default mode network (DMN) is mainly composed of three subdivisions, namely, the ventral medial prefrontal cortex, the dorsal medial prefrontal cortex, the posterior cingulate cortex, and adjacent precuneus (PCu) plus the lateral parietal cortex (Raichle, 2015). Prior to this study, there have been many studies on the DMN of mental disorders, such as schizophrenia (Guo et al., 2014, 2015b; Hu et al., 2017; Hare et al., 2019; Fan et al., 2020; Martin-Subero et al., 2021), MDD (Guo et al., 2015a; Fang et al., 2016; Posner et al., 2016; Yan et al., 2019; Zhou et al., 2020), post-traumatic stress disorder (King et al., 2016; Miller et al., 2017; Viard et al., 2019), and attention deficit hyperactivity disorder (Sidlauskaite et al., 2016; Bozhilova et al., 2018). The increased amplitude of low-frequency fluctuation and functional connectivity (FC) in the DMN have been reported in patients with ulcerative colitis (Fan et al., 2019). Visceral sensory abnormalities are very common in IBS (Song et al., 2006). The DMN plays a critical role in gastric sensations (Skrobisz et al., 2020). A previous study has suggested that somatic symptom disorders may be associated with altered processing of sensory discrimination of pain and other somatic symptoms (Kim et al., 2019). It was indicated that brain areas involved in the process of pain sensory shifted to those involved in the subjective states of emotion and motivation in the majority of chronic pain diseases (Apkarian et al., 2011). Moreover, chronic visceral pain might lead to functional reorganization in the DMN (Farmer et al., 2012; Qi et al., 2016; Kano et al., 2018). Therefore, the abovementioned studies indicated that the DMN may change with the onset and development of GI symptoms. Thus, we were curious about whether there were special brain imaging changes of the DMN in these MDD patients with GI symptoms.

In this study, we applied a network homogeneity (NH) approach to examine whether the NH of the DMN in MDD patients with GI symptoms was abnormal and whether abnormal NH of the DMN could be used as brain imaging markers to separate MDD patients with GI symptoms from MDD patients without GI symptoms. We hypothesized that MDD patients with

GI symptoms exhibited altered NH in certain areas of the DMN, which might be used to discriminate the MDD patients with GI symptoms from those without GI symptoms.

# MATERIALS AND METHODS

## Participants

A total of 35 patients with at least one GI symptom were recruited as the GI group, and 17 patients without GI symptoms were recruited and assigned to the non-GI group. Main GI symptoms included medically unexplained gastralgia, gastric distention, heartburn, acid reflux, nausea, vomiting, constipation, and diarrhea. All patients were aged from 18 to 55 years and were from the outpatients of the Second Xiangya Hospital of Central South University, China. Their final diagnoses were independently confirmed by two psychiatrists, using the DSM-5 criteria for MDD. The inclusion criteria for all patients were as follows: (1) first major depressive episode; (2) 17-item Hamilton Rating Scale for Depression (HRSD-17) (Hamilton, 1967) total scores $\geq$18; (3) with no history of antipsychotics and physical therapy (such as electroconvulsive therapy, ECT); and (4) with no confirmed digestive diseases.

A total of 28 healthy controls (HCs) were recruited from the community; the patient groups were matched in age, gender, and education. They would not be recruited if they had a suspicious or explicit family history of mental illness/disorders, especially their first-degree relatives. Besides, HCs with any history of digestive diseases, neurological diseases, substance abuse, or psychotic symptoms would not be enrolled.

All participants were Han Chinese and right-handed. The exclusion criteria for all participants were as follows: (a) other mental disorders meeting DSM-5 diagnostic criteria; (b) any history of neurological diseases, severe physical illnesses, and substance abuse; (c) being pregnant; (d) structural abnormalities of the brain after the initial magnetic resonance imaging (MRI) scan; and (e) any contraindications to MRI scans.

The severity of MDD was evaluated by using the HRSD-17. It can be divided into five types of factors: (1) anxiety/somatization (six items, namely, psychic anxiety, somatic anxiety, GI symptoms, hypochondriasis, insight, and general symptoms); (2) weight loss (one item); (3) cognitive disturbances (three items, namely, self-guilt, suicide, and agitation); (4) retardation symptoms (four items, namely, depression, work and interests, retardation, and sexual symptoms); and (5) sleep disturbances (three items, namely, difficulty in falling asleep, superficial sleep, and early awakening).

The study was approved by the Medical Research Ethics Committee of the Second Xiangya Hospital of Central South University, China. It was conducted in accordance with the Helsinki Declaration. Each participant has submitted a written informed consent before enrollment.

## Image Acquisition

By using a 3.0 T Siemens scanner (Germany) at the Second Xiangya Hospital of Central South University, resting-state fMRI data were obtained. All subjects were instructed to close their eyes, stay still, and awake throughout the scan. The resting-state functional images were acquired using the echo-planar imaging sequence. Specific parameters were as follows: 2,000/30 ms of repetition time/echo time, 30 slices, 64 × 64 matrix, 90° flip angle, 24 cm field of view, 4 mm slice thickness, 0.4 mm gap, and 250 volumes lasting for 500 s.

## Data Preprocessing

A Data Processing Assistant for Resting-State fMRI was used for data preprocessing in MATLAB (MathWorks) (Chao-Gan and Yu-Feng, 2010). Considering that data errors may increase due to initial signal instability and subjects' early adaptation time, we deleted the first 10 original images to minimize these potential impacts. Specific processes were as follows: (a) correction for slice timing and head motion: all data were with a maximum displacement of *x*-, *y*-, or *z*-axis less than 2 mm and maximum angular rotation less than 2°; (b) normalization: the corrected imaging data then got spatially normalized to the MNI space with 3 mm × 3mm × 3 mm; and (c) band-pass filtering and detrending: after normalization, the imaging data were temporally band-pass filtered at 0.01–0.08 Hz and got linearly detrended. Several spurious covariates (such as the signal from the ventricular seed-based region of interest, white matter-centered region, and 24-head motion parameters acquired by rigid body correction) were removed from the imaging data. The global signal was not regressed out during data preprocessing according to a previous study (Hahamy et al., 2014).

## Default Mode Network Identification

After being preprocessed, all groups were subjected to construct the DMN mask by using Group Independent Component Analysis (ICA) of fMRI toolbox (GIFT).[1] Three main steps were included in the analysis as follows: data reduction, independent component separation, and back reconstruction. The DMN components were selected based on the templates provided by GIFT. The specific calculation process of generating the final DMN mask was similar to our previous study (Guo et al., 2018b). The generated DMN mask was applied in the following NH analysis.

## Network Homogeneity Analysis

The NH analysis was conducted using MATLAB (MathWorks). Correlation coefficients between each voxel and all other voxels within the DMN mask were calculated for each subject. The average correlation coefficient was defined as the homogeneity of a given voxel. The NH of each voxel in the DMN mask was generated. The NH maps were smoothed with a Gaussian kernel of 4 mm full width at half maximum and were used for group comparisons.

## Statistical Analyses

Group differences (such as age, years of education, HRSD-17 total, and the five-factor scores across the three groups) were compared by performing an analysis of variance (ANOVA) using SPSS19.0 (LSD between two group comparisons). A Chi-square

[1] http://mialab.mrn.org/software/#gica

**TABLE 1 |** Demographic and clinical characteristics of the participants.

| | S1 (*n* = 35) | S0 (*n* = 17) | HCs (*n* = 28) | *F*, *t* or $\chi^2$ value | *Post hoc t*-tests or *p*-values |
|---|---|---|---|---|---|
| Age (years) | 30.86 ± 6.84 | 30.29 ± 8.05 | 30.14 ± 5.00 | 0.102 | 0.903[a] |
| Gender (male/female) | 13/22 | 6/11 | 14/14 | 1.377 | 0.502[b] |
| Handedness (right/left) | 35/0 | 17/0 | 28/0 | | |
| Education (years) | 14.51 ± 3.28 | 12.94 ± 3.46 | 14.61 ± 2.69 | 1.797 | 0.173[a] |
| Illness duration (months) | 6.23 ± 4.63 | 6.94 ± 3.98 | | 0.544 | 0.589[c] |
| HRSD-17 scores | 22.69 ± 3.41 | 20.18 ± 2.67 | 0.89 ± 0.88 | 585.979 | S1 > S0 > Nor |
| Anxiety/somatization | 7.31 ± 1.92 | 6.41 ± 1.66 | 0.39 ± 0.57 | 174.531 | S1 > S0 > Nor |
| Weight loss | 0.80 ± 0.83 | 0.06 ± 0.24 | 0 | 18.741 | S1 > S0, Nor |
| Cognitive disturbances | 3.71 ± 1.78 | 3.41 ± 1.50 | 0 | 64.213 | S1, S0 > Nor |
| Retardation symptoms | 6.40 ± 1.42 | 6.76 ± 1.56 | 0.18 ± 0.39 | 253.030 | S1, S0 > Nor |
| Sleep disturbances | 4.46 ± 1.42 | 3.53 ± 1.28 | 0.32 ± 0.55 | 103.570 | S1 > S0 > Nor |

*HRSD-17, 17-item Hamilton Rating Scale for Depression.*
[a]*The p-value was obtained by analyses of variance.*
[b]*The p-value was obtained by a Chi-square test.*
[c]*The p-value was obtained by two-sample t-tests.*
*S1, gastrointestinal (GI) symptoms group.*
*S0, non-gastrointestinal (non-GI) symptoms group.*
*HCs, healthy controls.*

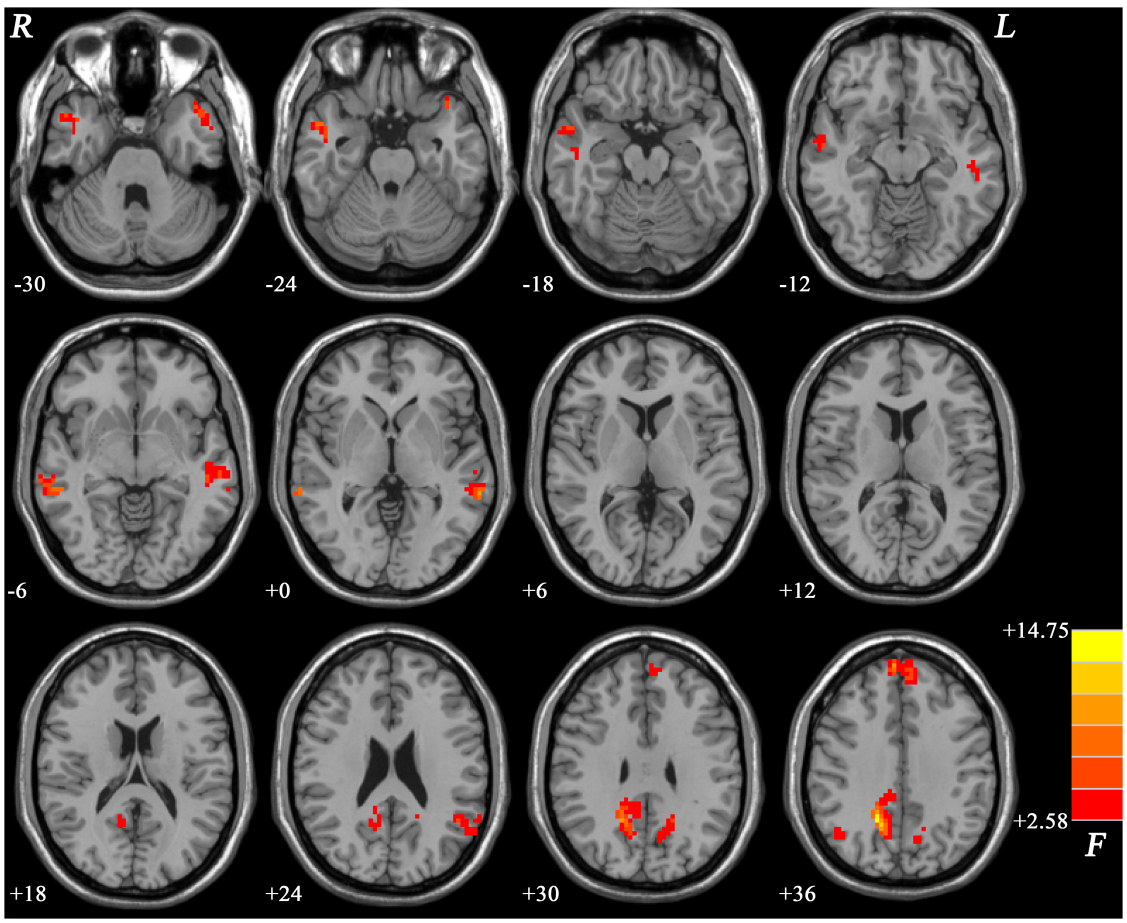


**FIGURE 1 |** Brain regions within the DMN showing group differences in NH values across the three groups. Color bar indicates *F* values from ANCOVA (age, sex, years of education, and frame-wise displacement as covariates). NH, network homogeneity; DMN, default mode network; ANCOVA, analysis of covariance.

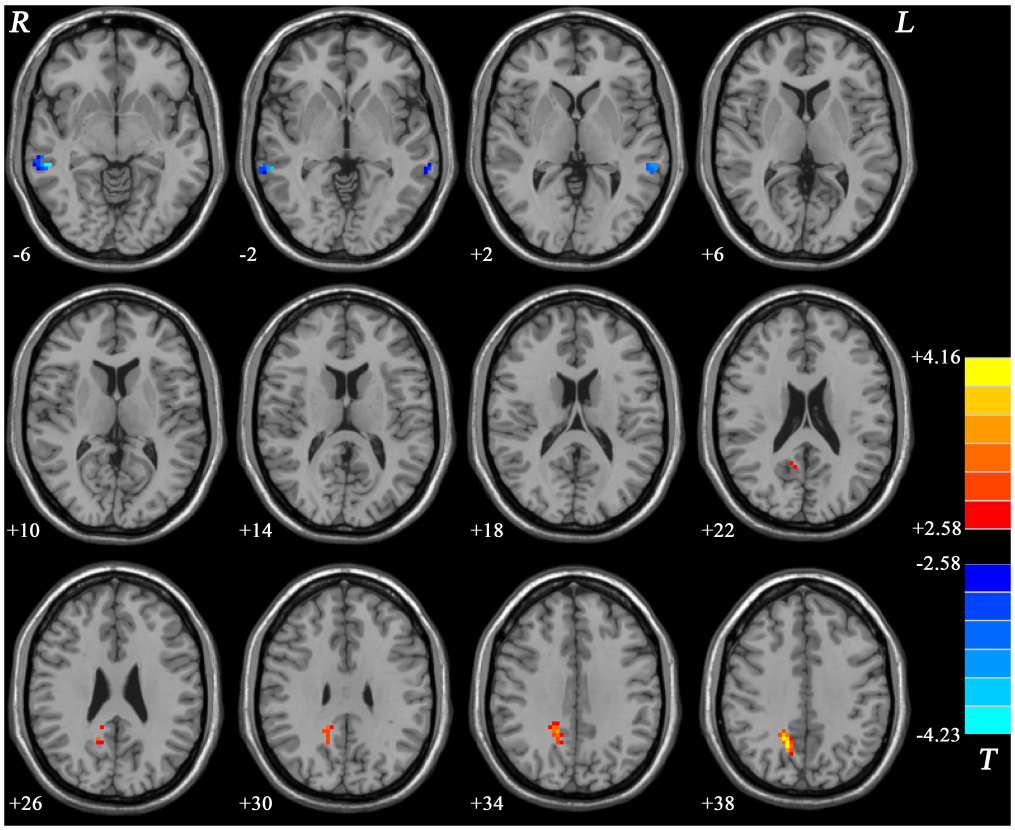


**FIGURE 2 |** Statistical map depicts higher and lower NH of MDD patients with GI symptoms compared with MDD patients without GI symptoms. The threshold was set at $p < 0.05$. Blue denotes lower NH, and red denotes higher NH. Color bar indicates *T* values from the two-sample *t*-test. NH, network homogeneity; GI, gastrointestinal symptoms.

test was applied to describe gender distribution. And we applied a two-sample *t*-test to analyze whether there were differences in the illness duration between the GI and non-GI groups. The *p*-value of <0.05 was considered statistically significant.

The NH analysis was performed using an analysis of covariance (ANCOVA) across the three groups, followed by *post hoc t*-tests. The significance threshold for multiple comparisons was set at $p < 0.05$ by using Gaussian random field (GRF) theory (voxel significance at $p < 0.001$ and cluster significance at $p < 0.05$). Frame-wise displacement (FD) values were calculated for every subject, and the average FD was used as one of the covariates according to the previous study (Power et al., 2012). Age, sex, and years of education were other covariates.

## Correlation Analyses

The NH values were extracted from the brain clusters with abnormal NH values. Pearson's correlation analysis was used to determine the correlations between NH abnormality and HRSD-17 total scores as well as the five-factor scores with the Benjamini–Hochberg correction threshold of $p < 0.05$.

## Classification Analyses

The support vector machine (SVM) approach is a popular supervised machine-learning model, which has gotten many applications for classifications in the researches of psychiatry in recent years (Steardo et al., 2020). It can map training examples to points in space and construct a hyperplane with the maximum distance from the nearest training data point of any one of the two predefined categories, known as the maximum-margin hyperplane (Shan et al., 2020). These nearest points are support vectors (Du et al., 2015). For more details about SVM, a previous study (Shan et al., 2020) is available. In this study, SVM was applied to use NH values extracted from the brain regions with abnormal NH values to discriminate MDD patients with GI symptoms from those without GI symptoms by employing the library for SVM (LIBSVM) software package[2] in MATLAB. In this study, the method of "leave-one-out" was applied.

# RESULTS

## Demographic Characteristics and Clinical Information

The three groups did not show any significant group differences in age, years of education, and gender distribution. No significant illness-duration difference was observed between the two patient

[2]http://www.csie.ntu.edu.tw/~{}cjlin/libsvm/

**TABLE 2 |** Significant NH differences of DMN across groups.

| Cluster location | Peak (MNI) | | | Number of voxels | *T* value |
|---|---|---|---|---|---|
| | *x* | *y* | *z* | | |
| **S1 vs. S0** | | | | | |
| Right middle temporal gyrus | 54 | −36 | −6 | 26 | −4.2276 |
| Left middle temporal gyrus | −63 | −39 | 3 | 20 | −3.5664 |
| Right precuneus | 15 | −57 | 39 | 88 | 4.1589 |
| **S1 vs. HC** | | | | | |
| Bilateral superior medial frontal cortex | 6 | 57 | 36 | 35 | −4.1248 |
| Left middle temporal pole | −45 | 15 | −30 | 24 | −3.4925 |
| Right middle temporal gyrus | 45 | 3 | −27 | 52 | −4.3309 |
| Right precuneus | 18 | −54 | 36 | 76 | 5.2115 |
| **S0 vs. HCs** | | | | | |
| None | | | | | |

*NH, network homogeneity.*
*DMN, default mode network.*
*MNI, Montreal Neurological Institute.*
*S1, gastrointestinal (GI) symptoms group.*
*S0, non-gastrointestinal (non-GI) symptoms group.*
*HCs, healthy controls.*

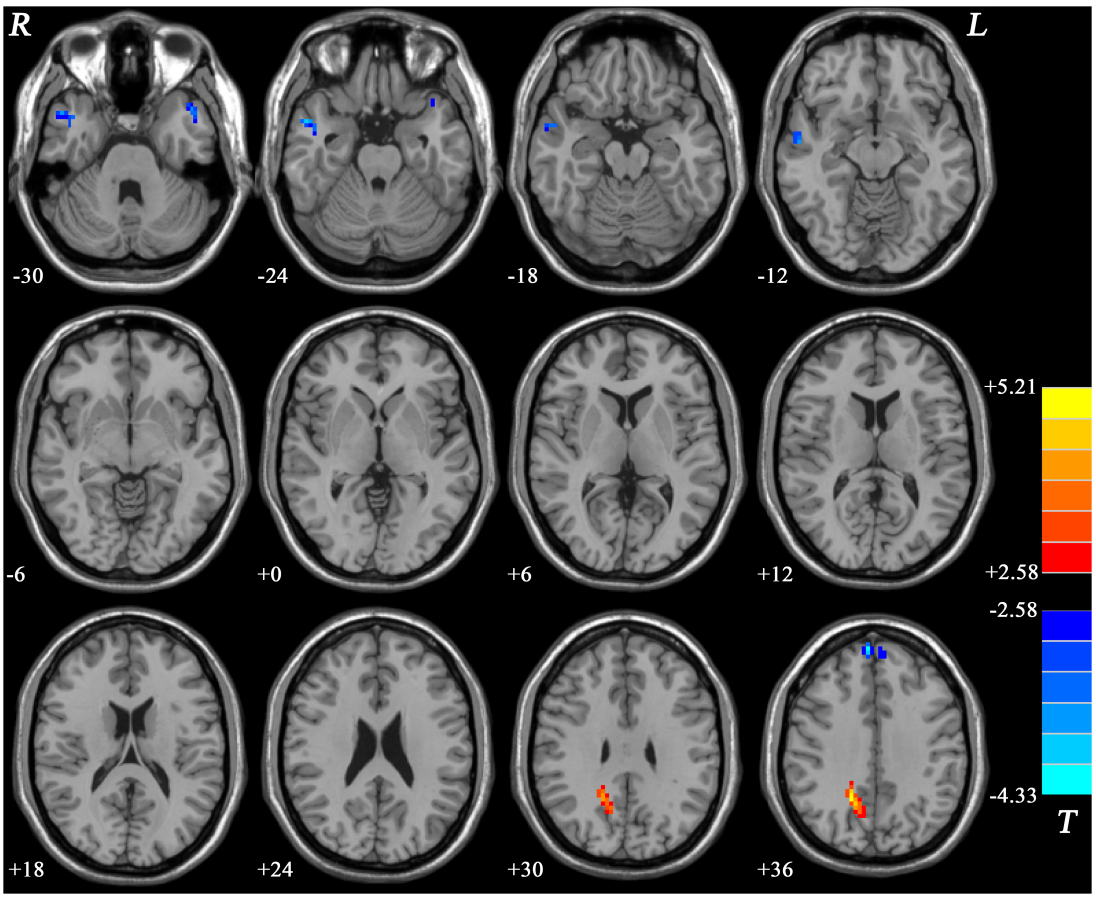


**FIGURE 3 |** Statistical map depicts higher and lower NH of MDD patients with GI symptoms compared with healthy controls. The threshold was set at $p < 0.05$. Blue denotes lower NH, and red denotes higher NH. Color bar indicates *T* values from two-sample *t*-test. NH, network homogeneity; GI, gastrointestinal symptoms.

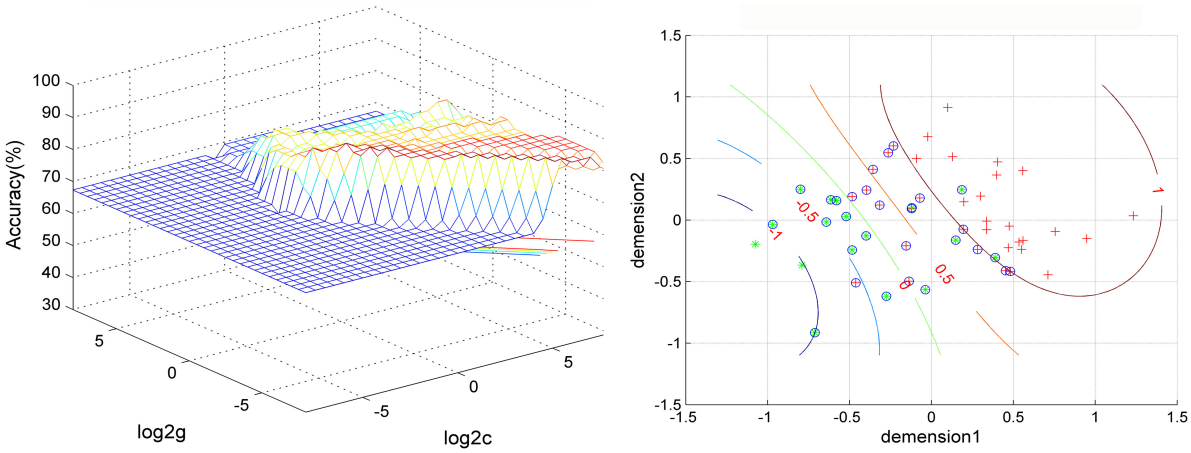


**FIGURE 4 |** Visualization of classifications through support vector machine (SVM) using a combination of NH values in the right precuneus and right middle temporal gyrus. Left: SVM parameters result of 3D view. Right: dimension 1 and dimension 2 represent the NH values in the right precuneus and right middle temporal gyrus, respectively. Red crosses represent MDD patients with GI symptoms, and green crosses represent MDD patients without GI symptoms. The circles mean support vectors. MDD, major depressive disorder; GI, gastrointestinal symptoms.

groups. Both patient groups showed higher HRSD-17 total and factor scores (except for scores of weight loss) than HCs. The weight loss scores of the GI group were higher than those of both the non-GI group and HCs, but there was no significant difference in weight loss scores between the non-GI group and HCs. Besides, the GI group showed higher HRSD-17 total scores, factor scores of anxiety/somatization, and sleep disturbances than those of the non-GI group (**Table 1**).

## Network Homogeneity Differences Across Groups

The NH values showed significant differences mainly in the frontal and temporal regions across the three groups (**Figure 1**).

Compared with MDD patients without GI symptoms, MDD patients with GI symptoms showed decreased NH in the bilateral MTG and increased NH in the right PCu (**Figure 2** and **Table 2**). Compared with HCs, MDD patients with GI symptoms exhibited decreased NH in the bilateral superior medial frontal cortex, left middle temporal pole, right MTG, and increased NH in the right PCu (**Figure 3** and **Table 2**). No abnormal NH in any brain region was found in the non-GI group relative to HCs.

## Support Vector Machine Analysis in Major Depressive Disorder With and Without Gastrointestinal Symptoms

The SVM results showed that a combination of NH values of the right PCu and the right MTG exhibited the highest accuracy of 88.46% (46/52) to discriminate MDD patients with GI symptoms from those without GI symptoms, with a sensitivity and specificity of 97.14% (34/35) and 70.56% (12/17), respectively. The accuracy of using abnormal NH in different brain regions was 78.85% (41/52) of the right PCu, 76.92% (40/52) of the left MTG, 80.77% (42/52) of the right MTG, 86.54% (45/52) of a combination of the right PCu and the left MTG, and 78.85% (41/52) of a combination of the bilateral MTG (**Figure 4** and **Figure 5**).

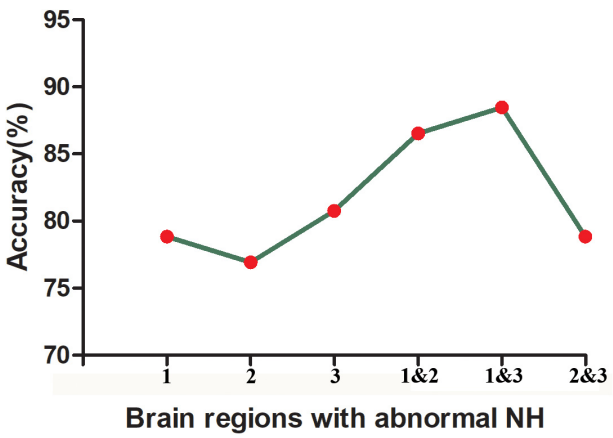


**FIGURE 5 |** The accuracy of using abnormal NH values of different brain regions to classify two patient groups. 1, right precuneus; 2, left middle temporal gyrus; 3, right middle temporal gyrus; 1&2, right precuneus and left middle temporal gyrus; 1&3, right precuneus and right middle temporal gyrus; 2&3, left middle temporal gyrus and right precuneus and right middle temporal gyrus.

## Correlations Between Network Homogeneity and Clinical Characteristics

There was no significant correlation between abnormal NH and the HRSD-17 total scores as well as the five-factor scores for both GI and non-GI symptom groups.

## DISCUSSION

Major depressive disorder patients with GI symptoms showed greater severity of depressive symptoms than MDD patients without GI symptoms. Distinctive NH patterns existed in MDD patients with GI symptoms. Compared with the non-GI group and HCs, the GI group showed decreased NH in the right MTG and increased NH in the right PCu. SVM results showed that a combination of NH values of the right PCu and the right MTG might be a potential brain imaging marker to discriminate MDD patients with GI symptoms from those without GI symptoms.

Depression, anxiety, and other psychological factors were considered as one of the important causes or inducements of some digestive system diseases (Drossman et al., 1999; Fond et al., 2014; Lee et al., 2017). A previous study has reported more serious depression in MDD patients with GI symptoms (Liu et al., 2020). Consistent with it, we observed that the GI group showed higher HRSD-17 total scores, factor scores of anxiety/somatization, weight loss, and sleep disturbances than the non-GI group in this study, indicating that the GI symptoms may be related to more severe depression.

The temporal gyrus is involved in attention control with the frontal and parietal lobe together (Sani et al., 2021), in which the MTG participated in cued attention (Corbetta and Shulman, 2002). Our previous study has observed that melancholic MDD showed lower NH in the right MTG than HCs (Cui et al., 2017). Reduced gray matter (Peng et al., 2011; Ma et al., 2012) and abnormal functional network connectivity (Zhi et al., 2018) were also observed in the MTG in MDD compared with HCs. Furthermore, a previous study found that MDD patients with somatic symptoms showed lower ReHo in the right MTG compared with MDD patients without somatic symptoms (Geng et al., 2019). In line with these studies, we observed decreased NH in the right MTG in MDD patients with GI symptoms compared with both MDD patients without GI symptoms and HCs. These issues might explain the phenomenon that MDD patients with GI symptoms pay much more attention to their somatic symptoms. Thus, we suspected that the right MTG might play an important role in the pathophysiology of MDD with GI symptoms. Additionally, we observed increased NH in the right PCu in MDD patients with GI symptoms compared with both MDD patients without GI symptoms and HCs. Some previous studies have reported abnormal PCu in MDD, including higher activity (Sheline et al., 2010) and lower activity (Chen et al., 2012; Guo et al., 2013a; Shi et al., 2020). It was proposed that PCu was involved in consciousness, specifically in the processes of self-reflection and episodic memory retrieval (Cavanna and Trimble, 2006; Cavanna, 2007). PCu would selectively deactivate during sleep (Cavanna and Trimble, 2006; Cavanna, 2007). Thus, we suspected that abnormal NH in the right PCu might be correlated with the phenomenon that the GI group showed more severe sleep disturbance than the non-GI group. Unfortunately, we did not find any statistically significant correlation between abnormal NH in the right PCu and clinical features. It was inconsistent with the results of the abovementioned study since we recruited different types of patients with MDD. Interestingly, a previous study reported that the interregional FC of the DMN between the MTG and PCu was reduced in IBS patients compared with HCs (Qi et al., 2016). Although we did not obtain more interregional FC data here to further test it, it makes us sure that decreased NH in the right MTG and increased NH in the right PCu might be distinctive NH patterns in MDD with GI symptoms.

We performed the SVM analysis to test whether abnormal NH in the DMN region could be used as a brain imaging marker to screen MDD patients with GI symptoms from MDD patients without GI symptoms. The results showed that a combination of NH values of the right PCu and right MTG showed the highest accuracy of 88.46% (46/52) to discriminate MDD patients with GI symptoms from those without GI symptoms, with a sensitivity of 97.14% (34/35) and a specificity of 70.56% (12/17). The establishment of good diagnostic indicators requires sensitivity or specificity of at least 60%, preferably greater than 70% (Swets, 1988; Gong et al., 2011). Thus, the combination of NH values of the right PCu and right MTG may be a potential brain imaging marker to screen MDD patients with GI symptoms from MDD patients without GI symptoms.

There were some limitations. First, we did not evaluate the severity of GI symptoms and did not further classify them. Second, we did not know whether changes in NH occurred before or as a result of GI symptoms. A long-term follow-up observation in the non-GI group may help us to understand the cause and effect. If the NH changes are prior, we could use the neuroimaging marker to identify patients who may have GI symptoms in advance in the future, provide appropriate intervention to prevent more serious symptoms, and then save medical resources. On the contrary, if abnormal NH is the result of GI symptoms, it will provide a new research direction for related treatments.

## CONCLUSION

Major depressive disorder with GI symptoms shows more severe depressive symptoms than MDD without GI symptoms. Distinctive NH patterns in DMN exist in MDD with GI symptoms that can be applied as a potential brain imaging marker to discriminate MDD with GI symptoms from those without GI symptoms.

## DATA AVAILABILITY STATEMENT

The raw data supporting the conclusions of this article will be made available by the authors, without undue reservation.

## ETHICS STATEMENT

The studies involving human participants were reviewed and approved by the Medical Research Ethics Committee of the Second Xiangya Hospital of Central South University, China. The patients/participants provided their written informed consent to participate in this study.

## AUTHOR CONTRIBUTIONS

MY, HL, and WG contributed to the conception and design of the study. HL, JC, and JZ supervised the progress of the study. MY, FL, and WG performed the data analysis. MY wrote the manuscript. All authors contributed to manuscript revision, read, and approved it for publication.

## FUNDING

This study was supported by grants from the National Natural Science Foundation of China (Grant Nos. 82171508 and 81771447), Natural Science Foundation of Hunan (Grant No. 2020JJ4784), Science and Technology Program of Hunan Province (Grant No. 2020SK53413), Key-Area Research and Development Program of Guangdong Province (Grant No. 2018B030334001), and Natural Science Foundation of Tianjin (Grant No. 18JCQNJC10900).

## ACKNOWLEDGMENTS

We thank all the participants who served as research participants.

## REFERENCES

Apkarian, V. A., Hashmi, J. A., and Baliki, M. N. (2011). Pain and the brain: specificity and plasticity of the brain in clinical chronic pain. *Pain* 152(3 Suppl.), S49–S64. doi: 10.1016/j.pain.2010.11.010

Bekhuis, E., Boschloo, L., Rosmalen, J. G., de Boer, M. K., and Schoevers, R. A. (2016). The impact of somatic symptoms on the course of major depressive disorder. *J. Affect. Disord.* 205, 112–118. doi: 10.1016/j.jad.2016.06.030

Bell-McGinty, S., Butters, M. A., Meltzer, C. C., Greer, P. J., Reynolds, C. F. III, and Becker, J. T. (2002). Brain morphometric abnormalities in geriatric depression: long-term neurobiological effects of illness duration. *Am. J. Psychiatry* 159, 1424–1427.

Blankstein, U., Chen, J., Diamant, N. E., and Davis, K. D. (2010). Altered brain structure in irritable bowel syndrome: potential contributions of pre-existing and disease-driven factors. *Gastroenterology* 138, 1783–1789. doi: 10.1053/j.gastro.2009.12.043

Bluhm, R., Williamson, P., Lanius, R., Théberge, J., Densmore, M., Bartha, R., et al. (2009). Resting state default-mode network connectivity in early depression using a seed region-of-interest analysis: decreased connectivity with caudate nucleus. *Psychiatry Clin. Neurosci.* 63, 754–761. doi: 10.1111/j.1440-1819.2009.02030.x

Bozhilova, N. S., Michelini, G., Kuntsi, J., and Asherson, P. (2018). Mind wandering perspective on attention-deficit/hyperactivity disorder. *Neurosci. Biobehav. Rev.* 92, 464–476. doi: 10.1016/j.neubiorev.2018.07.010

Cavanna, A. E. (2007). The precuneus and consciousness. *CNS Spectr.* 12, 545–552. doi: 10.1017/s1092852900021295

Cavanna, A. E., and Trimble, M. R. (2006). The precuneus: a review of its functional anatomy and behavioural correlates. *Brain* 129(Pt 3), 564–583. doi: 10.1093/brain/awl004

Chao-Gan, Y., and Yu-Feng, Z. (2010). DPARSF: a MATLAB toolbox for "Pipeline" data analysis of resting-state fMRI. *Front. Syst. Neurosci.* 4:13. doi: 10.3389/fnsys.2010.00013

Chen, J. D., Liu, F., Xun, G. L., Chen, H. F., Hu, M. R., Guo, X. F., et al. (2012). Early and late onset, first-episode, treatment-naive depression: same clinical symptoms, different regional neural activities. *J. Affect. Disord.* 143, 56–63. doi: 10.1016/j.jad.2012.05.025

Chen, Y., Wang, C., Zhu, X., Tan, Y., and Zhong, Y. (2015). Aberrant connectivity within the default mode network in first-episode, treatment-naive major depressive disorder. *J. Affect. Disord.* 183, 49–56. doi: 10.1016/j.jad.2015.04.052

Corbetta, M., and Shulman, G. L. (2002). Control of goal-directed and stimulus-driven attention in the brain. *Nat. Rev. Neurosci.* 3, 201–215. doi: 10.1038/nrn755

Cui, X., Guo, W., Wang, Y., Yang, T. X., Yang, X. H., Wang, Y., et al. (2017). Aberrant default mode network homogeneity in patients with first-episode treatment-naive melancholic depression. *Int. J. Psychophysiol.* 112, 46–51. doi: 10.1016/j.ijpsycho.2016.12.005

Depping, M. S., Wolf, N. D., Vasic, N., Sambataro, F., Hirjak, D., Thomann, P. A., et al. (2016). Abnormal cerebellar volume in acute and remitted major depression. *Prog. Neuropsychopharmacol. Biol. Psychiatry* 71, 97–102. doi: 10.1016/j.pnpbp.2016.06.005

Drossman, D. A., Creed, F. H., Olden, K. W., Svedlund, J., Toner, B. B., and Whitehead, W. E. (1999). Psychosocial aspects of the functional gastrointestinal disorders. *Gut* 45(Suppl. 2), Ii25–Ii30. doi: 10.1136/gut.45.2008.ii25

Du, Y., Pearlson, G. D., Liu, J., Sui, J., Yu, Q., He, H., et al. (2015). A group ICA based framework for evaluating resting fMRI markers when disease categories are unclear: application to schizophrenia, bipolar, and schizoaffective disorders. *Neuroimage* 122, 272–280. doi: 10.1016/j.neuroimage.2015.07.054

Fan, F., Tan, S., Huang, J., Chen, S., Fan, H., Wang, Z., et al. (2020). Functional disconnection between subsystems of the default mode network in schizophrenia. *Psychol. Med.* [Epub ahead of print]. doi: 10.1017/s003329172000416x

Fan, W., Zhang, S., Hu, J., Liu, B., Wen, L., Gong, M., et al. (2019). Aberrant brain function in active-stage ulcerative colitis patients: a resting-state functional MRI study. *Front. Hum. Neurosci.* 13:107. doi: 10.3389/fnhum.2019.00107

Fang, J., Rong, P., Hong, Y., Fan, Y., Liu, J., Wang, H., et al. (2016). Transcutaneous vagus nerve stimulation modulates default mode network in major depressive disorder. *Biol. Psychiatry* 79, 266–273. doi: 10.1016/j.biopsych.2015.03.025

Farmer, M. A., Baliki, M. N., and Apkarian, A. V. (2012). A dynamic network perspective of chronic pain. *Neurosci. Lett.* 520, 197–203. doi: 10.1016/j.neulet.2012.05.001

Fond, G., Loundou, A., Hamdani, N., Boukouaci, W., Dargel, A., Oliveira, J., et al. (2014). Anxiety and depression comorbidities in irritable bowel syndrome (IBS): a systematic review and meta-analysis. *Eur. Arch. Psychiatry Clin. Neurosci.* 264, 651–660. doi: 10.1007/s00406-014-0502-z

Foster, J. A., and McVey Neufeld, K. A. (2013). Gut-brain axis: how the microbiome influences anxiety and depression. *Trends Neurosci.* 36, 305–312. doi: 10.1016/j.tins.2013.01.005

García-Campayo, J., Ayuso-Mateos, J. L., Caballero, L., Romera, I., Aragonés, E., Rodríguez-Artalejo, F., et al. (2008). Relationship of somatic symptoms with depression severity, quality of life, and health resources utilization in patients with major depressive disorder seeking primary health care in Spain. *Prim. Care Companion J. Clin. Psychiatry* 10, 355–362. doi: 10.4088/pcc.v10n0502

Geng, J., Yan, R., Shi, J., Chen, Y., Mo, Z., Shao, J., et al. (2019). Altered regional homogeneity in patients with somatic depression: a resting-state fMRI study. *J. Affect. Disord.* 246, 498–505. doi: 10.1016/j.jad.2018.12.066

Gong, Q., Wu, Q., Scarpazza, C., Lui, S., Jia, Z., Marquand, A., et al. (2011). Prognostic prediction of therapeutic response in depression using high-field MR imaging. *Neuroimage* 55, 1497–1503. doi: 10.1016/j.neuroimage.2010.11.079

Greenberg, P. E., Fournier, A. A., Sisitsky, T., Pike, C. T., and Kessler, R. C. (2015). The economic burden of adults with major depressive disorder in the United States (2005 and 2010). *J. Clin. Psychiatry* 76, 155–162. doi: 10.4088/JCP.14m09298

Guo, W., Cui, X., Liu, F., Chen, J., Xie, G., Wu, R., et al. (2018a). Decreased interhemispheric coordination in the posterior default-mode network and visual regions as trait alterations in first-episode, drug-naive major depressive disorder. *Brain Imaging Behav.* 12, 1251–1258. doi: 10.1007/s11682-017-9794-8

Guo, W., Cui, X., Liu, F., Chen, J., Xie, G., Wu, R., et al. (2018b). Increased anterior default-mode network homogeneity in first-episode, drug-naive major

depressive disorder: a replication study. *J. Affect. Disord.* 225, 767–772. doi: 10.1016/j.jad.2017.08.089

Guo, W., Liu, F., Xue, Z., Gao, K., Liu, Z., Xiao, C., et al. (2013b). Abnormal resting-state cerebellar-cerebral functional connectivity in treatment-resistant depression and treatment sensitive depression. *Prog. Neuropsychopharmacol. Biol. Psychiatry* 44, 51–57. doi: 10.1016/j.pnpbp.2013.01.010

Guo, W., Liu, F., Dai, Y., Jiang, M., Zhang, J., Yu, L., et al. (2013a). Decreased interhemispheric resting-state functional connectivity in first-episode, drug-naive major depressive disorder. *Prog. Neuropsychopharmacol. Biol. Psychiatry* 41, 24–29. doi: 10.1016/j.pnpbp.2012.11.003

Guo, W., Liu, F., Zhang, Z., Liu, G., Liu, J., Yu, L., et al. (2015b). Increased cerebellar functional connectivity with the default-mode network in unaffected siblings of schizophrenia patients at rest. *Schizophr. Bull.* 41, 1317–1325. doi: 10.1093/schbul/sbv062

Guo, W., Liu, F., Liu, J., Yu, M., Zhang, Z., Liu, G., et al. (2015a). Increased cerebellar-default-mode-network connectivity in drug-naive major depressive disorder at rest. *Medicine* 94:e560. doi: 10.1097/md.0000000000000560

Guo, W., Yao, D., Jiang, J., Su, Q., Zhang, Z., Zhang, J., et al. (2014). Abnormal default-mode network homogeneity in first-episode, drug-naive schizophrenia at rest. *Prog. Neuropsychopharmacol. Biol. Psychiatry* 49, 16–20. doi: 10.1016/j.pnpbp.2013.10.021

Hahamy, A., Calhoun, V., Pearlson, G., Harel, M., Stern, N., Attar, F., et al. (2014). Save the global: global signal connectivity as a tool for studying clinical populations with functional magnetic resonance imaging. *Brain Connect.* 4, 395–403. doi: 10.1089/brain.2014.0244

Hamilton, M. (1967). Development of a rating scale for primary depressive illness. *Br. J. Soc. Clin. Psychol.* 6, 278–296. doi: 10.1111/j.2044-8260.1967.tb00530.x

Hare, S. M., Ford, J. M., Mathalon, D. H., Damaraju, E., Bustillo, J., Belger, A., et al. (2019). Salience-default mode functional network connectivity linked to positive and negative symptoms of schizophrenia. *Schizophr. Bull.* 45, 892–901. doi: 10.1093/schbul/sby112

Hillilä, M. T., Hämäläinen, J., Heikkinen, M. E., and Färkkilä, M. A. (2008). Gastrointestinal complaints among subjects with depressive symptoms in the general population. *Aliment. Pharmacol. Ther.* 28, 648–654. doi: 10.1111/j.1365-2036.2008.03771.x

Hu, M. L., Zong, X. F., Mann, J. J., Zheng, J. J., Liao, Y. H., Li, Z. C., et al. (2017). A review of the functional and anatomical default mode network in schizophrenia. *Neurosci. Bull.* 33, 73–84. doi: 10.1007/s12264-016-0090-1

Hyett, M. P., Perry, A., Breakspear, M., Wen, W., and Parker, G. B. (2018). White matter alterations in the internal capsule and psychomotor impairment in melancholic depression. *PLoS One* 13:e0195672. doi: 10.1371/journal.pone.0195672

Kano, M., Dupont, P., Aziz, Q., and Fukudo, S. (2018). Understanding neurogastroenterology from neuroimaging perspective: a comprehensive review of functional and structural brain imaging in functional gastrointestinal disorders. *J. Neurogastroenterol. Motil.* 24, 512–527. doi: 10.5056/jnm18072

Kim, S. M., Hong, J. S., Min, K. J., and Han, D. H. (2019). Brain functional connectivity in patients with somatic symptom disorder. *Psychosom. Med.* 81, 313–318. doi: 10.1097/psy.0000000000000681

King, A. P., Block, S. R., Sripada, R. K., Rauch, S., Giardino, N., Favorite, T., et al. (2016). ALTERED DEFAULT MODE NETWORK (DMN) RESTING STATE FUNCTIONAL CONNECTIVITY FOLLOWING A MINDFULNESS-BASED EXPOSURE THERAPY FOR POSTTRAUMATIC STRESS DISORDER (PTSD) IN COMBAT VETERANS OF AFGHANISTAN AND IRAQ. *Depress. Anxiety* 33, 289–299. doi: 10.1002/da.22481

Kirmayer, L. J., Robbins, J. M., Dworkind, M., and Yaffe, M. J. (1993). Somatization and the recognition of depression and anxiety in primary care. *Am. J. Psychiatry* 150, 734–741. doi: 10.1176/ajp.150.5.734

Kochar, B., Barnes, E. L., Long, M. D., Cushing, K. C., Galanko, J., Martin, C. F., et al. (2018). Depression is associated with more aggressive inflammatory bowel disease. *Am. J. Gastroenterol.* 113, 80–85. doi: 10.1038/ajg.2017.423

Kwan, C. L., Diamant, N. E., Pope, G., Mikula, K., Mikulis, D. J., and Davis, K. D. (2005). Abnormal forebrain activity in functional bowel disorder patients with chronic pain. *Neurology* 65, 1268–1277. doi: 10.1212/01.wnl.0000180971.95473.cc

Lee, C., Doo, E., Choi, J. M., Jang, S. H., Ryu, H. S., Lee, J. Y., et al. (2017). The increased level of depression and anxiety in irritable bowel syndrome patients compared with healthy controls: systematic review and meta-analysis. *J. Neurogastroenterol. Motil.* 23, 349–362. doi: 10.5056/jnm16220

Liu, P., Li, G., Zhang, A., Yang, C., Liu, Z., Sun, N., et al. (2020). Brain structural and functional alterations in MDD patient with gastrointestinal symptoms: a resting-state MRI study. *J. Affect. Disord.* 273, 95–105. doi: 10.1016/j.jad.2020.03.107

Ma, C., Ding, J., Li, J., Guo, W., Long, Z., Liu, F., et al. (2012). Resting-state functional connectivity bias of middle temporal gyrus and caudate with altered gray matter volume in major depression. *PLoS One* 7:e45263. doi: 10.1371/journal.pone.0045263

Malhi, G. S., and Mann, J. J. (2018). Depression. *Lancet* 392, 2299–2312. doi: 10.1016/s0140-6736(18)31948-2

Martin-Subero, M., Fuentes-Claramonte, P., Salgado-Pineda, P., Salavert, J., Arevalo, A., Bosque, C., et al. (2021). Autobiographical memory and default mode network function in schizophrenia: an fMRI study. *Psychol. Med.* 51, 121–128. doi: 10.1017/s0033291719003052

Mayer, E. A., Tillisch, K., and Gupta, A. (2015). Gut/brain axis and the microbiota. *J. Clin. Invest.* 125, 926–938. doi: 10.1172/jci76304

Miller, D. R., Hayes, S. M., Hayes, J. P., Spielberg, J. M., Lafleche, G., and Verfaellie, M. (2017). Default mode network subsystems are differentially disrupted in posttraumatic stress disorder. *Biol. Psychiatry Cogn. Neurosci. Neuroimaging* 2, 363–371. doi: 10.1016/j.bpsc.2016.12.006

Navabi, S., Gorrepati, V. S., Yadav, S., Chintanaboina, J., Maher, S., Demuth, P., et al. (2018). Influences and impact of anxiety and depression in the setting of inflammatory bowel disease. *Inflamm. Bowel Dis.* 24, 2303–2308. doi: 10.1093/ibd/izy143

Novick, D., Montgomery, W., Aguado, J., Kadziola, Z., Peng, X., Brugnoli, R., et al. (2013). Which somatic symptoms are associated with an unfavorable course in Asian patients with major depressive disorder? *J. Affect. Disord.* 149, 182–188. doi: 10.1016/j.jad.2013.01.020

Painchault, C., Brignone, M., Lamy, F. X., Diamand, F., and Saragoussi, D. (2014). Economic Burden of Major Depressive Disorder (Mdd) in five european countries: description of resource use by health state. *Value Health* 17:A465. doi: 10.1016/j.jval.2014.08.1300

Peng, J., Liu, J., Nie, B., Li, Y., Shan, B., Wang, G., et al. (2011). Cerebral and cerebellar gray matter reduction in first-episode patients with major depressive disorder: a voxel-based morphometry study. *Eur. J. Radiol.* 80, 395–399. doi: 10.1016/j.ejrad.2010.04.006

Posner, J., Cha, J., Wang, Z., Talati, A., Warner, V., Gerber, A., et al. (2016). Increased default mode network connectivity in individuals at high familial risk for depression. *Neuropsychopharmacology* 41, 1759–1767. doi: 10.1038/npp.2015.342

Power, J. D., Barnes, K. A., Snyder, A. Z., Schlaggar, B. L., and Petersen, S. E. (2012). Spurious but systematic correlations in functional connectivity MRI networks arise from subject motion. *Neuroimage* 59, 2142–2154. doi: 10.1016/j.neuroimage.2011.10.018

Qi, R., Ke, J., Schoepf, U. J., Varga-Szemes, A., Milliken, C. M., Liu, C., et al. (2016). Topological reorganization of the default mode network in irritable bowel syndrome. *Mol. Neurobiol.* 53, 6585–6593. doi: 10.1007/s12035-015-9558-7

Raichle, M. E. (2015). The brain's default mode network. *Annu. Rev. Neurosci.* 38, 433–447. doi: 10.1146/annurev-neuro-071013-014030

Sani, I., Stemmann, H., Caron, B., Bullock, D., Stemmler, T., Fahle, M., et al. (2021). The human endogenous attentional control network includes a ventro-temporal cortical node. *Nat. Commun.* 12:360. doi: 10.1038/s41467-020-20583-5

Scott, K. M., Bruffaerts, R., Tsang, A., Ormel, J., Alonso, J., Angermeyer, M. C., et al. (2007). Depression-anxiety relationships with chronic physical conditions: results from the World Mental Health Surveys. *J. Affect. Disord.* 103, 113–120. doi: 10.1016/j.jad.2007.01.015

Shan, X., Liao, R., Ou, Y., Ding, Y., Liu, F., Chen, J., et al. (2020). Metacognitive training modulates default-mode network homogeneity during 8-week olanzapine treatment in patients with schizophrenia. *Front. Psychiatry* 11:234. doi: 10.3389/fpsyt.2020.00234

Sheline, Y. I., Price, J. L., Yan, Z., and Mintun, M. A. (2010). Resting-state functional MRI in depression unmasks increased connectivity between networks via the dorsal nexus. *Proc. Natl. Acad. Sci. U.S.A.* 107, 11020–11025. doi: 10.1073/pnas.1000446107

Shi, Y., Li, J., Feng, Z., Xie, H., Duan, J., Chen, F., et al. (2020). Abnormal functional connectivity strength in first-episode, drug-naive adult patients with major depressive disorder. *Prog. Neuropsychopharmacol. Biol. Psychiatry* 97:109759. doi: 10.1016/j.pnpbp.2019.109759

Sidlauskaite, J., Sonuga-Barke, E., Roeyers, H., and Wiersema, J. R. (2016). Default mode network abnormalities during state switching in attention deficit hyperactivity disorder. *Psychol. Med.* 46, 519–528. doi: 10.1017/s0033291715002019

Skrobisz, K., Piotrowicz, G., Naumczyk, P., Sabisz, A., Markiet, K., Rydzewska, G., et al. (2020). Imaging of morphological background in selected functional and inflammatory gastrointestinal diseases in fMRI. *Front. Psychiatry* 11:461. doi: 10.3389/fpsyt.2020.00461

Smith, K. (2014). Mental health: a world of depression. *Nature* 515:181. doi: 10.1038/515180a

Song, G. H., Venkatraman, V., Ho, K. Y., Chee, M. W., Yeoh, K. G., and Wilder-Smith, C. H. (2006). Cortical effects of anticipation and endogenous modulation of visceral pain assessed by functional brain MRI in irritable bowel syndrome patients and healthy controls. *Pain* 126, 79–90. doi: 10.1016/j.pain.2006.06.017

Steardo, L. Jr., Carbone, E. A., de Filippis, R., Pisanu, C., Segura-Garcia, C., Squassina, A., et al. (2020). Application of support vector machine on fMRI data as biomarkers in schizophrenia diagnosis: a systematic review. *Front. Psychiatry* 11:588. doi: 10.3389/fpsyt.2020.00588

Swets, J. A. (1988). Measuring the accuracy of diagnostic systems. *Science* 240, 1285–1293. doi: 10.1126/science.3287615

Verster, G. C., and Gagiano, C. A. (1995). [Masked depression]. *S. Afr. Med. J.* 85, 759–762.

Viard, A., Mutlu, J., Chanraud, S., Guenolé, F., Egler, P. J., Gérardin, P., et al. (2019). Altered default mode network connectivity in adolescents with post-traumatic stress disorder. *Neuroimage Clin.* 22:101731. doi: 10.1016/j.nicl.2019.101731

Whitehead, W. E. (1996). Psychosocial aspects of functional gastrointestinal disorders. *Gastroenterol. Clin. North Am.* 25, 21–34. doi: 10.1016/s0889-8553(05)70363-0

Yan, C. G., Chen, X., Li, L., Castellanos, F. X., Bai, T. J., Bo, Q. J., et al. (2019). Reduced default mode network functional connectivity in patients with recurrent major depressive disorder. *Proc. Natl. Acad. Sci. U.S.A.* 116, 9078–9083. doi: 10.1073/pnas.1900390116

Zhi, D., Calhoun, V. D., Lv, L., Ma, X., Ke, Q., Fu, Z., et al. (2018). Aberrant dynamic functional network connectivity and graph properties in major depressive disorder. *Front. Psychiatry* 9:339. doi: 10.3389/fpsyt.2018.00339

Zhou, H. X., Chen, X., Shen, Y. Q., Li, L., Chen, N. X., Zhu, Z. C., et al. (2020). Rumination and the default mode network: meta-analysis of brain imaging studies and implications for depression. *Neuroimage* 206:116287. doi: 10.1016/j.neuroimage.2019.116287

**Conflict of Interest:** The authors declare that the research was conducted in the absence of any commercial or financial relationships that could be construed as a potential conflict of interest.

**Publisher's Note:** All claims expressed in this article are solely those of the authors and do not necessarily represent those of their affiliated organizations, or those of the publisher, the editors and the reviewers. Any product that may be evaluated in this article, or claim that may be made by its manufacturer, is not guaranteed or endorsed by the publisher.

frontiers | Frontiers in Aging Neuroscience

ORIGINAL RESEARCH
published: 22 April 2022
doi: 10.3389/fnagi.2022.872867

# Advanced Brain-Age in Psychotic Psychopathology: Evidence for Transdiagnostic Neurodevelopmental Origins

*Caroline Demro[1,2], Chen Shen[2], Timothy J. Hendrickson[3], Jessica L. Arend[1,2], Seth G. Disner[1,4] and Scott R. Sponheim[1,2,4]**

[1] Department of Psychiatry and Behavioral Sciences, University of Minnesota, Minneapolis, MN, United States, [2] Department of Psychology, University of Minnesota, Minneapolis, MN, United States, [3] Informatics Institute, University of Minnesota, Minneapolis, MN, United States, [4] Minneapolis Veterans Affairs Health Care System, Minneapolis, MN, United States

OPEN ACCESS

**Edited by:**
*Wenjing Zhang,*
*Sichuan University, China*

**Reviewed by:**
*Yann Quidé,*
*University of New South Wales, Australia*
*Anna S. Huang,*
*Vanderbilt University Medical Center, United States*

***Correspondence:**
*Scott R. Sponheim*
*sponh001@umn.edu*

**Specialty section:**
*This article was submitted to Neurocognitive Aging and Behavior, a section of the journal Frontiers in Aging Neuroscience*

**Received:** *10 February 2022*
**Accepted:** *11 March 2022*
**Published:** *22 April 2022*

**Citation:**
*Demro C, Shen C, Hendrickson TJ, Arend JL, Disner SG and Sponheim SR (2022) Advanced Brain-Age in Psychotic Psychopathology: Evidence for Transdiagnostic Neurodevelopmental Origins. Front. Aging Neurosci. 14:872867. doi: 10.3389/fnagi.2022.872867*

Schizophrenia is characterized by abnormal brain structure such as global reductions in gray matter volume. Machine learning models trained to estimate the age of brains from structural neuroimaging data consistently show advanced brain-age to be associated with schizophrenia. Yet, it is unclear whether advanced brain-age is specific to schizophrenia compared to other psychotic disorders, and whether evidence that brain structure is "older" than chronological age actually reflects neurodevelopmental rather than atrophic processes. It is also unknown whether advanced brain-age is associated with genetic liability for psychosis carried by biological relatives of people with schizophrenia. We used the Brain-Age Regression Analysis and Computation Utility Software (BARACUS) prediction model and calculated the residualized brain-age gap of 332 adults (163 individuals with psychotic disorders: 105 schizophrenia, 17 schizoaffective disorder, 41 bipolar I disorder with psychotic features; 103 first-degree biological relatives; 66 controls). The model estimated advanced brain-ages for people with psychosis in comparison to controls and relatives, with no differences among psychotic disorders or between relatives and controls. Specifically, the model revealed an enlarged brain-age gap for schizophrenia and bipolar disorder with psychotic features. Advanced brain-age was associated with lower cognitive and general functioning in the full sample. Among relatives, cognitive performance and schizotypal symptoms were related to brain-age gap, suggesting that advanced brain-age is associated with the subtle expressions associated with psychosis. Exploratory longitudinal analyses suggested that brain aging was not accelerated in individuals with a psychotic disorder. In sum, we found that people with psychotic disorders, irrespective of specific diagnosis or illness severity, show indications of non-progressive, advanced brain-age. These findings support a transdiagnostic, neurodevelopmental formulation of structural brain abnormalities in psychotic psychopathology.

**Keywords: brain-age, schizophrenia, bipolar, psychosis, advanced aging, neurodevelopment**

## INTRODUCTION

Schizophrenia is a debilitating mental disorder, characterized by psychotic symptoms and cognitive impairments, and individuals with the illness often have difficulties functioning in social and community settings. Crucially, it is unclear whether the neuropathology underlying the syndrome is neurodevelopmental or neurodegenerative in nature (Walker et al., 2010; Kochunov and Hong, 2014). Evidence for aberrant neurodevelopment in schizophrenia includes increased rates of adverse events during pregnancy and birth that lead to abnormal prenatal brain development, early signs of cognitive and behavioral abnormalities during childhood, and brain structural abnormalities that are evident during adolescence, either prior to illness onset or early in the course of the illness (Lewis and Levitt, 2002: Rapoport et al., 2005). Nevertheless, schizophrenia, which was originally described as *dementia praecox* [premature dementia; Kraepelin et al. (1971)], has recently been hypothesized to be associated with accelerated cell aging such that normal age-related physiological changes occur at an earlier age. The premature aging hypothesis is supported by evidence of increased rates of cardiovascular and metabolic syndromes (Hennekens et al., 2005; von Hausswolff-Juhlin et al., 2009) and lower cognitive performance in schizophrenia that is similar to older healthy controls (Kirkpatrick et al., 2008).

In the current investigation, we examined whether abnormalities in brain structure associated with schizophrenia are consistent with a pattern of atypical neurodevelopment or premature aging, whether such abnormalities extend beyond schizophrenia to other disorders with psychotic symptoms, and if increased genetic liability for psychotic psychopathology is associated with aberrant brain structure. Because structural brain abnormalities in schizophrenia are widespread and diverse, we used a recently developed brain-age algorithm to quantify and summarize the degree of overall deviation in brain morphology. We further investigated how such deviation is related to symptomatology and cognitive impairments that are central to the disorder.

A neurodevelopmental pattern of abnormalities—where the brain fails to achieve a normative state—is consistent with global structural brain abnormalities that appear early in the course of schizophrenia and are highly heritable (Keshavan et al., 2008). For example, whole brain and total gray matter volumes are reduced in schizophrenia compared to what is seen in typical development (Daniel et al., 1991; Ward et al., 1996; Wright et al., 2000; Shenton et al., 2001; Steen et al., 2006; Gupta et al., 2015; Van Erp et al., 2018). Meta-analyses of first-episode psychosis studies (Steen et al., 2006; Vita et al., 2006) have provided evidence of smaller whole brain and hippocampal volumes as well as larger ventricular spaces in comparison to controls. Also, gray matter perturbations in the absence of medication effects are evident early in the course of the illness (Cahn et al., 2002; Hietala et al., 2003; Szeszko et al., 2003).

To characterize advanced aging of the brain, researchers have developed machine learning tools to quantify the aggregate impact of gray matter loss in a variety of health conditions. One commonly used model estimates a person's age based on T1-weighted structural imaging data (Franke et al., 2010; Liem et al., 2017). The difference between the model-estimated age and chronological age is the estimated brain-age gap.[1] The brain-age gap gives an estimate of gray matter abnormalities throughout the brain. Brain-age models generally produce brain-age estimates for people with schizophrenia that are older than true chronological age, by about 2.5–8 years (Koutsouleris et al., 2014; Schnack et al., 2016; Nenadić et al., 2017; Shahab et al., 2019; Truelove-Hill et al., 2020; Constantinides et al., 2022). This pattern extends to early phases of illness, including first-episode psychosis (Kolenic et al., 2018; Hajek et al., 2019), schizophreniform and psychotic disorder not otherwise specified (Shahab et al., 2019), and clinical high risk (Chung et al., 2018) or ultra-high risk (Iftimovici et al., 2020) for psychosis. Despite evidence that abnormalities in brain morphology occur prior to the development of psychosis, the gap between model-estimated and chronological age widens with illness duration such that chronic schizophrenia has the largest gap, followed by recent-onset schizophrenia, and then ultra-high risk for psychosis (Koutsouleris et al., 2014), which could reflect a neurodegenerative process. Importantly, longitudinal data suggest that the brain-age gap may progressively increase over time in schizophrenia (Schnack et al., 2016). Thus, research to date has generated evidence for both neurodevelopmental and neurodegenerative processes in schizophrenia.

Regardless of the origins of aberrant brain morphology in schizophrenia, detection of advanced brain aging may have clinical utility. A large brain-age gap in combination with an early onset of clinical high risk symptoms may predict an insidious onset of psychosis (Chung et al., 2019a,b). Such information could be used in a risk calculator, and possibly be clinically useful in connecting those individuals at highest risk of developing a severe and persistent mental illness with appropriate treatments. However, a critical test for a clinical detection tool is whether it differentiates between individuals who develop psychotic psychopathology from those who do not. Contrasting brain-age of affected and unaffected individuals in a family is one way to appraise the potential for using an index to predict development of the disorder. Before any clinical implementation, however, more research is needed to replicate previous findings, explore diagnostic specificity, and test generalizability to a wider population, as well as understand the influence of confounds (e.g., obesity) to the link between brain-age gap and psychotic illness (Nenadić et al., 2017; Andreou and Borgwardt, 2020).

Whether advanced brain-age is specific to schizophrenia among mental disorders is unclear. There is some evidence for specificity to schizophrenia based on lack of abnormally large age gaps among mixed samples of bipolar disorder with and without psychosis (Nenadić et al., 2017; Shahab et al., 2019), offspring of people with bipolar disorder (Hajek et al., 2019), and non-psychotic major depressive disorder

[1]Brain-age gap here is the same construct as Brain Age Gap Estimate (BrainAGE), as it is sometimes referred to in this literature.

[Besteher et al., 2019; although, see Han et al. (2021)]. However, there is some evidence of larger age gaps among major depressive disorder and borderline personality disorder in comparison to controls, though these gaps are attenuated in comparison to that of the schizophrenia group (Koutsouleris et al., 2014). Structural brain abnormalities such as ventricular enlargement which underlie advanced brain-age estimation do not seem to be specific to schizophrenia, but extend to other psychotic disorders such as psychotic bipolar disorder (Strasser et al., 2005; Keshavan et al., 2008). Further, when comparing bipolar disorder participants with and without a history of psychosis, no difference in brain-age gap was found (Shahab et al., 2019). Based on this previous work, advanced brain-age is most evident in schizophrenia among psychiatric illnesses, but is present to a lesser degree in other mental health conditions; however, few studies to date have specifically compared schizophrenia with other psychotic disorders, including bipolar disorder with psychotic features and schizoaffective disorder. Therefore, it is unknown whether a larger brain-age gap is more generally evident in psychotic psychopathology rather than specific to the diagnostic category of schizophrenia.

In the current study, we examined whether schizophrenia and other psychotic disorders are associated with an advanced brain-age gap. Additionally, we tested the degree to which biological relatives demonstrate brain-age gaps similar to their family members who exhibit psychotic psychopathology. We hypothesized that people with schizophrenia would demonstrate the most advanced brain-age followed by other psychotic disorders and then relatives, who were expected to show attenuated abnormality to people with psychotic disorders (PwP). We also investigated the relationship of brain-age gap with cognitive impairment, functioning, and symptom severity. In order to examine whether brain-age gap suggests neurodegeneration, we conducted exploratory analyses in a subgroup of participants with longitudinal data. Finally, we tested for group differences in gray matter volume, cortical thickness, and surface area in order to approximate specific brain regions with structural deficits that lead to an advanced brain-age gap estimated by the model.

# MATERIALS AND METHODS

## Participants

Data were collected as part of two family studies focusing on psychosis. Study 1 recruited adults aged 18–65, including people with major mental illness (schizophrenia, schizoaffective disorder, bipolar I disorder without psychotic features, and bipolar I disorder with psychotic features), their first-degree biological relatives, and unrelated healthy controls. Only patients with a history of psychotic symptoms were included in primary analyses, though a separate analysis was completed comparing participants with bipolar I disorder with and without psychotic features (see below). Study 2, the Psychosis Human Connectome Project, recruited people aged 18–65 with a psychotic disorder (schizophrenia, schizoaffective disorder, or bipolar I disorder with psychotic features), their first-degree biological relatives (aged 18–69), and unrelated healthy controls. Exclusion criteria for study 2 have been described previously (Demro et al., 2021) and match those of study 1. In total, 332 participants (48 from study 1; 284 from study 2) were included in primary analyses: 163 participants with psychosis (105 schizophrenia, 17 schizoaffective, 41 bipolar I disorder with psychotic features), 103 first-degree biological relatives (57 siblings, 35 parents, 11 offspring), and 66 controls. Of the 103 relatives, 63 were related to a person with schizophrenia, seven to a person with schizoaffective disorder, and 33 to a person with bipolar I disorder with psychotic features. Forty-two participants (nine controls, 13 relatives, 20 PwP) completed both studies (within 2 weeks–4 years; mean time between scans = 633.55 days, *SD* = 415.10 days), allowing for exploratory analyses of longitudinal data. For the primary analyses, study 2 data were used for participants who completed both studies. An additional 15 individuals with bipolar I disorder without psychosis and seven relatives of people with such a diagnosis were included in exploratory analyses. Groups were matched on basic demographic characteristics as much as possible during study enrollment. For descriptive statistics of the full sample, see **Table 1**.

## Clinical Assessment

The Structured Clinical Interview for DSM-IV-TR disorders (First et al., 2002) was used to assess clinical diagnosis and estimate Global Assessment of Functioning (GAF) for participants in both studies. The Brief Psychiatric Rating Scale [BPRS; Ventura et al. (2000)] was administered to all participants as a broad measure of psychiatric symptom severity. Participants with psychosis were additionally assessed with the Scale for the Assessment of Negative/Positive Symptoms [SANS/SAPS; Andreasen (1984, 1989)]. This measure provides an estimate of current psychotic symptom severity. The Schizotypal Personality Questionnaire [SPQ; Raine (1991)] was used to capture subtle psychosis-like traits. Similarly, to capture variation in propensity for dysregulated negative emotional states the trait domain "negative affect" of the Personality Inventory for DSM-5 (PID-5) was used in analyses (Longenecker et al., 2020). Cognitive functioning was assessed using subscales of the Wechsler Adult Intelligence Scale (WAIS; Wechsler, 2008) to yield an estimate of IQ.

## Neuroimaging Data Acquisition

Study 1 collected structural Magnetic Resonance Imaging (MRI) data using a 10-min T1-weighted MPRAGE sequence (TE = 2.12 ms, TR = 2,400 ms, flip angle = 8, resolution = 256) on a 3 Tesla Siemens Prisma scanner using a 32 channel head coil. Imaging data for study 2 were collected on a separate Siemens 3 Tesla Prisma scanner with a Siemens 32 channel head coil. An 8-min HCP T1w MPRAGE (TE = 1.81/3.6/5.39/7.18 ms, TR = 2,500 ms, flip angle = 8, resolution = 256) with volumetric navigators for real-time motion correction was performed. Both studies completed MRI scanning at the Center for Magnetic Resonance Research of the University of Minnesota.

**TABLE 1 |** Demographic and clinical characteristics.

| | Controls $n$ = 66 | Relatives $n$ = 103 | PwP $n$ = 163 | Statistic |
|---|---|---|---|---|
| Mean age in years (*SD*) | 41.16 (12.69) | 45.93$^{c}$ (14.24) | 40.18$^{c}$ (12.65) | $F_{(2,329)} = 6.26$, $p = 0.002$ |
| Female sex | 35 (53.0%) | 65$^{c}$ (63.1%) | 68$^{c}$ (41.7%) | $\chi^2_{(2,332)} = 11.75$, $p = 0.003$ |
| Racial/ethnic minority identity | 6$^{a}$ (9.1%) | 13$^{c}$ (12.6%) | 52$^{ac}$ (31.9%) | $\chi^2_{(2,332)} = 21.36$, $p < 0.001$ |
| Parent education | 5.77 (1.18) | 5.56 (1.22) | 5.39 (1.28) | $H_{(2)} = 4.44$, $p = 0.108$ |
| Participant education (years) | 16.08$^{ab}$ (2.27) | 15.10$^{bc}$ (2.30) | 13.96$^{ac}$ (2.02) | $F_{(2,329)} = 24.62$, $p < 0.001$ |
| BMI (kg/m$^2$) | 26.15$^{a}$ (5.18) | 28.39$^{c}$ (5.93) | 31.25$^{ac}$ (7.40) | $F_{(2,328)} = 15.60$, $p < 0.001$ |
| BPRS total | 27.03$^{ab}$ (3.51) | 32.41$^{bc}$ (6.84) | 44.87$^{ac}$ (12.45) | $F_{(2,329)} = 100.44$, $p < 0.001$ |
| SPQ total | 7.85$^{ab}$ (7.51) | 14.96$^{bc}$ (13.09) | 31.14$^{ac}$ (16.33) | $F_{(2,327)} = 81.12$, $p < 0.001$ |
| PID-5 negative affect | 0.89$^{a}$ (0.32) | 0.98$^{c}$ (0.37) | 1.31$^{ac}$ (0.42) | $F_{(2,320)} = 35.82$, $p < 0.001$ |
| WAIS IQ | 109.09$^{ab}$ (12.28) | 101.88$^{bc}$ (11.35) | 97.40$^{ac}$ (12.15) | $F_{(2,328)} = 22.81$, $p < 0.001$ |

*Groups that share a superscript reflect a significant ($p < 0.05$) pairwise comparison; Participant racial/ethnic identities were as follows, in order of group (controls/relatives/PwP): 90.9/87.4/68.1% White, 4.5/6.8/20.9% Black, 1.5/2.9/3.7% Latino/a, 1.5/1.0/3.1% Asian/Asian American, 0/0/0.6% Native American, 1.5/1.9/3.7% Other; Number of participants who were missing data: nine on parent education, two on SPQ and one on WAIS IQ; Parent education = highest of either parent's level of education achieved, coded on an ordinal scale: 1 = 7th grade or less, 2 = 7th–9th grade, 3 = 10th–12th grade, 4 = high school graduate/GED, 5 = partial college/vocational/technical/RN, 6 = 4 year college/university graduate, 7 = graduate degree; BMI = body mass index calculated as [weight/(height * height)] and then multiplied by 703 to convert to metric units; BPRS = Brief Psychiatric Rating Scale (minimum score = 24); SPQ = Schizotypal Personality Questionnaire; PID-5 = Personality Inventory for DSM-5; WAIS IQ = estimated from Wechsler Adult Intelligence Scale.*

## Neuroimaging Data Processing

The T1-weighted DICOM data was converted to NIfTI by following the standardized brain imaging data structure (BIDS) format (Gorgolewski et al., 2016). The BIDS-organized NifTI data was then processed through the Brain-Age Regression Analysis and Computation Utility Software [BARACUS; Liem et al. (2017)] using a containerized version of the software (Liem and Gorgolewski, 2017). The BARACUS container was downloaded locally and used to produce the BARACUS model estimate of brain-age. The BARACUS container includes all functionality and software dependencies to take raw NIFTI data, run the FreeSurfer processing, and calculate the brain-age estimate based on the BARACUS model. We used BARACUS version 1.1.2. The BARACUS framework uses previously trained machine learning based prediction models to estimate the age of a participant based on their anatomical data. To perform the prediction, BARACUS utilizes metrics from the cortical reconstruction and volumetric segmentation tool FreeSurfer v5.3.0 (Dale and Sereno, 1993; Sled et al., 1998; Dale et al., 1999; Fischl et al., 1999a,b, 2001, 2002, 2004a,b; Fischl and Dale, 2000; Rosas et al., 2002; Kuperberg et al., 2003; Salat et al., 2004; Segonne et al., 2004; Desikan et al., 2006; Han et al., 2006; Jovicich et al., 2006; Segonne et al., 2007; Reuter et al., 2010, 2012; Reuter and Fischl, 2011) such as cortical thickness, cortical surface area, and subcortical volumes. The BARACUS model was trained and implemented in a two-level approach. The first level predicted ages with a support vector regression model (SVR) (Drucker et al., 1996) from each FreeSurfer metric separately. The second level stacked all of the SVR models from the first level with a random forest (RF) model (Breiman, 2001). Previous research suggests that generating a predictive model with this two-level strategy with neuroimaging data produces prediction with smaller variability (Rahim et al., 2016). The present analysis used the previously trained BARACUS model "Liem (2016)__OCI_norm," which was trained on 1,166 participants (566F/600M, age: $\mu = 59.1$, $\sigma = 15.2$, range = 20–80) with no objective cognitive impairment (OCI), because it most closely matched the demographics of our sample.

## Brain-Age Gap Estimate

The brain-age gap estimate is the difference between a person's chronological age and their model-estimated age. The model-estimated age was calculated using the publicly available BARACUS model. We used a corrected version of brain-age gap [see Smith et al. (2019)] because chronological age correlates with brain-age gap, leading to overestimation of age in younger people and underestimation in older people due to regression to the mean (Le et al., 2018). In order to correct for this, we computed the age gap by subtracting chronological age from the model-estimated age. We then fit a regression line to our data, predicting the age gap from chronological age and saving the unstandardized residuals. The residual values were then used for subsequent analyses and are hereafter referred to as brain-age gap estimates.[2]

## Statistical Analysis

Data analyses were completed using SPSS version 25 and R version 4.1.1. We conducted multilevel modeling to examine whether participants were nested due to family relatedness. We then used multilevel modeling to assess group differences in brain-age gap, accounting for family relatedness. Scanner type was used as a covariate in analyses to control for possible effects related to each study using a different MRI scanner. Additional covariates included race, sex, and BMI, as groups differed on these variables and previous studies, as well as our own analyses, suggest that these variables are associated with brain-age gap (Nenadić et al., 2017; Kolenic et al., 2018). We first tested for a main effect of group on brain-age gap by comparing healthy controls, relatives, and PwP.

[2]This type of corrected brain-age gap estimate is sometimes referred to as "BrainAGER" (Brain Age Gap Estimate Residualized) scores in the literature.

We then split the group of PwP into subgroups reflecting clinical diagnosis (schizophrenia, schizoaffective disorder, bipolar disorder with psychotic features). We conducted multilevel modeling (controlling for scanner, race, sex, and BMI) to assess the relation between brain-age gap and various clinical and cognitive measures, using False Discovery Rate (FDR) to correct for multiple comparisons.

In terms of exploratory analyses, we used linear regression to examine relations between brain-age gap and clinical and cognitive measures among subgroups of participants, controlling for scanner, race, sex, and BMI. We used mixed analysis of variance (ANOVA) to examine group differences in brain-age gap over time for a subset of participants who completed both study 1 and study 2. Using a subset of participants from study 1 that are not included in primary analyses, we conducted an analysis of covariance (ANCOVA; controlling for sex, race, and BMI) to test for group differences between 15 individuals with bipolar I disorder without psychosis, seven relatives of people with such a diagnosis, and the other groups previously described. Finally, we used ANCOVA to test for group differences in cortical thickness, cortical surface area, and subcortical volume. We entered cortical thickness, cortical surface area, and subcortical volume measures for all regions as dependent variables, group status (control, relative, PwP) as the independent variable, and sex, age, scanner, and estimated total intra-cranial volume as covariates. We corrected for multiple comparisons using FDR.

## RESULTS

Demographic and clinical characteristics of the sample are provided in **Table 1**. Groups differed in terms of age, sex, and race (see **Table 1**) largely due to relatives who were older, more female, and more White than PwP. Controls and PwP had similar demographic characteristics (i.e., no differences with the exception of race) and there were no group-by-age [$F_{(70,210)} = 1.26$, $p = 0.109$], group-by-sex [$F_{(2,326)} = 0.43$, $p = 0.653$] or group-by-race [$F_{(8,316)} = 0.62$, $p = 0.760$] interactions in predicting brain-age gap. As in previous studies, obesity [defined as BMI > 30 kg/m$^2$; Weir and Jan (2021)] was associated with more advanced brain-age [$F_{(1,330)} = 7.23$, $p = 0.008$] but there was no group-by-obesity status interaction in predicting brain-age gap [$F_{(2,326)} = 1.96$, $p = 0.143$]. Even though only 50 of the 163 PwP were related to one or more relatives in the study, and families in our sample were small (the modal PwP-relative family contained one relative), results of multilevel modeling suggest that brain-age gap data were nested within families. Primary analyses were conducted with the following covariates: sex, race, BMI, family relatedness, and scanner.

We tested our hypothesis that people with psychotic disorders (PwP), and to a lesser degree their first-degree biological relatives, would demonstrate advanced brain-age compared to healthy controls. The results of multilevel modeling indicated that participant group predicted brain-age gap after accounting for sex, race, BMI, family relatedness, and scanner [$\chi^2_{(2,332)} = 17.95$, $p < 0.001$]. Specifically, PwP demonstrated a larger brain-age gap compared to their biological relatives [$p = 0.001$] and healthy controls [$p = 0.002$], indicating that the estimated brain-age of individuals with a history of psychosis was further beyond their chronological age than the other groups (see **Figure 1**). In order to examine whether the particular form of psychotic psychopathology was relevant, we compared subgroups of PwP along clinical diagnostic boundaries. A multilevel model showed

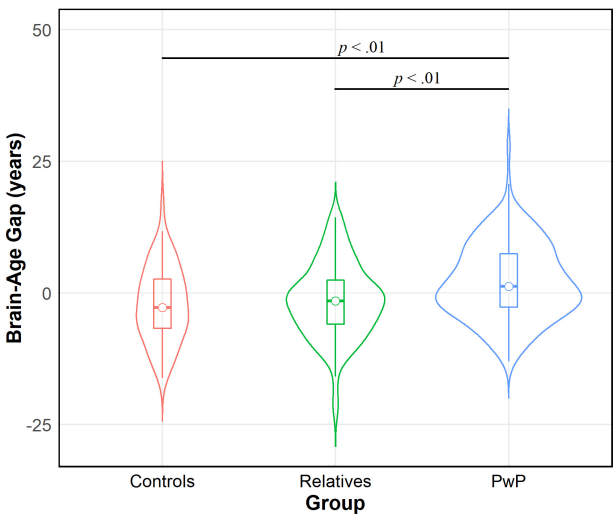


**FIGURE 1 |** Violin density plot of group comparison on brain-age gap. People with psychotic disorders (PwP) demonstrated a greater estimated brain-age than chronological age (i.e., brain-age gap) in contrast to biological relatives of people with psychotic psychopathology and healthy controls.

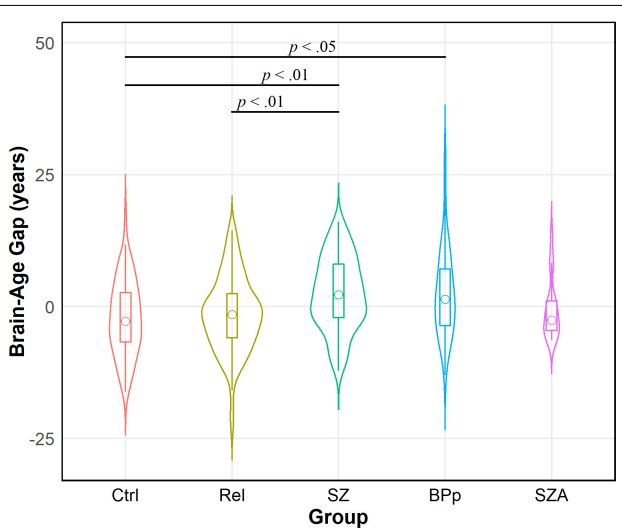


**FIGURE 2 |** Violin density plot of brain-age gap across diagnostic groups within people with psychotic disorders (PwP). Schizophrenia (SZ) and bipolar I disorder with psychotic features (BPp) groups demonstrated larger brain-age gaps than healthy controls (Ctrl). There were no differences in brain-age gap between the forms of psychotic disorders. Relatives (Rel) had smaller brain-age gaps than SZ; relatives did not differ from BPp, schizoaffective (SZA), or controls. Sample size for SZA is small and interpretation requires caution.

that a five-category diagnostic group variable (see **Figure 2**) predicted brain-age gap when controlling for sex, race, BMI, family relatedness, and scanner [$\chi^2_{(4,332)} = 20.26$, $p < 0.001$]. Pairwise comparisons indicated that people with schizophrenia and bipolar I disorder with psychotic features demonstrated larger brain-age gaps compared to controls ($p = 0.008$ and $p = 0.049$, respectively; Tukey-corrected), with no group differences between any of the psychotic disorders ($p > 0.584$; see **Figure 2**). Contrary to hypotheses, biological relatives of PwP failed to have greater brain-age gaps than healthy controls ($p = 0.990$; see **Supplementary Material** for more details). A multilevel model was run to determine whether IQ and community functioning predicted brain-age gap in the full sample (with scanner, race, sex, BMI, and family relatedness as variables of non-interest in the model). The results of this model indicated that lower IQ ($p = 0.007$), lower functioning ($p = 0.003$), and female sex ($p < 0.001$; see **Figure 3**) predicted greater brain-age gap.

In exploratory analyses, we examined these relations among subgroups of participants. Among relatives of PwP, multiple regression was run to predict brain-age gap from IQ, community functioning (GAF score), schizotypal symptoms (SPQ total), and emotion dysregulation (PID-5 negative affect), maintaining scanner, race, sex, and BMI as variables of non-interest in the model. Among relatives, lower IQ ($p = 0.028$), lower SPQ ($p = 0.032$), and study 1 scanner ($p = 0.040$) predicted larger brain-age gap [$F_{(8,89)} = 3.39$, $p = 0.002$, $R^2 = 0.233$]. Since scanner was entered as a variable of non-interest, and there were no group differences to suggest disproportionate assessment by scanner type [$\chi^2_{(2,332)} = 4.56$, $p = 0.102$], we did not further interpret the contribution of scanner in this analysis. Among PwP, multiple regression with IQ, community functioning, current symptom severity (BPRS total), duration of psychotic illness, and current antipsychotic medication dosage [quantified using chlorpromazine equivalents, see Leucht et al. (2016)] failed to predict brain-age gap, with scanner, race, sex, and BMI entered as covariates [$F_{(9,122)} = 1.74$, $p = 0.086$, $R^2 = 0.114$]. These results suggest that larger brain-age gap in biological relatives is associated with lower cognitive functioning, while in PwP, brain-age gap is not a marker of current cognitive functioning, symptoms, medication load, or time since disorder onset. This is consistent with brain-age gaps reflecting developmental abnormalities, rather than neurodegeneration, of brain structure in individuals with psychotic disorders.

Additional exploratory analyses included a longitudinal examination of brain-age gap among the subgroup of participants who completed both study 1 and study 2. The intraclass correlation coefficient between predicted brain-age scores from the study 1 and study 2 scans was 0.90 (95% CI: 0.81–0.95), suggesting good reliability and stability. A mixed ANOVA controlling for amount of time between scans 1 and 2 revealed that brain-age gap scores increased over time [$F_{(1,38)} = 4.15$, $p = 0.049$], but there was no interaction to suggest a group difference in changes in brain-age gap over time [$F_{(2,39)} = 0.49$, $p = 0.615$; see **Figure 4**]. In terms of years of brain-age gap reflected in the unadjusted values, PwP increased from an average brain-age gap of 7.94 years ($SD = 9.03$) at the first scan to 9.08 years ($SD = 10.01$) at the follow-up scan; controls increased from -0.75 ($SD = 10.73$) to 0.89 ($SD = 10.33$) years; and relatives increased from -1.35 ($SD = 10.66$) to 2.18 ($SD = 8.27$) years. The brain-age acceleration rate was calculated as the change in uncorrected brain-age gap over the change in chronological age. Aging accelerated at a rate of 2.56 years per chronological year ($SD = 10.76$) for PwP, 2.21 years per chronological year ($SD = 4.62$) for controls, and 1.54 years per chronological year ($SD = 11.61$) for relatives.

In an exploratory analysis to specifically examine the dependency of brain-age gap on history of psychosis, we compared participants with bipolar I disorder without a history of psychosis to the other groups. We found an effect of group on brain-age gap [$F_{(4,163)} = 4.16$, $p = 0.003$] such that participants with bipolar I disorder without psychotic features, surprisingly, had a greater brain-age gap in comparison to bipolar I disorder participants with psychotic features ($p = 0.029$), biological relatives of people with bipolar I disorder with ($p = 0.003$) and without psychotic features ($p = 0.003$), and healthy controls ($p < 0.001$). Although based on a small sample, this effect suggests that other factors beyond psychosis are related to altered brain morphology in bipolar disorder.

In order to investigate which brain regions may be driving brain-age gap findings, we compared groups on cortical thickness and surface area as well as subcortical volume. We found an effect of group in a range of regions when controlling for sex, scanner, age, and intra-cranial volume (see **Supplementary Material**). Briefly, groups differed in frontal regions (bilateral: caudal middle frontal, lateral orbitofrontal, paracentral, pars opercularis, pars orbitalis, pars triangularis, precentral, superior frontal; left medial orbitofrontal; and right rostral middle frontal), parietal regions (bilateral: inferior parietal, isthmus cingulate, precuneus, postcentral, superior parietal, supramarginal; and right posterior cingulate), temporal regions (bilateral: inferior temporal; fusiform; middle temporal, superior temporal, temporal pole, transverse temporal; and right parahippocampal), and occipital regions (bilateral: lateral occipital, lingual, pericalcarine; and left cuneus) as well as the right banks of superior temporal sulcus (see **Supplementary Table 1**). People with psychotic disorders had lower cortical thickness, surface area, and/or subcortical volume values than controls and relatives in all these regions; relatives had lower values than controls in only a few regions (surface area in left: lateral orbitofrontal, medial orbitofrontal, middle temporal, and pars opercularis regions; left transverse temporal cortical thickness; and right pericalcarine surface area; see **Supplementary Table 1**).

## DISCUSSION

Our analysis revealed evidence of advanced brain-age (quantified by a larger gap between chronological and model-estimated age) for individuals with a primary psychotic disorder as well as people with bipolar I disorder with a history of psychotic symptoms. There were no differences in brain-age gap across the types of psychotic disorders, indicating that advanced brain-age is

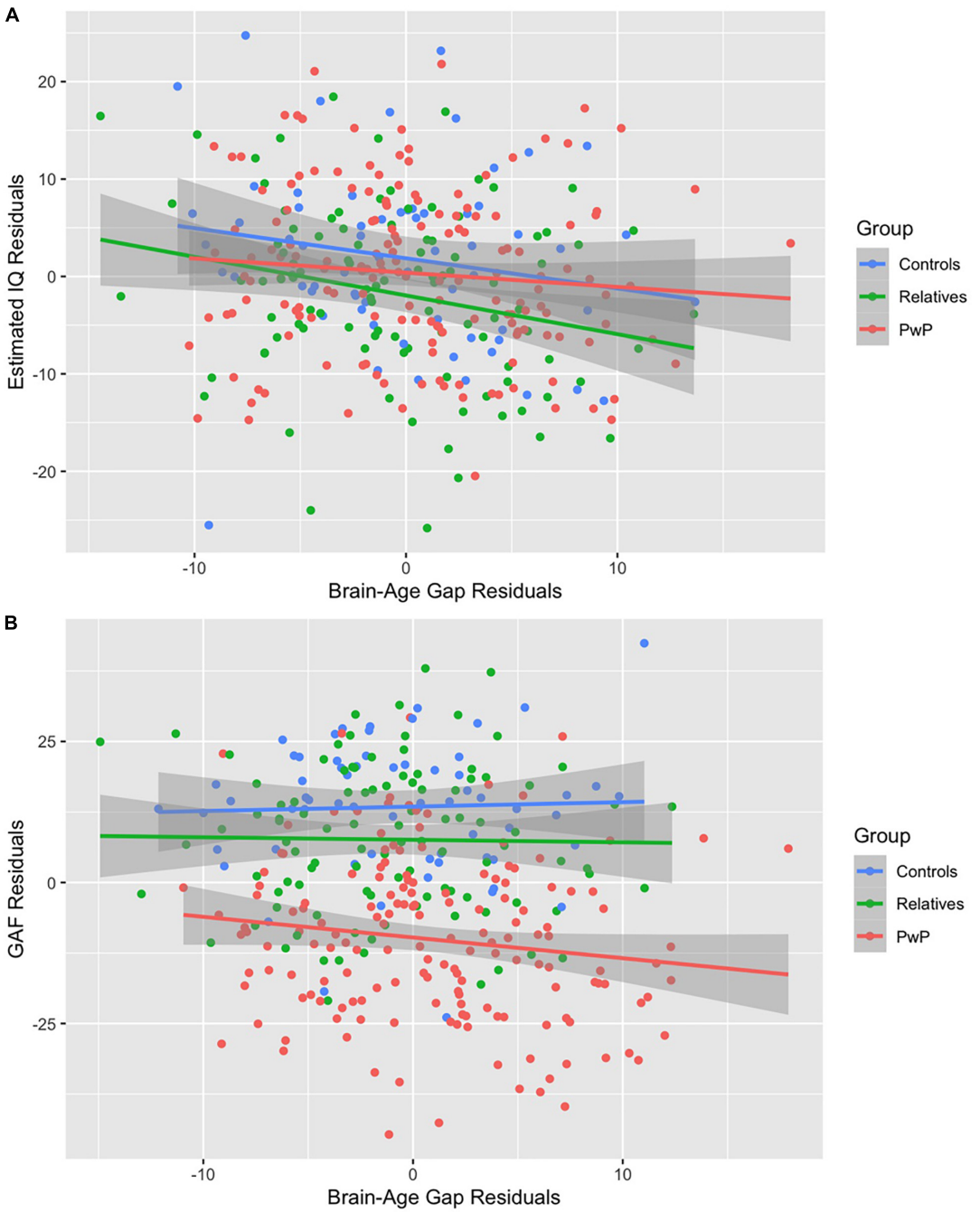


**FIGURE 3 | (A,B)** Correlations among the full sample. Lower IQ **(A)** and lower Global Assessment of Functioning **(B)** predicted larger brain-age gap after adjusting for covariates.

not diagnostically specific in our sample. Biological first-degree relatives, unaffected and affected, demonstrated model-estimated ages that did not differ from their chronological age and did not have an intermediate brain-age gap compared to people with psychosis and healthy controls. Thus, advanced brain-age may possess clinical utility for identifying individuals within a family who are likely to develop psychosis. Exploratory analyses of a subset of individuals with longitudinal data revealed that over an average period of 21 months, psychotic psychopathology failed to be associated with acceleration in brain aging. This supports the assertion that excessive advance in brain-age occurs earlier in the disorder and could reflect neurodevelopmental abnormalities.

Our findings support the presence of an abnormal neurodevelopmental process in psychotic disorders. Brain-age gap was unrelated to duration of psychotic illness, antipsychotic load, or current symptom severity, suggesting

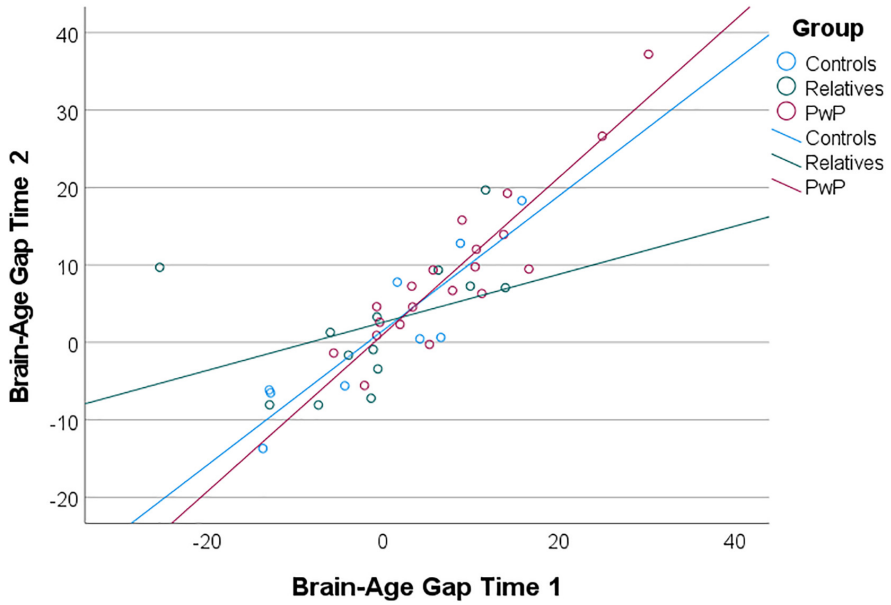


**FIGURE 4 |** Scatterplot of uncorrected brain-age gap scores from exploratory longitudinal analysis. Brain-age gap scores increased over time for all groups; groups did not differ in change in brain-age gap over time (i.e., brain-age acceleration).

that early disruptions to brain development—rather than current clinical severity—are indicative of advanced brain-age. Based on our longitudinal analyses, the large brain-age gap that we observed in schizophrenia and bipolar disorder does not seem to worsen over time. Morphological abnormalities underlying advanced brain aging likely occur early in the course of illness without progressing throughout the lifespan, thus reflecting neurodevelopmental processes [see Shahab et al. (2019)]. However, it is possible that our follow-up period of 21 months on average was too short to observe accelerated atrophy and that there may exist subgroups of persons with psychosis for whom neurodegenerative processes are implicated (Murray et al., 1992).

The current study involved a transdiagnostic sample of individuals with a history of psychotic symptomatology that allowed us to directly compare across diagnostic boundaries. Our primary findings suggest that the presence of psychotic psychopathology, regardless of specific diagnostic category, is implicated in advanced brain-age. Exploratory analysis revealed that advanced brain-age is evident in bipolar disorder regardless of a history of psychosis, which suggests that there are additional factors that affect brain structure in bipolar disorder. However, given the small sample, future studies would be more informative if they included more individuals with bipolar disorder who are classified based on their history of psychosis. The utility of examining brain-age gaps across different psychotic disorders lies in informing transdiagnostic, biologically-based classification. Classifying patients according to biological rather than clinical parameters can identify specific pathophysiological processes that contribute to the manifestation of psychotic symptoms and perhaps explain the heterogeneity within diagnoses (Clementz et al., 2016). Brain-age gap could characterize individual differences in overall brain morphology within psychotic disorders, which may improve the ability to predict the development and course of psychotic psychopathology (Cole et al., 2019). Our findings add to the growing literature by demonstrating cross-disorder associations between brain-age gap and IQ and community functioning. Specifically, we found among biological relatives that lower general cognitive performance predicted greater brain-age gap, suggesting that advanced brain-age could be a measure of subtle effects of genetic liability for psychosis that is more sensitive than the clinical presentation of psychotic psychopathology.

Our study provides further evidence of an association between lower cognitive performance and advanced brain-age. However, the association between advanced brain-age and lower cognitive functioning in our sample appears not to depend on the presence of clinically significant psychopathology. Similarly, lower cognitive performance has been associated with more advanced brain-age gap in healthy controls (Liem et al., 2017; Richard et al., 2018, 2020; Elliott et al., 2021) and in adults with various medical conditions, such as HIV (Kuhn et al., 2018), Alzheimer's disease (Franke and Gaser, 2012), and TBI (Cole et al., 2015). Within psychotic psychopathology, cognitive performance has been associated with cortical thickness throughout the brain in both schizophrenia and bipolar disorder (Shahab et al., 2019) and structural connectivity in schizophrenia (Yeo et al., 2016), and evidence suggests that different brain regions are related to cognitive function for people with schizophrenia versus controls (Hanford et al., 2019). Further, people with schizophrenia can be classified according to cognitive deficits in specific domains, which correspond to unique structural brain alterations (Geisler et al., 2015).

In terms of brain morphology, our analyses revealed widespread gray matter perturbations among people with

psychotic disorders. Brain-age provides an estimate of the aggregate impact of such gray matter deficits. Previous brain-age research has also linked larger brain-age gap with lower gray matter volume: in the prefrontal cortex in typical development (Truelove-Hill et al., 2020), throughout the brain among first-episode psychosis patients (Hajek et al., 2019), and in the left temporal and insular cortices as well as the left frontal and parietal lobes in schizophrenia spectrum disorders (Shahab et al., 2019). These regions are involved in higher-order processing and highly implicated in psychotic disorders. We found evidence of gray matter abnormalities throughout the brain for people with psychosis, overlapping with previous research. Finally, schizophrenia is associated with physical health issues, including cardiovascular disease, obesity, and metabolic syndrome (von Hausswolff-Juhlin et al., 2009). Such comorbid physical conditions require more hospitalizations (Šprah et al., 2017), further increasing the emotional and financial burden of the disorder and contributing to a shorter life span for people with schizophrenia. This increased mortality, in combination with evidence of impaired cognitive performance and abnormal brain development, may well be manifestations of compromised cellular health. The brain-age gap offers a summary value that provides an estimate of the degree to which abnormalities in brain morphology could be characterized using a cell aging algorithm.

There are several strengths of our study. First, the clinical sample included people with a range of psychotic disorders and therefore allowed for transdiagnostic examination of the brain-age gap model. Second, the study included biological first-degree relatives, which allowed for the testing of hypotheses related to genetic loading. Third, the sample size was relatively large for a single site study. Fourth, we used a corrected version of the brain-age gap to address the correlation between chronological age and brain-age gap, which leads to an overestimation of age in younger people and underestimation in older people due to regression to the mean (Le et al., 2018; Smith et al., 2019). The correlation suggests that chronological age can confound the relationship between brain-age gap and variables of interest, yielding spurious correlations. Thus, previous studies that did not correct for this statistical dependency should be interpreted with caution. Much of the data from the current study will be publicly available to allow other investigators to examine brain morphology in psychosis.

There are also some limitations of our study, including using a brain-age gap model that is based on only structural T1-weighted neuroimaging data, rather than incorporating functional data. Previous findings suggest that multimodal data, combining both anatomical and whole-brain functional connectivity information, improves brain-based age prediction in healthy controls (Liem et al., 2017). Another limitation is that our current findings are based on two studies that used different MRI scanners, which limited statistical power in our analyses as we had to covary for scanner type in our models. Further, because the two time points were collected on different scanners, results of longitudinal analyses are considered exploratory and require replication. Our sample was more diverse than the training sample in terms of racial identity and our groups differed on this variable, which is a potential limitation for the effectiveness of the brain-age model as acknowledged by the BARACUS authors (Liem and Gorgolewski, 2017). Body mass index was calculated from body measurements for a subset of participants, whereas it was based on participants' self-reported estimates of height and weight for all study 1 participants (body measurements were not part of the study 1 protocol) and for 25 study 2 participants (body measurements were not completed during the COVID-19 pandemic). Thus, our BMI variable may contain additional measurement error. However, the results of our group comparisons did not change when we controlled for body mass index. Finally, psychotic disorders have high rates of comorbidity with, for example, mood episodes, trauma, and metabolic health issues. There is a body of research documenting larger brain-age gap among such conditions, including major depressive disorder (Han et al., 2021), post-traumatic stress disorder (Liang et al., 2019; Clausen et al., 2022), and obesity, which co-occurs with both psychosis and cognitive impairment (Bora et al., 2017; Kolenic et al., 2018). Importantly, certain medications, such as those to treat obesity and bipolar disorder, may have neuroprotective effects [see Kolenic et al. (2018)]. These findings highlight the need to understand more about potential confounding factors to advanced brain-age in psychotic psychopathology, not all of which we could address in the current study.

Overall, our study revealed evidence of advanced brain-age in schizophrenia and bipolar disorder. Interestingly, analysis of a subset of individuals with longitudinal data failed to provide evidence of accelerated brain aging in psychotic psychopathology. This is consistent with early, and perhaps neurodevelopmental, neural abnormalities. Relatives of people with psychosis demonstrated an association between brain-age and cognitive performance, suggesting that lower cognitive function in individuals with genetic liability for psychosis may be tied to cellular abnormalities that result in aberrant brain morphology.

## DATA AVAILABILITY STATEMENT

The datasets presented in this article are not readily available because the data from study 2 will be made publicly available through the NIMH Data Archive. Requests to access the datasets should be directed to hodgem@wustl.edu.

## ETHICS STATEMENT

The studies involving human participants were reviewed and approved by the Institutional Review Board at the University of Minnesota. The patients/participants provided their written informed consent to participate in this study.

## AUTHOR CONTRIBUTIONS

SS and SD contributed to the conception and design of the study. CD, CS, TH, and JA contributed to the acquisition, analysis, and interpretation of the data. TH processed the study neuroimaging

data with machine-learning based software. CD and CS organized the database and performed the statistical analysis. CD wrote the first draft of the manuscript. CD, TH, and SS wrote sections of the manuscript. SS provided supervision throughout the study and contributed to all stages of the manuscript. All authors contributed to manuscript revision and approved the submitted version.

## FUNDING

This work was supported by the National Institutes of Health (U01MH108150 to SS; P50MH119569), the VA Rehabilitation Research and Development Service (1IK2RX002922 to SD), and the Center for Magnetic Resonance Research (P41 EB027061; 1S10OD017974). This work was also supported in part by a Merit Review Award (#I01CX000227 to SS) from the United States (U.S.) Department of Veterans Affairs Clinical Science Research and Development Service.

## ACKNOWLEDGMENTS

We are grateful to the families who participated in our studies and the many lab members who collected the data.

## SUPPLEMENTARY MATERIAL

The Supplementary Material for this article can be found online at: https://www.frontiersin.org/articles/10.3389/fnagi.2022.872867/full#supplementary-material

## REFERENCES

Andreasen, N. C. (1984). *Scale for the Assessment of Positive Symptoms (SAPS)*. Iowa City: University of Iowa.

Andreasen, N. C. (1989). Scale for the assessment of negative symptoms (SANS). *Br. J. Psychiatry* 155, 53–58. doi: 10.1192/S0007125000291496

Andreou, C., and Borgwardt, S. (2020). Structural and functional imaging markers for susceptibility to psychosis. *Mol. Psychiatry* 25, 2773–2785. doi: 10.1038/s41380-020-0679-7

Besteher, B., Gaser, C., and Nenadiæ, I. (2019). Machine-learning based brain age estimation in major depression showing no evidence of accelerated aging. *Psychiatry Res.* 290, 1–4. doi: 10.1016/j.pscychresns.2019.06.001

Bora, E., Akdede, B. B., and Alptekin, K. (2017). The relationship between cognitive impairment in schizophrenia and metabolic syndrome: A systematic review and meta-analysis. *Psychol. Med.* 47, 1030–1040. doi: 10.1017/S0033291716003366

Breiman, L. (2001). Random forests. *Machin. Learn.* 45, 5–32. doi: 10.1023/A:1010933404324

Cahn, W., Hulshoff Pol, H. E., Bongers, M., Schnack, H. G., Mandl, R. C., Van Haren, N. E., et al. (2002). Brain morphology in antipsychotic-naïve schizophrenia: A study of multiple brain structures. *Br. J. Psychiatry* 43, s66–s72. doi: 10.1192/bjp.181.43.s66

Chung, Y., Addington, J., Bearden, C. E., Cadenhead, K., Cornblatt, B., Mathalon, D. H., et al. (2018). Use of machine learning to determine deviance in neuroanatomical maturity associated with future psychosis in youths at clinically high risk. *JAMA Psychiatry* 75, 960–968. doi: 10.1001/jamapsychiatry.2018.1543

Chung, Y., Allswede, D., Addington, J., Bearden, C. E., Cadenhead, K., Cornblatt, B., et al. (2019a). Cortical abnormalities in youth at clinical high-risk for psychosis: Findings from the NAPLS2 cohort. *NeuroImage* 23:101862. doi: 10.1016/j.nicl.2019.101862

Chung, Y., Addington, J., Bearden, C. E., Cadenhead, K., Cornblatt, B., Mathalon, D. H., et al. (2019b). Adding a neuroanatomical biomarker to an individualized risk calculator for psychosis: A proof-of-concept study. *Schizophr. Res.* 208, 41–43. doi: 10.1016/j.schres.2019.01.026

Clausen, A. N., Fercho, K. A., Monsour, M., Disner, S., Salminen, L., Haswell, C. C., et al. (2022). Assessment of brain age in posttraumatic stress disorder: Findings from the ENIGMA PTSD and brain age working groups. *Brain Behav.* 12:e2413. doi: 10.1002/brb3.2413

Clementz, B. A., Sweeney, J. A., Hamm, J. P., Ivleva, E. I., Ethridge, L. E., Pearlson, G. D., et al. (2016). Identification of distinct psychosis biotypes using brain-based biomarkers. *Am. J. Psychiatry* 173, 373–384. doi: 10.1176/appi.ajp.2015.14091200

Cole, J. H., Leech, R., Sharp, D. J., and Alzheimer's Disease Neuroimaging Initiative. (2015). Prediction of brain-age suggests accelerated atrophy after traumatic brain injury. *Ann. Neurol.* 77, 571–581. doi: 10.1002/ana.24367

Cole, J. H., Marioni, R. E., Harris, S. E., and Deary, I. J. (2019). Brain age and other bodily 'ages': Implications for neuropsychiatry. *Mol. Psychiatry* 24, 266–281. doi: 10.1038/s41380-018-0098-1

Constantinides, C., Han, L. K. M., Alloza, C., Antonucci, L., Arango, C., Ayesa-Arriola, R., et al. (2022). Brain ageing in schizophrenia: Evidence from 26 international cohorts via the ENIGMA Schizophrenia consortium. *medRxiv* [Preprint], doi: 10.1101/2022.01.10.21267840

Dale, A. M., Fischl, B., and Sereno, M. I. (1999). Cortical surface-based analysis: I. Segmentation and surface reconstruction. *NeuroImage* 9, 179–194. doi: 10.1006/nimg.1998.0395

Dale, A. M., and Sereno, M. I. (1993). Improved localization of cortical activity by combining EEG and MEG with MRI cortical surface reconstruction: A linear approach. *J. Cogn. Neurosci.* 5, 162–176. doi: 10.1162/jocn.1993.5.2.162

Daniel, D. G., Goldberg, T. E., Gibbons, R. D., and Weinberger, D. R. (1991). Lack of a bimodal distribution of ventricular size in schizophrenia: A Gaussian mixture analysis of 1056 cases and controls. *Biol. Psychiatry* 30, 887–903. doi: 10.1016/0006-3223(91)90003-5

Demro, C., Mueller, B. A., Kent, J. S., Burton, P. C., Olman, C. A., Schallmo, M. P., et al. (2021). The psychosis Human Connectome Project: An overview. *NeuroImage* 241:118439. doi: 10.1016/j.neuroimage.2021.118439

Desikan, R. S., Segonne, F., Fischl, B., Quinn, B. T., Dickerson, B. C., Blacker, D., et al. (2006). An automated labeling system for subdividing the human cerebral cortex on MRI scans into gyral based regions of interest. *NeuroImage* 31, 968–980. doi: 10.1016/j.neuroimage.2006.01.021

Drucker, H., Burges, C. J. C., Kaufman, L., Smola, A. J., and Vapnik, V. (1996). "Support vector regression machines," in *In Advances in Neural Information Processing Systems*, eds M. C. Mozer, M. Jordan, and T. Petsche (USA: NIPS, Denver, CO). 9, 155–161.

Elliott, M. L., Belsky, D. W., Knodt, A. R., Ireland, D., Melzer, T. R., Poulton, R., et al. (2021). Brain-age in midlife is associated with accelerated biological aging and cognitive decline in a longitudinal birth cohort. *Mol. Psychiatry* 26, 3829–3838. doi: 10.1038/s41380-019-0626-7

First, M. B., Spitzer, R. L., Gibbon, M., and Williams, J. B. W. (2002). *Structured Clinical Interview for DSM-IV-TR Axis I Disorders, Patient Edition (SCID-I/NP, 11/2002 revision)*. (New York, NY: Biometrics Research Department, New York State Psychiatric Institution).

Fischl, B., and Dale, A. M. (2000). Measuring the thickness of the human cerebral cortex from magnetic resonance images. *Proc. Natl. Acad. Sci. U.S.A.* 97, 11050–11055. doi: 10.1073/pnas.200033797

Fischl, B., Liu, A., and Dale, A. M. (2001). Automated manifold surgery: Constructing geometrically accurate and topologically correct models of the human cerebral cortex. *IEEE Trans. Med. Imag.* 20, 70–80. doi: 10.1109/42.906426

Fischl, B., Salat, D. H., Busa, E., Albert, M., Dieterich, M., Haselgrove, C., et al. (2002). Whole brain segmentation: Automated labeling of neuroanatomical

structures in the human brain. *Neuron* 33, 341–355. doi: 10.1016/s0896-6273(02)00569-x

Fischl, B., Salat, D. H., van der Kouwe, A. J., Makris, N., Segonne, F., Quinn, B. T., et al. (2004a). Sequence-independent segmentation of magnetic resonance images. *NeuroImage* 23, S69–S84. doi: 10.1016/j.neuroimage.2004.07.016

Fischl, B., van der Kouwe, A., Destrieux, C., Halgren, E., Segonne, F., Salat, D. H., et al. (2004b). Automatically parcellating the human cerebral cortex. *Cereb. Cortex* 14, 11–22. doi: 10.1093/cercor/bhg087

Fischl, B., Sereno, M. I., and Dale, A. M. (1999a). Cortical surface-based analysis. II: Inflation, flattening, and a surface-based coordinate system. *NeuroImage* 9, 195–207. doi: 10.1006/nimg.1998.0396

Fischl, B., Sereno, M. I., Tootell, R. B., and Dale, A. M. (1999b). High-resolution intersubject averaging and a coordinate system for the cortical surface. *Hum. Brain Mapp.* 8, 272–284. doi: 10.1002/(sici)1097-019319998:4<272::aid-hbm10<3.0.co;2-4

Franke, K., and Gaser, C. (2012). Longitudinal changes in individual BrainAGE in healthy aging, mild cognitive impairment, and Alzheimer's disease. *GeroPsych* 25, 235. doi: 10.1024/1662-9647/a000074

Franke, K., Ziegler, G., Klöppel, S., Gaser, C., Alzheimer's Disease, and Neuroimaging Initiative. (2010). Estimating the age of healthy subjects from T1-weighted MRI scans using kernel methods: Exploring the influence of various parameters. *NeuroImage* 50, 883–892. doi: 10.1016/j.neuroimage.2010.01.005

Geisler, D., Walton, E., Naylor, M., Roessner, V., Lim, K. O., Charles Schulz, S., et al. (2015). Brain structure and function correlates of cognitive subtypes in schizophrenia. *Psychiatry Res.* 234, 74–83. doi: 10.1016/j.pscychresns.2015.08.008

Gorgolewski, K. J., Auer, T., Calhoun, V. D., Craddock, R. C., Das, S., Duff, E. P., et al. (2016). The brain imaging data structure, a format for organizing and describing outputs of neuroimaging experiments. *Sci. Data* 3:160044. doi: 10.1038/sdata.2016.44

Gupta, C. N., Calhoun, V. D., Rachakonda, S., Chen, J., Patel, V., Liu, J., et al. (2015). Patterns of gray matter abnormalities in schizophrenia based on an international mega-analysis. *Schizophr. Bull.* 41, 1133–1142. doi: 10.1093/schbul/sbu177

Hajek, T., Franke, K., Kolenic, M., Capkova, J., Matejka, M., Propper, L., et al. (2019). Brain age in early stages of bipolar disorders or schizophrenia. *Schizophr. Bull.* 45, 190–198. doi: 10.1093/schbul/sbx172

Han, L., Dinga, R., Hahn, T., Ching, C., Eyler, L. T., Aftanas, L., et al. (2021). Brain aging in major depressive disorder: Results from the ENIGMA major depressive disorder working group. *Mol. Psychiatry* 26, 5124–5139. doi: 10.1038/s41380-020-0754-0

Han, X., Jovicich, J., Salat, D., van der Kouwe, A., Quinn, B., Czanner, S., et al. (2006). Reliability of MRI-derived measurements of human cerebral cortical thickness: The effects of field strength, scanner upgrade and manufacturer. *NeuroImage* 32, 180–194. doi: 10.1016/j.neuroimage.2006.02.051

Hanford, L. C., Pinnock, F., Hall, G. B., and Heinrichs, R. W. (2019). Cortical thickness correlates of cognitive performance in cognitively-matched individuals with and without schizophrenia. *Brain Cogn.* 132, 129–137. doi: 10.1016/j.bandc.2019.04.003

Hennekens, C. H., Hennekens, A. R., Hollar, D., and Casey, D. E. (2005). Schizophrenia and increased risks of cardiovascular disease. *Am. Heart J.* 150, 1115–1121. doi: 10.1016/j.ahj.2005.02.007

Hietala, J., Cannon, T. D., van Erp, T. G., Syvälahti, E., Vilkman, H., Laakso, A., et al. (2003). Regional brain morphology and duration of illness in never-medicated first-episode patients with schizophrenia. *Schizophr. Res,* 64, 79–81. doi: 10.1016/s0920-9964(03)00065-3

Iftimovici, A., Douchesnay, E., Kebir, O., Plaze, M., Gay, O., Bourgin, J., et al. (2020). "Epigenetic and brain aging during conversion to psychosis in a longitudinal cohort of ultra-high risk individuals". *The Organization for Human Brain Mapping conference, virtual*. https://cdn-akamai.6connex.com/645/1827/Poster_OHBM_1591973577292772.pdf.

Jovicich, J., Czanner, S., Greve, D., Haley, E., van der Kouwe, A., Gollub, R., et al. (2006). Reliability in multi-site structural MRI studies: Effects of gradient non-linearity correction on phantom and human data. *NeuroImage* 30, 436–443. doi: 10.1016/j.neuroimage.2005.09.046

Keshavan, M. S., Tandon, R., Boutros, N. N., and Nasrallah, H. A. (2008). Schizophrenia,"just the facts": What we know in 2008: Part 3: Neurobiology. *Schizophr. Res.* 106, 89–107. doi: 10.1016/j.schres.2008.07.020

Kirkpatrick, B., Messias, E., Harvey, P. D., Fernandez-Egea, E., and Bowie, C. R. (2008). Is schizophrenia a syndrome of accelerated aging? *Schizophr. Bull.* 34, 1024–1032. doi: 10.1093/schbul/sbm140

Kochunov, P., and Hong, L. E. (2014). Neurodevelopmental and neurodegenerative models of schizophrenia: White matter at the center stage. *Schizophr. Bull.* 40, 721–728. doi: 10.1093/schbul/sbu070

Kolenic, M., Franke, K., Hlinka, J., Matejka, M., Capkova, J., Pausova, Z., et al. (2018). Obesity, dyslipidemia and brain-age in first-episode psychosis. *J. Psychiatric Res.* 99, 151–158. doi: 10.1016/j.jpsychires.2018.02.012

Koutsouleris, N., Davatzikos, C., Borgwardt, S., Gaser, C., Bottlender, R., Frodl, T., et al. (2014). Accelerated brain aging in schizophrenia and beyond: A neuroanatomical marker of psychiatric disorders. *Schizophr. Bull.* 40, 1140–1153. doi: 10.1093/schbul/sbt142

Kraepelin, E., Barclay, R. M., and Robertson, G. M. (1971). *Dementia Praecox and Paraphrenia*. Livingston: Edinburgh. Original work published 1919.

Kuhn, T., Kaufmann, T., Doan, N. T., Westlye, L. T., Jones, J., Nunez, R. A., et al. (2018). An augmented aging process in brain white matter in HIV. *Hum. Brain Mapp.* 39, 2532–2540. doi: 10.1002/hbm.24019

Kuperberg, G. R., Broome, M. R., McGuire, P. K., David, A. S., Eddy, M., et al. (2003). Regionally localized thinning of the cerebral cortex in schizophrenia. *Arch. Gen. Psychiatry* 60, 878–888. doi: 10.1001/archpsyc.60.9.878

Le, T. T., Kuplicki, R. T., McKinney, B. A., Yeh, H. W., Thompson, W. K., Paulus, M. P., et al. (2018). A nonlinear simulation framework supports adjusting for age when analyzing BrainAGE. *Front. Aging Neurosci.* 10:317. doi: 10.3389/fnagi.2018.00317

Leucht, S., Samara, M., Heres, S., and Davis, J. M. (2016). Dose equivalents for antipsychotic drugs: The DDD method. *Schizophr. Bull.* 42, S90–S94. doi: 10.1093/schbul/sbv167

Lewis, D. A., and Levitt, P. (2002). Schizophrenia as a disorder of neurodevelopment. *Annu. Rev. Neurosci.* 25, 409–432. doi: 10.1146/annurev.neuro.25.112701.142754

Liang, H., Zhang, F., and Niu, X. (2019). Investigating systematic bias in brain age estimation with application to post-traumatic stress disorders. *Hum. Brain Mapp.* 40, 3143–3152. doi: 10.1002/hbm.24588

Liem, F., and Gorgolewski, C. (2017). *BIDS-Apps/baracus: v1.1.2 (Version v1.1.2)*. Available online at: https://github.com/BIDS-Apps/baracus (accessed October 7, 2021).

Liem, F., Varoquaux, G., Kynast, J., Beyer, F., Kharabian Masouleh, S., Huntenburg, J. M., et al. (2017). Predicting brain-age from multimodal imaging data captures cognitive impairment. *NeuroImage* 148, 179–188. doi: 10.1016/j.neuroimage.2016.11.005

Longenecker, J. M., Krueger, R. F., and Sponheim, S. R. (2020). Personality traits across the psychosis spectrum: A Hierarchical Taxonomy of Psychopathology conceptualization of clinical symptomatology. *Personal. Mental Health* 14, 88–105. doi: 10.1002/pmh.1448

Murray, R. M., O'Callaghan, E., Castle, D. J., and Lewis, S. W. (1992). A neurodevelopmental approach to the classification of schizophrenia. *Schizophr. Bull.* 18, 319–332. doi: 10.1093/schbul/18.2.319

Nenadić, I., Dietzek, M., Langbein, K., Sauer, H., and Gaser, C. (2017). BrainAGE score indicates accelerated brain aging in schizophrenia, but not bipolar disorder. *Psychiatry Res.* 266, 86–89. doi: 10.1016/j.pscychresns.2017.05.006

Rahim, M., Thirion, B., Comtat, C., and Varoquaux, G. (2016). Transmodal learning of functional networks for Alzheimer's disease prediction. *IEEE J. Select. Topics Sign. Proc.* 10, 120–1213. doi: 10.1109/JSTSP.2016.2600400

Raine, A. (1991). The SPQ: A scale for the assessment of schizotypal personality based on DSM-III-R. *Schizophr. Bull.* 17, 555–564. doi: 10.1093/schbul/17.4.555

Rapoport, J. L., Addington, A. M., Frangou, S., and Psych, M. R. (2005). The neurodevelopmental model of schizophrenia: Update 2005. *Mol. Psychiatry* 10, 434–449. doi: 10.1038/sj.mp.4001642

Reuter, M., and Fischl, B. (2011). Avoiding asymmetry-induced bias in longitudinal image processing. *NeuroImage* 57, 19–21. doi: 10.1016/j.neuroimage.2011.02.076

Reuter, M., Rosas, H. D., and Fischl, B. (2010). Highly accurate inverse consistent registration: A robust approach. *NeuroImage* 53, 1181–1196. doi: 10.1016/j.neuroimage.2010.07.020

Reuter, M., Schmansky, N. J., Rosas, H. D., and Fischl, B. (2012). Within-subject template estimation for unbiased longitudinal image analysis. *NeuroImage* 61, 1402–1418. doi: 10.1016/j.neuroimage.2012.02.084

Richard, G., Kolskår, K., Sanders, A. M., Kaufmann, T., Petersen, A., Doan, N. T., et al. (2018). Assessing distinct patterns of cognitive aging using tissue-specific brain-age prediction based on diffusion tensor imaging and brain morphometry. *PeerJ* 6:e5908. doi: 10.7717/peerj.5908

Richard, G., Kolskår, K., Ulrichsen, K. M., Kaufmann, T., Alnćs, D., Sanders, A. M., et al. (2020). Brain age prediction in stroke patients: Highly reliable but limited sensitivity to cognitive performance and response to cognitive training. *NeuroImage* 25:102159. doi: 10.1016/j.nicl.2019.102159

Rosas, H. D., Liu, A. K., Hersch, S., Glessner, M., Ferrante, R. J., Salat, D. H., et al. (2002). Regional and progressive thinning of the cortical ribbon in Huntington's disease. *Neurology* 58, 695–701. doi: 10.1212/wnl.58.5.695

Salat, D. H., Buckner, R. L., Snyder, A. Z., Greve, D. N., Desikan, R. S., Busa, E., et al. (2004). Thinning of the cerebral cortex in aging. *Cereb. Cortex* 14, 721–730. doi: 10.1093/cercor/bhh032

Schnack, H. G., Van Haren, N. E., Nieuwenhuis, M., Hulshoff Pol, H. E., Cahn, W., and Kahn, R. S. (2016). Accelerated brain aging in schizophrenia: A longitudinal pattern recognition study. *Am. J. Psychiatry* 173, 607–616. doi: 10.1176/appi.ajp.2015.15070922

Segonne, F., Dale, A. M., Busa, E., Glessner, M., Salat, D., Hahn, H. K., et al. (2004). A hybrid approach to the skull stripping problem in MRI. *NeuroImage* 22, 1060–1075. doi: 10.1016/j.neuroimage.2004.03.032

Segonne, F., Pacheco, J., and Fischl, B. (2007). Geometrically accurate topology-correction of cortical surfaces using nonseparating loops. *IEEE Trans. Med. Imag.* 26, 518–529. doi: 10.1109/TMI.2006.887364

Shahab, S., Mulsant, B. H., Levesque, M. L., Calarco, N., Nazeri, A., Wheeler, A. L., et al. (2019). Brain structure, cognition, and brain-age in schizophrenia, bipolar disorder, and healthy controls. *Neuropsychopharmacology* 44, 898–906. doi: 10.1038/s41386-018-0298-z

Shenton, M. E., Dickey, C. C., Frumin, M., and McCarley, R. W. (2001). A review of MRI findings in schizophrenia. *Schizophr. Res.* 49, 1–52. doi: 10.1016/s0920-9964(01)00163-3

Sled, J. G., Zijdenbos, A. P., and Evans, A. C. (1998). A nonparametric method for automatic correction of intensity nonuniformity in MRI data. *IEEE Trans. Med. Imag.* 17, 87–97. doi: 10.1109/42.668698

Smith, S. M., Vidaurre, D., Alfaro-Almagro, F., Nichols, T. E., and Miller, K. L. (2019). Estimation of brain-age delta from brain imaging. *NeuroImage* 200, 528–539. doi: 10.1016/j.neuroimage.2019.06.017

Šprah, L., Dernovšek, M. Z., Wahlbeck, K., and Haaramo, P. (2017). Psychiatric readmissions and their association with physical comorbidity: A systematic literature review. *BMC Psychiatry* 17:2. doi: 10.1186/s12888-016-1172-3

Steen, R. G., Mull, C., Mcclure, R., Hamer, R. M., and Lieberman, J. A. (2006). Brain volume in first-episode schizophrenia: Systematic review and meta-analysis of magnetic resonance imaging studies. *Br. J. Psychiatry* 188, 510–518. doi: 10.1192/bjp.188.6.510

Strasser, H. C., Lilyestrom, J., Ashby, E. R., Honeycutt, N. A., Schretlen, D. J., Pulver, A. E., et al. (2005). Hippocampal and ventricular volumes in psychotic and nonpsychotic bipolar patients compared with schizophrenia patients and community control subjects: a pilot study. *Biol. Psychiatry* 57, 633–639. doi: 10.1016/j.biopsych.2004.12.009

Szeszko, P. R., Goldberg, E., Gunduz-Bruce, H., Ashtari, M., Robinson, D., Malhotra, A. K., et al. (2003). Smaller anterior hippocampal formation volume in antipsychotic-naive patients with first-episode schizophrenia. *Am. J. Psychiatry* 160, 2190–2197. doi: 10.1176/appi.ajp.160.12.2190

Truelove-Hill, M., Erus, G., Bashyam, V., Varol, E., Sako, C., Gur, R. C., et al. (2020). A multidimensional Neural Maturation Index reveals reproducible developmental patterns in children and adolescents. *J. Neurosci.* 40, 1265–1275. doi: 10.1523/JNEUROSCI.2092-19.2019

Van Erp, T., Walton, E., Hibar, D. P., Schmaal, L., Jiang, W., Glahn, D. C., et al. (2018). Cortical brain abnormalities in 4474 individuals with schizophrenia and 5098 control subjects via the Enhancing Neuro Imaging Genetics Through Meta Analysis (ENIGMA) Consortium. *Biol. Psychiatry* 84, 644–654. doi: 10.1016/j.biopsych.2018.04.023

Ventura, J., Nuechterlein, K. H., Subotnik, K. L., Gutkind, D., and Gilbert, E. A. (2000). Symptom dimensions in recent-onset schizophrenia and mania: A principal components analysis of the 24-item Brief Psychiatric Rating Scale. *Psychiatry Res.* 97, 129–135. doi: 10.1016/s0165-1781(00)00228-6

Vita, A., De Peri, L., Silenzi, C., and Dieci, M. (2006). Brain morphology in first-episode schizophrenia: A meta-analysis of quantitative magnetic resonance imaging studies. *Schizophr. Res.* 82, 75–88. doi: 10.1016/j.schres.2005.11.004

von Hausswolff-Juhlin, Y., Bjartveit, M., Lindström, E., and Jones, P. (2009). Schizophrenia and physical health problems. *Acta Psychiatrica Scandinavica* 119, 15–21. doi: 10.1111/j.1600-0447.2008.01309.x

Walker, E., Shapiro, D., Esterberg, M., and Trotman, H. (2010). Neurodevelopment and schizophrenia: Broadening the focus. *Curr. Direct. Psychol. Sci.* 19, 204–208. doi: 10.1177/0963721410377744

Ward, K. E., Friedman, L., Wise, A., and Schulz, S. C. (1996). Meta-analysis of brain and cranial size in schizophrenia. *Schizophr. Res.* 22, 197–213. doi: 10.1016/S0920-9964(96)00076-X

Wechsler, D. (2008). *Wechsler Adult Intelligence Scale*, 4th Edn. San Antonio, TX: Pearson Assessment.

Weir, C. B., and Jan, A. (2021). *BMI Classification Percentile And Cut Off Points*. Treasure Island (FL): StatPearls Publishing.

Wright, I. C., Rabe-Hesketh, S., Woodruff, P. W., David, A. S., Murray, R. M., and Bullmore, E. T. (2000). Meta-analysis of regional brain volumes in schizophrenia. *Am. J. Psychiatry* 157, 16–25. doi: 10.1176/ajp.157.1.16

Yeo, R. A., Ryman, S. G., van den Heuvel, M. P., de Reus, M. A., Jung, R. E., Pommy, J., et al. (2016). Graph metrics of structural brain networks in individuals with schizophrenia and healthy controls: Group differences, relationships with intelligence, and genetics. *J. Int. Neuropsychol. Soc.* 22, 240–249. doi: 10.1017/S1355617715000867

**Author Disclaimer:** The contents do not represent the views of the U.S. Department of Veterans Affairs or the United States Government.

**Conflict of Interest:** The authors declare that the research was conducted in the absence of any commercial or financial relationships that could be construed as a potential conflict of interest.

**Publisher's Note:** All claims expressed in this article are solely those of the authors and do not necessarily represent those of their affiliated organizations, or those of the publisher, the editors and the reviewers. Any product that may be evaluated in this article, or claim that may be made by its manufacturer, is not guaranteed or endorsed by the publisher.

frontiers | Frontiers in Aging Neuroscience

ORIGINAL RESEARCH
published: 26 May 2022
doi: 10.3389/fnagi.2022.857940

# Decreased Cerebral Amyloid-β Depositions in Patients With a Lifetime History of Major Depression With Suspected Non-Alzheimer Pathophysiology

*Kuan-Yi Wu[1], Kun-Ju Lin[2,3,4], Chia-Hsiang Chen[1], Chia-Yih Liu[1], Yi-Ming Wu[5], Cheng-Sheng Chen[6], Tzu-Chen Yen[2,3] and Ing-Tsung Hsiao[2,3,4]**

[1] Department of Psychiatry, Chang Gung Memorial Hospital, College of Medicine, Chang Gung University, Taoyuan City, Taiwan, [2] Department of Nuclear Medicine, Center for Advanced Molecular Imaging and Translation, Chang Gung Memorial Hospital, Taoyuan City, Taiwan, [3] Department of Medical Imaging and Radiological Sciences, College of Medicine and Healthy Aging Research Center, Chang Gung University, Taoyuan City, Taiwan, [4] Neuroscience Research Center, Chang Gung Memorial Hospital, Linkou Medical Center, Taoyuan City, Taiwan, [5] Department of Radiology, Chang Gung Memorial Hospital, Taoyuan City, Taiwan, [6] Department of Psychiatry, Kaohsiung Medical University Hospital, College of Medicine, Kaohsiung Medical University, Kaohsiung City, Taiwan

OPEN ACCESS

**Edited by:**
*Wenjing Zhang,*
*Sichuan University, China*

**Reviewed by:**
*Valeria Isella,*
*University of Milano-Bicocca, Italy*
*Jorge Matias-Guiu,*
*Complutense University of Madrid, Spain*

***Correspondence:**
*Ing-Tsung Hsiao*
*ihsiao@mail.cgu.edu.tw*

**Specialty section:**
*This article was submitted to Neurocognitive Aging and Behavior, a section of the journal Frontiers in Aging Neuroscience*

**Received:** *19 January 2022*
**Accepted:** *11 April 2022*
**Published:** *26 May 2022*

**Citation:**
*Wu K-Y, Lin K-J, Chen C-H, Liu C-Y, Wu Y-M, Chen C-S, Yen T-C and Hsiao I-T (2022) Decreased Cerebral Amyloid-β Depositions in Patients With a Lifetime History of Major Depression With Suspected Non-Alzheimer Pathophysiology. Front. Aging Neurosci. 14:857940. doi: 10.3389/fnagi.2022.857940*

Cerebral amyloid-β (Aβ) depositions in depression in old age are controversial. A substantial proportion of individuals with late-life major depressive disorder (MDD) could be classified as having suspected non-Alzheimer's disease pathophysiology (SNAP) by a negative test for the biomarker amyloid-β (Aβ−) but positive neurodegeneration (ND+). This study aimed to evaluate subthreshold Aβ loads in amyloid-negative MDD, particularly in SNAP MDD patients. This study included 46 amyloid-negative MDD patients: 23 SNAP (Aβ−/ND+) MDD and 23 Aβ−/ND− MDD, and 22 Aβ−/ND− control subjects. All subjects underwent $^{18}$F-florbetapir PET, FDG-PET, and MRI. Regions of interest (ROIs) and voxel-wise group comparisons were performed with adjustment for age, gender, and level of education. The SNAP MDD patients exhibited significantly deceased $^{18}$F-florbetapir uptakes in most cortical regions but not the parietal and precuneus cortex, as compared with the Aβ−/ND− MDD and control subjects (FDR correction, $p < 0.05$). No correlations of neuropsychological tests or depression characteristics with global cortical uptakes, but significant positive correlations between cognitive functions and adjusted hippocampal volumes among different groups were observed. The reduced Aβ depositions in the amyloid-negative MDD patients might be attributed mainly to the SNAP MDD patients. Our results indicated that meaningfully low amounts of subclinical Aβ might contain critical information on the non-amyloid-mediated pathogenesis.

**Keywords: suspected non-Alzheimer pathophysiology (SNAP), major depressive disorder (MDD), amyloid-β (Aβ), $^{18}$F-florbetapir (AV-45/Amyvid), neurodegeneration, depression in old age**

## INTRODUCTION

Converging evidence from multiple meta-analyses (Jorm, 2001; Ownby et al., 2006; Diniz et al., 2013) suggests that depression approximately doubles an individual's risk of developing dementia later in life. Brain amyloid-β (Aβ) deposition serves as a gold-standard hallmark of pathogenesis in Alzheimer's disease (AD). Early autopsy studies (Rapp et al., 2006) have shown more pronounced Aβ plaque in AD patients who have lifetime major depressive disorder (MDD) as compared with those without MDD. Depression in old age has been increasingly investigated in terms of the relationship with *in vivo* cerebral Aβ via validated amyloid imaging in the past decade. However, the results regarding cerebral Aβ amounts in depression have been inconsistent and controversial. Butters et al. (2008) and Wu et al. (2014) found that MDD patients have increased cortical Aβ in comparison with non-depressed healthy controls; however, Madsen et al. (2012) found no difference between midlife MDD and cognitively normal individuals. Unexpectedly, a recent study by Mackin et al. (2021) showed an even more reduced cortical Aβ level in depressed elderly patients as compared with non-depressed cognitively normal subjects. Therefore, to date, related studies have yielded variable and conflicting results.

Depression in old age, not surprisingly, might represent an etiological entity with both clinical and pathophysiological heterogeneity. Our previous study (Wu et al., 2018) provided evidence of the diversity of involved neurodegenerative processes in elderly depressed individuals. We found that some depressed elderly patients entered the AD prodrome; others might be subject to a neurodegenerative pathway completely distinct from AD. In the past, we have always paid more attention to amyloid positivity for an accurate diagnosis of AD; however, the impact of subthreshold Aβ is gradually being explored (Bischof and Jacobs, 2019). Recent studies reported subthreshold Aβ and Aβ accumulation rate could predict early tau deposition in those who were nominally amyloid negative (Leal et al., 2018). Additionally, non-amyloid-mediated neurodegeneration could be associated with subthreshold Aβ changes (Jack et al., 2013). Subthreshold Aβ might provide clinically meaningful and useful information that may reflect various individual neurodegenerative processes. To date, a subthreshold Aβ condition among amyloid-negative MDD patients remains largely unclear. In order to make group comparisons on the same basis of amyloid negativity status, both samples of amyloid-negative MDD and control subjects were included in this study.

Among the amyloid-negative individuals, a suspected non-Alzheimer disease pathophysiology (SNAP) can be indicated by a negative test for β-amyloid (Aβ−) but a positive test for neurodegeneration (ND+). Hippocampal atrophy and glucose hypometabolism within AD-vulnerable regions have been widely adopted as ND biomarkers (Jack et al., 2012; Caroli et al., 2015; Mormino et al., 2016). In this study, amyloid-negative MDD patients were further classified into SNAP (Aβ−/ND+) MDD and Aβ−/ND− MDD groups. This study aimed to investigate the subthreshold Aβ characteristics in amyloid-negative MDD subjects, particularly in SNAP MDD patients, utilizing $^{18}$F-florbetapir PET imaging.

## MATERIALS AND METHODS

### Subjects

This prospective, cross-sectional study, performed at Chang Gung Memorial Hospital Geriatric Psychiatry Center from July 2015 to June 2017, enrolled 50 MDD patients and 12 non-depressed control subjects. Of the enrolled subjects, 4 MDD patients and 1 control subject were excluded due to amyloid-positive results on $^{18}$F-florbetapir PET scanning. To increase the control sample size, another 11 control subjects were recruited from the Taiwan-Alzheimer's Disease Neuroimaging Initiative (T-ADNI) study cohort (Lin et al., 2016) owing to the availability of complete information with regards to the Aβ−/ND− profile in that cohort. Thus, a total of 46 amyloid-negative MDD and 22 Aβ−/ND− control subjects were included in the study.

Each MDD patient was assessed for the presence of lifetime major depressive episodes according to the DSM-IV [DSM-5 (American Psychiatric Association, 2013) after 2016] via a clinical structured interview and retrospective medical chart review. The lifetime course of major depression was also clarified, including age at onset of major depression, number of major depressive episodes, late-onset major depression (cut-off set at 60 years) and time since onset of first depression. Control subjects were confirmed as having an absence of lifetime psychiatric illnesses, and were deemed cognitively normal (MMSE $\geq$ 27 and CDR = 0). All subjects were aged > 50 years; had no definite neurologic diseases affecting brain structure (e.g., completed stroke, traumatic head injury or epilepsy); suffered no unstable medical diseases involving the heart, lungs, liver or kidneys; and did not have alcohol or other substance abuse currently or in the past 1 year. None of the subjects met the NIA-AA criteria for dementia due to AD (Jack et al., 2018), the IWG criteria for typical/atypical AD dementia (Dubois et al., 2014), or the DSM-5 criteria for any type of dementia (American Psychiatric Association, 2013).

All eligible subjects underwent scans of $^{18}$F-florbetapir PET, FDG-PET, and brain MRI. Apolipoprotein E (APOE) genotypes were determined by polymerase chain reaction (PCR) study, and vascular risk factors as defined by the Framingham Stroke Risk Score (FSRS) were also identified. Except for the 11 control subjects recruited from the T-ADNI study cohort, comprehensive neuropsychological tests were performed by all subjects as per our previous study, and the results are presented as standard z-scores transformed using regression-based norms, adjusted for age and level of education (Wu et al., 2016). Written informed consent was obtained from all subjects, and the study protocol was approved by the Institutional Review Boards of the Ministry of Health and Welfare and Chang Gung Medical Center.

Amyloid-negative results were evaluated according to visual rating criteria from $^{18}$F-florbetapir PET scans (Sabri et al., 2015), which were confirmed by the same experienced nuclear physician who was blind to the clinical data and imaging analysis of each

subject. The adjusted hippocampal volume (HVa) atrophy, a cut-off value described previously (Wu et al., 2018), and glucose hypometabolism within AD-vulnerable regions, as defined by the FDG t-sum score (Herholz et al., 2002), were adopted as ND biomarkers. Subjects were classified as neurodegeneration-positive (ND+) when positive for one of HVa atrophy or glucose hypometabolism (cut-off value of 6,879 $mm^3$ for HVa and 11,089.681 for FDG t-sum score). All control subjects met the Aβ−/ND− profile.

## Magnetic Resonance Imaging Acquisition and Data Preprocessing

T1-weighted MRI was performed for all subjects using a 3T Siemens Magnetom TIM Trio scanner on PET/MR (Siemens Medical Solutions, Malvern, PA, United States). An acquisition protocol using a sagittal T1-weighted magnetization prepared rapid acquisition gradient echo (MPRAGE) sequence was applied with the following acquisition parameters: Repetition Time (TR)/Echo Time (TE) = 2,600/3.12 ms, TI = 900 ms, flip angle = 13°, voxel size = 0.5 mm × 0.5 mm × 1.1 mm. Structural scans were processed using FreeSurfer version 5.3 image analysis software[1] for total bilateral hippocampal and intracranial volumes (Dale et al., 1999). A linear-regression normalization method was applied (Voevodskaya et al., 2014), with the total bilateral hippocampal volume adjusted by the estimated total intracranial volume to obtain the adjusted hippocampal volume (HVa), as described in our previous study (Wu et al., 2018), to reduce inter-subject variability.

## Positron Emission Tomography Imaging Acquisition and Data Preprocessing

Radiosynthesis of $^{18}$F-florbetapir (Yao et al., 2010) and amyloid PET data acquisition followed the same procedures as previously described (Lin et al., 2010). During the study, each $^{18}$F-florbetapir PET scan (380 ± 5 MBq) at 50–60 min post-injection was obtained using a Biograph mMR PET/MR System (Siemens Medical Solutions). The 3-D OSEM PET reconstruction algorithm (three iterations, 21 subsets; Gaussian filter: 2 mm; zoom: 3) with MR-based attenuation correction, scatter and random corrections was applied to obtain PET images with a matrix size of 344 × 344 × 127 and a voxel size of 0.83 $mm^3$ × 0.83 $mm^3$ × 2.03 $mm^3$.

$^{18}$F-FDG data were acquired at 30–50 min post-injection with a dose of 374 ± 13 MBq using a Biograph mCT PET/CT system (Siemens Medical Solutions). PET images were reconstructed using the 3D ordered subsets expectation maximization reconstruction algorithm with the parameters of four iterations, 24 subsets, Gaussian filter 2 mm, Zoom 3. In addition, CT-based attenuation correction, scatter and random corrections were performed using the correction methods provided by the manufacturer. The resulting reconstructed images were of a matrix size of 400 × 400 × 109 and a voxel size of 0.68 $mm^3$ × 0.68 $mm^3$ × 2.03 $mm^3$.

Subsequent image quantitation analysis was performed using PMOD image analysis software (version 3.7, PMOD Technologies Ltd., Zurich, Switzerland). PET images were spatially normalized to the Montreal Neurological Institute (MNI) MRI template (Hsiao et al., 2013) using an MR-based method. Standardized uptake value ratio (SUVR) images for $^{18}$F-florbetapir were generated using the whole cerebellum as the reference region for subsequent analysis.

## Statistical Analysis

Demographic and clinical data are expressed as means ± SD or absolute numbers with proportions for descriptive statistics. Continuous variables were analyzed by non-parametric statistics using the Kruskal-Wallis test with Dunn's *post hoc* multiple comparison. Categorical data were analyzed using the $X^2$ test (Fisher's exact test for APOE4, given the small numbers). Regions of interest (ROIs) comparisons of $^{18}$F-florbetapir SUVRs were conducted using the Kruskal-Wallis test with Dunn's *post hoc* analysis. In addition, analyses of covariance (ANCOVA) were conducted to compare regional $^{18}$F-florbetapir SUVRs among the three groups, with adjustment for age and years of education; pairwise differences among the adjusted means were further evaluated with Bonferroni correction. Partial correlations between global $^{18}$F-florbetapir SUVRs and the neuropsychological test data or depression characteristics were evaluated using Pearson correlation analysis, with adjustment for age, years of education and HVa. Statistical analyses were performed using IBM SPSS version 25.0 (IBM Corp., Armonk, NY, United States), and $p < 0.05$ was considered to indicate statistical significance.

Voxel-wise group comparisons were performed in Statistical Parametric Mapping 12 (SPM 12[2]) using an ANCOVA model with age, gender and level of education as covariates. Pairwise group contrasts were performed between the SNAP MDD, Aβ−/ND− MDD and control groups. To reduce the likelihood of volume effects on the results, both ROIs and voxel-wise analyses in the study were conducted with atrophy-corrected data using partial volume correction (PVC) (Gonzalez-Escamilla et al., 2017) unless otherwise specified. Furthermore, comparison results were corrected for multiple comparisons using a false discovery rate (FDR) correction at $p$ values ($p_{FDR}$) < 0.05 at the voxel level.

# RESULTS

## Subjects

The demographic and clinical characteristics of each group are shown in **Table 1**. The groups did not differ significantly in age, gender, ApoEε4 carriers, and vascular risk factors. The SNAP MDD and Aβ−/ND− MDD patients had similar HAM-D scores, in addition to similar clinical depressive features (age at onset, disease duration, depressive episodes, and late-onset depression).

In terms of neuropsychological testing, the SNAP MDD patients had greater cognitive deficits than the control subjects in all neuropsychological tests after *post hoc* analyses; the most severe deficits occurred in the executive function ($p < 0.001$) and processing speed domains ($p < 0.001$).

[1]https://surfer.nmr.mgh.harvard.edu/

[2]https://www.fil.ion.ucl.ac.uk/spm/

**TABLE 1 |** Demographic and clinical characteristics of the SNAP MDD patients, Aβ−/ND− MDD patients, and control subjects.

| Characteristic | SNAP (Aβ −/ND+) MDD (*n* = 23) | Aβ −/ND− MDD (*n* = 23) | Controls (*n* = 22) | *p* Value |
|---|---|---|---|---|
| **Age (years)[c]** | | | | |
| Mean ± SD | 65.3 ± 6.6 | 62.8 ± 4.0 | 64.1 ± 5.0 | 0.172 |
| Female gender, *n* (%) | 19 (82.6) | 19 (82.6) | 14 (63.6) | 0.226 |
| **Education (years)** | | | | |
| Mean ± SD | 8.3 ± 4.2*[a] | 8.1 ± 3.6*[a] | 11.9 ± 4.5 | 0.006 |
| **HAM-D[e]** | | | | |
| Mean ± SD | 11.1 ± 6.0***[a] | 9.3 ± 5.3**[a] | 2.6 ± 1.9 | < 0.001 |
| **MMSE** | | | | |
| Mean ± SD | 24.4 ± 4.2***[a] | 26.47 ± 2.5*[a] | 28.5 ± 1.1 | < 0.001 |
| CDR 0.5, *n* (%) | 17 (73.9)***[a] | 10 (43.5)***[a] | 0 | < 0.001 |
| APOE4, *n* (%)[d] | 5 (21.7) | 2 (8.7) | 1 (9.1) | 0.538 |
| **FSRS[d]** | | | | |
| Mean ± SD | 9.1 ± 4.3 | 9.6 ± 3.2 | 8.1 ± 1.5 | 0.317 |
| **Age at onset (years)** | | | | |
| Mean ± SD | 53.9 ± 10.7 | 52.6 ± 9.7 | – | 0.904 |
| **Duration since onset of depression (years)** | | | | |
| Mean ± SD | 11.3 ± 9.5 | 10.0 ± 9.6 | – | 0.552 |
| **Number of depressive episodes** | | | | |
| Mean ± SD | 2.3 ± 1.3 | 2.0 ± 1.3 | – | 0.366 |
| Late-onset MDD, *n* (%) | 7 (30.4) | 4 (17.4) | – | 0.494 |
| **Cognitive domain z-scores, Mean ± SD[d]** | | | | |
| Executive function | −0.8 ± 0.7***[a,*b] | −0.2 ± 0.7 | 0.3 ± 0.4 | < 0.001 |
| Memory | −1.0 ± 0.9**[a] | −0.5 ± 1.0 | 0.1 ± 0.6 | 0.004 |
| Processing speed | −1.3 ± 0.9***[a] | −0.7 ± 0.9*[a] | 0.3 ± 0.9 | < 0.001 |
| Visuospatial function | −0.4 ± 1.1*[a] | 0.2 ± 0.8 | 0.6 ± 0.6 | 0.016 |
| Language | 0.8 ± 0.8 | 1.1 ± 0.8 | 1.5 ± 0.9 | 0.058 |
| Attention | −0.4 ± 0.8**[a] | 0.1 ± 1.1 | 0.7 ± 1.0 | 0.012 |

*SNAP, suspected non-Alzheimer's disease pathophysiology; MDD, major depressive disorder; ND, neurodegeneration; HAM-D, 17-item Hamilton Depression Rating Scale; MMSE, Mini Mental Status Examination; CDR, Clinical Dementia Rating; APOE 4, Apolipoprotein E ε4 carrier; FSRS, Framingham Stroke Risk Score. p Values denote the significance of differences among the SNAP MDD, Aβ−/ND− MDD and control groups using the Kruskal-Wallis test (continuous variables) or the $x^2$ test (categorical variables).*

*[a]Dunn's post hoc analysis, significant difference between the SNAP MDD or Aβ−/ND− MDD group and the control subjects; *p < 0.05, **p < 0.01, ***p < 0.001.*

*[b]Dunn's post hoc analysis, significant difference between the SNAP MDD patients and the Aβ−/ND− MDD patients; *p < 0.05.*

*[c]Age at time of $^{18}$F-florbetapir PET scan.*

*[d]Data available for 11 control subjects only owing to recruitment of control subjects from different projects.*

Of the 23 SNAP MDD patients, there were five subjects with only hippocampal atrophy, and 11 subjects with only hypometabolism, and seven subjects with the presence of both. The neurodegeneration biomarker distributions are displayed in the **Supplementary Figure 1**.

## Regions of Interest Group Comparisons

The 46 amyloid-negative MDD patients showed significantly decreased $^{18}$F-florbetapir SUVRs as compared with the controls in most cortices except the parietal and precuneus cortex (**Supplementary Table 1**). The three-group comparisons among the SNAP MDD, Aβ−/ND− MDD and control subjects are shown in **Table 2**. There were significant differences among the three groups in all ROIs assessed except the precuneus cortex. *Post hoc* analyses showed that, as compared with the controls, the SNAP MDD patients exhibited significantly decreased $^{18}$F-florbetapir uptakes in the frontal, anterior and posterior cingulate, occipital, temporal, hippocampus, basal ganglia and global cortex. Compared with the Aβ−/ND− MDD patients, the SNAP MDD patients showed $^{18}$F-florbetapir regions with greater decreases in the parietal cortex in addition to the ROIs observed in a *post hoc* comparison of the SNAP MDD and control subjects. No differences in $^{18}$F-florbetapir uptake were observed between the Aβ−/ND− MDD and control subjects in the *post hoc* ROI analyses. The differences among the three groups are shown in **Figure 1**. In order to confirm our findings, analyses were repeated using non-PVC original data; furthermore, ANCOVA analyses were conducted using PVC data with age and level of education as covariates. Comparable results were found, and are shown in **Supplementary Tables 2**, **3**.

## Voxel-Wise Group Comparisons

The SNAP MDD patients exhibited much lower $^{18}$F-florbetapir uptakes than the control subjects in the lateral and medial frontal, anterior and posterior cingulate, temporoparietal junction, and occipital cortices, but this was not the case in the superior parietal

**TABLE 2 |** Region of interest (ROI) group comparisons among the SNAP MDD, Aβ−/ND− MDD, and control groups.

| Characteristic | SNAP (Aβ −/ND+) MDD | Aβ −/ND− MDD | Controls | *p* Value |
|---|---|---|---|---|
| | *n* = 23 | *n* = 23 | *n* = 22 | |
| Frontal | 1.06 ± 0.10****a, *b | 1.15 ± 0.06 | 1.20 ± 0.09 | < 0.0001 |
| Anterior cingulate | 1.14 ± 0.16****a, *b | 1.27 ± 0.11 | 1.36 ± 0.12 | < 0.0001 |
| Posterior cingulate | 1.23 ± 0.13**a, *b | 1.35 ± 0.11 | 1.39 ± 0.16 | 0.0008 |
| Occipital | 1.19 ± 0.10**a, *b | 1.27 ± 0.07 | 1.29 ± 0.10 | 0.0015 |
| Parietal | 1.08 ± 0.12*b | 1.16 ± 0.11 | 1.15 ± 0.08 | 0.024 |
| Precuneus | 1.06 ± 0.11 | 1.11 ± 0.07 | 1.11 ± 0.08 | 0.1607 |
| Temporal | 1.01 ± 0.09***a, *b | 1.09 ± 0.07 | 1.14 ± 0.10 | 0.0004 |
| Global cortex | 1.07 ± 0.09****a, **b | 1.15 ± 0.05 | 1.19 ± 0.08 | < 0.0001 |
| Hippocampus | 1.00 ± 0.11****a, **b | 1.11 ± 0.09 | 1.15 ± 0.09 | < 0.0001 |
| Basal ganglia | 1.05 ± 0.12****a, **b | 1.16 ± 0.08 | 1.22 ± 0.09 | < 0.0001 |

*ROI, region of interest; SNAP, suspected non-Alzheimer's disease pathophysiology; MDD, major depressive disorder; ND, neurodegeneration. p Values denote the significance of differences among the SNAP MDD, Aβ−/ND− MDD and control groups using the Kruskal-Wallis test.*

*[a]Dunn's post hoc analysis, significant difference between the SNAP MDD or Aβ−/ND− MDD group and the control subjects; *p < 0.05, **p < 0.01, ***p < 0.001, ****p < 0.0001.*

*[b]Dunn's post hoc analysis, significant difference between the SNAP MDD patients and the Aβ−/ND− MDD patients; *p < 0.05, **p < 0.01.*

and precuneus areas. The most prominent decreases in $^{18}$F-florbetapir SUVR were observed in the bilateral mesial temporal cortex and hippocampus (**Figure 2**, $p_{FDR} < 0.05$, adjusted for age, gender and level of education). Moreover, the SNAP MDD patients showed significantly decreased $^{18}$F-florbetapir retention as compared with the Aβ−/ND− MDD patients in similar areas to varying degrees, involving the frontal, anterior and posterior cingulate, occipital and mesial temporal cortices (**Figure 2**, $p_{FDR} < 0.05$, adjusted for age and years of education). Regions of decreased retention were overall symmetrical.

However, in contrast, no areas of differing $^{18}$F-florbetapir retention were found between the Aβ−/ND− MDD patients and controls. Besides, reverse contrast revealed no areas of increased $^{18}$F-florbetapir retention in the SNAP MDD patients as compared with the Aβ−/ND− MDD and control groups.

## Correlation of $^{18}$F-Florbetapir Retention and Cognition, and Characteristics of Depression

Given Aβ differences among the groups, separate partial correlation analyses were conducted in the SNAP MDD, Aβ−/ND− MDD, all MDD, and the whole MDD and control subject groups. After controlling for age, level of education, and HVa, there were no correlations between the global cortical $^{18}$F-florbetapir retention and cognitive functions, including the Mini Mental State Examination (MMSE) results and each domain-specific cognitive score in each group subset. However, significant positive correlations between HVa and cognitive functions were observed in different sample groups after controlling for age, level of education, and global cortical $^{18}$F-florbetapir retention. Details of partial correlation coefficients are shown in **Table 3**.

The global $^{18}$F-florbetapir retention was not significantly correlated with HAM-D ($r = -0.149$, $p = 0.336$), age at onset of depression ($r = -0.084$, $p = 0.587$), number of major depressive episodes ($r = 0.037$, $p = 0.812$), or time since onset of depression ($r = 0.064$, $p = 0.682$), after controlling for age and level of education.

# DISCUSSION

Unexpectedly, the SANP MDD group not only met the predefined criteria of an amyloid-negative status, but even exhibited a significantly reduced cerebral Aβ burden relative to the control and Aβ−/ND− MDD subjects in several brain regions. The most prominent decrease emerged in the bilateral mesial temporal cortex. The lack of differences of Aβ burden in the parietal and precuneus cortex between the SNAP MDD and control groups supported that the SNAP MDD patients had no preexisting early AD pathophysiology into the amyloid pathway. HVa atrophy, but not Aβ burden, had significant correlations with cognitive deficits in the total MDD and Aβ−/ND− MDD samples. However, in the SNAP MDD patients, neither HVa nor Aβ deposition were correlated with cognitive functions.

In the context of depression increasing the risk of incident dementia, early evidence connecting Aβ to depression came from postmortem studies of AD dementia patients, revealing an association between Aβ plaque and a lifetime history of MDD (Rapp et al., 2006). The advances of validated amyloid PET imaging enabled study of Aβ *in vivo*. In our previous studies (Wu et al., 2014, 2016), elderly patients with lifetime MDD, especially those with amnestic mild cognitive impairment, carried a greater Aβ burden in the parietal and precuneus cortex as compared with the controls. However, among subjects with midlife MDD, Madsen et al. (2012) demonstrated no global Aβ difference between cognitively normal MDD patients and control subjects. A population-based longitudinal study performed in Rotterdam (Mirza et al., 2016) provided some insight into the inconsistent results regarding Aβ in depression in old age, as that study uncovered that a substantially higher risk of dementia appeared in elderly depressed groups with an increasing depression trajectory, suggesting that depression might be a prodrome of dementia. In response to the postulation regarding depression as an AD prodrome, longitudinal studies have identified incident depressive symptoms corresponding to the baseline Aβ burden in cognitively normal older adults (Harrington et al., 2017; Donovan et al., 2018; Gatchel et al., 2019). Taken together, current evidence indicates that depression, especially late-onset depression, appears more likely to be a marker of incipient dementia than a true risk factor.

Challenging existing assumptions, Mackin et al. (2021) presented a shocking finding contrary to expectations, in that depressed elderly patients showed less Aβ accumulation than non-depressed subjects. Compared with the non-depressed group, which included individuals with a matched proportion of MCI, the depressed group exhibited decreased global Aβ

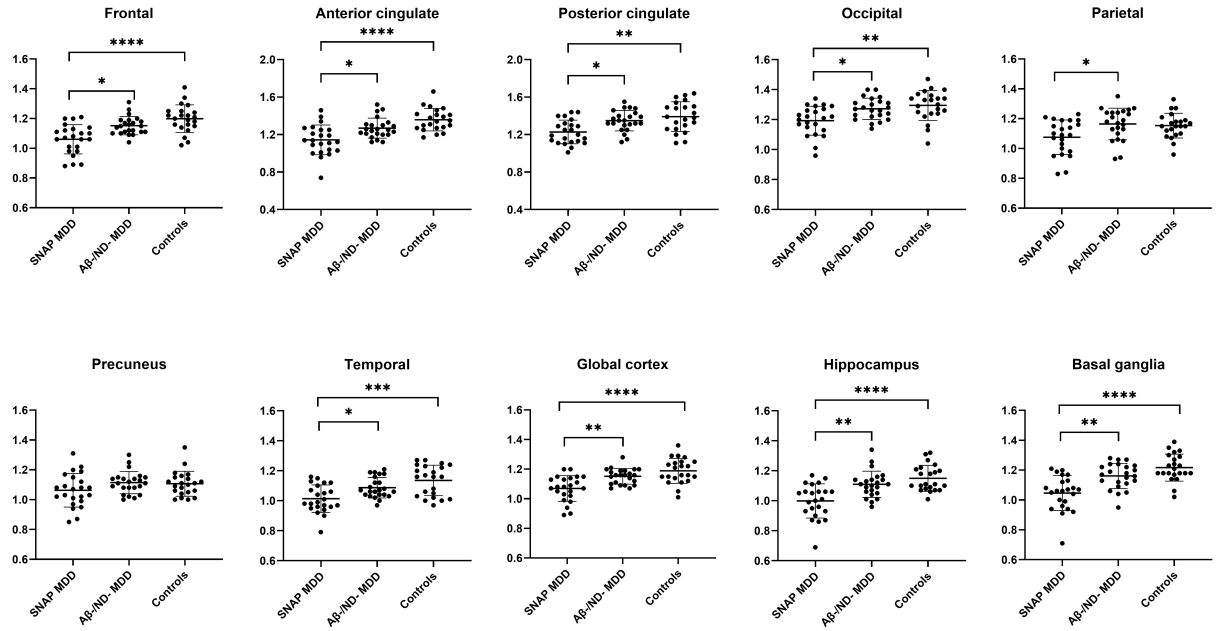


**FIGURE 1 |** Regions of interest comparisons of $^{18}$F-florbetapir SUVRs in the SNAP ($n$ = 23) and Aβ–/ND– MDD ($n$ = 23) patients and controls ($n$ = 22) using data of partial volume correction (PVC). *$p < 0.05$, **$p < 0.01$, ***$p < 0.001$, ****$p < 0.0001$ using the Kruskal-Wallis test with Dunn's *post hoc* analysis.

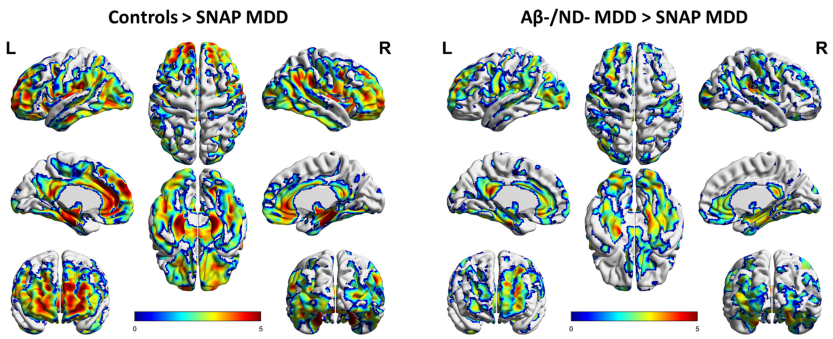


**FIGURE 2 |** Voxel-wise comparisons of $^{18}$F-florbetapir uptakes in the SNAP ($n$ = 23) and Aβ–/ND– MDD ($n$ = 23) patients and controls ($n$ = 22) using data of partial volume correction (PVC). Voxel-wise analyses were performed, including age, gender and level of education as covariates. Shown are T-maps using false discovery rate (FDR) correction for multiple comparisons ($p_{FDR} < 0.05$), with 3D brain renderings of $^{18}$F-florbetapir PET analysis on the ch2 template brain. Renders were created using BrainNet Viewer (https://www.nitrc.org/projects/bnv/).

**TABLE 3 |** Correlations of cognitive functions with global cortical Aβ depositions and HVa in the different sample groups.

| | SNAP MDD ($n$ = 23) | | Aβ −/ND− MDD ($n$ = 23) | | MDD ($n$ = 46) | | MDD and controls ($n$ = 68) | |
|---|---|---|---|---|---|---|---|---|
| | Global Aβ | HVa | Global Aβ | HVa | Global Aβ | HVa | Global Aβ | HVa |
| MMSE | −0.215 | 0.468* | 0.057 | 0.234 | −0.013 | 0.388* | 0.050 | 0.267* |
| Processing Speed | −0.247 | 0.406 | −0.064 | 0.274 | −0.087 | 0.388* | −0.028 | 0.418** |
| Executive | −0.434 | 0.072 | 0.164 | 0.395 | −0.031 | 0.267 | −0.064 | 0.324* |
| Language | −0.203 | 0.285 | −0.174 | 0.603** | −0.103 | 0.434** | −0.253 | 0.372** |
| Visuospatial | 0.126 | −0.104 | 0.250 | 0.534* | 0.231 | 0.141 | 0.150 | 0.184 |
| Memory | −0.073 | 0.389 | 0.269 | 0.486* | 0.085 | 0.412** | 0.070 | 0.416** |
| Attention | 0.036 | 0.310 | −0.325 | 0.392 | −0.044 | 0.351* | −0.127 | 0.381** |

*SNAP, suspected non-Alzheimer's disease pathophysiology; MDD, major depressive disorder; ND, neurodegeneration; HVa, adjusted hippocampal volume; MMSE, Mini Mental Status Examination. *$p < 0.05$, **$p < 0.01$ after adjustment for age, years of education and global cortical Aβ burden.*

accumulation and a lower proportion of Aβ positivity. They performed a second similar analysis restricting the sample to subsets of cognitively normal participants both in the depressed and non-depressed groups, which yielded results indicating a significant difference with regards to Aβ positivity, but not for Aβ burden.

In the present study, we observed that the amyloid-negative MDD patients had a significantly lesser Aβ burden than the control subjects. Moreover, the SNAP MDD population was the group that contributed most strongly to the result of reduced Aβ deposition. Corresponding to the reports by Mackin et al. (2021), our findings might provide a possibility as well as evidence to explain that other non-amyloid-mediated pathways may be associated with potential cortical Aβ reduction in depressed older adults. Nevertheless, we did not agree with the interpretation speculated by Mackin et al. that reduced cerebral blood flow or hypometabolism in depression may limit regional Aβ uptake (Mackin et al., 2021). Regional cerebral hypometabolism in SNAP by definition would mimic the metabolism pattern in AD; however, AD patients present with a typical abundant Aβ burden, and therefore decreased Aβ accumulation in the SNAP MDD group might be related to their own pathology-specific factors. To date, no study has investigated the characteristic Aβ patterns showing reduced Aβ depositions in SNAP patients with or without depression (Jack et al., 2012; Burnham et al., 2016).

Even though our findings demonstrated that other non-amyloid-mediated pathways were likely associated with reduced Aβ in the SNAP MDD patients, we did not refute the possibility that an increased Aβ burden is associated with the AD pathway in depression in old age. We very much agree with the comments of Christopher et al. (Van Dyck et al., 2021) that these diverse results should remind us of the tremendous heterogeneity regarding neurodegenerative pathophysiology in depression in old age. We should not expect most of depression in old age to have a uniform relationship with dementia pathogenesis. Some depressed individuals who enter the Aβ cascade in preclinical or prodromal AD stages may carry a greater Aβ burden; other depressed individuals have diverse Aβ depositions when they are on other non-AD pathways. Global cortical Aβ deposition was not found to be associated with any neuropsychological tests, whether in SNAP, Aβ−/ND− MDD, or all amyloid-negative MDD patients. However, HVa was positively associated with several neuropsychological tests in the amyloid-negative MDD sample, and when restricting the MDD sample to the Aβ−/ND− MDD patients. These correlations disappeared when further restricting the sample to the SNAP MDD subjects, the lack of a correlation in the SNAP MDD sample perhaps being associated with unrevealed factors other than Aβ and HVa.

Several limitations of this study must be acknowledged. First, this study was limited to small sample sizes; however, our results remained robust, even when using atrophy-corrected PVC data and a stringent threshold of FDR for multiple comparisons. Second, there are amyloid-positive individuals in the cognitively healthy general population, but we included control subjects with the Aβ−/ND− profile for group comparisons on the same amyloid-negative basis. However, the SNAP MDD patients exhibited much lower Aβ depositions, while amyloid-positive control subjects were also included in the study. Third, although atrophy and hypometabolism are widely recognized as ND biomarkers in relevant SNAP studies (Caroli et al., 2015; Jack et al., 2016; Mormino et al., 2016), an operational standardized approach to measurement remains lacking a consensus (Jack et al., 2012). Individuals may be misclassified due to arbitrary cut-off values. Moreover, the pathophysiology of SNAP should remain heterogeneous. Other non-amyloid neuropathological changes, such as Aβ-independent tauopathy, hippocampal sclerosis with TDP-43, α-synucleinopathy, or argyrophilic grain disease, might contribute to and coexist with each other (Wirth et al., 2013; Mormino et al., 2016; Villeneuve, 2016). Data regarding specific pathologies of the SNAP subjects were unavailable in this study. Finally, interpretation and generalization of the findings to non-depressive subjects must acknowledge the potential limitations of this study. Notably, the finding that the SNAP and Aβ-/ND-MDD groups differed in amyloid burden despite similar psychopathological features between these two depressed groups, supported that SNAP, but not depression, is associated with reduced amyloid burden. Future studies in non-depressed subjects with SNAP are critical to determine the role of isolated SNAP on brain Aβ changes.

## CONCLUSION

In this study, the amyloid-negative MDD patients had a significantly lesser Aβ burden than the control subjects. The SNAP MDD patients were the group that contributed most strongly to the result of reduced Aβ deposition. SNAP MDD subjects represent a distinct study population with ND biomarkers mimicking AD, but pathological biomarkers not doing so. Our findings might provide a possible evidence that other non-amyloid-mediated pathways may be involved in underlying cortical Aβ reduction in depressed older adults. We envisage that the currently labeled entity "amyloid-negative individuals" might be further refined to discern individuals with substantially low amounts of Aβ. Meaningfully low amounts of subclinical Aβ might provide critical information on the pathogenesis of non-AD individuals.

## DATA AVAILABILITY STATEMENT

The data that support the findings of this study are available from the corresponding author upon reasonable request.

## ETHICS STATEMENT

The studies involving human participants were reviewed and approved by Chang Gung Medical Foundation Institutional Review Board. The patients/participants provided their written informed consent to participate in this study.

## AUTHOR CONTRIBUTIONS

K-YW, K-JL, and I-TH designed the study. K-YW, K-JL, I-TH, C-HC, Y-MW, and C-YL acquired the data. K-YW, K-JL, Y-MW, T-CY, C-SC, and I-TH analyzed the data. K-YW, K-JL, T-CY, and I-TH wrote the manuscript. All authors revised and approved the article for publication.

## FUNDING

This study was carried out with financial support from the Ministry of Science and Technology, Taiwan (MOST-108-2314-B-182A-067-MY3, MOST-110-2314-B-182A-039-MY3, MOST-106-2314-B-182-017-MY3, MOST 109-2314-B-182A-043-MY3, and MOST-109-2314-B-182-019-MY3), and grants from the Research Fund of Chang Gung Memorial Hospital (CMRPG5H0041-3, CMRPD1H0391-3, BMRP488, CORPG3J0342, CMRPG3J0371, and CMRPG3J0361). The authors also acknowledge the administrative support of the Chang Gung Memorial Hospital Clinical Trial Center, which was funded by the Ministry of Health and Welfare, Taiwan (MOHW104-TDU-B-212-113003, MOHW105-TDU-B-212-13302, MOHW106-TDU-B-212-113005, MOHW107-TDU-B-212-123005, MOHW108-TDU-B-212-133005, and MOHW109-TDU-B-212-114005).

## ACKNOWLEDGMENTS

We thank Avid Radiopharmaceuticals Inc. (Philadelphia, PA, United States) for providing the precursor for the preparation of $^{18}$F-florbetapir. We also thank the Center for Advanced Molecular Imaging and Translation, Chang Gung Memorial Hospital, Linkou, for technical support.

## SUPPLEMENTARY MATERIAL

The Supplementary Material for this article can be found online at: https://www.frontiersin.org/articles/10.3389/fnagi.2022.857940/full#supplementary-material

## REFERENCES

American Psychiatric Association (2013). *Diagnostic and Statistical Manual of Mental Disorders*. Washington, DC: American Psychiatric Association.

Bischof, G. N., and Jacobs, H. I. L. (2019). Subthreshold amyloid and its biological and clinical meaning: Long way ahead. *Neurology* 93, 72–79. doi: 10.1212/WNL.0000000000007747

Burnham, S. C., Bourgeat, P., Dore, V., Savage, G., Brown, B., Laws, S., et al. (2016). Clinical and cognitive trajectories in cognitively healthy elderly individuals with suspected non-Alzheimer's disease pathophysiology (SNAP) or Alzheimer's disease pathology: a longitudinal study. *Lancet Neurol.* 15, 1044–1053. doi: 10.1016/S1474-4422(16)30125-9

Butters, M. A., Klunk, W. E., Mathis, C. A., Price, J. C., Ziolko, S. K., and Hoge, J. A. (2008). Imaging Alzheimer pathology in late-life depression with PET and Pittsburgh Compound-B. *Alzheimer. Dis. Assoc. Disord.* 22, 261–268. doi: 10.1097/WAD.0b013e31816c92bf

Caroli, A., Prestia, A., Galluzzi, S., Ferrari, C., Der Flier, W. M., and Ossenkoppele, R. (2015). Mild cognitive impairment with suspected nonamyloid pathology (SNAP): prediction of progression. *Neurology* 84, 508–515. doi: 10.1212/WNL.0000000000001209

Dale, A. M., Fischl, B., and Sereno, M. I. (1999). Cortical surface-based analysis. *Neuroimage* 9, 179–194. doi: 10.1006/nimg.1998.0395

Diniz, B. S., Butters, M. A., Albert, S. M., Dew, M. A., and Reynolds, C. F. III (2013). Late-life depression and risk of vascular dementia and Alzheimer's disease: systematic review and meta-analysis of community-based cohort studies. *Br. J. Psychiatry* 202, 329–335. doi: 10.1192/bjp.bp.112.118307

Donovan, N. J., Locascio, J. J., Marshall, G. A., Gatchel, J., Hanseeuw, B. J., Rentz, D. M., et al. (2018). Longitudinal Association of Amyloid Beta and Anxious-Depressive Symptoms in Cognitively Normal Older Adults. *Am. J. Psychiatry* 175, 530–537. doi: 10.1176/appi.ajp.2017.17040442

Dubois, B., Feldman, H. H., Jacova, C., Hampel, H., Molinuevo, J. L., and Blennow, K. (2014). Advancing research diagnostic criteria for Alzheimer's disease: the IWG-2 criteria. *Lancet Neurol.* 13, 614–629.

Gatchel, J. R., Rabin, J. S., Buckley, R. F., Locascio, J. J., Quiroz, Y. T., and Yang, H. S. (2019). Longitudinal Association of Depression Symptoms With Cognition and Cortical Amyloid Among Community-Dwelling Older Adults. *JAMA Netw. Open.* 2:e198964. doi: 10.1001/jamanetworkopen.2019.8964

Gonzalez-Escamilla, G., Lange, C., Teipel, S., Buchert, R., Grothe, M. J., and Initiative, A. S. D. N. (2017). PETPVE12: an SPM toolbox for Partial Volume Effects correction in brain PET - Application to amyloid imaging with AV45-PET. *Neuroimage* 147, 669–677. doi: 10.1016/j.neuroimage.2016.12.077

Harrington, K. D., Gould, E., Lim, Y. Y., Ames, D., Pietrzak, R. H., and Rembach, A. (2017). Amyloid burden and incident depressive symptoms in cognitively normal older adults. *Int. J. Geriatr. Psychiatry* 32, 455–463. doi: 10.1002/gps.4489

Herholz, K., Salmon, E., Perani, D., Baron, J. C., Holthoff, V., and Frolich, L. (2002). Discrimination between Alzheimer dementia and controls by automated analysis of multicenter FDG PET. *Neuroimage* 17, 302–316. doi: 10.1006/nimg.2002.1208

Hsiao, T., Huang, C.-C., Hsieh, C.-J., Wey, S.-P., Kung, M.-P., Yen, T.-C., et al. (2013). Perfusion-like template and standardized normalization-based brain image analysis using 18F-florbetapir (AV-45/Amyvid) PET. *Eur. J. Nucl. Med. Mol. I.* 40, 908–920. doi: 10.1007/s00259-013-2350-x

Jack, C. R. Jr., Bennett, D. A., Blennow, K., Carrillo, M. C., Dunn, B., and Haeberlein, S. B. (2018). NIA-AA Research Framework: Toward a biological definition of Alzheimer's disease. *Alzheimers Dement.* 14, 535–562. doi: 10.1016/j.jalz.2018.02.018

Jack, C. R. Jr., Knopman, D. S., Weigand, S. D., Wiste, H. J., Vemuri, P., Lowe, V., et al. (2012). An operational approach to National Institute on Aging-Alzheimer's Association criteria for preclinical Alzheimer disease. *Ann. Neurol.* 71, 765–775. doi: 10.1002/ana.22628

Jack, C. R., Knopman, D. S., Chetelat, G., Dickson, D., Fagan, A. M., Frisoni, G. B., et al. (2016). Suspected non-Alzheimer disease pathophysiology - concept and controversy. *Nat. Rev. Neurol.* 12, 117–124. doi: 10.1038/nrneurol.2015.251

Jack, C. R., Wiste, H. J., Weigand, S. D., Knopman, D. S., Lowe, V., Vemuri, P., et al. (2013). Amyloid-first and neurodegeneration-first profiles characterize incident amyloid PET positivity. *Neurology* 81, 1732–1740. doi: 10.1212/01.wnl.0000435556.21319.e4

Jorm, A. F. (2001). History of depression as a risk factor for dementia: an updated review. *Aust. N. Z. J. Psychiatry.* 35, 776–781. doi: 10.1046/j.1440-1614.2001.00967.x

Leal, S. L., Lockhart, S. N., Maass, A., Bell, R. K., and Jagust, W. J. (2018). Subthreshold amyloid predicts tau deposition in aging. *J. Neurosci.* 38, 4482–4489. doi: 10.1523/JNEUROSCI.0485-18.2018

Lin, K. J., Hsu, W. C., Hsiao, I. T., Wey, S. P., Jin, L. W., Skovronsky, D., et al. (2010). Whole-body biodistribution and brain PET imaging with [18F]AV-45, a novel amyloid imaging agent–a pilot study. *Nucl. Med. Biol.* 37, 497–508. doi: 10.1016/j.nucmedbio.2010.02.003

Lin, K.-J., Hsiao, T., Hsu, J.-L., Huang, C.-C., Huang, K.-L., Hsieh, C.-J., et al. (2016). Imaging characteristic of dual-phase 18F-florbetapir (AV-45/Amyvid) PET for the concomitant detection of perfusion deficits and beta-amyloid

deposition in Alzheimer's disease and mild cognitive impairment. *Eur. J. Nucl. Med. Mol. I.* 43, 1304–1314. doi: 10.1007/s00259-016-3359-8

Mackin, R. S., Insel, P. S., Landau, S., Bickford, D., Morin, R., Rhodes, E., et al. (2021). Late-life depression is associated with reduced cortical amyloid burden: Findings from the Alzheimer's Disease Neuroimaging Initiative Depression Project. *Biol. Psychiatry* 89, 757–765. doi: 10.1016/j.biopsych.2020.06.017

Madsen, K., Hasselbalch, B. J., Frederiksen, K. S., Haahr, M. E., Gade, A., Law, I., et al. (2012). Lack of association between prior depressive episodes and cerebral [11C]PiB binding. *Neurobiol. Aging* 33, 2334–2342. doi: 10.1016/j.neurobiolaging.2011.11.021

Mirza, S. S., Wolters, F. J., Swanson, S. A., Koudstaal, P. J., Hofman, A., Tiemeier, H., et al. (2016). 10-year trajectories of depressive symptoms and risk of dementia: a population-based study. *Lancet Psychiat.* 3, 628–635. doi: 10.1016/S2215-0366(16)00097-3

Mormino, E. C., Papp, K. V., Rentz, D. M., Schultz, A. P., Lapoint, M., Amariglio, R., et al. (2016). Heterogeneity in Suspected Non-Alzheimer Disease Pathophysiology Among Clinically Normal Older Individuals. *JAMA Neurol.* 73, 1185–1191. doi: 10.1001/jamaneurol.2016.2237

Ownby, R. L., Crocco, E., Acevedo, A., John, V., and Loewenstein, D. (2006). Depression and risk for Alzheimer disease: systematic review, meta-analysis, and metaregression analysis. *Arch. Gen. Psychiatry* 63, 530–538. doi: 10.1001/archpsyc.63.5.530

Rapp, M. A., Schnaider-Beeri, M., Grossman, H. T., Sano, M., Perl, D. P., Purohit, D. P., et al. (2006). Increased hippocampal plaques and tangles in patients with Alzheimer disease with a lifetime history of major depression. *Arch. Gen. Psychiatry* 63, 161–167. doi: 10.1001/archpsyc.63.2.161

Sabri, O., Seibyl, J., Rowe, C., and Barthel, H. (2015). Beta-amyloid imaging with florbetaben. *Clin. Transl. I.* 3, 13–26. doi: 10.1007/s40336-015-0102-6

Van Dyck, C. H., O'dell, R. S., and Mecca, A. P. (2021). Amyloid-Associated Depression-or Not? *Biol. Psychiatry* 89, 737–738. doi: 10.1016/j.biopsych.2021.02.008

Villeneuve, S. (2016). Cause of Suspected Non-Alzheimer Disease Pathophysiology If Not Tau Pathology. Then What? *JAMA Neurol.* 73, 1177–1179. doi: 10.1001/jamaneurol.2016.2842

Voevodskaya, O., Simmons, A., Nordenskjold, R., Kullberg, J., Ahlstrom, H., Lind, L., et al. (2014). The effects of intracranial volume adjustment approaches on multiple regional MRI volumes in healthy aging and Alzheimer's disease. *Front. Aging Neurosci.* 6:264. doi: 10.3389/fnagi.2014.00264

Wirth, M., Villeneuve, S., Haase, C. M., Madison, C. M., Oh, H., Landau, S. M., et al. (2013). Associations between Alzheimer disease biomarkers, neurodegeneration, and cognition in cognitively normal older people. *JAMA Neurol.* 70, 1512–1519. doi: 10.1001/jamaneurol.2013.4013

Wu, K. Y., Hsiao, I. T., Chen, C. S., Chen, C. H., Hsieh, C. J., Wai, Y. Y., et al. (2014). Increased brain amyloid deposition in patients with a lifetime history of major depression: evidenced on 18F-florbetapir (AV-45/Amyvid) positron emission tomography. *Eur. J. Nucl. Med. Mol. I.* 41, 714–722. doi: 10.1007/s00259-013-2627-0

Wu, K. Y., Lin, K. J., Chen, C. H., Chen, C. S., Liu, C. Y., Huang, S. Y., et al. (2018). Diversity of neurodegenerative pathophysiology in nondemented patients with major depressive disorder: Evidence of cerebral amyloidosis and hippocampal atrophy. *Brain Behav.* 8:e01016. doi: 10.1002/brb3.1016

Wu, K. Y., Liu, C. Y., Chen, C. S., Chen, C. H., Hsiao, I. T., Hsieh, C. J., et al. (2016). Beta-amyloid deposition and cognitive function in patients with major depressive disorder with different subtypes of mild cognitive impairment: (18)F-florbetapir (AV-45/Amyvid) PET study. *Eur. J. Nucl. Med. Mol. I.* 43, 1067–1076. doi: 10.1007/s00259-015-3291-3

Yao, C. H., Lin, K. J., Weng, C. C., Hsiao, I. T., Ting, Y. S., Yen, T. C., et al. (2010). GMP-compliant automated synthesis of [(18)F]AV-45 (Florbetapir F 18) for imaging beta-amyloid plaques in human brain. *Appl. Radiat. Isot.* 68, 2293–2297. doi: 10.1016/j.apradiso.2010.07.001

**Conflict of Interest:** The authors declare that the research was conducted in the absence of any commercial or financial relationships that could be construed as a potential conflict of interest.

**Publisher's Note:** All claims expressed in this article are solely those of the authors and do not necessarily represent those of their affiliated organizations, or those of the publisher, the editors and the reviewers. Any product that may be evaluated in this article, or claim that may be made by its manufacturer, is not guaranteed or endorsed by the publisher.

frontiers | Frontiers in Aging Neuroscience

ORIGINAL RESEARCH
published: 27 May 2022
doi: 10.3389/fnagi.2022.873148

# The Alternation of Gray Matter Morphological Topology in Drug-Naïve Tourette's Syndrome in Children

*Yi Liao[1,2], Xiuli Li[3], Fenglin Jia[1,2], Yuexin Jiang[4], Gang Ning[1,2], Xuesheng Li[1,2], Chuan Fu[1,2], Hui Zhou[2,5], Xuejia He[1,2], Xiaotang Cai[2,5*†] and Haibo Qu[1,2*†]*

[1] Department of Radiology, West China Second University Hospital, Sichuan University, Chengdu, China, [2] Key Laboratory of Birth Defects and Related Diseases of Women and Children (Sichuan University), Ministry of Education, Chengdu, China, [3] Department of Radiology, West China Hospital, Sichuan University, Chengdu, China, [4] Department of Radiology, Chengdu Office Hospital of People's Government of Tibet Autonomous Region, Chengdu, China, [5] Department of Rehabilitation, West China Second University Hospital, Sichuan University, Chengdu, China

Tourette syndrome (TS) is a neurodevelopment disorder characterized by motor and phonic tics. We investigated the topological alterations in pediatric TS using morphological topological analysis of brain structures. We obtained three-dimensional T1-weighted magnetic resonance imaging (MRI) sequences from 59 drug-naïve pediatric patients with TS and 87 healthy controls. We identified morphological topographical alterations in the brains of patients with TS compared to those of the healthy controls *via* GRETNA software. At the global level, patients with TS exhibited increased global efficiency ($E_{glob}$) ($p = 0.012$) and decreased normalized characteristic path length ($\lambda$) ($p = 0.027$), and characteristic path length (Lp) ($p = 0.025$) compared to healthy controls. At the nodal level, we detected significant changes in the nodal betweenness, nodal degree, and nodal efficiency in the cerebral cortex-striatum-thalamus-cortex circuit. These changes mainly involved the bilateral caudate nucleus, left thalamus, and gyri related to tics. Nodal betweenness, nodal degree, and nodal efficiency in the right superior parietal gyrus were negatively correlated with the motor tic scores of the Yale Global Tic Severity Scale (YGTSS) ($r = -0.328$, $p = 0.011$; $r = -0.310$, $p = 0.017$; and $r = -0.291$, and $p = 0.025$, respectively). In contrast, nodal betweenness, nodal degree, and nodal efficiency in the right posterior cingulate gyrus were positively correlated with the YGTSS phonic tic scores ($r = 0.353$, $p = 0.006$; $r = 0.300$, $p = 0.021$; $r = 0.290$, and $p = 0.026$, respectively). Nodal betweenness in the right supplementary motor area was positively correlated with the YGTSS phonic tic

OPEN ACCESS

**Edited by:**
*Wei Deng,*
*Affiliated Mental Health Center and Hangzhou Seventh People's Hospital, China*

**Reviewed by:**
*Natalia Szejko,*
*Yale University, United States*
*Xize Jia,*
*Hangzhou Normal University, China*

***Correspondence:**
*Xiaotang Cai*
*cxt_1999@126.com*
*Haibo Qu*
*windowsqhb@126.com*

*† These authors have contributed equally to this work*

**Specialty section:**
*This article was submitted to Neurocognitive Aging and Behavior, a section of the journal Frontiers in Aging Neuroscience*

**Received:** *10 February 2022*
**Accepted:** *29 April 2022*
**Published:** *27 May 2022*

**Citation:**
*Liao Y, Li X, Jia F, Jiang Y, Ning G, Li X, Fu C, Zhou H, He X, Cai X and Qu H (2022) The Alternation of Gray Matter Morphological Topology in Drug-Naïve Tourette's Syndrome in Children. Front. Aging Neurosci. 14:873148. doi: 10.3389/fnagi.2022.873148*

scores ($r$ = 0.348, $p$ = 0.007). The nodal degree in the right supplementary motor area was positively correlated with the YGTSS phonic tic scores ($r$ = 0.259, $p$ = 0.048). Diagnosis by age interactions did not display a significant effect on brain network properties at either the global or nodal level. Overall, our findings showed alterations in the gray matter morphological networks in drug-naïve children with TS. These findings enhance our understanding of the structural topology of the brain in patients with TS and provide useful clues for exploring imaging biomarkers of TS.

**Keywords: magnetic resonance imaging, morphological topology, Tourette's syndrome, children, gray matter**

## INTRODUCTION

Tourette syndrome (TS) is a neurodevelopmental disorder characterized by multiple motor tics and at least one vocal tic present for greater than 1 year (American Psychiatric Association [APA], 2013). The symptoms wax and wane in frequency (American Psychiatric Association [APA], 2013). The age of onset is before 18 years (American Psychiatric Association [APA], 2013). Motor tics start at the age of 3–8 years, while phonic tics can begin as early as 3 years, but typically they follow the onset of motor tics by several years (Leckman and Cohen, 1999; Leckman, 2002). Some symptoms gradually decrease with age, whereas others persist into adulthood. TS may be comorbid with autism spectrum disorder (ASD), obsessive-compulsive disorder (OCD), attention deficit hyperactivity disorder (ADHD), or other mental disorders. The symptoms of TS are complex, recurrent, difficult to treat, and are often accompanied by a variety of behavioral disorders, which greatly impact children's ability to learn, live, and interact socially (Robertson, 2000). The neural mechanisms, by which tics arise, are not fully understood. The pathogenesis of TS remains unclear, and genetic defects can lead to neuroanatomical abnormalities and neurobiochemical dysfunction. Most scholars speculate that the disease is related to neuronal dysfunction in the basal ganglia, prefrontal lobe, and limbic system, and its onset is related to various factors, such as psychiatric, environmental, genetic, and epigenetic factors, as well as embryonic development and infections, biochemical metabolism, and improper medication. Dysregulation of the actions of brain dopamine and 5-hydroxytryptamine and their interactions are currently considered to be related to tics, and abnormalities in the cerebral cortex-striatum-thalamus-cortex (CSTC) circuit are associated with the development of TS (Leckman, 2002).

In recent years, MRI has rapidly developed. It is non-invasive and has a high temporal and spatial resolution. MRI can provide physiopathological information at multiple levels, from macroscopic tissue morphology to microscopic subcellular structures, from blood flow and energy metabolism to functional changes in brain regions for the diagnosis, prediction, treatment, and evaluation of diseases. The development of multimodal neuroimaging with MRI has provided an opportunity to achieve a breakthrough in elucidating the neurological mechanisms of neuropsychiatric disorders and to explore objective indicators for clinical diagnosis and treatment (Gong, 2020). This provides strong technical support for investigating the structure and function of the brain. Several studies have explored structural brain imaging changes in patients with TS compared to those of healthy controls. Kong et al. (2020) conducted a surface-based study and detected alterations in cortical thickness, sulcus, cortical curvature, and local gyrification index in 52 patients with TS compared with those structures in 52 healthy controls. Greene et al. conducted a study on altered gray matter and white matter in 103 children with TS and 103 healthy controls. They observed an increase in the volume of the gray matter of the posterior thalamus, hypothalamus, and midbrain and a decrease in the volume of the white matter bilaterally in the orbital and medial prefrontal cortex using the voxel-based morphometry approach (Greene et al., 2017). Draper et al. (2016) reported that premonitory sensory phenomena are negatively related to the thicknesses of the insula and sensorimotor cortex. White matter abnormalities of the cortical-striatal-pallido-thalamic were explored in a study by Worbe et al. (2015) and they determined that there was an increase in the brain volume in the thalamus and right cingulum bundle. A decrease in white matter volume in the right frontal pole was reported by Liu et al. (2013), and brain volume changes were observed in the bilateral frontal and left temporal lobes. A reduction in gray matter volume in the bilateral frontal lobe and cingulum was reported by Draganski et al. (2010). Müller-Vahl et al. (2009) detected both gray matter volume and white matter volume reductions in the frontal lobe. Increases were found in the left middle frontal gyrus and left sensorimotor areas. The YGTSS scores were negatively correlated with the gray matter volume.

The aforementioned studies demonstrated gray and white matter alterations in brain regions involved CSTC in pediatric patients with TS. However, there have been no structure-based topological analyses on TS in children. A novel approach called structural covariance network (SCN) analysis has been utilized for brain structure analysis in 3D T1-weighted imaging (Seidlitz et al., 2018; Sun et al., 2018). The analysis was performed using structural brain data to construct a structural network with correlations (He et al., 2007; Alexander-Bloch et al., 2013). The analysis was performed using structural brain data to construct correlations between structural networks. It is a useful tool for morphological topological analysis of the brain (Tijms et al., 2012). We aimed to explore the morphological topological alterations in the gray matter of pediatric patients with TS. This study hypothesized that gray matter morphological topology differed in pediatric patients with TS from healthy controls.

# MATERIALS AND METHODS

## Participants

Participants were recruited from July 2015 to June 2020 at West China Second University Hospital, Sichuan University. This study was approved by the Ethics Committee of the West China Second University of Sichuan University. The legal guardians of all pediatric patients provided written informed consent. A total of 59 pediatric and adolescent patients with TS were recruited from West China Second University Hospital, Sichuan University. The diagnosis criteria of pediatrics were made according to the Diagnostic and Statistical Manual of Mental Disorders-5 (*DSM-V*) (American Psychiatric Association [APA], 2013). The *DSM-V* criteria for Tourette disorder are as follows (American Psychiatric Association [APA], 2013): (i) both multiple motor and one or more vocal tics were present at some time during the illness, though not necessarily concurrently (a tic is a sudden, rapid, recurrent, non-rhythmic, stereotyped motor movement, or vocalization); (ii) the tics may wax and wane in frequency, but have persisted for more than 1 year since the onset of the first tic; (iii) onset occurred before 18 years of age; and (iv) the disturbance is not due to the direct physiological effects of a substance (e.g., cocaine) or a general medical condition (e.g., Huntington's disease or post-viral encephalitis). The exclusion criteria were as follows: (1) concomitant with other neurological, psychiatric, or metabolic diseases; (2) MRI scans indicated structural or signal abnormalities of intracranial lesions; (3) claustrophobia or otherwise unsuitable for MRI scans; and (4) medication used for TS treatment. Initially, 85 patients with TS were recruited. Fourteen patients with TS were concomitant with ADHD. Three patients with TS were concomitant with OCD. No patient with TS were concomitant with OCD and ADHD or ASD. One of the patients with TS had a combination of abnormal thyroid function. Six patients were excluded because of image quality issues. Two patients fail to persist through the examination. All above 26 patients were excluded. Finally, 59 patients with TS were included in this study.

A total of 87 age- and gender-matched healthy pediatric controls participated in this study. The exclusion criteria were as follows: (1) neurological, psychiatric, or other metabolic diseases; (2) MRI scans indicated structural or signal abnormalities of intracranial lesions; (3) claustrophobia or otherwise unsuitable for MRI scans; and (4) a history of mental disorders.

## Data Acquisition

Clinical data are collected using a standardized process for assessment and collection by clinicians. All the participants are drug- naïve.

Imaging data were collected from pediatric patients with TS and healthy controls (HCs). All participants were scanned using 1.5T MRI and 3D T1 structural images were obtained. The scan parameters for T1-weighted imaging were as follows: echo time = 4.6 ms; repetition time = 9.6 ms; flip angle = 8°; slice thickness = 1 mm; no interslice gap; voxel size = 0.8 × 0.8 × 0.6 $mm^3$; field of view = 240 mm × 240 mm; and matrix size = 256 × 256. The total number of slices was 162.

## Data Preprocessing

Magnetic resonance images were evaluated by two expert radiologists (YL and HQ with 11 years and 16 years of MRI diagnosis experience, respectively) for artifacts, structural, or signal abnormalities, and 6 subjects were excluded from the study. Routine image processing, such as spatial smoothing and spatial normalization, was performed using the Statistical Parametric Mapping (SPM) software package (version 12[1]) for voxel-based morphometry (VBM) analysis (Ashburner et al., 2000). Specifically, tissue segmentation was performed with structural images (Ashburner and Friston, 2005) and the segmented gray matter (GM) of each subject was non-linearly co-registered to the generated study-specific template using Diffeomorphic Anatomical Registration Through Exponentiated

[1]http://www.fil.ion.ucl.ac.uk/spm/software/spm12/

**TABLE 1 |** Demographic characteristics of patients with Tourette's syndrome (TS) and healthy controls (HCs).

| Characteristics | Tourette's syndrome | | Healthy control | | |
|---|---|---|---|---|---|
| | Mean | SD | Mean | SD | *P*-value |
| Age (years) | 7.97 | 1.91 | 8.67 | 2.63 | 0.136 |
| Education (years) | 2.24 | 1.70 | 2.89 | 1.72 | 0.642 |
| Gender (Male/Female) | 36/23 | NA | 48/39 | NA | 0.483 |
| Age at onset (years) | 5.38 | 2.79 | NA | NA | NA |
| Disease duration (month) | 23.00 | 21.42 | NA | NA | NA |
| Total YGTSS score | 22.84 | 7.56 | NA | NA | NA |
| Total motor tic score | 13.96 | 4.32 | NA | NA | NA |
| Total phonic tic score | 8.88 | 4.60 | NA | NA | NA |

**TABLE 2 |** Regions showing altered node centrality (including nodal betweenness, nodal degree, and nodal efficiency) in patients with TC and HCs.

| Brain regions | *P*-values | | |
|---|---|---|---|
| | Nodal betweenness | Nodal degree | Nodal efficiency |
| **TS > HC** | | | |
| SMA.R | 0.0371* | 0.0006* | 0.0006* |
| ORBsupmed.R | 0.0645 | 0.0027* | 0.0080 |
| PCG.R | 0.3837 | 0.0002* | 0.0002* |
| SOG.L | 0.0022* | 0.0002* | 0.0004* |
| CAU.L | 0.0073 | 0.0024* | 0.0025 |
| CAU.R | 0.1313 | 0.0024* | 0.0043 |
| THA.L | 0.0002* | 0.0004* | 0.1222 |
| **TS < HC** | | | |
| ORBinf.R | 0.0022* | 0.0159 | 0.1013 |
| SPG.R | 0.0002* | 0.0041* | 0.0621 |
| TROsup.R | 0.0031* | 0.0020* | 0.0039 |

**Significant differences with FDR correction were applied to each nodal measure. A permutation test was conducted to get the p-values. CAU, caudate nucleus; HC, healthy control; L, left; ORBinf, inferior frontal gyrus, orbital part; ORBsupmed, superior frontal gyrus, medial orbital; PCG, posterior cingulate gyrus; R, right; SMA, supplementary motor area; SOG, superior occipital gyrus; SPG, superior parietal gyrus; THA, thalamus; TPOsup, temporal pole: superior temporal gyrus; TS, Tourette's syndrome.*

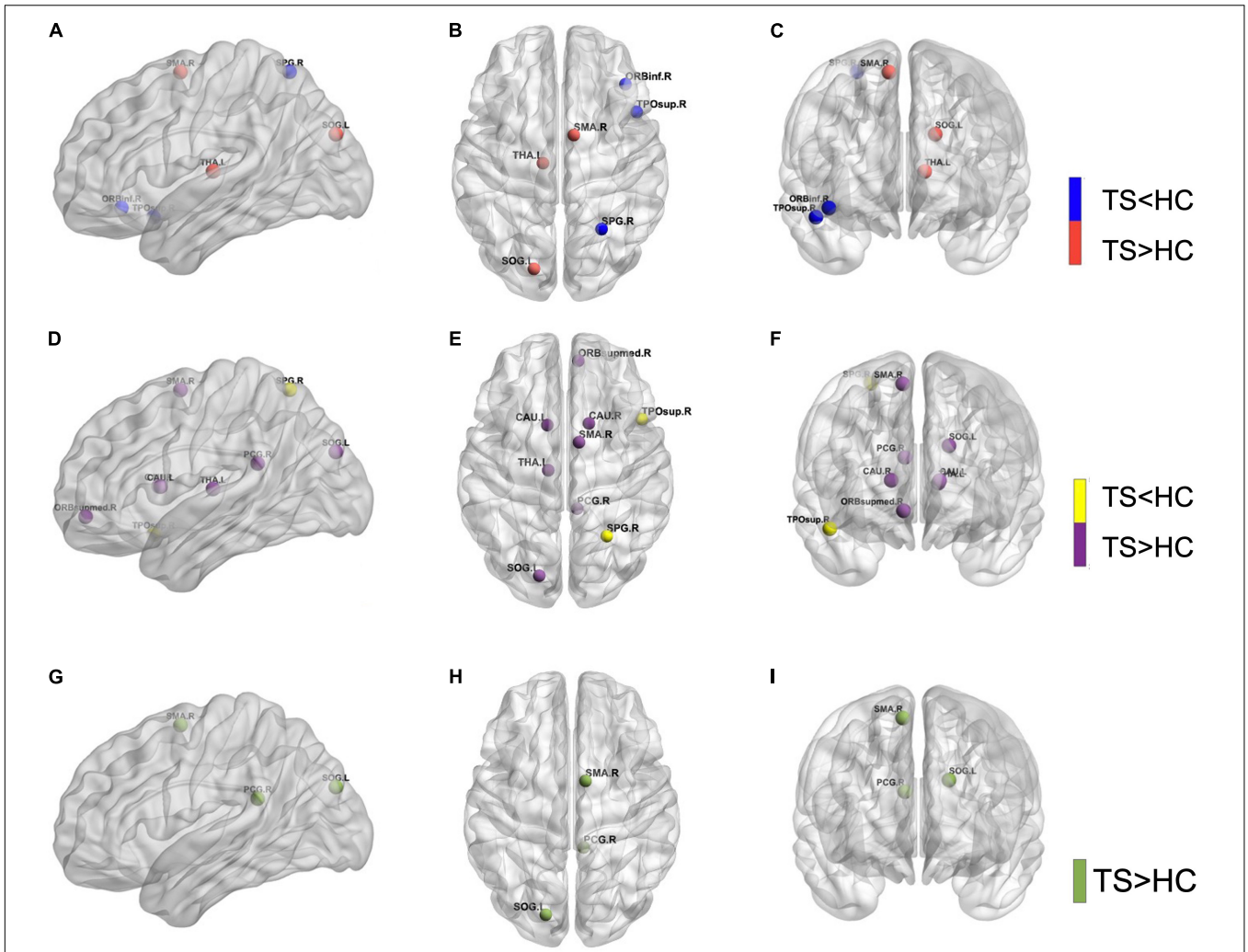


**FIGURE 1 |** The significant alternations of nodal betweenness **(A–C)**, nodal degree **(D–F)**, and nodal efficiency **(G–I)** of gray matter (GM) in pediatric Tourette syndrome and healthy controls. CAU, caudate nucleus; HC, healthy control; L, left; ORBinf, inferior frontal gyrus, orbital part; ORBsupmed, superior frontal gyrus, medial orbital; PCG, posterior cingulate gyrus; R, right; SMA, supplementary motor area; SOG, superior occipital gyrus; SPG, superior parietal gyrus; THA, thalamus; TPOsup, temporal pole: superior temporal gyrus; TS, Tourette syndrome.

Lie Algebra (DARTEL) software (Ashburner, 2007). Co-registered images were then transformed to the standard Montreal Neurological Institute (MNI) space, the same space as the brain parcellation, modulated by the Jacobian determinants derived from the spatial normalization to preserve tissue volume after warping, resampled to a 2-mm isotropic resolution, and finally smoothed using a Gaussian kernel with a 6-mm full-width half-maximum (FWHM).

## Construction of Gray Matter Morphological Networks

For each subject, the nodes of the GM network were defined as the 90 cortical regions of interest (ROIs) (Tzourio-Mazoyer et al., 2002) utilizing the automated anatomical labeling (AAL) algorithm. The edges were defined as the Kullback–Leibler divergence-based similarity (KLS) measurement (Kong et al., 2014) of morphological distributions between different cortical regions, which was previously described in detail (Kong et al., 2014, 2015; Wang et al., 2016). Briefly, kernel density estimation (KDE) (Wang et al., 2016) was used to estimate the probability density functions (PDFs) of image intensities within each cortical region from the AAL method, with the KDE bandwidths estimated by Scott's rule (Scott, 2015) using public Matlab codes (function: kde[2]). The similarity of image intensity PDFs of different cortical regions was quantified as the Kullback–Leibler (KL) divergence, which is a probability theory index calculating the differences between two probability distributions (Burnhan and Anderson, 2002). KLS values range between 0 and 1, where 1 represents an identical distribution for the two regions. The KL-based similarity values between all possible pairs of 90 cortical

[2]http://www.mathworks.com/matlabcentral/fileexchange/14034-kernel-density-estimator

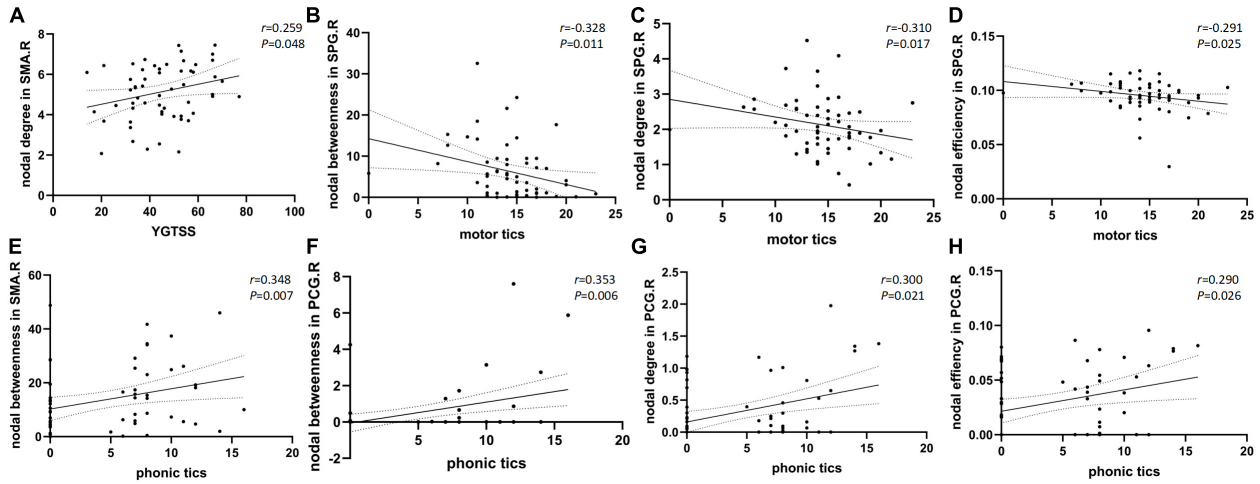


**FIGURE 2 |** Scatter plots with 95% confidence interval (CI) of nodal brain network properties of different regions compared to YGTSS total scores **(A)** and sub scores of motor tics **(B–D)** and phonic tics **(E–H)**.

regions formed a 90×90 similarity matrix, in which each element represents the similarity of morphological distributions between two cortical regions.

The GM structural network properties were calculated using the Matlab-based GRETNA software (Wang et al., 2015). This method was sensitive in detecting the morphological topology (e.g., He et al., 2009; Zhang et al., 2011). A wide range of the sparsity (S) thresholds was set up with a wide range for each correlation matrix. The range values of S were set to make sure that the thresholded networks were measured for the small-worldness with sparse properties and had the minimum number of spurious edges (Watts and Strogatz, 1998). Consequently, threshold values, ranging between 0.10 and 0.34 with an interval of 0.01, were used. All global and nodal network metrics were measured at each sparsity value. For each network metric, the area under the curve (AUC) was calculated to reflect measures across the sparsity parameter S. Nodes with statistically significant differences in network efficiency of local brain regions between the two groups of subjects were visualized using the BrainNet Viewer software (Version 1.6[3]).

At the global level, global efficiency ($E_{glob}$), characteristic path length (Lp), normalized characteristic path length (λ), clustering coefficient (Cp), normalized clustering coefficient (γ), and small-worldness (σ) were calculated. At the nodal level, the nodal degree, nodal efficiency ($E_{loc}$), and nodal betweenness were computed (Rubinov and Sporns, 2010). Briefly, Cp reflects the local interconnectivity extent. Lp measures the average distance or routing efficiency between any pair of network nodes, with higher values indicating lower routing efficiency. Small-world attributes (γ, λ, and σ) indicate the degree of organization of the small world. $E_{glob}$ indicates the global efficiency of parallel information transfer in the network. $E_{loc}$ reflects the communication efficiency among the first neighbors of a node. The nodal degree reflects the capacity to communicate information. The nodal efficiency indicates the nodal efficiency of parallel information transfer. The nodal betweenness centrality means the influence of a node over information flow between other nodes in the network. Detailed information on these metrics was previously provided (Rubinov and Sporns, 2010).

## STATISTICAL ANALYSIS

Group comparisons of demographic and clinical data were conducted using IBM SPSS software (IBM SPSS Statistics for Windows, Version 24.0, IBM Corp., Armonk, NY, United States). Two-tailed independent-sample *t*-tests and chi-square tests were performed. The threshold was set at $P < 0.05$.

A non-parametric substitution test was used for morphological topology metric comparison analysis (e.g., Zhang et al., 2011; Lei et al., 2015). The AUC of each network metric was calculated across the S values to determine differences. All values were randomly reclassified into two groups, and the mean difference between the two groups was calculated for each network metric for multiple comparisons. This randomization procedure was repeated 10,000 times. The 95th percentile of each distribution was used as the threshold for significance testing. In addition, the Benjamini–Hochberg procedure was used to test for nodal centrality and to correct for multiple comparisons by controlling for false discovery rate (FDR) (Benjamini et al., 2001).

As children's brains are undergoing development, we proposed to analyze the age and diagnosis interaction effect. This analysis used a general linear model to examine the interaction effects of the network with age and diagnosis at global and node levels. In this analysis, gender and years of education were used as covariates, diagnosis, and age and the interaction of diagnosis and age were the dependent variables. The results were corrected for FDR, setting $P < 0.05$, as the threshold. We also analyzed

[3]https://www.nitrc.org/projects/bnv/

the correlation between the morphological metrics and clinical data. For the global and nodal attributes, where differences were detected earlier, correlation analysis was performed with the clinical scale separately. The above analysis was conducted by the IBM SPSS software (version 24.0).

# RESULTS

## Clinical Information

The basic clinical information and YGTSS scores are shown in **Table 1**. Age and sex were matched between the TS and HCs ($p > 0.05$).

## Brain Network Properties Alterations

Compared to HCs, patients with TS indicated a significant increase in $E_{glob}$ ($p = 0.012$) and a decrease in λ ($p = 0.027$) and Lp ($p = 0.025$). Increased $E_{global}$ means increased global efficiency of parallel information transfer in the network, lower Lp values indicate higher routing efficiency. No significant differences were identified in the Eloc ($p = 0.063$), Cp ($p = 0.217$), γ ($p = 0.267$), or σ ($p = 0.435$). The $p$-value has been FDR corrected.

## Differences in Nodal Brain Network Metrics

The nodal betweenness, nodal degree, and nodal efficiency differences are presented in **Table 2**. The significantly different regions included the right frontal lobe, right temporal lobe, right parietal lobe, right post-cingulum, bilateral caudate nucleus, and left thalamus (**Figure 1**).

## Relationships Between Topological Metrics and Clinical Data

Nodal betweenness, nodal degree, and nodal efficiency in the right superior parietal gyrus were negatively correlated with the motor tics scores of the YGTSS ($r = -0.328$, $p = 0.011$; $r = -0.310$, $p = 0.017$; $r = -0.291$, and $p = 0.025$, respectively). Nodal betweenness, nodal degree, and nodal efficiency in the right posterior cingulate gyrus were positively correlated with the YGTSS phonic tics scores ($r = 0.353$, $p = 0.006$; $r = 0.300$, $p = 0.021$; $r = 0.290$, and $p = 0.026$, respectively). Nodal betweenness in the right supplementary motor area was positively correlated with the YGTSS phonic tics scores ($r = 0.348$, $p = 0.007$). The nodal degree in the right supplementary motor area was positively correlated with the YGTSS phonic tics scores ($r = 0.259$, $p = 0.048$). The correlations were exhibited in **Figure 2**. The metrics of the structural connectome of the sparsity threshold were shown in **Figure 3**.

## Age and Diagnosis Interaction on Network Properties

The $E_{glob}$, λ, Lp revealed no significant main effect of age and diagnosis interaction at the global level. At the nodal level, our findings revealed no significant main effect of diagnosis-by-age interaction on nodal betweenness, nodal degree, or nodal efficiency (**Table 3**).

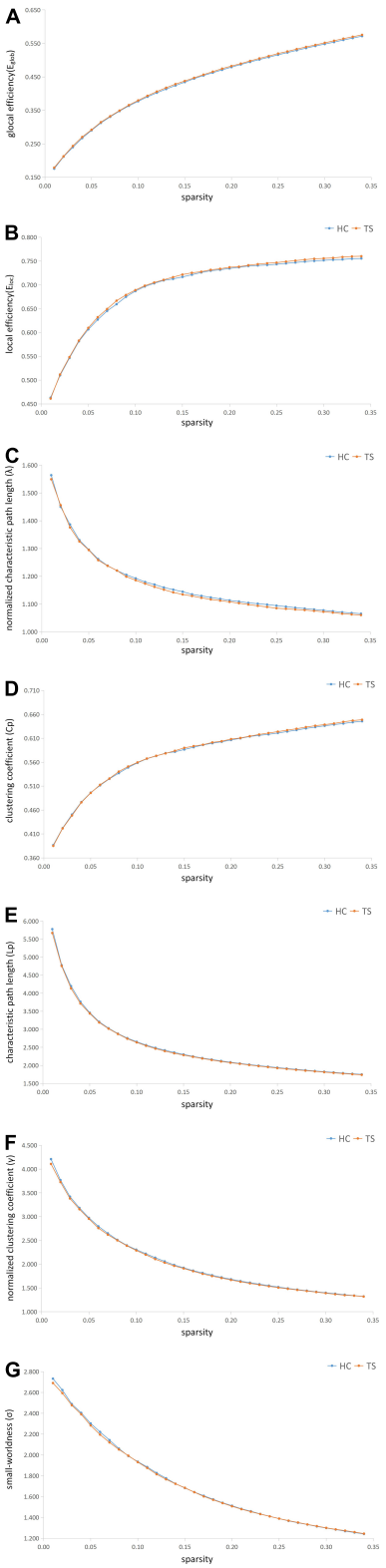


**FIGURE 3 |** The metrics of the structural connectome of the sparsity threshold in global efficiency **(A)**, local efficiency **(B)**, normalized characteristic path length (λ) **(C)**, clustering coefficient (Cp) **(D)**, characteristic path length (Lp) **(E)**, normalized clustering coefficient (γ) **(F)**, small-worldness (σ) **(G)**, respectively.

**TABLE 3 |** Linear modeling of age effects on node-level average controllability in drug-naïve patients with TS and HCs.

| Source | Dependent variable | Type III sum source of squares | df | Mean square | F value | *P*-value |
|---|---|---|---|---|---|---|
| Diagnosis*age | $E_{glob}$ | 1.25E-06 | 1 | 1.254E-6 | 0.363 | 0.548 |
| | $E_{loc}$ | 9.67E-07 | 1 | 9.674E-7 | 0.119 | 0.730 |
| | Cp | 3.53E-06 | 1 | 3.529E-6 | 0.353 | 0.553 |
| | γ | 3.92E-05 | 1 | 3.922E-5 | 0.027 | 0.869 |
| | λ | 7.26E-05 | 1 | 7.260E-5 | 3.294 | 0.072 |
| | Lp | 3.34E-05 | 1 | 3.342E-5 | 0.301 | 0.584 |
| | Nodal betweenness in ORBinf.R | 1.020 | 1 | 1.020 | 0.018 | 0.895 |
| | Nodal betweenness in SMA.R | 269.783 | 1 | 269.783 | 1.779 | 0.184 |
| | Nodal betweenness in SOG.L | 11.679 | 1 | 11.679 | 0.039 | 0.844 |
| | Nodal betweenness in SPG.R | 8.774 | 1 | 8.774 | 0.094 | 0.759 |
| | Nodal betweenness in TPOsup.R | 93.188 | 1 | 93.188 | 0.487 | 0.486 |
| | Nodal degree in SMA.R | 1.221 | 1 | 1.221 | 0.702 | 0.404 |
| | Nodal degree in ORBsupmed.R | 4.325 | 1 | 4.325 | 0.753 | 0.387 |
| | Nodal degree in PCG.R | 0.050 | 1 | 0.050 | 0.505 | 0.479 |
| | Nodal degree in SOG.L | 0.015 | 1 | 0.015 | 0.005 | 0.946 |
| | Nodal degree in SPG.R | 0.042 | 1 | 0.042 | 0.044 | 0.834 |
| | Nodal degree in CAU.L | 0.678 | 1 | 0.678 | 0.800 | 0.373 |
| | Nodal degree in CAU.R | 1.656 | 1 | 1.656 | 1.610 | 0.207 |
| | Nodal degree in TPOsup.R | 2.082 | 1 | 2.082 | 0.891 | 0.347 |
| | Nodal efficiency in SMA.R | 5.836E-5 | 1 | 5.836E-5 | 0.401 | 0.528 |
| | Nodal efficiency in PCG.R | 0.000 | 1 | 0.000 | 0.436 | 0.510 |
| | Nodal efficiency in SOG.L | 1.985E-6 | 1 | 1.985E-6 | 0.008 | 0.931 |

*CAU, caudate nucleus; HC, healthy control; L, left; ORBinf, inferior frontal gyrus, orbital part; ORBsupmed, superior frontal gyrus, medial orbital; PCG, posterior cingulate gyrus; R, right; SMA, supplementary motor area; SOG, superior occipital gyrus; SPG, superior parietal gyrus; THA, thalamus; TPOsup, temporal pole: superior temporal gyrus; TS, Tourette's syndrome. *Means the interaction effect of age and diagnosis.*

## DISCUSSION

This study explored gray matter topological alterations in drug-naïve pediatric patients with TS. Patients with TS showed a significant increase in $E_{global}$ and a decrease in λ and Lp. Altered nodal characteristics were observed, some of which were correlated with the YGTSS total scores, phonic tics scores, and motor tics scores. Nodal characteristic metrics are mainly involved in the cortex-striatum-thalamus-cortex (CSTC) circuit. This result is consistent with the results of previous structural studies. Furthermore, this result explores the structural abnormalities from a topological perspective.

The function of the supplementary motor area (SMA) is to control movement (Chen et al., 2010). The SMA can produce complex movement synergies and vocalizations. In the present study, the YGTSS total score was positively correlated with the nodal degree in the right SMA. In addition, phonic tics scores were positively correlated with nodal betweenness in the right SMA. The total tic severity increased as the nodal degree increased, and the phonic tic severity increased as the nodal betweenness increased. The nodal degree indicates the ability of information communication, and the nodal betweenness reflects the interaction between a node and the surrounding nodes. SMA plays a role in maintaining postural stability and physical coordination (Fujimoto et al., 2014). The SMA is closely linked to the basal ganglia. The SMA projects to both the presenter's motor cortex and spinal cord (Tanji, 1994). Therefore, the SMA may be associated with motor tic and compulsive behaviors in TS (Tübing et al., 2018). Studies with probabilistic fiber tractography revealed reduced connectivity between the SMA and basal ganglia, as well as between frontal cortico-cortical circuits (Cheng et al., 2013) in patients with TS.

In this study, we found that nodal betweenness and nodal degree increased in the left thalamus of patients with TS. Previous structural studies showed an increased volume of the thalamus in both adults and children with TS (Miller et al., 2010). In patients with TS, the altered volume of the thalamus may be related to compensatory mechanisms related to its control of twitching and the formation of overactive motor circuits (Greene et al., 2017). The thalamus is the core nucleus that connects the peripheral tissues, is involved in the interactions between the cortical connections, and accelerates the synchronous oscillatory activity of the functional areas of the cortex (Benarroch, 2015). Convulsions may be related to the CSTC circuit (Draper et al., 2016). Studies have suggested that thalamic-striatal projections may act as positive reinforcement for striatal neurons, which have behaviorally selected roles. They monitor "top-down" control by modulating the activity of cortico-basal ganglia loops (Kimura et al., 2004; Smith et al., 2004).

We observed that nodal degree and nodal efficiency increased in the right posterior cingulate gyrus in patients with TS. The posterior cingulate gyrus is metabolically active and has extensive connections with surrounding brain regions

(Leech and Sharp, 2014). It is temporally and spatially associated with common activities. The cingulate gyrus is a component of the limbic lobe and is associated with emotion, learning, and memory. The posterior cingulate gyrus amplifies tic impulses more than inhibits them. Structural MRI showed cortical thinning and/or below-normal volume in the cingulate cortex, correlating with tic severity. Moreover, in the posterior middle cingulate cortex, dorsal posterior cingulate cortex, and ventral posterior cingulate cortex, cortical thickness is a candidate biomarker shared across siblings with TS (O'Neill et al., 2019). This study indicated the right posterior cingulate gyrus played an essential role in topological perspective.

In this study, the nodal degree increased in the bilateral caudate nucleus in the TS group compared with that in the healthy controls. The caudate nucleus is part of the striatum, and its role includes correlating motor behavior with spatial information, as well as limb posture maintenance, speed, and accuracy of directed movements (Takakusaki et al., 2004; Turner and Desmurget, 2010). A previous study showed caudate nucleus volume reduction in both adults and children with TS (Gerard and Peterson, 2003). Our study showed a nodal degree alteration may result in tics.

The nodal betweenness and nodal degree in the superior parietal lobule were lower in patients with TS than in those of healthy controls. Motor tics scores were positively correlated with nodal betweenness, degree, and efficiency in the superior parietal lobule. The superior parietal lobule is involved in spatial orientation, which may be related to the tics. Generally, the nodal brain network properties were in the circuit.

While previous studies have explored brain structural abnormalities in TS from a structural perspective, our study explored structural topological alterations in TS. Brain structural abnormalities underlie the altered brain topology. Our study is consistent with previous structural studies that have identified altered brain structure topology in the CSTC circuit.

As the brain develops in children, diagnosis and age interaction analyses were conducted. The results showed no significant main effect of diagnosis-by-age interactions on the global or nodal brain network properties. Therefore, the changes in the global or nodal brain network properties between the patients with TS and healthy controls were not related to age.

## CONCLUSION

Using a novel gray matter morphological topology method and a moderate patient group, we showed alterations in global or nodal brain topological properties in patients with TS compared with those of healthy controls. The nodal brain network properties are included in the CSTC circuit. These alterations were not affected by age of the developing brains of children.

## DATA AVAILABILITY STATEMENT

The raw data supporting the conclusions of this article will be made available by the authors, without undue reservation.

## ETHICS STATEMENT

The studies involving human participants were reviewed and approved by the Human Ethics Committee of West China Second University Hospital of Sichuan University. Written informed consent to participate in this study was provided by the participants' legal guardian/next of kin.

## AUTHOR CONTRIBUTIONS

YL, XC, and HQ proposed the conception and design of the study and wrote the manuscript. YL and XLL analyzed the data. YJ, FJ, XH, and GN analyzed the clinical data and imaging data. XSL and CF collected the imaging data and analyzed the data. HZ and XC assessed the patients and collected the clinical data. All authors contributed to the article, critically reviewed the manuscript, and approved the submitted version.

## FUNDING

This research work was supported by the youth fund of the National Natural Science Foundation of China (Grant number 81601460).

## ACKNOWLEDGMENTS

We thank Qiyuan Tian and Hong Li for their helpful discussions.

## REFERENCES

Alexander-Bloch, A., Giedd, J. N., and Bullmore, E. (2013). Imaging structural co-variance between human brain regions. *Nat. Rev. Neurosci.* 14, 322–336. doi: 10.1038/nrn3465

American Psychiatric Association [APA] (2013). *Diagnostic and Statistical Manual of Mental Disorders (DSM-5§)*. Washington, DC: American Psychiatric Pub.

Ashburner, J. (2007). A fast diffeomorphic image registration algorithm. *Neuroimage* 38, 95–113. doi: 10.1016/j.neuroimage.2007.07.007

Ashburner, J., Andersson, J. L., and Friston, K. J. (2000). Image registration using a symmetric prior–in three dimensions. *Hum. Brain Mapp.* 9, 212–225. doi: 10.1002/(sici)1097-0193(200004)9:4<212::aid-hbm3>3.0.co;2-#

Ashburner, J., and Friston, K. J. (2005). Unified segmentation. *Neuroimage* 26, 839–851. doi: 10.1016/j.neuroimage.2005.02.018

Benarroch, E. E. (2015). Pulvinar: associative role in cortical function and clinical correlations. *Neurology* 84, 738–747. doi: 10.1212/WNL.0000000000001276

Benjamini, Y., Drai, D., Elmer, G., Kafkafi, N., and Golani, I. (2001). Controlling the false discovery rate in behavior genetics research. *Behav. Brain Res.* 125, 279–284. doi: 10.1016/s0166-4328(01)00297-2

Burnhan, K. P., and Anderson, D. R. (2002). Model selection and multi-model inference: a practical information-theoretic approach. *Technometrics* 45:181. doi: 10.1198/tech.2003.s146

Chen, X., Scangos, K. W., and Stuphorn, V. (2010). Supplementary motor area exerts proactive and reactive control of arm movements. *J. Neurosci.* 30, 14657–14675. doi: 10.1523/JNEUROSCI.2669-10.2010

Cheng, B., Braass, H., Ganos, C., Treszl, A., Biermann-Ruben, K., Hummel, F. C., et al. (2013). Altered intrahemispheric structural connectivity in Gilles de la Tourette syndrome. *Neuroimage Clin.* 4, 174–181. doi: 10.1016/j.nicl.2013.11.011

Draganski, B., Martino, D., Cavanna, A. E., Hutton, C., Orth, M., Robertson, M. M., et al. (2010). Multispectral brain morphometry in Tourette syndrome persisting into adulthood. *Brain* 133, 3661–3675. doi: 10.1093/brain/awq300

Draper, A., Jackson, G. M., Morgan, P. S., and Jackson, S. R. (2016). Premonitory urges are associated with decreased grey matter thickness within the insula and sensorimotor cortex in young people with Tourette syndrome. *J. Neuropsychol.* 10, 143–153. doi: 10.1111/jnp.12089

Fujimoto, H., Mihara, M., Hattori, N., Hatakenaka, M., Kawano, T., Yagura, H., et al. (2014). Cortical changes underlying balance recovery in patients with hemiplegic stroke. *Neuroimage* 85, 547–554. doi: 10.1016/j.neuroimage.2013.05.014

Gerard, E., and Peterson, B. S. (2003). Developmental processes and brain imaging studies in Tourette syndrome. *J. Psychosom. Res.* 55, 13–22. doi: 10.1016/s0022-3999(02)00581-0

Gong, Q. (2020). *Psychoradiology, Neuroimaging Clinics of North America*. New York: Elsevier Inc.

Greene, D. J., Williams Iii, A. C., Koller, J. M., Schlaggar, B. L., and Black, K. J. (2017). The Tourette Association of America neuroimaging C: brain structure in pediatric Tourette syndrome. *Mol. Psychiatry* 22, 972–980.

He, Y., Dagher, A., Chen, Z., Charil, A., Zijdenbos, A., Worsley, K., et al. (2009). Impaired small-world efficiency in structural cortical networks in multiple sclerosis associated with white matter lesion load. *Brain* 132, 3366–3379. doi: 10.1093/brain/awp089

He, Y., Chen, Z. J., and Evans, A. C. (2007). Small-world anatomical networks in the human brain revealed by cortical thickness from MRI. *Cereb. Cortex* 17, 2407–2419. doi: 10.1093/cercor/bhl149

Kimura, M., Minamimoto, T., Matsumoto, N., and Hori, Y. (2004). Monitoring and switching of cortico-basal ganglia loop functions by the thalamo-striatal system. *Neurosci. Res.* 48, 355–360. doi: 10.1016/j.neures.2003.12.002

Kong, L., Cao, S., Lv, B., Wu, T., Zhang, J., Yang, F., et al. (2020). Altered structural cerebral cortex in Children with Tourette syndrome. *Eur. J. Radiol.* 129:109119. doi: 10.1016/j.ejrad.2020.109119

Kong, X. Z., Liu, Z., Huang, L., Wang, X., Yang, Z., Zhou, G., et al. (2015). Mapping individual brain networks using statistical similarity in regional morphology from MRI. *PLoS One* 10:e0141840. doi: 10.1371/journal.pone.0141840

Kong, X. Z., Wang, X., Huang, L., Pu, Y., Yang, Z., Dang, X., et al. (2014). Measuring individual morphological relationship of cortical regions. *J. Neurosci. Methods* 237, 103–107. doi: 10.1016/j.jneumeth.2014.09.003

Leckman, J. F. (2002). Tourette's syndrome. *Lancet* 360, 1577–1586. doi: 10.1016/S0140-6736(02)11526-1

Leckman, J. F., and Cohen, D. J. (eds) (1999). *Tourette's Syndrome-tics, Obsessions, Compulsions: Developmental Psychopathology and Clinical Care*. New York: John Wiley and Sons Inc.

Leech, R., and Sharp, D. J. (2014). The role of the posterior cingulate cortex in cognition and disease. *Brain* 137, 12–32. doi: 10.1093/brain/awt162

Lei, D., Li, K., Li, L., Chen, F., Huang, X., Lui, S., et al. (2015). Disrupted functional brain Connectome in patients with posttraumatic stress disorder. *Radiology* 276, 818–827. doi: 10.1148/radiol.15141700

Liu, Y. M., Wang, W., Gao, J. Q., Yin, P. Y., Zhang, G. H., Lv, L. P., et al. (2013). Structural abnormalities in early Tourette syndrome children: a combined voxel-based Morphometry and tract-based spatial statistics study. *PLoS One* 8:e76105. doi: 10.1371/journal.pone.0076105

Miller, A. M. B. R., Hao, X., Sanchez-Pena, J. P., Sobel, L. J., and Liu, J. (2010). Enlargement of thalamic nuclei in Tourette syndrome. *Arch. Gen. Psychiatry* 67, 955–964. doi: 10.1001/archgenpsychiatry.2010.102

Müller-Vahl, K. R., Kaufmann, J., Grosskreutz, J., Dengler, R., Emrich, H. M., and Peschel, T. (2009). Prefrontal and anterior cingulate cortex abnormalities in Tourette syndrome: evidence from voxel-based morphometry and magnetization transfer imaging. *BMC Neurosci.* 10:47. doi: 10.1186/1471-2202-10-47

O'Neill, J., Piacentini, J. C., and Peterson, B. S. (2019). Cingulate role in Tourette syndrome. *Handb. Clin. Neurol.* 166, 165–221. doi: 10.1016/B978-0-444-64196-0.00011-X

Robertson, M. M. (2000). Tourette syndrome, associated conditions and the complexities of treatment. *Brain* 123, 425–462. doi: 10.1093/brain/123.3.425

Rubinov, M., and Sporns, O. (2010). Complex network measures of brain connectivity: uses and interpretations. *Neuroimage* 52, 1059–1069. doi: 10.1016/j.neuroimage.2009.10.003

Scott, D. W. (2015). *Multivariate Density Estimation: Theory, Practice, and Visualization, 2nd ed*. Hoboken, NJ: John Wiley & Sons.

Seidlitz, J., Váša, F., Shinn, M., Romero-Garcia, R., Whitaker, K. J., Vértes, P. E., et al. (2018). Morphometric similarity networks detect microscale cortical organization and predict inter-individual cognitive variation. *Neuron* 97, 231–247. doi: 10.1016/j.neuron.2017.11.039

Smith, Y., Raju, D. V., Pare, J. F., and Sidibe, M. (2004). The thalamostriatal system: a highly specific network of the basal ganglia circuitry. *Trends Neurosci.* 27, 520–527. doi: 10.1016/j.tins.2004.07.004

Sun, H., Chen, Y., Huang, Q., Lui, S., Huang, X., Shi, Y., et al. (2018). Psychoradiologic utility of MR imaging for diagnosis of attention deficit hyperactivity disorder: a radiomics analysis. *Radiology* 287, 620–630. doi: 10.1148/radiol.2017170226

Takakusaki, K., Saitoh, K., Harada, H., and Kashiwayanagi, M. (2004). Role of basal ganglia–brainstem pathways in the control of motor behaviors. *Neurosci. Res.* 50, 137–151. doi: 10.1016/j.neures.2004.06.015

Tanji, J. (1994). The supplementary motor area in the cerebral cortex. *Neurosci. Res.* 19, 251–268. doi: 10.1016/0168-0102(94)90038-8

Tijms, B. M., Seriès, P., Willshaw, D. J., and Lawrie, S. M. (2012). Similarity-based extraction of individual networks from gray matter MRI scans. *Cereb. Cortex* 22, 1530–1541. doi: 10.1093/cercor/bhr221

Tübing, J., Gigla, B., Brandt, V. C., Verrel, J., Weissbach, A., Beste, C., et al. (2018). Associative plasticity in supplementary motor area-motor cortex pathways in Tourette syndrome. *Sci. Rep.* 8, 1–8. doi: 10.1038/s41598-018-30504-8

Turner, R. S., and Desmurget, M. (2010). Basal ganglia contributions to motor control: a vigorous tutor. *Curr. Opin. Neurobiol.* 20, 704–716. doi: 10.1016/j.conb.2010.08.022

Tzourio-Mazoyer, N., Landeau, B., Papathanassiou, D., Crivello, F., Etard, O., Delcroix, N., et al. (2002). Automated anatomical labeling of activations in SPM using a macroscopic anatomical parcellation of the MNI MRI single-subject brain. *NeuroImage* 15, 273–289. doi: 10.1006/nimg.2001.0978

Wang, H., Jin, X., Zhang, Y., and Wang, J. (2016). Single-subject morphological brain networks: connectivity mapping, topological characterization and test-retest reliability. *Brain Behav.* 6:e00448. doi: 10.1002/brb3.448

Wang, J., Wang, X., Xia, M., Liao, X., Evans, A., and He, Y. (2015). Corrigendum: GRETNA: a graph theoretical network analysis toolbox for imaging connectomics. *Front. Hum. Neurosci.* 9:458. doi: 10.3389/fnhum.2015.00458

Watts, D. J., and Strogatz, S. H. (1998). Collective dynamics of 'small-world' networks. *Nature* 393, 440–442. doi: 10.1038/30918

Worbe, Y., Marrakchi-Kacem, L., Lecomte, S., Valabregue, R., Poupon, F., Guevara, P., et al. (2015). Altered structural connectivity of cortico-striato-pallido-thalamic networks in Gilles de la Tourette syndrome. *Brain* 138, 472–482. doi: 10.1093/brain/awu311

Zhang, J., Wang, J., Wu, Q., Kuang, W., Huang, X., He, Y., et al. (2011). Disrupted brain connectivity networks in drug-naive, firstepisode major depressive disorder. *Biol. Psychiatry* 70, 334–342. doi: 10.1016/j.biopsych.2011.05.018

**Conflict of Interest:** The authors declare that the research was conducted in the absence of any commercial or financial relationships that could be construed as a potential conflict of interest.

**Publisher's Note:** All claims expressed in this article are solely those of the authors and do not necessarily represent those of their affiliated organizations, or those of the publisher, the editors and the reviewers. Any product that may be evaluated in this article, or claim that may be made by its manufacturer, is not guaranteed or endorsed by the publisher.

# Advantages of publishing in Frontiers

**OPEN ACCESS**
Articles are free to read for greatest visibility and readership

**FAST PUBLICATION**
Around 90 days from submission to decision

**HIGH QUALITY PEER-REVIEW**
Rigorous, collaborative, and constructive peer-review

**TRANSPARENT PEER-REVIEW**
Editors and reviewers acknowledged by name on published articles

**Frontiers**
Avenue du Tribunal-Fédéral 34
1005 Lausanne | Switzerland

**Visit us:** www.frontiersin.org
**Contact us:** frontiersin.org/about/contact

**REPRODUCIBILITY OF RESEARCH**
Support open data and methods to enhance research reproducibility

**DIGITAL PUBLISHING**
Articles designed for optimal readership across devices

**FOLLOW US**
@frontiersin

**IMPACT METRICS**
Advanced article metrics track visibility across digital media

**EXTENSIVE PROMOTION**
Marketing and promotion of impactful research

**LOOP RESEARCH NETWORK**
Our network increases your article's readership